MycoKeys 88: 1–33 (2022)
doi: 10.3897/mycokeys.88.77106
https://mycokeys.pensoft.net

RESEARCH ARTICLE

A peer-reviewed open-access journal
MycoKeys
Launched to accelerate biodiversity research

Metabarcoding of insect-associated fungal communities: a comparison of internal transcribed spacer (ITS) and large-subunit (LSU) rRNA markers

Angelina Ceballos-Escalera[1,2], John Richards[1,2], Maria Belen Arias[1,4], Daegan J. G. Inward[3], Alfried P. Vogler[1,2]

1 *Department of Life Sciences, Natural History Museum, Cromwell Road, London SW7 5BD, UK* **2** *Department of Life Sciences, Imperial College London, Silwood Park Campus, Ascot SL5 7PY, UK* **3** *Forest Research, Alice Holt Research Station, Farnham, Surrey, GU10 4LH, UK* **4** *School of Life Sciences, University of Essex, Colchester Campus, CO4 3SQ, UK*

Corresponding author: Angelina Ceballos-Escalera (angelinaceballosescalera@gmail.com)

Academic editor: Francesco Dal Grande | Received 29 October 2021 | Accepted 25 January 2022 | Published 8 March 2022

Citation: Ceballos-Escalera A, Richards J, Arias MB, Inward DJG, Vogler AP (2022) Metabarcoding of insect-associated fungal communities: a comparison of internal transcribed spacer (ITS) and large-subunit (LSU) rRNA markers. MycoKeys 88: 1–33. https://doi.org/10.3897/mycokeys.88.77106

Abstract

Full taxonomic characterisation of fungal communities is necessary for establishing ecological associations and early detection of pathogens and invasive species. Complex communities of fungi are regularly characterised by metabarcoding using the Internal Transcribed Spacer (ITS) and the Large-Subunit (LSU) gene of the rRNA locus, but reliance on a single short sequence fragment limits the confidence of identification. Here we link metabarcoding from the ITS2 and LSU D1-D2 regions to characterise fungal communities associated with bark beetles (Scolytinae), the likely vectors of several tree pathogens. Both markers revealed similar patterns of overall species richness and response to key variables (beetle species, forest type), but identification against the respective reference databases using various taxonomic classifiers revealed poor resolution towards lower taxonomic levels, especially the species level. Thus, Operational Taxonomic Units (OTUs) could not be linked via taxonomic classifiers across ITS and LSU fragments. However, using phylogenetic trees (focused on the epidemiologically important Sordariomycetes) we placed OTUs obtained with either marker relative to reference sequences of the entire rRNA cistron that includes both loci and demonstrated the largely similar phylogenetic distribution of ITS and LSU-derived OTUs. Sensitivity analysis of congruence in both markers suggested the biologically most defensible threshold values for OTU delimitation in Sordariomycetes to be 98% for ITS2 and 99% for LSU D1-D2. Studies of fungal communities using the canonical ITS barcode require corroboration across additional loci. Phylogenetic analysis of OTU sequences aligned to the full rRNA cistron shows higher success rate and greater accuracy of species identification compared to probabilistic taxonomic classifiers.

Keywords
clustering, fungi, ITS, LSU, metabarcoding, pathogens, phylogeny, Scolytinae

Introduction

Fungal communities associated with insects have been widely studied to disentangle the ecological roles and specificities of these interactions (Ganter 2006; Raman et al. 2012; Li et al. 2016; Malacrinò et al. 2017; Jacobsen et al. 2018). For these studies to succeed, accurate and reliable fungal identifications are essential. However, identifications of fungi are challenging due to their cryptic morphology and incomplete taxonomy, with only 3–8% of fungal species described so far (Hibbett et al. 2016; Kandawatte Wedaralalage et al. 2020). Conventional studies of fungal communities have been conducted by isolating and culturing the fungi associated with insect specimens (Batra 1963), but this overlooked many unculturable species. High-throughput DNA sequencing has provided an alternative methodology by amplifying and sequencing short 'barcodes' from mixed communities (metabarcoding) (Yu et al. 2012). Metabarcoding is now widely applied in characterising the species composition and diversity of fungal communities associated with insects. In the specific case of fungal communities associated with bark beetles, metabarcoding usually detects dozens of species of fungi isolated from a single insect specimen (Bálint et al. 2014; Miller et al. 2016, 2019, Malacrinò et al. 2017; Johnson et al. 2018; Hulcr et al. 2020).

There is broad agreement that the internal transcribed spacer (ITS) of the nuclear rRNA gene cluster should be the standard DNA barcode in fungi (Schoch et al. 2012). Its utility in metabarcoding is now equally well established, and extensive reference databases and universal primer combinations are in wide use (Porras-Alfaro et al. 2014; Tedersoo et al. 2015b). However, various challenges remain for accurate characterisation of communities. PCR amplification biases may skew species recovery (Bellemain et al. 2010; Harrington et al. 2011; Dreaden et al. 2014; Tedersoo et al. 2015b; Li et al. 2020). For example, the ITS marker may not detect key pathogen species in the Ophiostomatales (Skelton et al. 2019; Hulcr et al. 2020). In addition, the recovered short sequence fragments have limited power for phylogenetic placement (Vrålstad 2011; Porras-Alfaro et al. 2014), exacerbated by the incompleteness of the reference databases (Porras-Alfaro et al. 2014; Tedersoo et al. 2015a; Miller et al. 2016; Agerbo Rasmussen et al. 2020). In response to these challenges, several fungal phylogenetic and barcoding studies have used a combination of ITS and partial large and small subunit (LSU and SSU) rRNA genes, as well as other markers such as RPB2 and TEF1α (Lutzoni et al. 2004; Zhang et al. 2006; Stielow et al. 2015). Extensive curated reference sets and analysis tools like SILVA and RDP (Ribosomal Database Project) have been built specifically for SSU and LSU genes (Wang et al. 2007; Quast et al. 2012).

In practice, both the ITS and LSU/SSU markers exhibit particularities whose benefits and drawbacks depend on the aim and scope of a study (Porras-Alfaro et al. 2014).

The LSU/SSU genes are less variable than the ITS intergenic regions, which favours alignment and tree-based analyses, but their low rate of molecular evolution reduces the taxonomic resolution at the species-level. In turn, ITS provides better species resolution due to its higher substitution rate but, as a non-coding RNA, the ITS region is prone to insertion/deletions, which causes difficulties with alignment and phylogenetic analysis (Vrålstad 2011; Porras-Alfaro et al. 2014). In addition, the higher substitution rate in ITS leads to intragenomic variation of the tandem repeat units, given the slow homogenisation among the various copies. However, in fungi this intraspecific and intragenomic variation is still poorly documented, and it may also affect the LSU/SSU coding regions (Lücking et al. 2020). The differences in evolutionary rates and in levels of intra-genomic variation have implications for the way the raw reads are processed in ecological and taxonomic studies. In metabarcoding, sequence reads are usually clustered into Operational Taxonomic Units (OTU) to circumscribe and identify fungal species (Hyde et al. 2013; Kõljalg et al. 2013; Hibbett et al. 2016; Kandawatte Wedaralalage et al. 2020; Lücking et al. 2020). However, if the two regions evolve at different rates, this may affect the optimal threshold values of clustering in establishing the species level entities, and equally may change the interpretation of quality filtered reads, the so-called Amplified Sequence Variants (ASVs) (Callahan et al. 2017), to represent the haplotypes of individuals.

The problem of marker choice and the comparability of metabarcoding studies using either type could be alleviated if both regions were sequenced for the same specimens. Whilst this is a powerful approach for cultured isolates (Vu et al. 2019), it is not possible to link ITS and SSU/LSU amplicons in the metabarcoding mixtures. A recent study attempted to perform metabarcoding of longer amplicons covering both markers with long-read technology, which is ultimately the way forward, but laboratory and bioinformatic procedures currently developed for short fragments could not be applied easily (Furneaux et al. 2021). Thus, short fragments of either marker remain the focus of metabarcoding for the immediate future, which leaves the question about the consequences of marker choice for the conclusions from such studies. To date the issue of ITS vs. LSU comparability has mainly been addressed by conducting amplification of both markers from the same mixture, both in mock (Bakker 2018; Egan et al. 2018; Frau et al. 2019) and natural communities (Parada et al. 2016; Jusino et al. 2019; Li et al. 2020). When applied to the study of ecological patterns these studies have found no major effect of the marker choice (Tedersoo et al. 2015b; George et al. 2019; Nilsson et al. 2019; Furneaux et al. 2021). However, these studies generally have applied a coarse-grain approach of higher-level taxonomic analysis, rather than the species level, where the effects of using different reference databases and different clustering methods may be more pronounced.

Here, we address the problem of identification and unification of information derived from both markers using phylogenetic approaches. Metabarcodes obtained from a given community, as those associated with a single insect, should be composed of the same lineages, and thus occupy the same positions in a phylogenetic tree. Generating trees independently for ITS and LSU does not overcome the problem of

associating the sequences from both amplicons, and hence the aim here is to integrate these sequences in the same tree. This may be achieved based on a scaffold of well-identified reference sequences covering the entire rRNA cluster, including ITS and LSU, to which the non-overlapping sequences for each marker are added for a joint tree search. If both markers represent the same fungal community, the corresponding ITS and LSU sequences should appear in a similar place in the tree, relative to a given reference sequence spanning both regions. Besides the greater precision of the phylogenetic position, the use of both barcodes in a single analysis also overcomes the problem of using different reference sets in the prevailing databases for ITS and rRNA markers.

We test this approach for fungal communities associated with bark beetles (Coleoptera: Scolytinae). These insects breed in living or dead trees and form close associations with fungi, which are important for access to nutrients from wood that cannot be utilised directly by the beetles themselves (Batra 1963). Fungal communities associated with these beetles are highly diverse and form symbioses of varying strength and specificity, and may involve the active transport of fungal hyphae or spores in specifically adapted pockets of the beetles' exoskeleton, the mycangia (Six 2020). The beetle-fungus complex can cause enormous damage to forest ecosystems, e.g., resulting in the demise of chestnuts in North America and elms across the Northern Hemisphere, or the recent large-scale decline of conifer forests in Central Europe and North America, which usually involve fungi from the ascomycete orders Ophiostomatales, Microascales and Hypocreales (Class Sordariomycetes) (Ploetz et al. 2013). Metabarcoding now provides a powerful tool for detailed studies of these complex communities, but the results may be influenced by the choice of barcode markers and various experimental problems in using short sequences from mixed amplicons, such as primer bias and co-amplification of paralogues. We used individuals from four bark beetle species obtained from three forest types to characterise the associated fungal communities, conducting a comparison of the two markers with regard to: (1) broad ecological trends of fungal associations taking a whole-community approach, and (2) species identifications against existing ITS and LSU fungal reference databases, using various taxonomic classifiers and explicit phylogenetic methods. The side-by-side comparison addresses the power of either marker to infer critical parameters of fungal community metabarcoding, such as the number and taxonomic identity of OTUs, their ecological associations, and inference of whole-community diversity and turnover. The phylogenetic approach also can improve upon the taxonomic placement of OTUs conducted with probabilistic classifiers.

Materials and methods

Samples used and laboratory procedures

Sequence data were generated from 20 specimens per species for four species (*Xylosandrus germanus*, *Xyleborinus saxesenii*, *Gnathotrichus materiarius*, and *Tomicus piniperda*),

Table 1. Beetle species included in the study and relevant life history information.

Forest type	Beetle species	Status	Adapted structures	Feeding mode
Spruce, oak	*Xylosandrus germanus*	Introduced	Mesonotal mycangia	Xylomycetophagous
Spruce, oak	*Xyleborinus saxesenii*	Native	Elytral mycangia	Xylomycetophagous
Pine, spruce	*Gnathotrichus materiarius*	Introduced	Tubular opening near precoxae	Xylomycetophagous
Pine, spruce	*Tomicus piniperda*	Native	No known mycangia	Xylophagous

for a total of 80 specimens (Table 1). Only the latter is a xylophagous 'bark beetle' in the strict sense, while the three others are considered mycelia feeding (xylomycetophagous) 'ambrosia beetles' that rely on active transport of fungi indicated by the presence of mycangia (see Six 2020). Specimens were collected by Forest Research UK (Alice Holt, Hampshire, UK, see https://www.forestresearch.gov.uk/) during 2013–2015 in the New Forest National Park (50°50'52.08"N, 1°35'33.51"W), Hampshire, UK, using Lindgren multiple-funnel traps (Lindgren 1983) (Phero Tech). These traps were placed in oak, spruce and pine forests and were baited with lures (100% ethanol, plus α-pinene) (Inward 2019). Propylene glycol (65%) was used as the preservation fluid at the bottom of the traps. Specimens were morphologically identified and selected at random to obtain the same number of specimens per beetle species and forest type.

In the laboratory, the specimens were rinsed with pure water to remove loosely adhering fungal tissue, and thoroughly macerated individually to ensure that all fungi associated with the specimens were released. DNA was extracted using the DNeasy Blood and Tissue spin column extraction kit (Qiagen, Valencia, CA, USA). Individual DNA extracts were first tested for correct beetle species identification using the COI barcode marker, which was amplified for a 418 bp fragment and sequenced on Illumina HiSeq following methods of Arribas et al. (2016). In all cases the most abundant read, as determined with the NAPselect script (Creedy et al. 2019), had an exact match to existing reference sequences of the respective species, confirming the morphological identification.

The DNA extracts were then used for fungal metabarcoding of the ITS2 region with primers ITS86F (5'-GTGAATCATCGAATCTTTGAA-3') (Op De Beeck et al. 2014)/ ITS4 (5'-TCCTCCGCTTATTGATATGC-3') (White et al. 1990) and LSU using primers LR0R (5'-ACCCGCTGAACTTAAGC-3 (Vilgalys and Hester 1990)/ JH-LSU-369rc (5'-CTTCCCTTTCAACAATTTCAC-3') (Li et al. 2016) targeting the D1-D2 region at the 5' end of the LSU gene immediately downstream of the ITS2 region. Both markers were amplified from each beetle DNA extraction in separate reactions. Unique six-nucleotide indices added to each primer pair were used to distinguish the libraries. PCRs were pooled from three replicates conducted under slightly different annealing temperatures (54 °C, 55 °C and 56 °C) to accommodate differences in optimal amplification conditions of the fungal species (Schmidt et al. 2013), and blank PCR reactions were used as negative control. Successful PCR amplicons were purified using the AMPure XP magnetic beads (Beckman Coulter). Amplicons were indexed using a secondary PCR with Nextera XT DNA Library Preparation Kit (Illumina Inc.) and sequenced on an Illumina HiSeq 2500 platform to generate 2 × 300 bp paired-end reads.

Bioinformatics

Raw reads were demultiplexed, primer sequences trimmed, and singleton reads removed with Cutadapt v. 2.10 (Martin 2011). Read quality was evaluated using FastQC v. 0.11.9 (Andrews et al. 2010). The raw reads generated for these analyses are available as Bio-Project PRJNA727174 (Sequence Read Archives) in the BioSample Submission Portal (Barrett et al. 2012).

Forward and reverse reads were merged and quality filtered (Phred score ≥ 30) using PEAR v. 0.9.8 (Zhang et al. 2014), while un-merged reads were discarded. After merging, the average read length was 252 bp for ITS2 and 357 bp for LSU D1-D2. Subsequent steps were carried out using VSEARCH v. 2.15.0 (Rognes et al. 2016) using the following commands. A further quality test was conducted using the --fastx_filter command and --fastq_maxee 1.0. After dereplication (--derep_fulllength), assemblies were denoised (--cluster_unoise --minsize 4 --unoise_alpha 2) and length filtered for a range of 100 to 500 bp (--fastx_filter) and all singletons removed. Chimera filtering was performed with --uchime3_denovo and reads were then clustered into Operational Taxonomic Units (OTUs) at various similarity thresholds (97%, 98%, 99%) using the --cluster_size command. The average length of the OTU representative sequences was 270 bp for ITS2 and 347 bp for LSU D1-D2 (Suppl. material 1: Fig. S1). Reads were then mapped to the 97% OTU clusters, outputting an OTU table of read abundances suitable for the ecological analysis.

OTU identification and classification

Fungal OTUs were classified following three widely used methods for species identification. The Ribosomal Database Project (RDP) Bayesian Classifier (Wang et al. 2007) was used for fungal identification employing the Warcup fungal ITS (v. 2, release March 2018) and UNITE (accessed on February 2020) training sets (Deshpande et al. 2016; Edgar 2018). In addition, OTUs were processed through the Protax-fungi pipeline (Abarenkov et al. 2018), implemented in the PlutoF platform (Abarenkov et al. 2010) and based on the UNITE fungal database (accessed February 2020). Protax-fungi hierarchically assigns the OTU identities from the root node of the taxonomy through to the species (Nilsson et al. 2019). It has not been implemented for LSU, and thus was applied to the ITS data only. A third classifier, IDTAXA, employs machine learning to reduce over-classification errors to obtain a higher accuracy (Murali et al. 2018). Taxonomic assignment was carried out separately on class, order, genus, and species level. A minimum threshold of 70% confidence for at least one of the classifiers was set, below which the OTUs were considered as "unclassified", together with other sequences that were identified with high confidence against database entries labelled as "unclassified", "unidentified" or "*incertae sedis*". Then, for the remaining identifications, the confidence values were averaged (average of three values for ITS2 and two for LSU D1-D2 data). When identifications disagreed among the classifiers, the one with the highest confidence value was selected, although this could give preference to over-confident classifiers, i.e., RDP (2018). Taxonomic composition of

samples was presented as the number of OTUs assigned to a given taxonomic level in a barplot created with *ggplot2* in Rstudio (Wickham 2016) and was used for the ecological analysis. In addition, in a more detailed study of OTU assignments in the ecologically important class Sordariomycetes, the identification provided by the three classifiers was compared to their position in a phylogenetic tree (see below).

The Sordariomycetes subset was also used to test the effect of variable sequence similarity thresholds on the classification, by generating OTUs under clustering at 97%, 98%, and 99% similarity and comparing the taxonomic assignments, using the RDP classifier (Warcup 2 and Fungal 11 training sets for ITS2 and LSU D1-D2, respectively) (Deshpande et al. 2016). All OTUs with a confidence of assignment > 70% to class Sordariomycetes were retained. Order-level assignments (the Sordariomycetes are split into 28 orders) with a confidence > 50% were taxonomised, while all others were kept as "unclassified Sordariomycetes". To assess the effects of differing clustering thresholds on downstream taxonomic assignment, OTUs at each clustering threshold were also closed-reference clustered (i.e., only retaining sequences with hits in the reference set) against the composite LSU/ITS reference sequences used to construct the tree (Edgar 2010; Rognes et al. 2016).

Alignment and tree building in Sordariomycetes

Reference sequences for the class Sordariomycetes were downloaded from Genbank, querying the database for various permutations of the gene names for the rRNA cluster composed of SSU, LSU and ITS, separately for each target fungal order. Only sequences that were complete for at least 2/3 of the rRNA operon were chosen (full list of accessions in Suppl. material 5: Table S1). 80% of species in this reference set were complete for all three regions. ITS2 reference sequences were processed through ITSx to eliminate redundancy in the concatenated alignment (Bengtsson-Palme et al. 2013).The subsequent steps were carried out separately for each OTU set at 97%, 98% and 99% clustering thresholds. The reference sequences and OTU representative sequences were aligned using MUSCLE (Edgar 2004) under default settings and the aligned matrices were concatenated. The concatenated three-region alignment (SSU, LSU, ITS1-2) was then inspected in Mesquite (Maddison and Maddison 2021) and Geneious Prime (v. 2020.0.4) and problematic accession sequences were removed. This alignment is available on TreeBase (www.treebase.org accession number S28904). The alignment was then partitioned for each marker region, and the best model for each partition was selected according to BIC values. Model testing, tree building, and ultrafast bootstrap approximation (n = 1000) were performed in IQ-Tree2 (Chernomor et al. 2016). Tree visualisation was improved using iTOL v. 6.5 (Letunic and Bork 2007).

Phylogenetic diversity metrics

Phylogenetic distribution of ITS2 and LSU D1-D2 copies was assessed by metrics of clustering and over-dispersion originally developed for community ecology (Webb

et al. 2008). In the ideal case of capturing the same species with both markers, copies of ITS2 and LSU D1-D2 corresponding to the same species should be in close vicinity on the tree, i.e., the copies of each marker should be 'over-dispersed' (more dispersed than a random phylogenetic structure). Deviations from this pattern can be assessed with the metrics calculating the Mean Pairwise Distances (MPD) and Mean Nearest Taxon Distances (MNTD) of each set (ITS2 and LSU D1-D2). We report standardised values as the net relatedness index (NRI) and nearest taxon index (NTI) relative to null models of randomly distributed communities. Positive NRI and NTI scores indicate phylogenetic clustering, negative values indicate phylogenetic over-dispersion, while random phylogenetic structure results in values not significantly different from zero (Webb et al. 2008). Calculations were performed with the *R* packages *picante*, *ape*, and *phylomeasures* (Webb et al. 2008; Tsirogiannis and Sandel 2016; Paradis and Schliep 2019).

Assessment of species richness and community composition

Community ecological analyses were carried out on samples rarefied to 1000 reads, which was sufficient for generating largely complete OTU sets as judged by species accumulation curves (Suppl. material 2: Fig. S2). Species accumulation curves were built with the *specaccum* function of the *vegan* package (Oksanen et al. 2013). An OTU table and species classification was generated for fungal communities separately from ITS2 and LSU D1-D2 sequencing, after singletons and doubletons were removed. For the OTU table, the 97% threshold was selected because it is the most generally applied in fungal studies (Nilsson et al. 2008). Fungal OTU richness among samples was assessed with a Generalised Linear Model (GLM) built with the *lme4* package (Bates et al. 2015), with fungal OTU richness as a response variable and beetle species and forest type as dependent variables. The Negative Binomial model was chosen, as it is suitable for overdispersed data. A post hoc pairwise comparison (Tukey HSD test at the 95% significance level) was carried out to compare the means among the distinct factors.

The Jaccard index was used to calculate beta-diversity between sample pairs based on OTU presence-absence data (richness) (*betapart* R package; Baselga and Orme 2012). The variation was visualised using Nonmetric Multidimensional Scaling (NMDS) (*metaMDS* function of the vegan package; Oksanen et al. 2013). To evaluate the stringency of association of fungal OTUs with tree species and beetle hosts for each assembly, a multilevel pattern analysis was carried out by calculating Pearson's phi coefficient of association ("p.g") (Chytrý et al. 2002) between sample pairs, correcting this index to account for the differences in specimen numbers among the compared groups (function *multipatt* of the *indicspecies R* package; (De Cáceres et al. 2011). OTUs for which the association values were significant were displayed as a heatmap (*aheatmap* function, NMF *R* package (Gaujoux and Seoighe 2010).

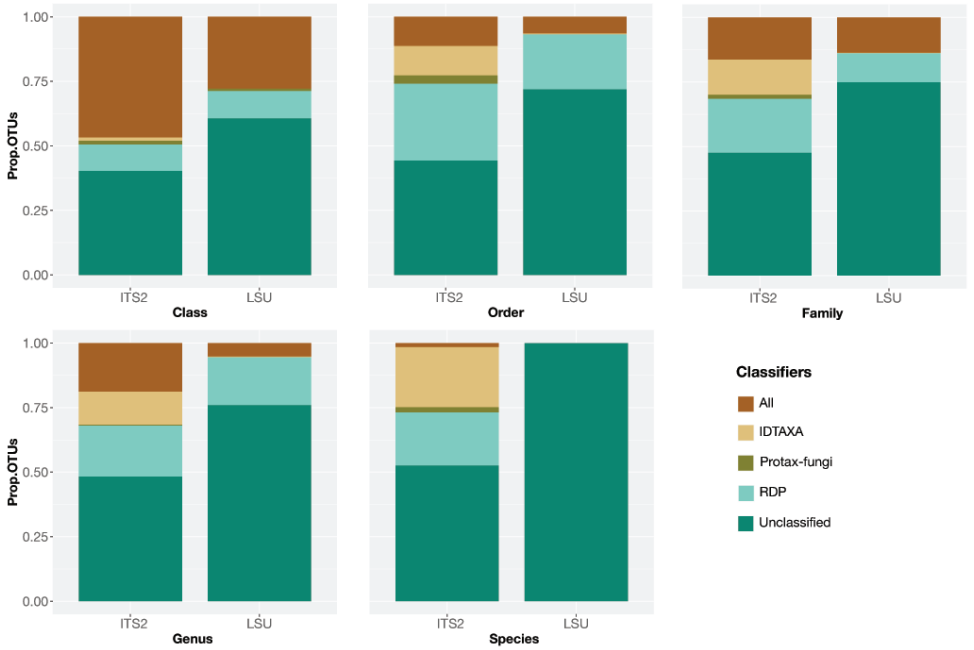

Figure 1. The proportion of fungi classified with IDTAXA, Protax-fungi and RDP from class to species level. "All" refers to the proportion of OTUs for which the three classifiers agreed in their classification.

Results

Composition of fungal communities from ITS and LSU markers

Sequencing of 80 libraries produced 2,436,075 quality-filtered, merged reads for ITS2 and 1,742,119 reads for LSU D1-D2, which resulted in 1157 OTUs from ITS2 and 548 OTUs from LSU D1-D2 after bioinformatics filtering and clustering at 97% threshold (1546 and 632 OTUs if singleton and doubleton reads were retained and without applying rarefaction on each library). Identifications of OTUs at ≥ 70% confidence level obtained with IDTAXA, Protax-fungi and RDP were higher for ITS2 than for LSU D1-D2 at all hierarchical levels from class to order, family, genus and species level (Fig. 1). However, the fraction of OTUs identified by one or multiple identifiers never exceeded 61.5% for ITS2 and 41.5% for LSU D1-D2 of the total OTUs. Identifications dropped consistently from class to species level, and with each hierarchical level an increasing proportion of identifications was due to a single classifier only, indicating the growing uncertainty of taxonomic assignments. A classification at species-level was generally not possible for LSU because of the limitations of the databases, which generally provide a taxonomy string to genus level only and nearly 100% of the OTUs remained unidentified at this level. Nearly 50% of the ITS2 OTUs were identified to species level but in almost all cases only a single classifier produced these assignments (Fig. 1).

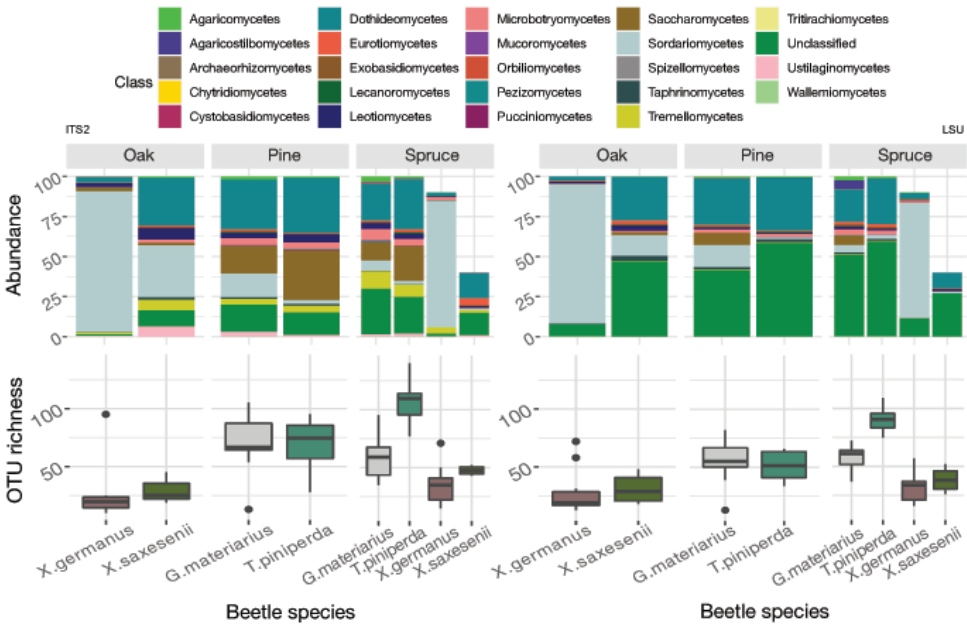

Figure 2. Top panel: The proportion of OTUs identified as members of a fungal Class determined by the ITS2 and LSU D1-D2 regions. For the spruce forest, only nine *X. germanus* and four *X. saxesenii* specimens were retained after rarefaction. Lower panel: The number of fungal OTUs per beetle specimen, separate for each beetle species and forest type, for ITS2 and LSU.

Libraries from 73 beetle specimens remained after rarefaction and harboured a total of 1180 OTUs for ITS2 and 553 OTUs for LSU D1-D2. Using taxonomic classifiers, OTUs were assigned to 24 classes, 66 orders, 129 families and 369 genera. Identification at class level revealed the presence of 23 classes for ITS2 and 17 classes for LSU. The dominant classes were Dothideomycetes for ITS2 and Sordariomycetes for LSU D1-D2 (Fig. 2, Suppl. material 6: Table S2). ITS2 produced twice as many identified OTUs compared to LSU D1-D2, and in the classes Leotiomycetes and Tremellomycetes more than five times as many, due to the greater total number of OTUs and the higher proportion being fully identified. ITS2 metabarcoding also detected seven fungal classes not retrieved with the LSU D1-D2 primers (Archaeorhizomycetes, Chytridiomycetes, Mucoromycetes, Orbiliomycetes, Spizellomycetes, Tritirachiomycetes and Ustilaginomycetes), while LSU D1-D2 metabarcoding recovered only one class not obtained with the ITS2 primers (Atractiellomycetes). Only for the Sordariomycetes and Agaricomycetes the proportion of OTUs detected with LSU D1-D2 was higher than with the ITS2 marker.

Comparison of the ITS and LSU markers in ecological analyses

Fungal communities obtained with either marker were compared with regard to total richness and differentiation across beetle species and forest type. For both markers,

species accumulation curves displayed a similar shape, despite the roughly twice higher OTU number in ITS2, with a slow increase and not reaching a plateau, although LSU D1-D2 generally showed a more pronounced 'shoulder' indicating a fraction of OTUs that is encountered commonly in multiple samples. Across the different forest types, species accumulation in oak forest clearly lagged pine and spruce forests (fewer total species, slower accumulation) in both markers (Suppl. material 2: Fig. S2).

Richness in a single-beetle extract ranged from 9 to 140 fungal OTUs (average 56 ± 32.34) in ITS2 and from 11 to 109 fungal OTUs (average 48 ± 24.27) in LSU D1-D2 (Fig. 2). Despite some scatter among individual beetles, the number of OTUs per sample differed in a characteristic way between beetle species and forest types, and these differences were closely correlated in ITS2 and LSU D1-D2, indicating that both markers detected a similar set of fungal species (beyond the classes unique to each marker, which only make a small contribution to overall species richness and relative abundances). This correlation was also evident at specimen level in the two outliers in each of the libraries corresponding to the same beetle individual. The variation in species richness explained by forest type and beetle species was broadly similar in ITS2 and LSU D1-D2 derived fungal communities (Table 2), although the LSU data attributed a greater proportion of the variation to the forest type alone (27.47% compared to 18.75% from ITS2), while the reverse was true for ITS2. Community composition analysed with both markers had around 8% of the variation explained by the interaction of beetle species and forest types. NMDS plots on the OTU composition revealed a very similar pattern of community separation of the three forest types in ITS2 and LSU (Fig. 3).

The *indval* function revealed significant levels of association with the tree species and or the beetle species for 50 and 60 OTUs, respectively, from the ITS2 and LSU

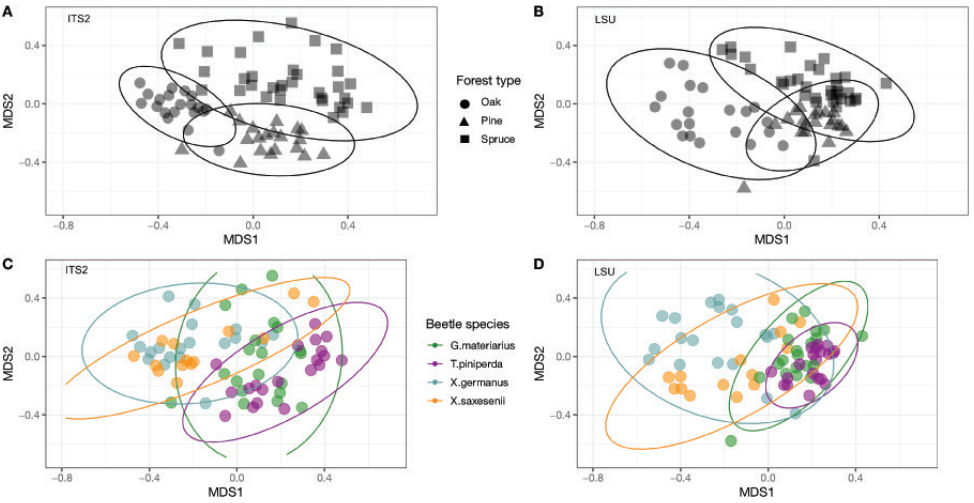

Figure 3. NMDS ordination plot of all specimens sampled with ITS2 and LSU D1-D2, based on the fungal community composition of the individual beetles. Shapes represent forest types and colours represent beetle species. Stress for this graph fell within acceptable ranges (<0.2).

Table 2. Correlation of species richness with beetle species and forest type. The table shows the result of a GLM analysis showing the percentage of explained variance for each predictor with the F parameter and significance level.

Factor	Explained variance		$F_{x,y}$		p	
	ITS2	LSU	ITS2	LSU	ITS2	LSU
Beetle + forest type	8.46%	7.58%	$F_{6, 65} = 2.809$	$F_{6, 65} = 3.521$	<0.1 *	<0.05 *
Beetle	27.07%	18.25%	$F_{3, 69} = 30.265$	$F_{3, 69} = 29.888$	<0.001 ***	<0.001 ***
Forest type	18.75%	27.47%	$F_{2, 67} = 6.772$	$F_{2, 67} = 5.236$	<0.01 **	<0.01 **
Unexplained	45.72%	46.68 %				

D1-D2 regions. Many OTUs showed positive associations with pine and spruce, but much fewer with oak. Regarding the associations with beetle species, many OTUs had positive associations with *T. piniperda*, and to some extent with *G. materiarius*, whereas positive associations with *Xs. germanus* and *Xb. saxesenii* were limited to a small number of oak associated OTUs. Most other associations in these species were negative; e.g., the pine/spruce associated OTUs were absent, despite the fact that both beetle species were also sampled from spruce. General patterns of OTU associations and non-associations were similar for the two xyleborine species, and they were quite similar to those associated with oak. In contrast, association patterns in *T. piniperda* and *G. materiarius* were similar to pine and spruce (Fig. 4). The similarity in these association patterns differed only slightly between the ITS2 and LSU-based OTUs (Fig. 4), even though the OTUs themselves could not be linked up between the two markers, as they mostly were not identified to species level, or the identifications did not overlap between the two marker sets.

OTU identifications across markers using phylogenetics

A phylogenetic approach was used to associate ITS-based and LSU-based OTUs with each other, focusing on the class Sordariomycetes that includes the Ophiostomatales of important tree pathogens for which ITS efficiency has been questioned (Skelton et al. 2019; Hulcr et al. 2020). OTUs were clustered at minimum similarity thresholds of 97, 98 and 99%, which resulted in between 120–150 OTUs for ITS2 and 80–120 OTUs for LSU D1-D2 classified as Sordariomycetes using the RDP classifier at > 80% confidence (Table 3). The most similar values for the number of OTUs were obtained at 98% and 99% thresholds for ITS2 and LSU D1-D2 (Table 3). As each species should produce one ITS and one LSU sequence, we used these as the preferred threshold values in further analyses. These conditions were used because they generated a similar number of OTUs for each marker (Table 3), and thus potentially represent a similar set of species.

OTU sequences from both markers were included in a phylogenetic analysis together with publicly available full-length sequences covering the full or most of the rRNA cluster, including the ITS2 and LSU D1-D2 regions, with the SSU gene also present in most accessions. These sequences served as a scaffold to represent the major

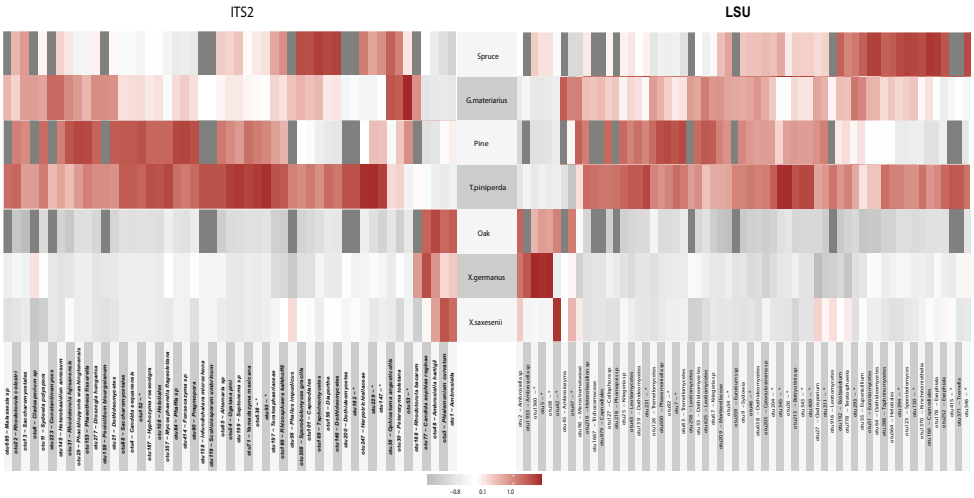

Figure 4. Heatmap using Pearson's correlation coefficient between the OTUs generated from the ITS2 and LSU D1-D2 metabarcodes and the analysed beetle species and forest types. Rectangles indicate the strength of association between an OTU and beetle/forest (strongly negative, grey, to strongly positive, red). Fungal OTUs (on the horizontal axis) were classified to genus or species level where possible; they are shown in random order and cannot be linked taxonomically between both markers.

Table 3. Sequence numbers and phylogenetic dispersion in Sordariomycetes OTUs under different threshold values. The table presents the Net relatedness index (NRI), nearest taxon index (NTI), and the number of OTUs recovered for ITS2 and LSU D1-D2. "Mixed" refers to a clustering threshold of 99% for LSU D1-D2 and 98% for ITS2. Reference sequences were included when building the trees used, though pruned (leaving only OTUs in the tree) for the above calculations. Positive NRI and NTI scores indicate phylogenetic clustering of either ITS and LSU sequences (indicating different species sets were sequenced), negative values indicate phylogenetic over-dispersions of ITS and LSU with respect to each other (indicating the same species was sequenced for the two markers).

	ITS2				LSU			
	97%	**98%**	**99%**	**Mixed**	**97%**	**98%**	**99%**	**Mixed**
NRI	-0,111	-0,805	1,497	-0,122	1,328	0,697	-2,55	-0,653
NTI	-1,212	-3,81	-2,386	-2,277	1,367	0,882	-0,183	-1,343
OTU count	138	144	158	144	80	102	150	150

orders of Sordariomycetes (full list of accessions in Suppl. material 5: Table S1), to which the OTU sequences were added. ML trees for the combined three-region reference alignment and OTUs from metabarcoding resolved relationships at the base of the tree similarly to those found in the literature (Zhang et al. 2006; Hongsanan et al. 2017) (Suppl. material 3: Fig. S3). All orders were monophyletic, given the taxonomic assignment of the reference sequences in their Genbank accessions. The positions of OTUs on this tree were then used to provide a taxonomic assignment at the level of orders. This was achieved by determining the node representing the hypothetical ancestor of all reference sequences representing an order (based on their Genbank taxonomy), and OTUs descended from this ancestor were assigned to the same order. OTUs placed on

branches outside of these clades were considered 'unassigned'. By using this approach, 254 of the 294 OTUs were placed into clades defined by the reference sequences, thus determining their identity at order level. This number compared to 212 OTUs classified by RDP, 150 OTUs by IDTAXA (141) and 31 OTUs by Protax-fungi (ITS only). Out of these, 8, 9 and 3 OTUs were misclassified by the three classifiers, respectively. The few cases of disagreement of the phylogenetic analysis with the classifiers affected mainly OTUs that showed discrepancies of assignments between the classifiers.

OTUs obtained from ITS2 and LSU D1-D2 were widely distributed on this tree, and across most orders, both types of sequences were interleaved, showing that overall community diversity at the order level could equally be inferred using either region (Suppl. material 2: Fig. S2). Order-level subsets of trees for these orders showed the placement of ITS2 and LSU sequence fragments relative to the reference set (Fig. 6A, B). If both sequences are derived from the same genomic template in the metabarcoding amplification they were expected to be represented by one OTU representative sequence for each marker, and these sequences to fall in proximity on the tree, taking the same phylogenetic position relative to the nearest full-length reference sequence (Fig. 6, species D). We found 15 instances where one ITS and one LSU barcode were in close proximity together with a reference sequence (84 reference species in total), potentially representing the same species. In an additional six instances, one or both barcodes formed a cluster on zero-length branches when matched to full-length rRNA reference sequences, i.e., representing an exact match to an existing database entry, but missing the other type of barcodes.

Closed-reference clustering against the reference dataset to each order within Sordariomycetes by the RDP classifier revealed species-level matches for both ITS2 and LSU sequences (Fig. 7A). Notably, four species had matches to both markers, i.e., the same species were amplified. In addition, one ITS2 sequence produced a hit not reciprocated in LSU. Vice versa, LSU sequences produced hits to a minimum of eight additional species not seen in ITS, which was increased to 11 and 17 species under the higher 98 and 99% threshold values, respectively, as the trees became increasingly populated with the additional taxa from splitting of larger OTUs (Fig. 7B). Under these lower threshold values closely related sequences apparently were less affected by 'lumping', which obscured the true diversity in the sequencing mixture.

Where closely related reference sequences were missing, ITS2 and LSU sequences may be matched based on their phylogenetic proximity, but the ITS2 and LSU sequences obtained from a single genome may not appear as sister taxa because the gene sequences are non-overlapping and thus lack characters that could group them. We tested the degree to which ITS2 and LSU sequences interleave on the tree, by assessing phylogenetic clustering and dispersion with the NRI and NTI (Table 3). For ITS2, most values were negative, indicating over-dispersion relative to the LSU sequences as expected if both markers pick up the same or closely related species. The exception was for the 99% similarity value, which produced positive NRI (clustering) possibly from selective over-splitting of OTUs that was not matched in the less variable LSU sequences. For LSU there was a progression from positive (clustering) at 97% similar-

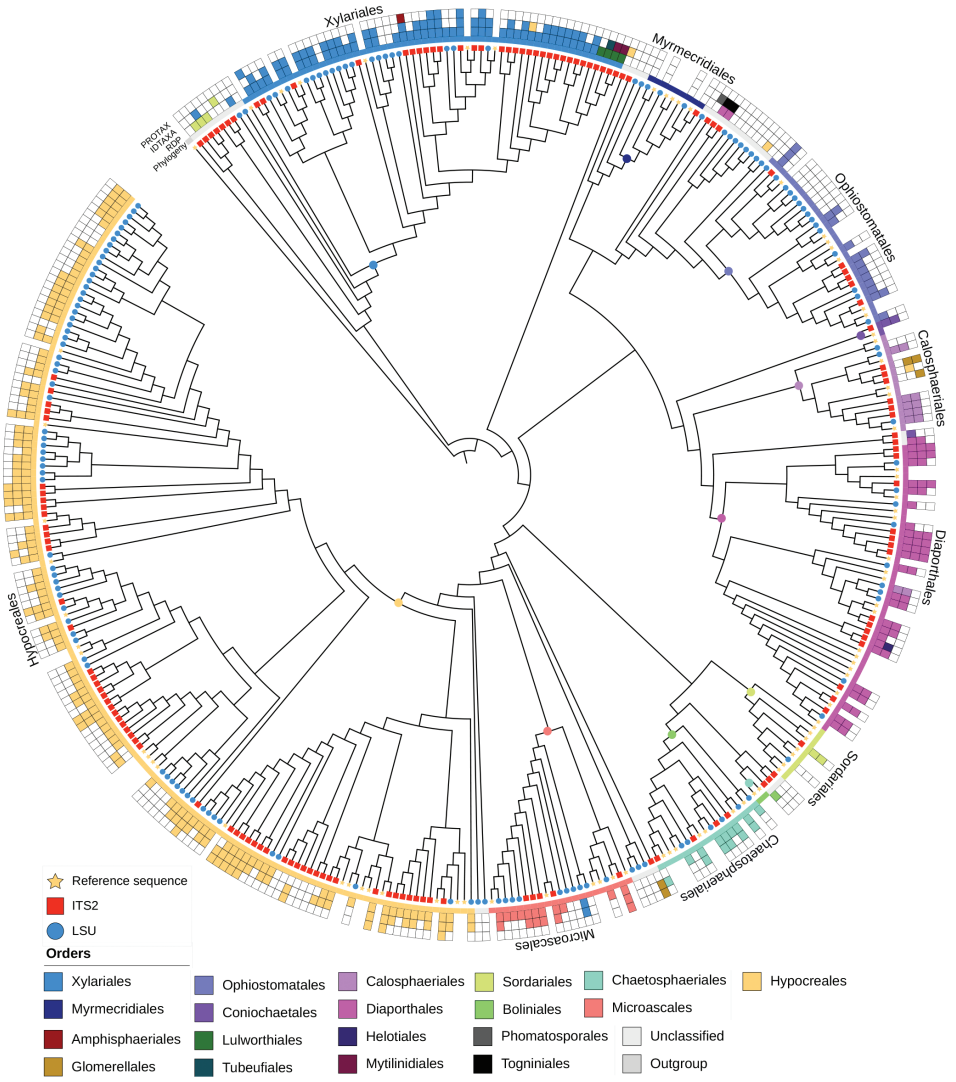

Figure 5. ML tree of Sordariomycetes constructed from the reference sequence alignments and OTUs for both markers (clustering thresholds: 98% ITS2, 99% LSU D1-D2). *Leotia lubrica* (Leotiomycetes) was specified as the outgroup. The assignment of OTUs by each of the three classifiers (RDP, IDTAXA, Protax-fungi) is shown by coloured boxes. Terminals missing these boxes are the reference sequences. Coloured dots on the nodes of the tree indicate the hypothetical ancestor defining monophyletic groups corresponding to the various orders of Sordariomycetes. The extent of each order is indicated by the coloured inner ring. Note that the ancestor of an order is defined by the youngest node from which all reference sequences are descended; OTUs falling outside of the resulting clades appear as 'unassigned' by the phylogenetic analysis approach. The distribution of ITS2 (red squares) and LSU D1-D2 (blue bullets) relative to the reference set (yellow stars) on each of the tips of the tree. Note the limited presence of ITS sequences in the Ophiostomatales (in top right quadrant).

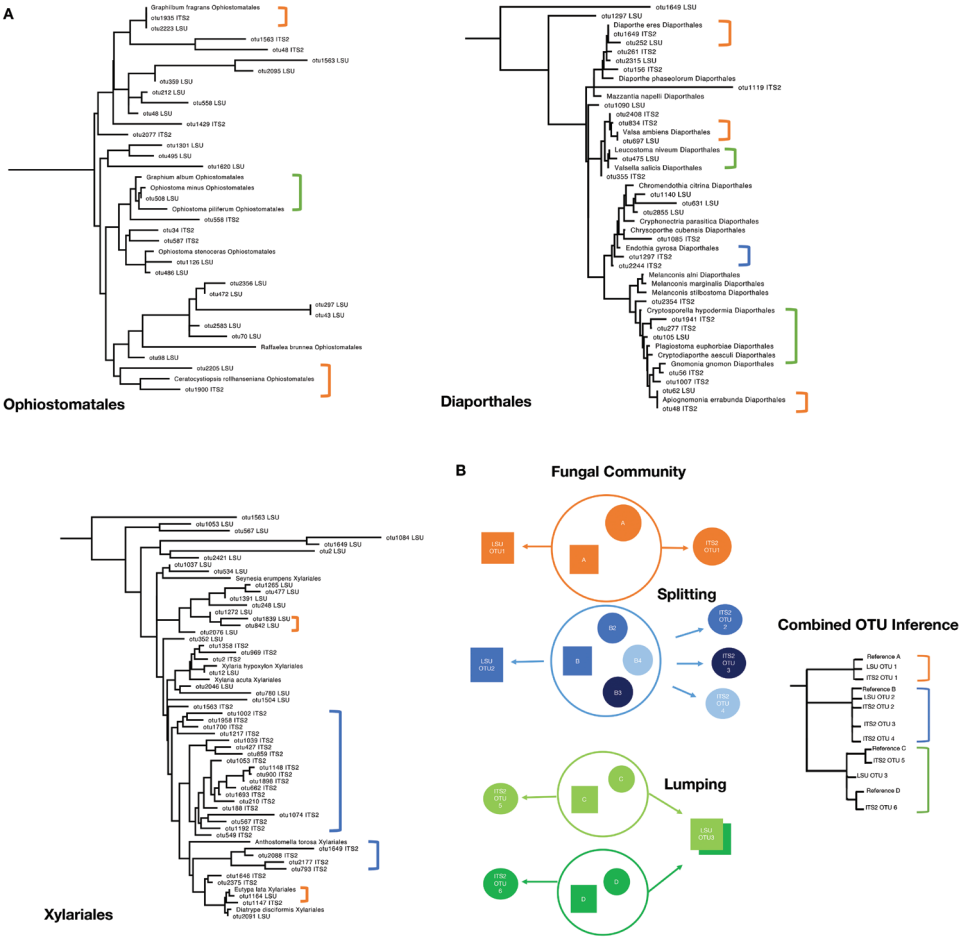

Figure 6. Order-level trees and splitting/lumping of OTUs at clustering **A** order-level ML trees with mixed OTU clustering thresholds (99% LSU D1-D2, 98% ITS2). Full tree in supplementary materials. *Leotia lubrica* was used as the outgroup (not pictured). Brackets indicate reference taxa linked to an ITS2 and/or LSU OTU, with colours indicating potential splitting/lumping (blue, splitting; green, lumping; orange, 1:1) **B** diagram illustrating the effects of splitting and lumping of an OTU in the fungal community on the tree inference. Four hypothetical species (A to D) in a community are treated under uniform clustering thresholds for ITS2 and LSU. This may result in deviation from the 1:1 ratio of OTUs expected if each species in the community is represented equally by both markers (species A). Threshold values may be too high, resulting in splitting of species into multiples OTUs, which is likely to affect the more variable ITS2 region (species B) or may be too low, resulting in lumping of multiple species into a single OTU, likely to affect the conservative LSU region (species C and D).

ity to negative (indicating over-dispersion) at 99% similarity, which coincided with a near doubling in the number of OTUs (against only a small increase in the ITS2 data) (Table 3). This indicated that OTUs newly formed by splitting were not clustered on the tree, unlike the ITS2-derived OTUs, but instead were interleaved with the ITS2

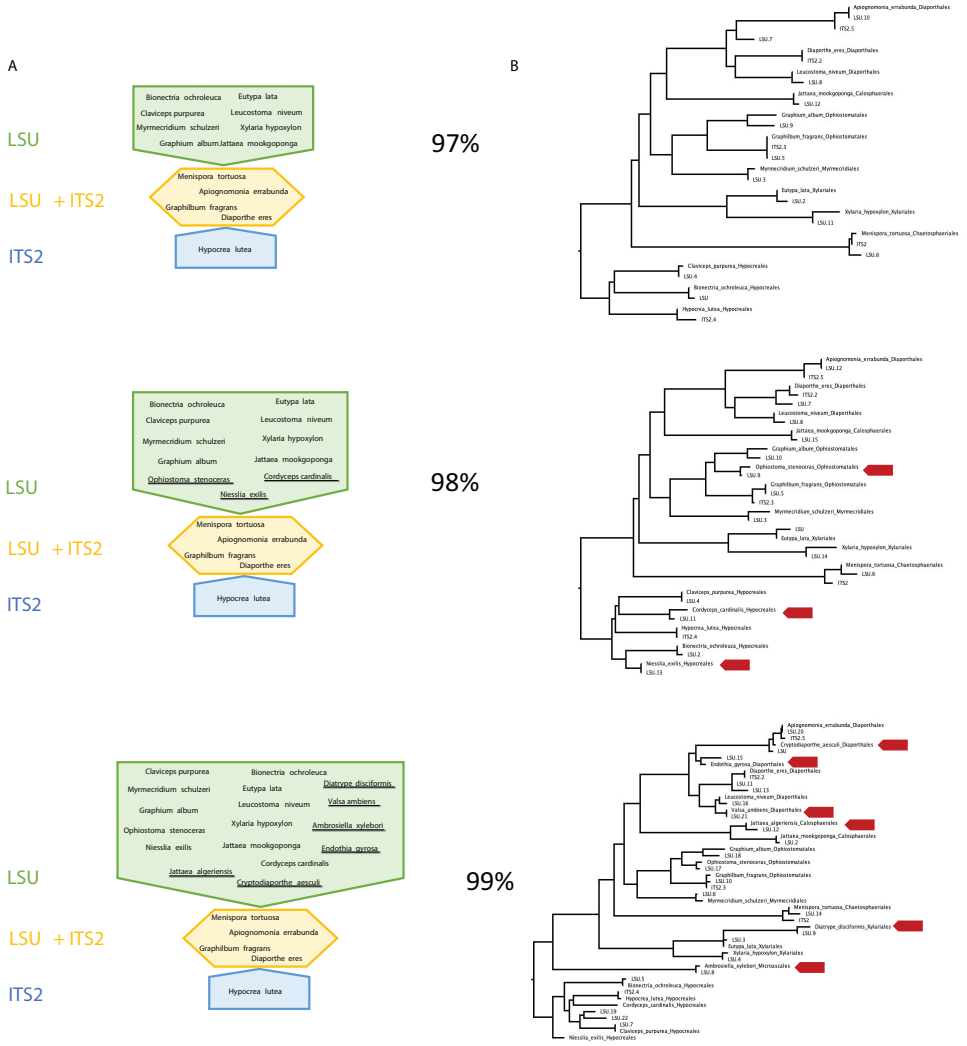

Figure 7. Closed reference clustering of OTUs and phylogenetic trees at different thresholds **A** results from the closed reference clustering of OTUs at each clustering threshold against composite LSU/ITS2 reference sequences. LSU matches in green, ITS2 matches in blue, linked matches (for which both an ITS2 and LSU OTU were matched to a reference sequence of the same species) in yellow. Underlined taxa indicate new matches at each clustering threshold **B** phylogenetic tree of LSU OTUs under increasingly stringent clustering thresholds, with arrows marking newly added taxa as threshold values are increased.

sequences, indicating more complete representation of species already on the tree based on their ITS2 sequences. The 'mixed' threshold value of 98% for ITS2 and 99% for LSU presented slightly negative NRI/NTI values for both markers (Table 3).

The detailed observations were confirmed by the global classification of OTUs at order level, which showed an increase in the proportion of identified OTUs with increasing threshold value for LSU, but not ITS2 (Fig. 8). Both markers produced

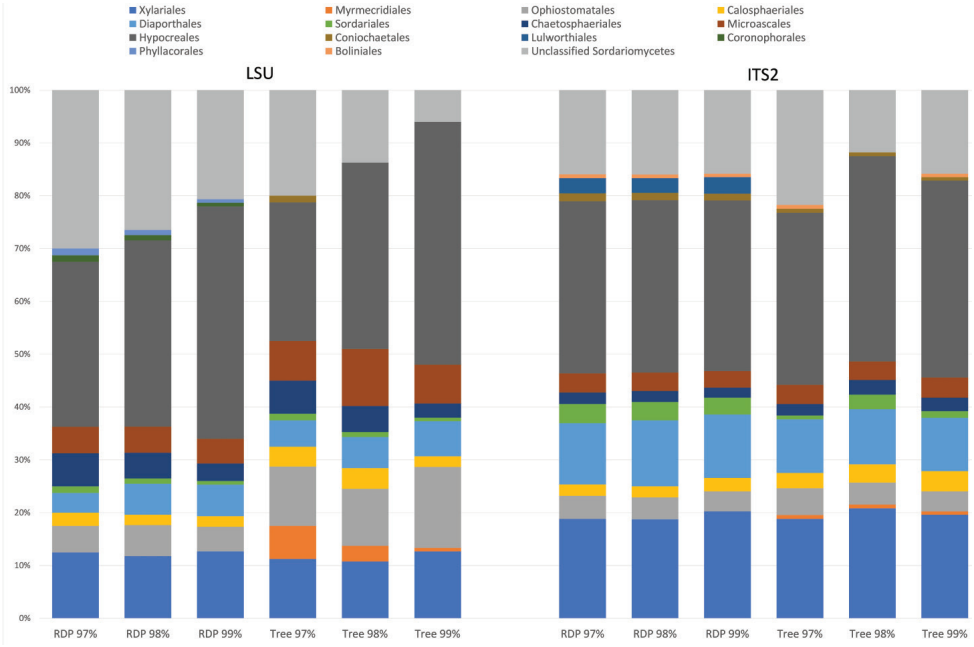

Figure 8. Proportion of OTUs assigned to each Order from metabarcoding with LSU (left panel) and ITS (right panel) markers based on the RDP classifier and the phylogenetic tree, under increasing threshold values.

broadly similar proportions of the four dominant orders, Xylariales, Ophiostomatales, Diaporthales and Hypocreales, but differed to various degrees in the assignment of the 'small' orders. It was also evident that OTU numbers in Ophiostomatales were comparatively lower in ITS2, as also suggested from the phylogenetic tree (Fig. 5). This is likely explained by the fact that the ITS2 forward primer binding site in this group differs from the consensus (Tedersoo et al. 2015b; also see Suppl. material 4: Fig. S4).

Discussion

Metabarcoding has revolutionised the study of fungal communities, revealing the huge proportion of hitherto unobserved species, including the unexpectedly high diversity of fungi associated with bark beetles (Miller et al. 2016; Hulcr et al. 2020; Větrovský et al. 2020). However, these inferences are based on short sequences and lack the biological information of conventional studies using fungal cultures. Independent corroboration of species limits is needed, and principally can be achieved by using multiple markers that each define the same entities (e.g. DeSalle et al. 2005). The test of phylogenetic congruence in metabarcoding data is complicated because the amplicons come from complex mixtures of species, which does not allow to establish genetic linkage (phasing) across the two markers, despite the proximity of the ITS2 and LSU D1-D2

regions in the genome. Instead, an indirect approach had to be used that identifies the amplicons of ITS2 and LSU separately relative to full-length reference sequences comprising the entire rRNA cistron.

We assessed the congruence of signal from ITS and LSU metabarcoding for the characterisation of fungal communities, by (1) comparing the ecological associations at various taxonomic levels as established with either marker (for the entire fungal set), and (2) testing the species-level correspondence of OTUs from both markers based on their phylogenetic positions (for the class Sordariomycetes only). As we showed in both cases, OTU identification is challenging and depends on the available reference databases, as well as the specific strategy for linking the metabarcode sequences into the taxonomic system. Taxonomic classifiers are now widely used and are becoming increasingly sophisticated. However, placement was possible mostly to higher taxonomic levels only (Fig. 1), in line with existing studies (Richardson et al. 2017). Just a small proportion of reads could be identified to genus or species, usually only with one of the three classifiers, while the LSU marker is not even annotated to species level in the RDP fungal training set. These difficulties in identifying species compromised the comparison of community composition obtained with either marker, as virtually none of the OTUs encountered in each set were labelled with the same Linnaean binomial (Suppl. material 3: Fig. S3).

In contrast, simple counts of OTU numbers (a proxy of species richness) produced a good correlation between both markers in several key parameters describing the community composition. First, the numbers of OTUs and the higher-level composition of fungal communities obtained from each treatment (beetle species, forest type) assessed with the ITS2 and LSU D1-D2 data closely mirror each other (Fig. 2). This also holds for the composition of orders within the class Sordariomycetes (Fig. 8). Equally, the proportions of explained OTU diversity by beetle species, forest type and beetle × forest interactions were remarkably similar between both markers, even if the absolute number of OTUs was much lower in LSU D1-D2 (Table 2). For both markers, communities from different forest types and beetle species occupy similar portions of the multivariate space (Fig. 3). Finally, the broad patterns of individual OTU associations in the *indval* analysis show similar affinities with the beetle species and tree type (Fig. 4), even if the correspondences of species between ITS2 and LSU D1-D2 datasets could not be determined. All these findings point to a high level of congruence between both markers and provide justification for the widely used approach of fungal community analysis using metabarcoding with either marker, based on higher level classification and read abundances. The utility of read abundance in these analyses is particularly remarkable given the frequently raised concern about skew in the number of reads in the PCR (Bálint et al. 2016; Krehenwinkel et al. 2017). Thus, even a single metabarcode marker can safely represent the broad ecological trends determining fungal communities, as previously found in studies addressing a wide range of ecological questions (Tedersoo et al. 2015b; George et al. 2019; Nilsson et al. 2019; Furneaux et al. 2021).

Yet, the difficulty of linking these metabarcoding sequences across multiple markers leaves some uncertainty about the biological relevance of the community data, which still may represent different species within the major taxonomic groups recovered by

either ITS2 and LSU D1-D2, as already suggested for the Ophiostomatales (Hulcr et al. 2020). Thus, ultimately, the metabarcoding approach may fall short of linking any particular fungal species to a beetle, unlike the conventional approaches of culturing particular isolates that reveal the specific symbioses. Phylogenetic analysis of individual sequences can improve the precision of identification with both markers individually and relative to each other, beyond the assignment to a broad taxonomic group, and thus link the corresponding reads representing a given species from either marker (Fig. 6D).

As illustrated for the Sordariomycetes, we found that OTU assignments obtained by taxonomic classifiers are broadly in agreement with the phylogenetic analysis. The backbone of the phylogenetic tree from the full-length rRNA reference sequences recovered each order of the Sordariomycetes as monophyletic (Fig. 5, Suppl. material 3: Fig. S3). OTUs placed on this tree can then be scored for membership in clades defined by the reference sequences. The RDP classifications and tree-based assignments were largely in agreement regarding the species composition at order-level, although generally the trees assigned a greater proportion of OTUs, reaching nearly 95%. When placed on the tree, the order level assignments were consistent with the identifications obtained by the classifiers, and disagreements mainly affected cases where only one of the classifiers disagreed or the alternative identifications differed between classifiers (Fig. 5). This observation suggests low confidence in the conflicting identifications, as also indicated by the average confidence scores from the RDP classifier that varied between orders, with LSU assignments having low confidence overall (see Suppl. material 7: Table S3). Many OTUs were not identified beyond the class level by the classifier, despite clear placement in the tree. The order Myrmecridiales was missing entirely from the classifier results, despite the presence of several OTUs placed clearly within the order and OTUs matching *Myrmecridium schulzeri* found in the closed-reference clustering at all three thresholds (Fig. 7A, B). The comparison with formal phylogenetic analyses thus highlights the limitations of classifiers that are dependent on reference databases and probabilistic *k-mer* matching, given the limited sequence length of metabarcoding reads (Wang et al. 2007; Porras-Alfaro et al. 2014; Bacci et al. 2015; Xue et al. 2019).

Second, we used the phylogenetic analysis to determine if both markers reveal the same species-level entities. Under ideal circumstances, each species is represented by exactly one sequence each of LSU and ITS, and these two sequences from both markers find themselves in the same position of the tree. As both markers are non-overlapping, they only can be placed relative to full-length reference sequences rather than to each other, and therefore if 1:1 represented for each species, sequences of ITS and LSU should be uniformly interleaved on the tree (Fig. 6D). However, if similarity thresholds are too low (incorrectly lumping of species) or too high (splitting of species) in one or both of these loci, deviations from the uniform distribution occur. Overall, the increase of the similarity threshold had a greater impact on the LSU D1-D2 than ITS2, almost doubling in numbers of recognised OTUs versus a small increase only (Table 3), and parity of OTUs in both markers was greatest at a 'mixed' threshold of 99% for LSU D1-D2 and 98% for ITS2. While simplistic, the logic of this analysis is straightforward and the results could be improved with greater density of reference sequences. Using the NRI/NTI framework under these OTU thresholds (Table 3), 'communities' of LSU and ITS2

sequences show over-dispersion, as expected for the 1:1 correspondence of each marker. The 99% threshold for LSU is also supported by the greater matches in the closed-reference clustering (Fig. 7). Because of the similarities in OTU counts and because of the NRI/NTI values indicating moderate levels of over-dispersion, we consider the 98/99% threshold mixed strategy as the best estimate of the OTU diversity in each marker. Thus, proximity on the tree is taken to indicate that the respective ITS2 and LSU sequences are derived from the same genomic template, or at least from closely related strains present in a community. Frequently this was corroborated by the fact that these closely related ITS2 and LSU sequences were obtained from the same specimen sample (not shown).

There are uncertainties associated with this inference. Across fungal species, intraspecific ITS variability varies considerably, highlighting the challenges and inevitable shortcomings resulting from the selection of a uniform OTU clustering threshold (Nilsson et al. 2008). For example, while a 97% clustering threshold is generally accepted and widely used in environmental sequencing studies (Kõljalg et al. 2013; Tedersoo et al. 2015b), other studies from sequencing of well-defined strains from culture collections have suggested a much higher optimal threshold of > 99.6% similarity (Vu et al. 2019). However, with the use of long-read technology the full extent of intraspecific and intragenomic variability is becoming evident. For example, in *Xylaria hypoxylon* more than a dozen copies of the rRNA cistron were detected in a single genome, with ITS sequence divergences ranging from 96.9–99.8% (Stadler et al. 2020). Although intra-genomic variation in other species of Xylariales was lower, this case demonstrates the difficulty of splitting vs. lumping in the analysis of both markers. Thus, the higher number of ITS2 OTUs in Xylariales compared to LSU OTUs from the same communities (Fig. 6) may be the result of over-splitting of distantly related copies of ITS2 present in a single genome (Nilsson et al. 2008; Stadler et al. 2020). Yet, even if the clustering is not a correct reflection of intra-genomic and intra-specific variation, the placement of sequences representing the OTUs can link close relatives across different markers. For greatest success, densely sampled reference sequences spanning both markers are required, but as shown for the Sordariomycetes, even an incomplete set can provide the scaffold for placing non-overlapping sequences, and in several instances the idealised placement of OTUs and reference sequences was found, in some cases across all clustering thresholds (Fig. 5), while uncertainties remain where reference sequences are distant. Matching of ITS2 and LSU sequences was even possible in the Ophiostomatales, despite the deviation in the ITS2 primer binding site in this group (Tedersoo et al. 2015b; Suppl. Fig. S4), as the bias against the amplification presumably is overcome by permissive PCR conditions, and similar effects can be expected in other groups where such sequence variation may exist, e.g. in a clade of Hypocreales composed entirely of LSU sequences, although this is an exception in the taxonomically broad set of fungal lineages used here.

Conclusion

We addressed the problem of marker choice in fungal metabarcoding for the study of biodiversity patterns and taxonomic identifications. Community-level diversity

metrics showed high consistency of results from metabarcoding with both the ITS2 and LSU D1-D2 regions, using OTU clustering under the widely used 97% threshold level. However, when identified with standard taxonomic classifiers, great discrepancies in the taxonomic composition at species level were evident between both markers. We attempted to reconcile the two distinct 'images' of the community using a phylogenetic approach that incorporates barcodes from both regions into a single phylogeny generated from reference sequences covering the full rRNA cistron. We find that the ITS2 and LSU D1-D2 metabarcodes are broadly interleaved in these trees, linking individual sequences across markers. This analysis also was used to select threshold values for clustering in each marker, recommending a mixed strategy of 98% similarity for ITS2 and 99% similarity for LSU D1-D2. Phylogenetic approaches which, unlike taxonomic classifiers, do not rely on sequence similarities with marker-specific reference sets, can link barcodes from different regions and provide greater precision of taxonomic placement. In addition, the approach provides a means to evaluate threshold values for clustering; despite the general tendency for the use of denoised 'exact sequence reads' (ASVs; Callahan et al. 2017), metabarcoding with ITS and LSU markers may continue to require OTU clustering due to the problem of intra-genomic variation in these tandemly repeated markers.

Acknowledgements

We express our gratitude for advice and consultations to Carola Gomez-Rodriguez (Santiago de Compostela), Kirsten Miller (Newcastle), and Ruth Bone (Kew Gardens). We thank Nicolas Magain and Brendan Furneaux for their most helpful comments on an earlier version of the manuscript. This work was funded by a PhD studentship of the John Spedan Lewis Foundation to ACE.

References

Abarenkov K, Somervuo P, Nilsson RH, Kirk PM, Huotari T, Abrego N, Ovaskainen O (2018) Protax -fungi: a web-based tool for probabilistic taxonomic placement of fungal internal transcribed spacer sequences. New Phytologist 220: 517–525. https://doi.org/10.1111/nph.15301

Abarenkov K, Tedersoo L, Nilsson RH, Vellak K, Saar I, Veldre V, Parmasto E, Prous M, Aan A, Ots M (2010) PlutoF – a web based workbench for ecological and taxonomic research, with an online implementation for fungal ITS sequences. Evolutionary Bioinformatics 6: EBO-S6271. https://doi.org/10.4137/EBO.S6271

Agerbo Rasmussen J, Nielsen M, Mak SS, Döring J, Klincke F, Gopalakrishnan S, Dunn RR, Kauer R, Gilbert MTP (2020) eDNA-based biomonitoring at an experimental German vineyard to characterize how management regimes shape ecosystem diversity. Environmental DNA. https://doi.org/10.1002/edn3.131

Andrews S, Krueger F, Segonds-Pichon A, Biggins L, Krueger C, Wingett S (2010) FastQC. https://www.bioinformatics.babraham.ac.uk/projects/fastqc/

Arribas P, Andújar C, Hopkins K, Shepherd M, Vogler AP (2016) Metabarcoding and mitochondrial metagenomics of endogean arthropods to unveil the mesofauna of the soil. Methods in Ecology and Evolution 7: 1071–1081. https://doi.org/10.1111/2041-210X.12557

Bacci G, Bani A, Bazzicalupo M, Ceccherini MT, Galardini M, Nannipieri P, Pietramellara G, Mengoni A (2015) Evaluation of the performances of ribosomal database project (RDP) classifier for taxonomic assignment of 16S rRNA metabarcoding sequences generated from Illumina-Solexa NGS. Journal of Genomics 3: e36. https://doi.org/10.7150/jgen.9204

Bakker MG (2018) A fungal mock community control for amplicon sequencing experiments. Molecular ecology resources 18: 541–556. https://doi.org/10.1111/1755-0998.12760

Bálint M, Schmidt P-A, Sharma R, Thines M, Schmitt I (2014) An Illumina metabarcoding pipeline for fungi. Ecology and Evolution 4: 2642–2653. https://doi.org/10.1002/ece3.1107

Bálint M, Bahram M, Eren AM, Faust K, Fuhrman JA, Lindahl B, O'Hara RB, Öpik M, Sogin ML, Unterseher M, Tedersoo L (2016) Millions of reads, thousands of taxa: microbial community structure and associations analyzed via marker genes. van der Meer JR (Ed.). FEMS Microbiology Reviews 40: 686–700. https://doi.org/10.1093/femsre/fuw017

Barrett T, Clark K, Gevorgyan R, Gorelenkov V, Gribov E, Karsch-Mizrachi I, Kimelman M, Pruitt KD, Resenchuk S, Tatusova T (2012) BioProject and BioSample databases at NCBI: facilitating capture and organization of metadata. Nucleic acids research 40: D57–D63. https://doi.org/10.1093/nar/gkr1163

Baselga A, Orme CDL (2012) Betapart: an R package for the study of beta diversity: *Betapart package*. Methods in Ecology and Evolution 3: 808–812. https://doi.org/10.1111/j.2041-210X.2012.00224.x

Bates D, Mächler M, Bolker B, Walker S (2015) Fitting linear mixed-effects models using lme4. Journal of Statistical Software 67 pp. https://doi.org/10.18637/jss.v067.i01

Batra LR (1963) Ecology of Ambrosia Fungi and Their Dissemination by Beetles. Transactions of the Kansas Academy of Science (1903-) 66: e213. https://doi.org/10.2307/3626562

Bellemain E, Carlsen T, Brochmann C, Coissac E, Taberlet P, Kauserud H (2010) ITS as an environmental DNA barcode for fungi: an in silico approach reveals potential PCR biases. BMC Microbiology 10: e189. https://doi.org/10.1186/1471-2180-10-189

Bengtsson-Palme J, Ryberg M, Hartmann M, Branco S, Wang Z, Godhe A, De Wit P, Sánchez-García M, Ebersberger I, de Sousa F, Amend AS, Jumpponen A, Unterseher M, Kristiansson E, Abarenkov K, Bertrand YJK, Sanli K, Eriksson KM, Vik U, Veldre V, Nilsson RH (2013) Improved software detection and extraction of ITS1 and ITS2 from ribosomal ITS sequences of fungi and other eukaryotes for analysis of environmental sequencing data. Bunce M (Ed.). Methods in Ecology and Evolution: 914–919. https://doi.org/10.1111/2041-210X.12073

Callahan BJ, McMurdie PJ, Holmes SP (2017) Exact sequence variants should replace operational taxonomic units in marker-gene data analysis. The ISME journal 11: 2639–2643. https://doi.org/10.1038/ismej.2017.119

Chytrý M, Tichý L, Holt J, Botta-Dukát Z (2002) Determination of diagnostic species with statistical fidelity measures. Journal of Vegetation Science 13: 79–90. https://doi.org/10.1111/j.1654-1103.2002.tb02025.x

Creedy TJ, Ng WS, Vogler AP (2019) Toward accurate species-level metabarcoding of arthropod communities from the tropical forest canopy. Ecology and evolution 9: 3105–3116. https://doi.org/10.1002/ece3.4839

De Cáceres M, Sol D, Lapiedra O, Legendre P (2011) A framework for estimating niche metrics using the resemblance between qualitative resources. Oikos 120: 1341–1350. https://doi.org/10.1111/j.1600-0706.2011.19679.x

DeSalle R, Egan MG, Siddall M (2005) The unholy trinity: taxonomy, species delimitation and DNA barcoding. Philosophical transactions of the royal society B: Biological sciences 360: 1905–1916. https://doi.org/10.1098/rstb.2005.1722

Deshpande V, Wang Q, Greenfield P, Charleston M, Porras-Alfaro A, Kuske CR, Cole JR, Midgley DJ, Tran-Dinh N (2016) Fungal identification using a Bayesian classifier and the Warcup training set of internal transcribed spacer sequences. Mycologia 108: 1–5. https://doi.org/10.3852/14-293

Dreaden TJ, Davis JM, de Beer ZW, Ploetz RC, Soltis PS, Wingfield MJ, Smith JA (2014) Phylogeny of ambrosia beetle symbionts in the genus Raffaelea. Fungal Biology 118: 970–978. https://doi.org/10.1016/j.funbio.2014.09.001

Edgar RC (2004) MUSCLE: multiple sequence alignment with high accuracy and high throughput. Nucleic acids research 32: 1792–1797. https://doi.org/10.1093/nar/gkh340

Edgar RC (2010) Search and clustering orders of magnitude faster than BLAST. Bioinformatics 26: 2460–2461. https://doi.org/10.1093/bioinformatics/btq461

Edgar RC (2018) Accuracy of taxonomy prediction for 16S rRNA and fungal ITS sequences. PeerJ 6: e4652. https://doi.org/10.7717/peerj.4652

Egan CP, Rummel A, Kokkoris V, Klironomos J, Lekberg Y, Hart M (2018) Using mock communities of arbuscular mycorrhizal fungi to evaluate fidelity associated with Illumina sequencing. Fungal Ecology 33: 52–64. https://doi.org/10.1016/j.funeco.2018.01.004

Frau A, Kenny JG, Lenzi L, Campbell BJ, Ijaz UZ, Duckworth CA, Burkitt MD, Hall N, Anson J, Darby AC, Probert CSJ (2019) DNA extraction and amplicon production strategies deeply influence the outcome of gut mycobiome studies. Scientific Reports 9: 9328. https://doi.org/10.1038/s41598-019-44974-x

Furneaux B, Bahram M, Rosling A, Yorou NS, Ryberg M (2021) Long- and short-read metabarcoding technologies reveal similar spatiotemporal structures in fungal communities. Molecular Ecology Resources 21: 1833–1849. https://doi.org/10.1111/1755-0998.13387

Ganter PF (2006) Yeast and Invertebrate Associations. In: Péter G, Rosa C (Eds) Biodiversity and Ecophysiology of Yeasts. Springer, Berlin, 303–370. https://doi.org/10.1007/3-540-30985-3_14

Gaujoux R, Seoighe C (2010) A flexible R package for nonnegative matrix factorization. BMC Bioinformatics 11: 367. https://doi.org/10.1186/1471-2105-11-367

George PB, Creer S, Griffiths RI, Emmett BA, Robinson DA, Jones DL (2019) Primer and database choice affect fungal functional but not biological diversity findings in a national soil survey. Frontiers in Environmental Science 7: e173. https://doi.org/10.3389/fenvs.2019.00173

Harrington TC, Yun HY, Lu S-S, Goto H, Aghayeva DN, Fraedrich SW (2011) Isolations from the redbay ambrosia beetle, *Xyleborus glabratus* , confirm that the laurel wilt path-

ogen, *Raffaelea lauricola*, originated in Asia. Mycologia 103: 1028–1036. https://doi.org/10.3852/10-417

Hibbett D, Abarenkov K, Kõljalg U, Öpik M, Chai B, Cole J, Wang Q, Crous P, Robert V, Helgason T (2016) Sequence-based classification and identification of Fungi. Mycologia 108: 1049–1068. https://doi.org/10.3852/16-130

Hulcr J, Barnes I, De Beer ZW, Duong TA, Gazis R, Johnson AJ, Jusino MA, Kasson MT, Li Y, Lynch S, Mayers C, Musvuugwa T, Roets F, Seltmann KC, Six D, Vanderpool D, Villari C (2020) Bark beetle mycobiome: collaboratively defined research priorities on a widespread insect-fungus symbiosis. Symbiosis 81: 101–113. https://doi.org/10.1007/s13199-020-00686-9

Hyde KD, Udayanga D, Manamgoda DS, Tedersoo L, Larsson E, Abarenkov K, Bertrand YJ, Oxelman B, Hartmann M, Kauserud H (2013) Incorporating molecular data in fungal systematics: a guide for aspiring researchers. arXiv preprint arXiv: 1302.3244. https://doi.org/10.5943/CREAM/3/1/1

Inward DJG (2019) Three new species of ambrosia beetles established in Great Britain illustrate unresolved risks from imported wood. Journal of Pest Science 93: 117–126. https://doi.org/10.1007/s10340-019-01137-1

Jacobsen RM, Sverdrup-Thygeson A, Kauserud H, Birkemoe T (2018) Revealing hidden insect-fungus interactions; moderately specialized, modular and anti-nested detritivore networks. Proceedings of the Royal Society B: Biological Sciences 285: e20172833. https://doi.org/10.1098/rspb.2017.2833

Johnson AJ, McKenna DD, Jordal BH, Cognato AI, Smith SM, Lemmon AR, Lemmon EM, Hulcr J (2018) Phylogenomics clarifies repeated evolutionary origins of inbreeding and fungus farming in bark beetles (Curculionidae, Scolytinae). Molecular Phylogenetics and Evolution 127: 229–238. https://doi.org/10.1016/j.ympev.2018.05.028

Jusino MA, Banik MT, Palmer JM, Wray AK, Xiao L, Pelton E, Barber JR, Kawahara AY, Gratton C, Peery MZ (2019) An improved method for utilizing high-throughput amplicon sequencing to determine the diets of insectivorous animals. Molecular Ecology Resources 19: 176–190. https://doi.org/10.1111/1755-0998.12951

Kandawatte Wedaralalage TC, Jayawardena RS, Hyde KD (2020) Hurdles in fungal taxonomy: Effectiveness of recent methods in discriminating taxa. Megataxa 1: 114–122. https://doi.org/10.11646/megataxa.1.2.2

Kõljalg U, Nilsson RH, Abarenkov K, Tedersoo L, Taylor AF, Bahram M, Bates ST, Bruns TD, Bengtsson-Palme J, Callaghan TM (2013) Towards a unified paradigm for sequence-based identification of fungi Molecular Ecology 22(21): 5271–5277. https://doi.org/10.1111/mec.12481

Krehenwinkel H, Wolf M, Lim JY, Rominger AJ, Simison WB, Gillespie RG (2017) Estimating and mitigating amplification bias in qualitative and quantitative arthropod metabarcoding. Scientific Reports 7: 1–12. https://doi.org/10.1038/s41598-017-17333-x

Letunic I, Bork P (2007) Interactive Tree Of Life (iTOL): an online tool for phylogenetic tree display and annotation. Bioinformatics 23: 127–128. https://doi.org/10.1093/bioinformatics/btl529

Li S, Deng Y, Wang Z, Zhang Z, Kong X, Zhou W, Yi Y, Qu Y (2020) Exploring the accuracy of amplicon-based internal transcribed spacer markers for a fungal community. Molecular Ecology Resources 20: 170–184. https://doi.org/10.1111/1755-0998.13097

Li Y, Simmons DR, Bateman CC, Short DPG, Kasson MT, Rabaglia RJ, Hulcr J (2016) Correction: New Fungus-Insect Symbiosis: Culturing, Molecular, and Histological Methods Determine Saprophytic Polyporales Mutualists of Ambrosiodmus Ambrosia Beetles. PLoS ONE 11: e0147305. https://doi.org/10.1371/journal.pone.0147305

Lindgren B (1983) A multiple funnel trap for scolytid beetles (Coleoptera). The Canadian Entomologist, 115: 299–302. https://doi.org/10.4039/Ent115299-3

Lücking R, Aime MC, Robbertse B, Miller AN, Ariyawansa HA, Aoki T, Cardinali G, Crous PW, Druzhinina IS, Geiser DM, Hawksworth DL, Hyde KD, Irinyi L, Jeewon R, Johnston PR, Kirk PM, Malosso E, May TW, Meyer W, Öpik M, Robert V, Stadler M, Thines M, Vu D, Yurkov AM, Zhang N, Schoch CL (2020) Unambiguous identification of fungi: where do we stand and how accurate and precise is fungal DNA barcoding? IMA Fungus 11: e14. https://doi.org/10.1186/s43008-020-00033-z

Lutzoni F, Kauff F, Cox CJ, McLaughlin D, Celio G, Dentinger B, Padamsee M, Hibbett D, James TY, Baloch E (2004) Assembling the fungal tree of life: progress, classification, and evolution of subcellular traits. American Journal of Botany 91: 1446–1480. https://doi.org/10.3732/ajb.91.10.1446

Maddison WP, Maddison RM (2021) Mesquite: a modular system for evolutionary analysis. http://www.mesquiteproject.org

Malacrinò A, Rassati D, Schena L, Mehzabin R, Battisti A, Palmeri V (2017) Fungal communities associated with bark and ambrosia beetles trapped at international harbours. Fungal Ecology 28: 44–52. https://doi.org/10.1016/j.funeco.2017.04.007

Martin M (2011) Cutadapt removes adapter sequences from high-throughput sequencing reads. EMBnet.journal 17: 10. https://doi.org/10.14806/ej.17.1.200

Miller KE, Hopkins K, Inward DJG, Vogler AP (2016) Metabarcoding of fungal communities associated with bark beetles. Ecology and Evolution 6: 1590–1600. https://doi.org/10.1002/ece3.1925

Miller KE, Inward DJG, Gomez-Rodriguez C, Baselga A, Vogler AP (2019) Predicting the unpredictable: How host specific is the mycobiota of bark and ambrosia beetles? Fungal Ecology 42: 100854. https://doi.org/10.1016/j.funeco.2019.07.008

Murali A, Bhargava A, Wright ES (2018) IDTAXA: a novel approach for accurate taxonomic classification of microbiome sequences. Microbiome 6: e140. https://doi.org/10.1186/s40168-018-0521-5

Nilsson RH, Kristiansson E, Ryberg M, Hallenberg N, Larsson K-H (2008) Intraspecific *ITS* Variability in the Kingdom Fungi as Expressed in the International Sequence Databases and Its Implications for Molecular Species Identification. Evolutionary Bioinformatics 4: EBO.S653. https://doi.org/10.4137/EBO.S653

Nilsson RH, Larsson K-H, Taylor AFS, Bengtsson-Palme J, Jeppesen TS, Schigel D, Kennedy P, Picard K, Glöckner FO, Tedersoo L, Saar I, Kõljalg U, Abarenkov K (2019) The UNITE database for molecular identification of fungi: handling dark taxa and parallel taxonomic classifications. Nucleic Acids Research 47: D259–D264. https://doi.org/10.1093/nar/gky1022

Oksanen J, Blanchet FG, Kindt R, Legendre P, Minchin PR, O'hara R, Simpson GL, Solymos P, Stevens MHH, Wagner H (2013) Package 'vegan.' Community ecology package, version 2: 1–295.

Op De Beeck M, Lievens B, Busschaert P, Declerck S, Vangronsveld J, Colpaert JV (2014) Comparison and Validation of Some ITS Primer Pairs Useful for Fungal Metabarcoding Studies. Neilan B (Ed.). PLoS ONE 9: e97629. https://doi.org/10.1371/journal.pone.0097629

Parada AE, Needham DM, Fuhrman JA (2016) Every base matters: assessing small subunit rRNA primers for marine microbiomes with mock communities, time series and global field samples. Environmental Microbiology 18: 1403–1414. https://doi.org/10.1111/1462-2920.13023

Paradis E, Schliep K (2019) ape 5.0: an environment for modern phylogenetics and evolutionary analyses in R. Bioinformatics 35: 526–528. https://doi.org/10.1093/bioinformatics/bty633

Ploetz RC, Hulcr J, Wingfield MJ, de Beer ZW (2013) Destructive Tree Diseases Associated with Ambrosia and Bark Beetles: Black Swan Events in Tree Pathology? Plant Disease 97: 856–872. https://doi.org/10.1094/PDIS-01-13-0056-FE

Porras-Alfaro A, Liu K-L, Kuske CR, Xie G (2014) From Genus to Phylum: Large-Subunit and Internal Transcribed Spacer rRNA Operon Regions Show Similar Classification Accuracies Influenced by Database Composition. Applied and Environmental Microbiology 80: 829–840. https://doi.org/10.1128/AEM.02894-13

Quast C, Pruesse E, Yilmaz P, Gerken J, Schweer T, Yarza P, Peplies J, Glöckner FO (2012) The SILVA ribosomal RNA gene database project: improved data processing and web-based tools. Nucleic Acids Research 41: D590–D596. https://doi.org/10.1093/nar/gks1219

Raman A, Wheatley W, Popay A (2012) Endophytic Fungus-Vascular Plant-Insect Interactions. Environmental Entomology 41: 433–447. https://doi.org/10.1603/EN11317

Richardson RT, Bengtsson-Palme J, Johnson RM (2017) Evaluating and optimizing the performance of software commonly used for the taxonomic classification of DNA metabarcoding sequence data. Molecular Ecology Resources 17: 760–769. https://doi.org/10.1111/1755-0998.12628

Rognes T, Flouri T, Nichols B, Quince C, Mahé F (2016) VSEARCH: a versatile open source tool for metagenomics. PeerJ 4: e2584. https://doi.org/10.7717/peerj.2584

Schmidt P-A, Bálint M, Greshake B, Bandow C, Römbke J, Schmitt I (2013) Illumina metabarcoding of a soil fungal community. Soil Biology and Biochemistry 65: 128–132. https://doi.org/10.1016/j.soilbio.2013.05.014

Schoch CL, Seifert KA, Huhndorf S, Robert V, Spouge JL, Levesque CA, Chen W, Fungal Barcoding Consortium, Fungal Barcoding Consortium Author List, Bolchacova E, Voigt K, Crous PW, Miller AN, Wingfield MJ, Aime MC, An K-D, Bai F-Y, Barreto RW, Begerow D, Bergeron M-J, Blackwell M, Boekhout T, Bogale M, Boonyuen N, Burgaz AR, Buyck B, Cai L, Cai Q, Cardinali G, Chaverri P, Coppins BJ, Crespo A, Cubas P, Cummings C, Damm U, de Beer ZW, de Hoog GS, Del-Prado R, Dentinger B, Dieguez-Uribeondo J, Divakar PK, Douglas B, Duenas M, Duong TA, Eberhardt U, Edwards JE, Elshahed MS, Fliegerova K, Furtado M, Garcia MA, Ge Z-W, Griffith GW, Griffiths K, Groenewald JZ, Groenewald M, Grube M, Gryzenhout M, Guo L-D, Hagen F, Hambleton S, Hamelin RC, Hansen K, Harrold P, Heller G, Herrera C, Hirayama K, Hirooka Y, Ho H-M, Hoffmann K, Hofstetter V, Hognabba F, Hollingsworth PM, Hong

S-B, Hosaka K, Houbraken J, Hughes K, Huhtinen S, Hyde KD, James T, Johnson EM, Johnson JE, Johnston PR, Jones EBG, Kelly LJ, Kirk PM, Knapp DG, Koljalg U, Kovacs GM, Kurtzman CP, Landvik S, Leavitt SD, Liggenstoffer AS, Liimatainen K, Lombard L, Luangsa-ard JJ, Lumbsch HT, Maganti H, Maharachchikumbura SSN, Martin MP, May TW, McTaggart AR, Methven AS, Meyer W, Moncalvo J-M, Mongkolsamrit S, Nagy LG, Nilsson RH, Niskanen T, Nyilasi I, Okada G, Okane I, Olariaga I, Otte J, Papp T, Park D, Petkovits T, Pino-Bodas R, Quaedvlieg W, Raja HA, Redecker D, Rintoul TL, Ruibal C, Sarmiento-Ramirez JM, Schmitt I, Schussler A, Shearer C, Sotome K, Stefani FOP, Stenroos S, Stielow B, Stockinger H, Suetrong S, Suh S-O, Sung G-H, Suzuki M, Tanaka K, Tedersoo L, Telleria MT, Tretter E, Untereiner WA, Urbina H, Vagvolgyi C, Vialle A, Vu TD, Walther G, Wang Q-M, Wang Y, Weir BS, Weiss M, White MM, Xu J, Yahr R, Yang ZL, Yurkov A, Zamora J-C, Zhang N, Zhuang W-Y, Schindel D (2012) Nuclear ribosomal internal transcribed spacer (ITS) region as a universal DNA barcode marker for Fungi. Proceedings of the National Academy of Sciences 109: 6241–6246. https://doi.org/10.1073/pnas.1117018109

Six DL (2020) Niche construction theory can link bark beetle-fungus symbiosis type and colonization behavior to large scale causal chain-effects. Current Opinion in Insect Science 39: 27–34. https://doi.org/10.1016/j.cois.2019.12.005

Skelton J, Jusino MA, Carlson PS, Smith K, Banik MT, Lindner DL, Palmer JM, Hulcr J (2019) Relationships among wood-boring beetles, fungi, and the decomposition of forest biomass. Molecular Ecology 28: 4971–4986. https://doi.org/10.1111/mec.15263

Stadler M, Lambert C, Wibberg D, Kalinowski J, Cox RJ, Kolařík M, Kuhnert E (2020) Intragenomic polymorphisms in the ITS region of high-quality genomes of the Hypoxylaceae (Xylariales, Ascomycota). Mycological Progress 19: 235–245. https://doi.org/10.1007/s11557-019-01552-9

Stielow JB, Levesque CA, Seifert KA, Meyer W, Iriny L, Smits D, Renfurm R, Verkley G, Groenewald M, Chaduli D (2015) One fungus, which genes? Development and assessment of universal primers for potential secondary fungal DNA barcodes. Persoonia: Molecular Phylogeny and Evolution of Fungi 35: e242. https://doi.org/10.3767/003158515X689135

Tedersoo L, Ramirez KS, Nilsson RH, Kaljuvee A, Kõljalg U, Abarenkov K (2015a) Standardizing metadata and taxonomic identification in metabarcoding studies. GigaScience 4: s13742-015. https://doi.org/10.1186/s13742-015-0074-5

Tedersoo L, Anslan S, Bahram M, Põlme S, Riit T, Liiv I, Kõljalg U, Kisand V, Nilsson H, Hildebrand F (2015b) Shotgun metagenomes and multiple primer pair-barcode combinations of amplicons reveal biases in metabarcoding analyses of fungi. MycoKeys 10: e1. https://doi.org/10.3897/mycokeys.10.4852

Tsirogiannis C, Sandel B (2016) PhyloMeasures: a package for computing phylogenetic biodiversity measures and their statistical moments. Ecography 39: 709–714. https://doi.org/10.1111/ecog.01814

Větrovský T, Morais D, Kohout P, Lepinay C, Algora C, Awokunle Hollá S, Bahnmann BD, Bílohnědá K, Brabcová V, D'Alò F, Human ZR, Jomura M, Kolařík M, Kvasničková J, Lladó S, López-Mondéjar R, Martinović T, Mašínová T, Meszárošová L, Michalčíková L,

Michalová T, Mundra S, Navrátilová D, Odriozola I, Piché-Choquette S, Štursová M, Švec K, Tláskal V, Urbanová M, Vlk L, Voříšková J, Žifčáková L, Baldrian P (2020) GlobalFungi, a global database of fungal occurrences from high-throughput-sequencing metabarcoding studies. Scientific Data 7: e228. https://doi.org/10.1038/s41597-020-0567-7

Vilgalys R, Hester M (1990) Rapid genetic identification and mapping of enzymatically amplified ribosomal DNA from several Cryptococcus species. Journal of Bacteriology 172: 4238–4246. https://doi.org/10.1128/jb.172.8.4238-4246.1990

Vrålstad T (2011) ITS, OTUs and beyond-fungal hyperdiversity calls for supplementary solutions. Molecular Ecology 20: 2873–2875. https://doi.org/10.1111/j.1365-294X.2011.05149.x

Vu D, Groenewald M, de Vries M, Gehrmann T, Stielow B, Eberhardt U, Al-Hatmi A, Groenewald JZ, Cardinali G, Houbraken J, Boekhout T, Crous PW, Robert V, Verkley GJM (2019) Large-scale generation and analysis of filamentous fungal DNA barcodes boosts coverage for kingdom fungi and reveals thresholds for fungal species and higher taxon delimitation. Studies in Mycology 92: 135–154. https://doi.org/10.1016/j.simyco.2018.05.001

Wang Q, Garrity GM, Tiedje JM, Cole JR (2007) Naïve Bayesian Classifier for Rapid Assignment of rRNA Sequences into the New Bacterial Taxonomy. Applied and Environmental Microbiology 73: 5261–5267. https://doi.org/10.1128/AEM.00062-07

Webb CO, Ackerly DD, Kembel SW (2008) Phylocom: software for the analysis of phylogenetic community structure and trait evolution. Bioinformatics 24(18): 2098–2100. https://doi.org/10.1093/bioinformatics/btn358

White TJ, Bruns T, Lee S, Taylor J (1990) Amplification and direct sequencing of fungal ribosomal RNA genes for phylogenetics. PCR protocols: a guide to methods and applications 18: 315–322. https://doi.org/10.1016/B978-0-12-372180-8.50042-1

Wickham H (2016) ggplot2: Elegant Graphics for Data Analysis. 2nd edn. 2016. Springer International, Cham, 1 pp. https://doi.org/10.1007/978-3-319-24277-4

Xue C, Hao Y, Pu X, Ryan Penton C, Wang Q, Zhao M, Zhang B, Ran W, Huang Q, Shen Q, Tiedje JM (2019) Effect of LSU and ITS genetic markers and reference databases on analyses of fungal communities. Biology and Fertility of Soils 55: 79–88. https://doi.org/10.1007/s00374-018-1331-4

Yu DW, Ji Y, Emerson BC, Wang X, Ye C, Yang C, Ding Z (2012) Biodiversity soup: metabarcoding of arthropods for rapid biodiversity assessment and biomonitoring: Biodiversity soup. Methods in Ecology and Evolution 3: 613–623. https://doi.org/10.1111/j.2041-210X.2012.00198.x

Zhang J, Kobert K, Flouri T, Stamatakis A (2014) PEAR: a fast and accurate Illumina Paired-End reAd mergeR. Bioinformatics 30: 614–620. https://doi.org/10.1093/bioinformatics/btt593

Zhang N, Castlebury LA, Miller AN, Huhndorf SM, Schoch CL, Seifert KA, Rossman AY, Rogers JD, Kohlmeyer J, Volkmann-Kohlmeyer B, Sung G-H (2006) An overview of the systematics of the Sordariomycetes based on a four-gene phylogeny. Mycologia 98: 1076–1087. https://doi.org/10.1080/15572536.2006.11832635

Supplementary material 1

Figure S1. Length distribution of the ITS (grey) and LSU (orange) OTUs

Authors: Angelina Ceballos-Escalera, John Richards, Maria Belen Arias, Daegan J. G. Inward, Alfried P. Vogler

Data type: Eps file.

Explanation note: The average length for each amplified region is indicated with a dashed line.

Link: https://doi.org/10.3897/mycokeys.88.77106.suppl1

Supplementary material 2

Figure S2. Species accumulation curves of the OTUs generated from the ITS (panel right) and LSU (panel left) metabarcodes

Authors: Angelina Ceballos-Escalera, John Richards, Maria Belen Arias, Daegan J. G. Inward, Alfried P. Vogler

Data type: Eps file.

Explanation note: Colours show the different forest types in which beetles were trapped: oak (red), spruce (blue) or pine (green).

Link: https://doi.org/10.3897/mycokeys.88.77106.suppl2

Supplementary material 3

Figure S3. Maximum-likelihood tree constructed in IQ-Tree2 based on three-gene (LSU D1-D2, SSU, ITS2) reference sequence alignments and OTUs for both markers (clustering thresholds: 99% LSU D1-D2 and 98% ITS2)

Authors: Angelina Ceballos-Escalera, John Richards, Maria Belen Arias, Daegan J. G. Inward, Alfried P. Vogler

Data type: Pdf file.

Explanation note: *Leotia lubrica* (Leotiomycetes) used as the outgroup. Node values indicate ultrafast bootstrap approximation support (n = 1000).

Link: https://doi.org/10.3897/mycokeys.88.77106.suppl3

Supplementary material 4

Figure S4. Binding site of ITS86 primer showing mismatched base pairs in Ophiostomatales

Authors: Angelina Ceballos-Escalera, John Richards, Maria Belen Arias, Daegan J. G. Inward, Alfried P. Vogler

Data type: Eps file.

Explanation note: Degenerate primer suggestion with variable base pairs in bold. While all other reference sequences were consistent with the non-Ophiostomatales sequences, only several are shown for clarity.

Link: https://doi.org/10.3897/mycokeys.88.77106.suppl4

Supplementary material 5

Table S1. Accession numbers corresponding with the reference sequences used to build the phylogenetic trees

Authors: Angelina Ceballos-Escalera, John Richards, Maria Belen Arias, Daegan J. G. Inward, Alfried P. Vogler

Data type: Xlsx file.

Link: https://doi.org/10.3897/mycokeys.88.77106.suppl5

Supplementary material 6

Table S2. Class level identification of OTUs showing the number of OTUs produced with ITS2 and LSU and the proportion of the total OTU set on the rarefied data

Authors: Angelina Ceballos-Escalera, John Richards, Maria Belen Arias, Daegan J. G. Inward, Alfried P. Vogler

Data type: Xlsx file.

Explanation note: OTUs classified at species level but not correctly classified at class level were considered as “Misclassified”.

Link: https://doi.org/10.3897/mycokeys.88.77106.suppl6

Supplementary material 7

Table S3. Number of OTUs assigned to each order based on RDP Bayesian classifier

Authors: Angelina Ceballos-Escalera, John Richards, Maria Belen Arias, Daegan J. G. Inward, Alfried P. Vogler

Data type: Xlsx file.

Explanation note: Average confidence scores were calculated over all order-level assignments, though only classifications with > 50% confidence were taxonomised, all others were kept as "unclassified Sordariomycetes".

Link: https://doi.org/10.3897/mycokeys.88.77106.suppl7

MycoKeys 88: 35–54 (2022)
doi: 10.3897/mycokeys.88.79346
https://mycokeys.pensoft.net

RESEARCH ARTICLE

A peer-reviewed open-access journal
MycoKeys
Launched to accelerate biodiversity research

Three novel species of *Distoseptispora* (Distoseptisporaceae) isolated from bamboo in Jiangxi Province, China

Zhi-Jun Zhai[1,2], Jun-Qing Yan[1,2], Wei-Wu Li[1], Yang Gao[1,2], Hai-Jing Hu[1,2], Jian-Ping Zhou[1,2], Hai-Yan Song[1,3], Dian-Ming Hu[1,2]

1 *Bioengineering and Technological Research Centre for Edible and Medicinal Fungi, College of Bioscience and Bioengineering, Jiangxi Agricultural University, Nanchang, Jiangxi 330045, China* **2** *Jiangxi Key Laboratory for Conservation and Utilization of Fungal Resources, College of Bioscience and Bioengineering, Jiangxi Agricultural University, Nanchang, Jiangxi 330045, China* **3** *Key Laboratory of Crop Physiology, Ecology and Genetic Breeding, Ministry of Education of the P. R. China, Jiangxi Agricultural University, Nanchang, Jiangxi 330045, China*

Corresponding author: Dian-Ming Hu (hudianming1@163.com)

Academic editor: Cecile Gueidan | Received 16 December 2021 | Accepted 24 February 2022 | Published 22 March 2022

Citation: Zhai Z-J, Yan J-Q, Li W-W, Gao Y, Hu H-J, Zhou J-P, Song H-Y, Hu D-M (2022) Three novel species of *Distoseptispora* (Distoseptisporaceae) isolated from bamboo in Jiangxi Province, China. MycoKeys 88: 35–54. https://doi.org/10.3897/mycokeys.88.79346

Abstract

Decaying bamboo in freshwater is a unique eco-environment for fungi. Three new *Distoseptispora* (*Distoseptisporaceae*) species, *D. meilingensis*, *D. yongxiuensis* and *D. yunjushanensis* from submerged decaying bamboo culms in Jiangxi Province, China, were discovered, based on phylogenetic analyses and morphological characters. The combined data of ITS-LSU-SSU-*Tef*1 sequences were used to infer the phylogenetic relationship between *D. meilingensis*, *D. yongxiuensis*, *D. yunjushanensis* and related species. Both molecular analyses and morphological data supported *D. meilingensis*, *D. yongxiuensis* and *D. yunjushanensis* as three independent taxa.

Keywords

Hyphomycetes, phylogenetic analysis, *Sordariomycetes*, taxonomy, three new taxa

Introduction

Distoseptispora was established by Su et al. (2016) as the single genus in *Distoseptisporaceae*. This genus morphologically resembles *Ellisembia* and *Sporidesmium* (Subramanian 1992; Shenoy et al. 2006; Yang et al. 2018), while they are not in sister clades in molecular phylogenetic trees (Su et al. 2016; Luo et al. 2019; Hyde et al. 2020, 2021). Multigene analysis showed that *Distoseptispora* formed a stable and well-supported clade within *Distoseptisporales* as a sister clade to *Aquapteridospora* (Luo et al. 2019; Hyde et al. 2020, 2021). *Aquapteridospora* has been raised as a new family *Aquapteridosporaceae* for the divergence time (110 million years ago (mya)) falling within the family-level range (50–130 mya) (Hyde et al. 2021). *Aquapteridospora* and *Distoseptispora* are similar in having macronematous, mononematous, unbranched conidiophores, mono- or polyblastic, holoblastic, conidiogenous cells and acrogenous, solitary conidia. *Distoseptispora* can easily be distinguished from *Aquapteridospora* by its short conidiophores and obclavate or cylindrical, rostrate, euseptate or distoseptate conidia. Additionally, *Distoseptispora* has terminal conidiogenous cells which lack circular scars (Hyde et al. 2021).

Distoseptispora was regarded as saprobic lignicolous fungal genus, which has the ability to decompose lignocelluloses in wood (Wong et al. 1998; Hyde et al. 2016). In recent years, the number of new taxa in *Distoseptispora* is steadily increasing and currently comprises 35 species, which have been discovered mostly in freshwater and some in terrestrial habitats (Su et al. 2016; Dong et al. 2021; Hyde et al. 2021; Li et al. 2021). Except for the two species, *D. adscendens* and *D. leonensis*, which were found from Hungary and Malaysia, respectively (Shoemaker and White 1985; Mckenzie 1995), 19 of the 33 species has been discovered in Thailand, while the remaining 14 species were introduced from China (Table 2). In China, *Distoseptispora* species are almost exclusively reported in Yunnan Province (Su et al. 2016; Luo et al. 2018; Hyde et al. 2019; Phookamsak et al. 2019; Li et al. 2021). Only three species, *D. martinii*, *D. bambusae* and *D. suoluoensis*, have been discovered from Guizhou Province (Xia et al. 2017; Yang et al. 2018; Sun et al. 2020). In this study, we introduce three new species of *Distoseptispora*, including *D. meilingensis*, *D. yongxiuensis* and *D. yunjushanensis* from Jiangxi Province in subtropical China. We describe the novel species, based on morphological illustrations and phylogenetic analyses. A synopsis of the morphological characters of *Distoseptispora* species is also provided.

Materials and methods

Samples collection, morphological observation and isolation

Dead bamboo samples from different freshwater habitats in Jiangxi Province, China, were taken to the lab for detection of fungi using a Nikon SMZ-1270 microscope (Nikon Corporation, Japan). Micro-morphological characteristics were observed and

captured using a Nikon ECLIPSE Ni-U compound microscope (Nikon Corporation, Japan), equipped with a Nikon DS-Fi3 camera. All measurements were calculated using PhotoRuler Ver. 1.1 software (The Genus Inocybe, Hyogo, Japan) and figures were processed using Adobe Photoshop CS6 Extended version 10.0 software (Adobe Systems, USA). Pure cultures of the fungi were obtained by the single spore isolation method (Chomnunti et al. 2014). The germinating conidia were transferred to potato dextrose agar (PDA) and incubated at 25 °C for two weeks. The fungal cultures were deposited in the Jiangxi Agricultural University Culture Collection (JAUCC) and the holotypic specimens with MycoBank numbers (842065, 842066, 842067) were deposited in the Herbarium of Fungi, Jiangxi Agricultural University (HFJAU) .

DNA extraction, PCR amplification and sequencing

Fungal genomes were extracted from fresh mycelium using a modified cetyltrimethylammonium bromide (CTAB) method (Doyle and Doyle 1987). Four deoxyribonucleic acid (DNA) barcodes (ITS, LSU, SSU and *Tef-1α*) were chosen for polymerase chain reaction (PCR) using the primer pairs ITS1/ITS4 (White et al. 1990), LR0R/LR7 (Hopple and Vilgalys 1999), NS1/NS4 (White et al. 1990) and EF983F/EF2218R (Örstadius et al. 2015), respectively. Amplification reactions were carried out in a volume of 25 μl, containing 12.5 μl 2 × Taq PCR MasterMix (Qingke, Changsha, China), 1 μl each forward and reverse primer (0.2 μM), 1 μl template DNA (circa 50–100 ng) and 9.5 μl ddH_2O. Amplifications were conducted under the following conditions: 3 min at 98 °C, 35 cycles of 10 s at 98 °C, 10 s of annealing at 55 °C and extension at 72 °C for 10 s, with a final 2-min extension at 72 °C. Sequencing reactions were conducted with the corresponding forward and reverse primers commercially by QingKe Biotechnology Co. (Changsha, China). All sequences were edited with Sequencher v.4.14 (GeneCodes Corporation, USA) and have been deposited in the NCBI GenBank database (Table 1).

Data analyses

Reference sequences of 35 *Distoseptispora* species and three *Aquapteridospora* species, based on recent publications (Luo et al. 2019; Hyde et al. 2020; Monkai et al. 2020; Dong et al. 2021, Li et al. 2021) were downloaded from GenBank. Detailed information on fungal strains used in this paper are provided in Table 1.

All obtained sequences were aligned using the online service of MAFFT (Madeira et al. 2019) and refined manually in MEGA v.7.0 (Kumar et al. 2016). Maximum Likelihood (ML) analysis was conducted with RAxML 8.0 using a GTR-GAMMA model of evolution (Stamatakis 2014). Non-parametric bootstrap analysis was implemented using 1,000 replicates to estimate ML bootstrap (BS) values. Bayesian Inference (BI) analysis was carried out with MrBayes v.3.2 under partitioned models (Ronquist et al. 2012). The best-fit models of nucleotide substitutions were selected according to the Akaike Information Criterion (AIC) implemented in jModelTest2.1.1

Table 1. Sequences used in this study.

Taxa	Voucher	LSU	ITS	SSU	*Tef-1α*
Aquapteridospora aquatica	MFLUCC 17-2371	NG_075413	NR_172447	—	—
Aquapteridospora fusiformis	MFLU 18-1601	MK849798	MK828652	—	MN194056
Aquapteridospora lignicola	MFLU 15-1172	KU221018	—	—	—
Distoseptispora adscendens	HKUCC 10820	DQ408561	—	—	—
Distoseptispora appendiculata	MFLUCC 18-0259	MN163023	MN163009	—	MN174866
Distoseptispora aquatica	GZCC 19-0452	MZ227216	MW133908	MW134689	—
Distoseptispora aquatica	MFLUCC 16-0904	MK849794	MK828649	MK828315	—
Distoseptispora aquatica	MFLUCC 18-0646	MK849793	MK828648	—	—
Distoseptispora aquatica	MFLUCC 16-1357	MK849796	MK828650	MK828317	—
Distoseptispora aquatica	S-965	MK849792	MK828647	MK828314	MN194051
Distoseptispora bambusae	MFLUCC 20-0091	NG_074430	NR_170068	NG_070348	—
Distoseptispora bambusae	MFLU 20-0261	MT232718	MT232713	MT232716	MT232880
Distoseptispora bambusae	MFLU 17-1653	MT232717	MT232712	—	—
Distoseptispora cangshanensis	MFLUCC 16-0970	MG979761	MG979754	—	MG988419
Distoseptispora caricis	CPC 36498	MN567632	NR_166325	—	—
Distoseptispora clematidis	MFLUCC 17-2145	MT214617	MT310661	MT226728	—
Distoseptispora clematidis	KUN-HKAS 112708	MW879523	MW723056	MW774580	—
Distoseptispora dehongensis	KUMCC 18-0090	MK079662	MK085061	—	MK087659
Distoseptispora euseptata	MFLUCC 20–0154	MW081544	MW081539	—	—
Distoseptispora euseptata	DLUCC S2024	MW081545	MW081540	—	MW084994
Distoseptispora fasciculata	KUMCC 19-0081	NG_075417	NR_172452	—	MW396656
Distoseptispora fluminicola	DLUCC 0391	MG979762	MG979755	—	MG988420
Distoseptispora fluminicola	DLUCC 0999	MG979763	MG979756	—	MG988421
Distoseptispora guttulata	MFLU 17-0852	MF077554	MF077543	MF077532	MF135651
Distoseptispora hydei	MFLUCC 20-0481	MT742830	MT734661	—	—
Distoseptispora leonensis	HKUCC 10822	DQ408566	—	—	—
Distoseptispora lignicola	MFLUCC 18-0198	MK849797	MK828651	MK828318	—
Distoseptispora longispora	HFJAU 0705	MH555357	MH555359	MH555431	—
Distoseptispora martinii	CGMCC 318651	KX033566	KU999975	KX033537	—
Distoseptispora meilingensis	**JAUCC 4727**	**OK562396**	**OK562390**	**OK562402**	**OK562408**
Distoseptispora meilingensis	**JAUCC 4728**	**OK562397**	**OK562391**	**OK562403**	**OK562409**
Distoseptispora multiseptata	MFLUCC 15-0609	KX710140	KX710145	NG_065693	MF135659
Distoseptispora multiseptata	MFLU 17-0856	MF077555	MF077544	MF077533	—
Distoseptispora neorostrata	MFLUCC 18-0376	MN163017	MN163008	—	—
Distoseptispora obclavata	MFLUCC 18-0329	MN163010	MN163012	—	—
Distoseptispora obpyriformis	DLUCC 0867	MG979765	MG979757	—	MG988423
Distoseptispora palmarum	MFLUCC 18-1446	MK079663	MK085062	MK079661	MK087660
Distoseptispora palmarum	MFLU 18-0588	NG_067856	NR_165897	—	MK087660
Distoseptispora phangngaensis	MFLU 17-0855	MF077556	MF077545	MF077534	MF135653
Distoseptispora phangngaensis	MFLUCC 16-0857	—	NR_166230	—	—
Distoseptispora rayongensis	MFLUCC 18-0415	NG_073624	NR_171938	NG_073504	—
Distoseptispora rayongensis	MFLU 18-1045	MH457137	MH457172	MH457169	—
Distoseptispora rostrata	MFLUCC 16-0969	MG979766	MG979758	—	MG988424
Distoseptispora rostrata	DLUCC 0885	MG979767	MG979759	—	MG988425
Distoseptispora rostrata	MFLU 18-0479	NG_064513	NR_157552	—	—
Distoseptispora saprophytica	MFLUCC 18-1238	NG_075419	NR_172454	—	MW396651
Distoseptispora songkhlata	MFLUCC 18-1234	MW287755	MW286482	—	MW396642
Distoseptispora submersa	MFLUCC 16-0946	MG979768	MG979760	—	MG988426
Distoseptispora suoluoensis	MFLUCC 17-0224	NG_068552	NR_168764	NG_070113	MF135654
Distoseptispora suoluoensis	MFLU 17-0854	MF077558	MF077547	MF077536	—
Distoseptispora tectonae	MFLUCC 15-0981	MW287763	MW286489	—	MW396641
Distoseptispora tectonae	MFLUCC 12-0291	KX751713	KX751711	—	KX751710

Taxa	Voucher	LSU	ITS	SSU	*Tef-1α*
Distoseptispora tectonae	S-2023	MW081543	MW081538	—	—
Distoseptispora tectonae	GZ 25	MH555358	MH555361	—	—
Distoseptispora tectonigena	MFLUCC 12-0292	KX751714	NR_154018	—	—
Distoseptispora thailandica	MFLUCC 16-0270	MH260292	MH275060	MH260334	MH412767
Distoseptispora thysanolaenae	KUN-HKAS 112710	MW879524	MW723057	—	—
Distoseptispora thysanolaenae	KUN-HKAS 102247	MK064091	MK045851	—	MK086031
Distoseptispora xishuangbannaensis	KUMCC 17-0290	MH260293	MH275061	MH260335	MH412768
Distoseptispora yongxiuensis	**JAUCC 4725**	**OK562394**	**OK562388**	**OK562400**	**OK562406**
Distoseptispora yongxiuensis	**JAUCC 4726**	**OK562395**	**OK562389**	**OK562401**	**OK562407**
Distoseptispora yunjushanensis	**JAUCC 4723**	**OK562398**	**OK562392**	**OK562404**	**OK562410**
Distoseptispora yunjushanensis	**JAUCC 4724**	**OK562399**	**OK562393**	**OK562405**	**OK562411**
Distoseptispora yunnansis	MFLUCC 20–0153	MW081546	MW081541	—	MW084995

"—", sequence is unavailable.

(Darriba et al. 2012) on XSEDE in the CIPRES web portal (Miller et al. 2010). The models for ITS, LSU, SSU and *Tef-1α* datasets used for phylogenetic analysis are GTR+I+G model (-lnL = 4965.1122), GTR+I+G model (-lnL = 2716.7536), TIM2+G (-lnL = 4344.2295) and TrN+I+G (-lnL = 4479.4914), respectively. The datasets were run for 10,000,000 generations, with four chains and trees sampled every 1,000 generations. The first 10% trees were discarded as burn-in. We used three *Aquapteridospora* species as outgroups. The Bayesian consensus tree with posterior probabilities (PP) was visualised with FigTree v.1.4.4 (Rambaut 2018) and was edited in Adobe Illustrator CS6. Our aligned matrices and trees can be obtained from TreeBASE (http://purl.org/phylo/treebase/phylows/study/TB2:S29465).

Results

Molecular phylogenetic results

According to the results of BLAST analysis and sequence alignment, the ITS sequence of *D. meilingensis* has 11 different loci from those of *D. yongxiuensis*, the ITS sequence of which shares 99% similarity (five different loci) with that of *D. suoluoensis*. The ITS sequence of *D. yunjushanensis* is 97% similar (22 different loci) to that of *D. obclavata*. The aligned matrix for the combined analysis, ITS + LSU + SSU + *Tef-1α*, had 4015 bp, including ITS 596 bp, LSU 799 bp, SSU 1715 bp and *Tef-1α* 905 bp. The topologies of trees generated by ML and BI analyses are highly similar. The Bayesian tree with BS and PP is shown in Fig. 1. All species of *Distoseptispora* form a monophyletic group (BS/PP = 100/1.00). *D. yongxiuensis* groups together with *D. suoluoensis* (BS/PP = 60/0.99). These two species and collections of *D. meilingensis* form a strong-supported clade (BS/PP = 99/1.00), which is strongly linked with sequences of *D. bambusae* (BS/PP = 100/1.00). Collections of *D. yunjushanensis* form a moderate-support clade (BS/PP = 81/1.00) with the lineage consisting of *D. obclavata* and *D. rayongensis*.

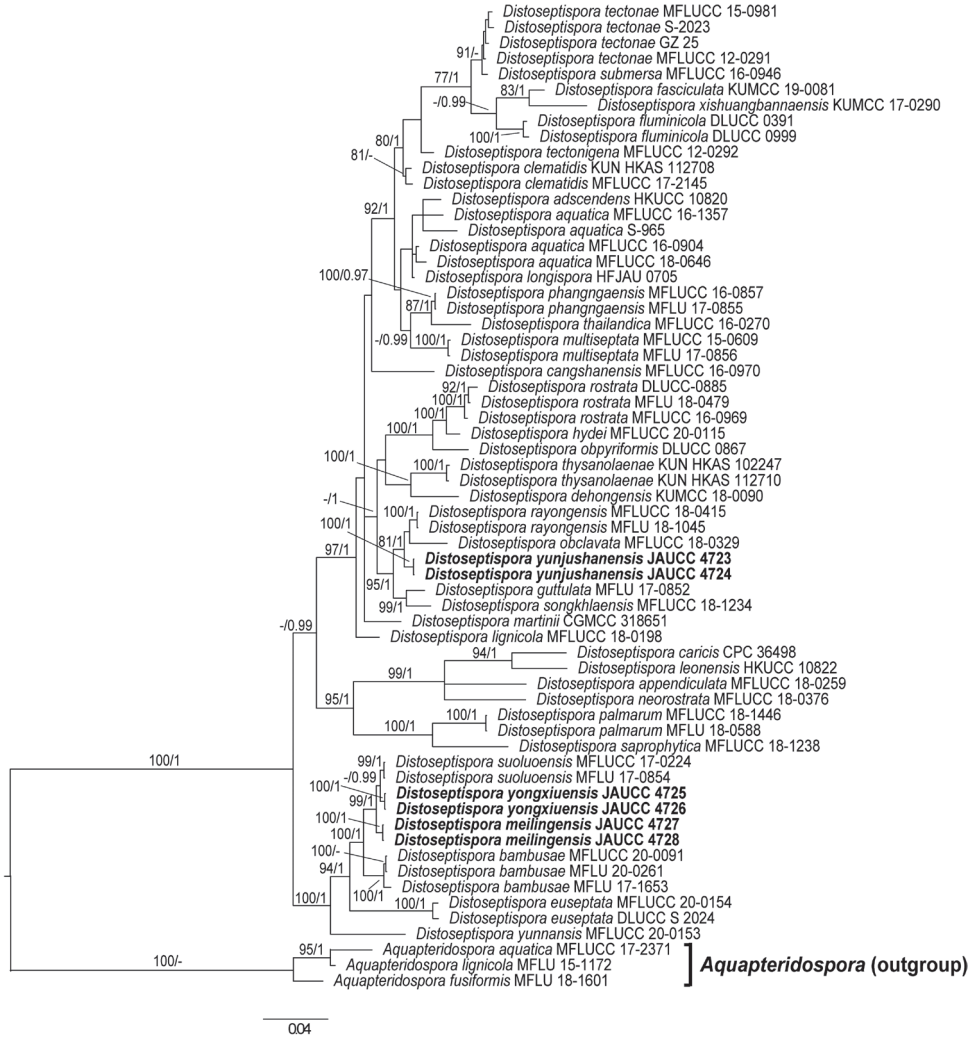

Figure 1. Phylogenetic tree of *Distoseptispora*, inferred from the combined regions (ITS-LSU-SSU-*Tef 1α*) using Bayesian Inference (BI) analysis. The *Aquapteridospora* clade was used as the outgroup. The lineages with new species were shown in bold. PP ≥ 0.95 and BS ≥ 75% were indicated around the branches. The new sequences generated in this study are given in bold.

Taxonomy

***Distoseptispora meilingensis* Z. J. Zhai & D. M. Hu, sp. nov.**
MycoBank No: 842067
Fig. 2

Etymology. Referring to the collecting site of the Meiling Mountain in Jiangxi Province, China.

Holotype. HFJAU 10009.

Figure 2. *Distoseptispora meilingensis* (HFJAU10009, holotype) **a, b** colonies on bamboo culms **c–e** conidiophores with conidia **f** conidiogenous cells **g, n** conidiogenous cells with conidia **h–m** conidia **o** germinating conidium **p** culture on PDA from above and reverse. Scale bars: 100 μm (**a, b**), 20 μm (**c–e, o**), 5 μm (**f-n**).

Description. Saprobic on culms of bamboo. ***Sexual morph*:** Undetermined. ***Asexual morph*:** Hyphomycetous. ***Colonies*** effuse, brown to dark brown, hairy. *Mycelium* mostly immersed, composed of pale to dark brown, septate, branched, smooth, hyaline to subhyaline hyphae. ***Conidiophores*** 69–192 × 4–7 μm ($\bar{x}$ = 120.6 × 5.5 μm, n = 25), macronematous, mononematous, erect, cylindrical, straight or slightly flexuous, 5–12-septate, yellowish-brown or brown, robust at the base. ***Conidiogenous cells*** holoblastic, mono- to polyblastic, integrated, terminal, cylindrical, yellowish-brown or brown. ***Conidia*** 32−64.5 × (7−)9−12.5 μm ($\bar{x}$ = 43.7 × 9.8 μm, n = 30), acrogenous, solitary, straight or slightly curved, obclavate, 5–7-distoseptate, thick-walled, rounded at the apex, truncate at the base, tapering towards apex, bud scars disjunctors at base, mostly brown when mature.

Cultural characteristics. Conidia germinating on PDA within 24 h and germ tubes produced from both ends. Colonies on PDA reaching 17–23 mm diam. at two weeks at 25 °C, in natural light, circular, with dense, light olivaceous mycelium on the surface with entire margin; reverse brown to dark brown.

Material examine. China, Jiangxi Province, Nanchang City, Meiling Mountain, alt. 305 m, near 28.79°N, 115.72°E, on decaying bamboo culms submerged in a freshwater stream, 16 Aug 2021, Z. J. Zhai, SLT-3 (HFJAU10009, ***holotype***), ex-type living culture, JAUCC 4727 = JAUCC 4728.

Notes. *Distoseptispora meilingensis* clusters with the clade including *D. suoluoensis* and *D. yongxiuensis* with high support in the phylogenetic tree (Fig. 1). *Distoseptispora meilingensis* is distinct from *D. suoluoensis* (Yang et al. 2018) and *D. yongxiuensis* by its conidial colour (mostly brown, yellowish-brown to dark olivaceous and yellowish-brown or brown, respectively). Furthermore, *D. meilingensis* has shorter conidia (32–64.5 μm vs. (65–)80–125(–145) μm) than those of *D. suoluoensis* (Yang et al. 2018) and slightly shorter conidiophores (69–192 μm vs. 112–253 μm) than those of *D. yongxiuensis*. *Distoseptispora meilingensis* resembles *D. bambusae* in similar habitats and polyblastic conidiogenous cells (Sun et al. 2020). However, *D. meilingensis* can be distinguished from *D. bambusae* in its longer conidiophores (69–192 μm vs. 40–96 μm), slightly wider (up to 12.5 μm vs. up to 9.5 μm) and brighter (light brown vs. brown) conidia (Sun et al. 2020). A comparison of morphological features of *Distoseptispora* species is provided in Table 2.

***Distoseptispora yongxiuensis* Z. J. Zhai & D. M. Hu, sp. nov.**
MycoBank No: 842066
Fig. 3

Etymology. With reference to Yongxiu, from where the holotype was collected.

Holotype. HFJAU10007

Description. Saprobic on decaying bamboo culms. ***Sexual morph*:** Undetermined. ***Asexual morph*:** Hyphomycetous. ***Colonies*** effuse, brown, hairy, glistening, often inconspicuous. ***Mycelium*** partly superficial, partly immersed in the substra-

Table 2. Synopsis of morphological characteristics, habitats, hosts and district compared across *Distoseptispora* species.

Species	Conidiophores (µm)	Conidia (µm)	Conidia septation	Conidia characteristics	Habitat	Host	District	References
Distoseptispora meilingensis	**69–192 × 4–7**	**32–64.5 × (7–)9–12.5**	**5–7-distoseptate**	**Obclavate, mostly bright brown when mature**	**Freshwater**	**Dead bamboo culms**	**China, Jiangxi**	**This study**
D. yongxiuensis	**112–253 × 4–9**	**46–74(–86) × 10–13(–16)**	**6–9-euseptate**	**Obclavate or obspathulate, olivaceous to yellowish-brown or brown, guttulate**	**Freshwater**	**Dead bamboo culms**	**China, Jiangxi**	**This study**
D. yunjushanensis	**100–175 × 5.5–10**	**39–67.5(–77) × (7–)9.5–13.5(–16.5)**	**7–13-distoseptate**	**Obpyriform or obclavate, olivaceous when young, dark brown when mature**	**Freshwater**	**Dead bamboo culms**	**China, Jiangxi**	**This study**
D. adscendens	28–46 × 8–10	(80–)350–500 × 15–18	80-distoseptate	Cylindrical, hemispherical apex, hyaline	Terrestrial	Decaying wood of *Fagus sylvatica*	Hungary	Shoemaker and White (1985), Réblová (1999)
D. appendiculata	62–86 × 4.5–5.5	67–89 × 10–16	13–17-distoseptate	Obpyriform or obclavate, olivaceous or dark brown, with gelatinous sheath around tip	Freshwater	Unidentified submerged wood	Thailand, Khwaeng Phra	Luo et al. (2019)
D. aquatica	29–41 × 7–9	110–157 × 13.5–16.5	15–28-distoseptate	Obclavate, dark brown with bluish-green to malachite green tinge	Freshwater	Unidentified submerged wood	China, Yunnan	Su et al. (2016)
D.bambusae	40–96 × 4–5.5	45–74 × 5.5–9.5	5–10-distoseptate	Obclavate, olivaceous or brown	Terrestrial	Dead bamboo culms	China and Thailand	Sun et al. (2020), Monkai et al. (2020)
D. cangshanensis	44–68 × 4–8	58–166(–287) × 10–14	Multi-distoseptate	Obclavate or lanceolate, rostrate, olivaceous or brown	Freshwater	Unidentified submerged wood	China, Yunnan	Luo et al. (2018)
D. caricis	35–90 × 6–7	(55–)65–85(–100) × 15–16(–17)	5–10-distoseptate	Obclavate, brown, septa with central pore, basal cell pale brown, with truncate hilum	Terrestrial	Leaves of *Carex* sp.	Thailand, Chiang Mai	Crous et al. (2019)
D. clematidis	22–40 × 4–10	120–210 × 12–20	28–35-distoseptate	Oblong, obclavate, cylindrical or rostrate, brown with green tinge, bud scars or disjunctors present at the site of attachment	Terrestrial	Dried branches of *Clematis sikkimensis*	Thailand, Chiang Rai	Phukhamsakda et al. (2020)
D. dehongensis	45–80 × 4–5	17–30 × 7.5–10	3–5-distoseptate	Obpyriform to obclavate, broad cylindrical or irregular, olivaceous	Freshwater	Unidentified submerged wood	China, Yunnan	Hyde et al. (2019)
D. euseptata	19–28 × 4–5	37–54 × 8–9	4–7-euseptate	Obpyriform to obclavate, often constricted at septa, olivaceous	Freshwater	Unidentified submerged wood	China, Yunnan	Li et al. (2021)

Species	Conidiophores (µm)	Conidia (µm)	Conidia septation	Conidia characteristics	Habitat	Host	District	References
D. fasciculata	12–16 × 5–6	46–200 × 10–16.5	10–40-distoseptate	Subcylindrical to obclavate, olivaceous when young, dark brown when mature	Freshwater	Unidentified submerged wood	Thailand, Nakhon Si Thammarat	Dong et al. (2021)
D. fluminicola	21–33 × 5.5–6.5	125–250 × 13–15	17–34-distoseptate	Oblong, obclavate, cylindrical or rostrate, brown with green tinge	Freshwater	Unidentified submerged wood	China, Yunnan	Su et al. (2016)
D. guttulata	55–90(–145) × 3.5–5.5	75–130(–165) × 7–11	11–14(–20)-euseptate	Obclavate or lanceolate, rostrate, mid to dark brown or olivaceous	Freshwater	Unidentified submerged wood	Thailand, Prachuap Khiri Khan	Yang et al. (2018)
D. hydei	87–145 × 3–7	32–58 × 10–15	7–9-distoseptate	Obpyriform to fusiform, olivaceous to brown, with a hyaline, globose, gelatinous sheath around tip	Terrestrial	Dead bamboo culms	Thailand, Phitsanulok	Monkai et al. (2020)
D. leonensis	Up to 175 × 6–7	(38–)50–75(–85) × 11–15	7–12-distoseptate	Obclavate, rostrate, brown	Terrestrial	Dead culms of *Freycinetia* sp.	Malaysia	McKenzie (1995)
D. lignicola	84–124 × 4–5	60–108 × 7–9	5–9-euseptate	Obclavate, curved, brown	Freshwater	Unidentified submerged wood	Thailand, Sai-Khu Waterfall	Luo et al. (2019)
D. longispora	17–37 × 6–10	189–297 × 16–23	31–56-distoseptate	Obclavate, elongated, brown to yellowish-brown	Freshwater	Unidentified submerged wood	China, Yunnan	Song et al. (2020)
D. martinii	50–110 × 3.5–4.5	15–20 × 11–16	Transversal septa	Transversal ellipsoid, oblate or subglobose, muriform, pale brown to brown	Terrestrial	Unidentified dead branches	China, Guizhou	Xia et al. (2017)
D. multiseptata	29–47 × 4–6	147–185 × 12–14	Multi-distoseptate	Obclavate, rostrate, dark olivaceous green	Freshwater	Unidentified submerged wood	Thailand, Prachuap Khiri Khan	Hyde et al. (2016)
D. neorostrata	93–117 × 5.5–6.5	109–147 × 13–15	Multi-distoseptate	Obclavate, rostrate, dark olivaceous to mid or dark brown	Freshwater	Unidentified submerged wood	Thailand, Khwaeng Phra Khanong Nuea	Luo et al. (2019)
D. obclavata	117.5–162.5 × 5–7	46–66 × 9–11	9-11-distoseptate	Obclavate, olivaceous to pale or dark brown, guttulate	Freshwater	Unidentified submerged wood	Thailand, Khwaeng Phra Khanong Nuea	Luo et al. (2019)
D. obpyriformis	97–119 × 5–7	53–71 × 12–16	9–11-distoseptate	Obpyriform, olivaceous to pale or dark brown, guttulate	Freshwater	Unidentified submerged wood	China, Yunnan	Luo et al. (2018)
D. palmarum	90–165 × 4–7	35–180 × 7–11	7–27-distoseptate	Oblong, obclavate, greenish-black to brown	Terrestrial	Rachis of *Cocos nucifera*	Thailand, Trat	Hyde et al. (2019)
D. phangngaensis	18–30(–40) × 4.3–6.5	165–350 × 14–19	Multi-distoseptate	Elongate, obclavate, rostrate, dark olivaceous to mid or dark brown	Freshwater	Unidentified submerged wood	Thailand, Phang Nga	Yang et al. (2018)

Species	Conidiophores (µm)	Conidia (µm)	Conidia septation	Conidia characteristics	Habitat	Host	District	References
D. rayongensis	75–125 × 3.5–5.5	(36–)60–106(–120) × 9–14.5	9–13-euseptate, rarely 14–15-septate	Obclavate or obspathulate, rostrate, pale brown or pale olivaceous, with percurrent proliferation	Freshwater	Unidentified submerged wood	Thailand, Rayong	Hyde et al. (2020)
D. rostrata	82–126 × 5–7	115–155 × 9–11	(15–)18–23-distoseptate	Obclavate or lanceolate, rostrate, olivaceous to pale brown	Freshwater	Unidentified submerged wood	China, Yunnan	Luo et al. (2018)
D. saprophytica	50–140 × 3.2–4.2	14.5–30 × 4.5–7.5	2–6-distoseptate	Subcylindrical to obclavate, olivaceous to brown	Freshwater	Unidentified submerged wood	Thailand, Songkhla	Dong et al. (2021)
D. songkhlaensis	70–90 × 4–5.5	44–125 × 9–14.5	9–16-distoseptate	Obclavate, constricted at septa, olivaceous to brown	Freshwater	Unidentified submerged wood	Thailand, Songkhla	Dong et al. (2021)
D. submersa	55–73 × 7–9	95–123 × 15–19	17–23(–28)-distoseptate	Obclavate, brown to dark brown or olivaceous	Freshwater	Unidentified submerged wood	China, Yunnan	Luo et al. (2018)
D. suoluoensis	80–250 × 4.5–5.8	(65–)80–125(–145) × 8–13	8–10-euseptate	Narrowly obclavate or obspathulate, yellowish-brown or dark olivaceous, verrucose, with percurrent proliferation	Freshwater	Unidentified submerged wood	China, Guizhou	Yang et al. (2018)
D. tectonae	19.5–95 × 4.5–9	45–270 × 11–16	10–40-distoseptate	Obclavate, brown to dark brown or olivaceous	Terrestrial/ Freshwater	Dead twig of *tectona grandis* (Lamiaceae)	Thailand, Prachuap Khiri Khan	Hyde et al. (2016)
D. tectonigena	Up to 110 × 5–11	(83–)148–225(360–) × (10–)11–12(–13)	20–46-distoseptate	Flexuous, cylindrical-obclavate, elongated, verruculose, dark reddish-brown	Terrestrial	Dead twig of *Tectona grandis* (Lamiaceae)	Thailand, Chiang Rai	Hyde et al. (2016)
D. thailandica	15–26 × 3–6	130–230 × 13.5–17	35–52-distoseptate	Oblong, obclavate, cylindrical or rostrate, reddish-brown to brown	Terrestrial	Dead leaves of *Pandanus* sp.	Thailand, Prachuap Khiri Khan	Tibpromma et al. (2018)
D. thysanolaenae	30–80 × 3.5–5.5	21.5–80 × 6.5–12.8	8–14-distoseptate	Elongated obclavate, light to dark brown, flat apex, with conspicuous spore attachment loci	Terrestrial	Dead culms of *Thysanolaena maxima*	China, Yunnan	Phookamsak et al. (2019)
D. xishuangbannaensis	12–17 × 2–5	160–305 × 8–15	Up to 40-distoseptate	Cylindrical-obclavate, green-brown to brown, tapering towards apex	Terrestrial	Dead leaf sheaths of *Pandanus utilis*	China, Yunnan	Tibpromma et al. (2018)
D. yunnanensis	131–175 × 6–7	58–108 × 8–10	6–10-euseptate	Obclavate, rostrate, mid-olivaceous to brown	Freshwater	Unidentified submerged wood	China, Yunnan	Li et al. (2021)

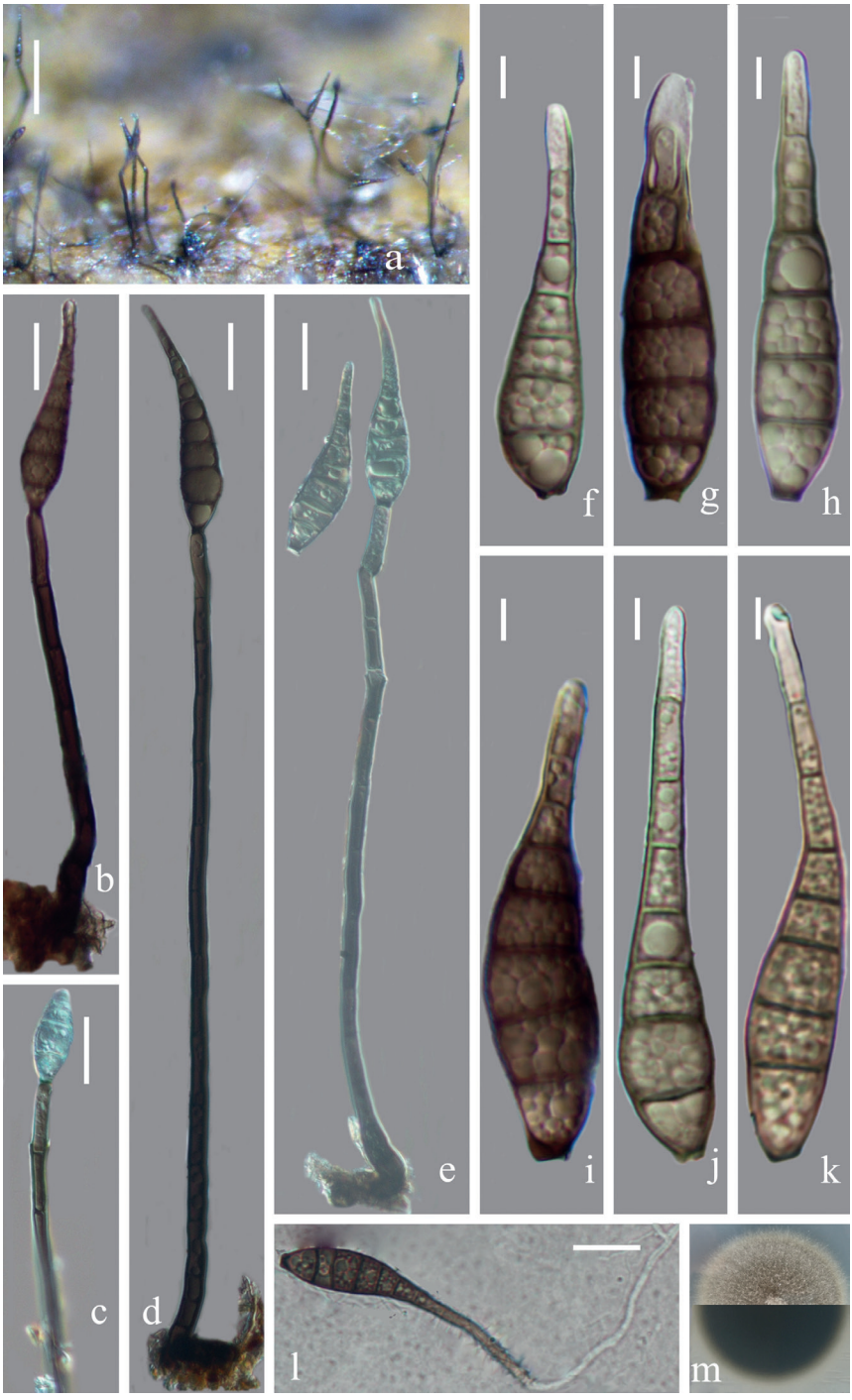

Figure 3. *Distoseptispora yongxiuensis* HFJAU 10007, holotype) **a** Colonies on bamboo culm **b, d** conidiophores with conidia **c** conidiogenous cell bearing conidium **e** conidiogenous cells with young conidia **f-k** conidia **l** germinating conidium **m** culture on PDA from above and reverse. Scale bars: 100 μm (**a**), 20 μm (**b–e, l**), 5 μm (**f–k**).

tum, composed of hyaline to pale brown, septate, branched hyphae. ***Conidiophores*** 112–253 × 4–9 μm ($\bar{x}$ = 198 × 6.9 μm, n = 15), macronematous, mononematous, solitary or aggregated at the base, cylindrical, straight or slightly flexuous, 8–13-septate, olivaceous to dark brown, sharply curving near the base, paler at the apical part, rounded at the apex. ***Conidiogenous cells*** integrated, terminal, monoblastic, rarely polyblastic, cylindrical, olivaceous to dark brown. ***Conidia*** 46–74(−86) × 10–13(−16) μm ($\bar{x}$ = 65.6 × 12.6 μm, n = 30), acrogenous, solitary, obclavate or obspathulate, straight or flexuous, rostrate, 6–9-euseptate, olivaceous to yellowish-brown or brown, becoming paler or hyaline towards the apex, guttulate, 2.5–4 μm wide at the base and 2.5–5 μm wide at the apex, with a darkened scar at the base.

Cultural characteristics. Conidia germinating on PDA within 24 h and germ tubes produced from both ends. Colonies on PDA reaching 24–32 mm diam. at two weeks at 25 °C, in natural light, circular, with dense, light olivaceous mycelium on the surface with entire margin; reverse dark brown to black.

Material examined. China, Jiangxi Province, Jiujiang City, Yongxiu County, alt. 680.5 m, 29.09°N, 115.62°E, on decaying bamboo culms submerged in a freshwater stream, 28 Apr 2020, Z. J. Zhai and W. W. Li, YJS-70 (HFJAU 10007, ***holotype***), ex-type living culture, JAUCC 4725 = JAUCC 4726.

Notes. In the multi-gene phylogenetic tree (Fig. 1), *D. yongxiuensis* clusters with *D. suoluoensis*. Nonetheless, *D. yongxiuensis* can be distinguished from *D. suoluoensis* by its shorter conidia (46–74(−86) μm vs. (65–)80–125(–145) μm) and polyblastic conidiogenous cells (Yang et al. 2018). Additionally, *D. suoluoensis* has the percurrent proliferation of conidia, while it was not observed in *D. yongxiuensis*. *Distoseptispora yongxiuensis* is similar with *D. bambusae* (Sun et al. 2020), *D. palmarum* (Hyde et al. 2019) and *D. meilingensis* for the polyblastic conidiogenous cells, but *D. yongxiuensis* has wider conidia than those of *D. bambusae* (10–13(−16) μm vs. 5.5–9.5 μm) (Sun et al. 2020), shorter conidia than those of *D. palmarum* (46–74(−86) μm vs. 35–180 μm) (Hyde et al. 2019) and paler (yellowish-brown or brown vs. bright brown) conidia than those of *D. meilingensis*.

Distoseptispora yunjushanensis **Z. J. Zhai & D. M. Hu, sp. nov.**
MycoBank No: 842065
Fig. 4

Etymology. The epithet refers to the collecting site from the Yunjushan Mountain in China.

Holotype. HFJAU10005

Description. Saprobic on decaying bamboo culms submerged in freshwater habitats. ***Sexual morph*****:** Undetermined. ***Asexual morph*****:** Hyphomycetous. ***Colonies*** effuse, olivaceous or dark brown, hairy, velvety. ***Mycelium*** mostly immersed, consisting of branched, septate, smooth, subhyaline to pale brown hyphae. ***Conidiophores*** 100–175 μm × 5.5–10 μm ($\bar{x}$ = 129×7.1 μm, n = 30), single or in groups of 2 or 3, macronematous, mononematous, erect, straight or slightly flexuous, 4–7-septate,

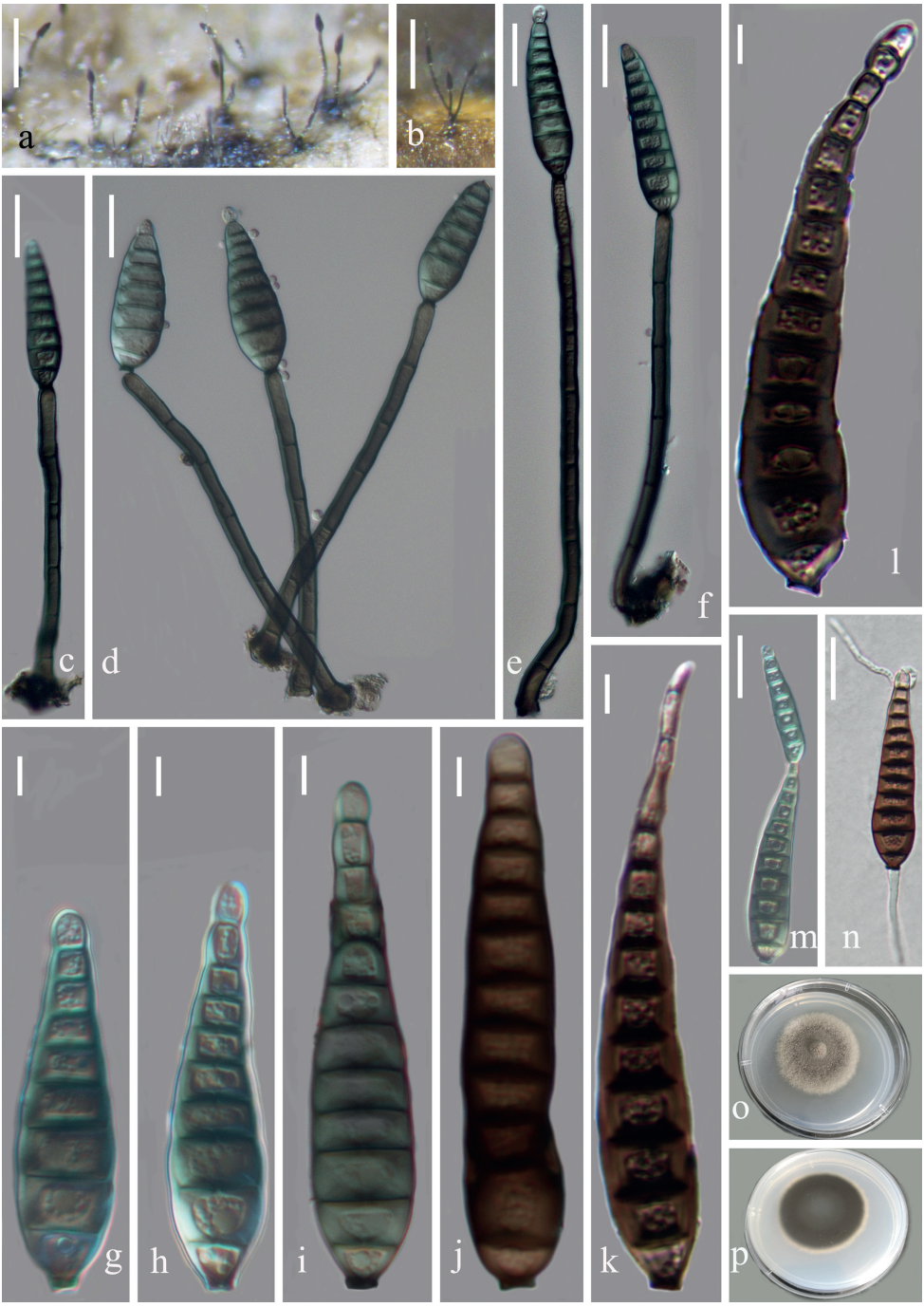

Figure 4. *Distoseptispora yunjushanensis* (HFJAU 10005, holotype) **a, b** colonies on bamboo culms **c–f** conidiophores with conidia **g-i** young conidia **j-l** mature conidia **m** conidium with proliferation **n** germinating conidium **o, p** culture on PDA from above and reverse. Scale bars: 100 μm (**a, b**), 20 μm (**c–f, m, n**), 5 μm (**g–l**).

unbranched, olivaceous to dark brown, smooth, cylindrical, rounded at the apex. ***Conidiogenous cells*** monoblastic, integrated, terminal, determinate, pale to dark brown, cylindrical. ***Conidia*** 39−67.5(−77) μm × (7–)9.5–13.5(–16.5) μm ($\bar{x}$ = 52 × 12 μm, n = 30), acrogenous, solitary, obpyriform or obclavate, thick-walled, tapering towards the rounded apex, slightly curved, truncate at the base, 7–13-distoseptate, guttulate, smooth-walled, olivaceous, dark brown when mature, sometimes with the percurrent proliferation which forms another conidium from the conidial apex.

Cultural characteristics. Conidia germinating on PDA within 24 h and germ tubes produced from both ends. Colonies on PDA reaching 12–18 mm diam. at 14 days at 25 °C, in natural light, with fluffy, dense, thin olivaceous mycelium in the centre, becoming sparse and paler at the entire margin; reverse dark brown, pale brown at the smooth margin.

Material examined. China, Jiangxi Province, Jiujiang City, Yongxiu County, Yunjushan Mountain, alt. 672.5 m, 29.23°N, 115.59°E, on decaying bamboo culms submerged in a freshwater stream, 28 Apr 2020, Z. J. Zhai and W. W. Li, YJS-42 (HFJAU 10005, ***holotype***), ex-type living culture, JAUCC 4723 = JAUCC 4724.

Notes. In the phylogenetic analysis, *D. yunjushanensis* clusters with *D. obclavata* and *D. rayongensis* with moderate support (BS/PP = 81/1.00). However, *D. yunjushanensis* is easily distinguished from *D. obclavata* by its comparatively wider (5.5–10 μm vs. 5–7 μm) conidiophores and conidia ((7–)9.5–13.5(–16.5) μm vs. 9–11 μm) (Luo et al. 2019). Moreover, the percurrent proliferation of conidia was not observed in *D. obclavata* (Luo et al. 2019). *Distoseptispora yunjushanensis* has shorter conidia (39−67.5(−77) μm vs. (36–)60–106(–120) μm) and wider conidiophores (5.5–10 μm vs. 3.5–5.5 μm) than those of *D. rayongensis* (Hyde et al. 2020). The morphology of *D. yunjushanensis* is similar to *D. guttulata* and *D. songkhlaensis* in having the obclavate conidia, but differs in having wider (5.5–10 μm vs. 3.5–5.5 μm and 4–5.5 μm) conidiophores, shorter (39–67.5(−77) μm vs. 75–130(–165) μm and 44–125 μm) and proliferating conidia (Yang et al. 2018; Dong et al. 2021). Additionally, *D. yunjushanensis* can be distinguished from *D. guttulata* by its distoseptate conidia (Yang et al. 2018).

Discussion

Previous reports of *Distoseptispora* were mainly concentrated in tropical areas, such as Thailand (Chiang Rai, Phitsanulok, Phang Nga; Luo et al. 2019) and southwest Yunnan, China (Su et al. 2016; Luo et al. 2018). Nonetheless, several new taxa were found sporadically in subtropical China, for example, *Distoseptispora martinii* (Xia et al. 2017), *D. suoluoensis* (Yang et al. 2018) and *D. bambusae* (Sun et al. 2020) in Guizhou Province and *D. euseptata* and *D. yunnansis* in northwest Yunnan (Li et al. 2021). The ongoing discovery of this taxa from other geographic regions in subtropical China will deepen our understanding of the species in this genus. In this study, we introduced another three new species of *Distoseptispora* from Jiangxi Province of subtropical China. It is interesting to note that all these species in subtropical China, except *D. yunjushanensis* and

D. martinii, formed a well-supported monophyletic clade in the phylogenetic tree and this clade was at the basal position (Fig. 1). *Distoseptispora yunjushanensis* and *D.martinii* were otherwise phylogenetically placed within other clades (Fig. 1) and, therefore, we suppose that other lineages might also comprise more *Distoseptispora* species distributed in subtropical China. Further discovery of *Distoseptispora* species in more extensive areas in subtropical and other regions of China are needed to be addressed if the phylogenetic position of species reflects their geographical and ecological distribution.

Distoseptisporaceae is a holomorphic group of *Sordariomycetes* that are saprobic on decaying wood and plant debris in terrestrial and freshwater habitats (Su et al. 2016). The genus *Distoseptispora* seems not to have specific habitat preferences, as most species were reported from submerged wood in freshwater habitats, while some were introduced from terrestrial habitats (Table 2). So far, only five species of *Distoseptispora* have been found on bamboo, two of them (*Distoseptispora bambusae* and *D. hydei*, Table 2) from terrestrial habitats, the other three (this study) from freshwater. There may be more species in this genus existing on bamboo waiting to be discovered and further studies are needed to clarify if a specific species in *Distoseptispora* is specific to its host.

Acknowledgements

We are grateful to Deng-Mei Fan and Yi Yang (Agricultural college, Jiangxi Agricultural University) for the valuable advice in the context of this study. This study was supported by the National Natural Science Foundation of China (NSFC 32070023 and NSFC 32060014), the Natural Science Foundation of Jiangxi Province (20151BAB214002) and Science and Technology Plan Project of Jiangxi Province (GJJ160417).

References

Chomnunti P, Hongsanan S, Aguirre-Hudson B, Tian Q, Peršoh D, Dhami MK, Alias AS, Xu J, Liu X, Stadler M, Hyde KD (2014) The sooty moulds. Fungal Diversity 66(1): 1–36. https://doi.org/10.1007/s13225-014-0278-5

Crous PW, Wingfield MJ, Lombard L, Roets F, Swart WJ, Alvarado P, Carnegie AJ, Moreno G, Luangsa-Ard J, Thangavel R, Alexandrova AV, Baseia IG, Bellanger JM, Bessette AE, Bessette AR, Delapeña-Lastra S, García D, Gené J, Pham THG, Heykoop M, Malysheva E, Malysheva V, Martín MP, Morozova OV, Noisripoom W, Overton BE, Rea AE, Sewall BJ, Smith ME, Smyth CW, Tasanathai K, Visagie CM, Adamčík S, Alves A, Andrade JP, Aninat MJ, Araújo RVB, Bordallo JJ, Boufleur T, Baroncelli R, Barreto RW, Bolin J, Cabero J, Cabo M, Cafà G, Caffot MLH, Cai L, Carlavilla JR, Chávez R, Decastro RRL, Delgat L, Deschuyteneer D, Dios MM, Domínguez LS, Evans HC, Eyssartier G, Ferreira BW, Figueiredo CN, Liu F, Fournier J, Galli-Terasawa LV, Gil-Durán C, Glienke C, Gonçalves MFM, Gryta H, Guarro J, Himaman W, Hywel-Jones N, Iturrieta-González I, Ivanushkina NE, Jargeat P, Khalid AN, Khan J, Kiran M, Kiss L, Kochkina GA, Kolařík M, Kubátová A, Lodge DJ, Loizides M, Luque D, Manjón JL, Marbach PAS, Massolajr NS,

Mata M, Miller AN, Mongkolsamrit S, Moreau PA, Morte A, Mujic A, Navarro-Ródenas A, Németh MZ, Nóbrega TF, Nováková A, Olariaga I, Ozerskaya SM, Palma MA, Petters-Vandresen DAL, Piontelli E, Popov ES, Rodríguez A, Requejo Ó, Rodrigues ACM, Rong IH, Roux J, Seifert KA, Silva BDB, Sklenář F, Smith JA, Sousa JO, Souza HG, Desouza JT, Švec K, Tanchaud P, Tanney JB, Terasawa F, Thanakitpipattana D, Torres-Garcia D, Vaca I, Vaghefi N, van Iperen AL, Vasilenko OV, Verbeken A, Yilmaz N, Zamora JC, Zapata M, Jurjević Ž, Groenewald JZ (2019) Fungal Planet description sheets: 951–1041. Persoonia 43(1): 223–425. https://doi.org/10.3767/persoonia.2019.43.06

Darriba D, Taboada GL, Doallo R, Posada D (2012) jModelTest 2: More models, new heuristics and parallel computing. Nature Methods 9(8): e772. https://doi.org/10.1038/nmeth.2109

Dong W, Hyde KD, Jeewon R, Doilom M, Yu XD, Wang GN, Liu NG, Hu DM, Nalumpang S, Zhang H (2021) Towards a natural classification of annulatascaceae-like taxa II: Introducing five new genera and eighteen new species from freshwater. Mycosphere : Journal of Fungal Biology 12(1): 1–88. https://doi.org/10.5943/mycosphere/12/1/1

Doyle JJ, Doyle JL (1987) A rapid DNA isolation procedure for small quantities of fresh leaf tissue. Phytochemical Bulletin 19: 11–15.

Hopple JJJ, Vilgalys R (1999) Phylogenetic relationships in the mushroom genus *Coprinus* and dark-spored allies based on sequence data from the nuclear gene coding for the large ribosomal subunit RNA: Divergent domains, outgroups, and monophyly. Molecular Phylogenetics and Evolution 13(1): 1–19. https://doi.org/10.1006/mpev.1999.0634

Hyde KD, Hongsanan S, Jeewon R, Bhat DJ, McKenzie EHC, Jones EBG, Phookamsak R, Ariyawansa HA, Boonmee S, Zhao Q, Abdel-Aziz FA, Abdel-Wahab MA, Banmai S, Chomnunti P, Cui BK, Daranagama DA, Das K, Dayarathne MC, deSilva NI, Dissanayake AJ, Doilom M, Ekanayaka AH, Gibertoni TB, Góes-Neto A, Huang SK, Jayasiri SC, Jayawardena RS, Konta S, Lee HB, Li WJ, Lin CG, Liu JK, Lu YZ, Luo ZL, Manawasinghe IS, Manimohan P, Mapook A, Niskanen T, Norphanphoun C, Papizadeh M, Perera RH, Phukhamsakda C, Richter C, Santiago ALCM, Drechsler-Santos ER, Senanayake IC, Tanaka K, Tennakoon TMDS, Thambugala KM, Tian Q, Tibpromma S, Thongbai B, Vizzini A, Wanasinghe DN, Wijayawardene NN, Wu HX, Yang J, Zeng XY, Zhang H, Zhang JF, Bulgakov TS, Camporesi E, Bahkali AH, Amoozegar MA, Araujo-Neta LS, Ammirati JF, Baghela A, Bhatt RP, Bojantchev D, Buyck B, Silva GA, Lima CLF, Oliveira RJV, Souza CAF, Dai YC, Dima B, Duong TT, Ercole E, Mafalda-Freire F, Ghosh A, Hashimoto A, Kamolhan S, Kang JC, Karunarathna SC, Kirk PM, Kytövuori I, Lantieri A, Liimatainen K, Liu ZY, Liu XZ, Lücking R, Medardi G, Mortimer PE, Nguyen TTT, Promputtha I, Raj KNA, Reck MA, Lumyong S, Shahzadeh-Fazeli SA, Stadler M, Soudi MR, Su HY, Takahashi T, Tangthirasunun N, Uniyal P, Wang Y, Wen TC, Xu JC, Zhang ZK, Zhao YC, Zhou JL , Zhu L (2016) Fungal diversity notes 367–490: Taxonomic and phylogenetic contributions to fungal taxa. Fungal Diversity 80: 1–270. https://doi.org/10.1007/s13225-016-0373-x

Hyde KD, Tennakoon DS, Jeewon R, Bhat DJ, Maharachchikumbura SS, Rossi W, Leonardi M, Lee HB, Mun HY, Houbraken J, Nguyen TT, Jeon SJ, Frisvad JC, Wanasinghe DN, Lücking R, Aptroot A, Cáceres ME, Karunarathna SC, Hongsanan S, Phookamsak R, Silva NI, Thambugala KM, Jayawardena RS, Senanayake IC, Boonmee S, Chen J, Luo ZL, Phukhamsakda C, Pereira OL, Abreu VP, Rosado AWC, Bart B, Randrianjohany E,

Hofstetter V, Gibertoni TB, Soares AMS, Plautz HL, Sotão HMP, Xavier WKS, Bezerra JDP, Oliveira TGL, Souza-Motta CM, Magalhães OMC, Bundhun D, Harishchandra D, Manawasinghe IS, Dong W, Zhang SN, Bao DF, Samarakoon MC, Pem D, Karunarathna A, Lin CG, Yang J, Perera RH, Kumar V, Huang SK, Dayarathne MC, Ekanayaka AH, Jayasiri SC, Xiao YP, Konta S, Niskanen T, Liimatainen K, Dai YC, Ji XH, Tian XM, Mešić A, Singh SK, Phutthacharoen K, Cai L, Sorvongxay T, Thiyagaraja V, Norphanphoun C, Chaiwan N, Lu YZ, Jiang HB, Zhang JF, Abeywickrama PD, Aluthmuhandiram JVS, Brahmanage RS, Zeng M, Chethana T, Wei DP, Réblová M, Fournier J, Nekvindová J, Barbosa RN, Santos JEF, Oliveira NT, Li GJ, Ertz D, Shang QJ, Phillips AJL, Kuo CH, Camporesi E, Bulgakov TS, Lumyong S, Jones EBG, Chomnunti P, Gentekaki E, Bungartz F, Zeng XY, Fryar S, Tkalčec Z, Liang JM, Li GS, Wen TC, Singh PN, Gafforov Y, Promputtha I, Yasanthika E, Goonasekara ID, Zhao RL, Zhao Q, Kirk PM, Liu JK, Yan JY, Mortimer PE, Xu JC, Doilom M (2019) Fungal diversity notes 1036–1150: Taxonomic and phylogenetic contributions on genera and species of fungal taxa. Fungal Diversity 96(1): 1–242. https://doi.org/10.1007/s13225-019-00429-2

Hyde KD, Norphanphoun C, Maharachchikumbura SSN, Bhat DJ, Jones EBG, Bundhun D, Chen YJ, Bao DF, Boonmee S, Calabon MS, Chaiwan N, Chethana KWT, Dai DQ, Dayarathne MC, Devadatha B, Dissanayake AJ, Dissanayake LS, Doilom M, Dong W, Fan XL, Goonasekara ID, Hongsanan S, Huang SK, Jayawardena RS, Jeewon R, Karunarathna A, Konta S, Kumar V, Lin CG, Liu JK, Liu NG, Luangsaard J, Lumyong S, Luo ZL, Marasinghe DS, McKenzie EHC, Niego AGT, Niranjan M, Perera RH, Phukhamsakda C, Rathnayaka AR, Samarakoon MC, Samarakoon SMBC, Sarma VV, Senanayake IC, Shang QJ, Stadler M, Tibpromma S, Wanasinghe DN, Wei DP, Wijayawardene NN, Xiao YP, Yang J, Zeng XY, Zhang SN, Xiang MM (2020) Refined families of *Sordariomycetes.* Mycosphere : Journal of Fungal Biology 11(1): 305–1059. https://doi.org/10.5943/mycosphere/11/1/7

Hyde KD, Bao DF, Hongsanan S, Chethana KWT, Yang J, Suwannarach N (2021) Evolution of freshwater Diaporthomycetidae (Sordariomycetes) provides evidence for five new orders and six new families. Fungal Diversity 107(1): 71–105. https://doi.org/10.1007/s13225-021-00469-7

Kumar S, Stecher G, Tamura K (2016) Mega7: Molecular evolutionary genetic analysis version 7.0 for bigger datasets. Molecular Biology and Evolution 33(7): 1870–1874. https://doi.org/10.1093/molbev/msw054

Li WL, Liu ZP, Zhang T, Dissanayake AJ, Luo ZL, Su HY, Liu JK (2021) Additions to *Distoseptispora* (Distoseptisporaceae) associated with submerged decaying wood in China. Phytotaxa 520(1): 75–86. https://doi.org/10.11646/phytotaxa.520.1.5

Luo ZL, Hyde KD, Liu JK, Bhat DJ, Bao DF, Li WL, Su HY (2018) Lignicolous freshwater fungi from China II: Novel *Distoseptispora* (Distoseptisporaceae) species from northwestern Yunnan Province and a suggested unified method for studying lignicolous freshwater fungi. Mycosphere: Journal of Fungal Biology 9(3): 444–461. https://doi.org/10.5943/mycosphere/9/3/2

Luo ZL, Hyde KD, Liu JK, Maharachchikumbura SSN, Jeewon R, Bao DF, Bhat DJ, Lin CG, Li WL, Yang J, Liu NG, Lu YZ, Jayawardena RS, Li JF, Su HY (2019) Freshwater *Sordariomycetes.* Fungal Diversity 99(1): 451–660. https://doi.org/10.1007/s13225-019-00438-1

Madeira F, Park YM, Lee J, Buso N, Gur T, Madhusoodanan N, Basutkar P, Tivey ARN, Potter SC, Finn RD, Lopez R (2019) The EMBL-EBI search and sequence analysis tools APIs in 2019. Nucleic Acids Research 47(W1): W636–W641. https://doi.org/10.1093/nar/gkz268

Mckenzie EHC (1995) Dematiaceous Hyphomycetes on Pandanaceae. V. *Sporidesmium* sensu lato. Mycotaxon 56: 9–29.

Miller MA, Pfeiffer W, Schwartz T (2010) Creating the CIPRES Science Gateway for inference of large phylogenetic trees. In: Proceedings of the 2010 Gateway Computing Environments Workshop (GCE), Institute of Electrical and Electronics Engineers, New Orleans, Louisiana, 1–8. https://doi.org/10.1109/GCE.2010.5676129

Monkai J, Boonmee S, Ren GC, Wei DP, Phookamsak R, Mortimer PE (2020) *Distoseptispora hydei* sp. nov. (Distoseptisporaceae), a novel lignicolous fungus on decaying bamboo in Thailand. Phytotaxa 459(2): 93–107. https://doi.org/10.11646/phytotaxa.459.2.1

Phookamsak R, Hyde KD, Jeewon R, Bhat DJ, Gareth Jones E, Maharachchikumbura SSN, Raspé O, Karunarathna SC, Wanasinghe DN, Hongsanan S, Doilom M, Tennakoon DS, Machado AR, Firmino AL, Ghosh A, Karunarathna A, Mešić A, Dutta AK, Thongbai B, Devadatha B, Norphanphoun C, Senwanna C, Wei DP, Pem D, Ackah FK, Wang GN, Jiang HB, Madrid H, Lee HB, Goonasekara ID, Manawasinghe IS, Kušan I, Cano J, Gené J, Li JF, Das K, Acharya K, Raj KNA, Latha KPD, Chethana KWT, He MQ, Dueñas M, Jadan M, Martín MP, Samarakoon MC, Dayarathne MC, Raza M, Park MS, Telleria MT, Chaiwan N, Matočec N, de Silva NI, Pereira OL, Singh PN, Manimohan P, Uniyal P, Shang QJ, Bhatt RP, Perera RH, Alvarenga RLM, Nogal-Prata S, Singh SK, Vadthanarat S, Oh SY, Huang SK, Rana S, Konta S, Paloi S, Jayasiri SC, Jeon SJ, Mehmood T, Gibertoni TB, Nguyen TTT, Singh U, Thiyagaraja V, Sarma VV, Dong W, Yu XD, Lu YZ, Lim YW, Chen Y, Tkalčec Z, Zhang ZF, Luo Z, Daranagama DA, Thambugala KM, Tibpromma S, Camporesi E, Bulgakov TS, Dissanayake AJ, Senanayake IC, Dai DQ, Tang LZ, Khan S, Zhang H, Promputtha I, Cai L, Chomnunti P, Zhao RL, Lumyong S, Boonmee S, Wen TC, Mortimer PE, Xu JC (2019) Fungal diversity notes 929–1035: Taxonomic and phylogenetic contributions on genera and species of fungi. Fungal Diversity 95(1): 1–273. https://doi.org/10.1007/s13225-019-00421-w

Phukhamsakda C, Mckenzie EHC, Phillips AJL, Jones EBG, Bhat DJ, Marc S, Bhunjun CS, Wanasinghe DN, Thongbai B, Camporesi E, Ertz D, Jayawardena RS, Perera RH, Ekanayake AH, Tibpromma S, Doilom M, Xu J, Hyde KD (2020) Microfungi associated with *Clematis* (Ranunculaceae) with an integrated approach to delimiting species boundaries. Fungal Diversity 102(1): 1–203. https://doi.org/10.1007/s13225-020-00448-4

Rambaut A (2018) FigTree v1.4.4: Tree figure drawing tool. https://github.com/rambaut/figtree/releases

Réblová M (1999) Studies in *Chaetosphaeria* sensu lato III. *Umbrinosphaeria* gen. nov. and *Miyoshiella* with *Sporidesmium* anamorphs. Mycotaxon 71: 13–43.

Ronquist F, Teslenko M, Van Der Mark P, Ayres DL, Darling A, Höhna S, Larget B, Liu L, Suchard MA, Huelsenbeck JP (2012) MrBayes 3.2: Efficient Bayesian phylogenetic inference and model choice across a large model space. Systematic Biology 61(3): 539–542. https://doi.org/10.1093/sysbio/sys029

Shenoy BD, Jeewon R, Wu WPP, Bhat DJ, Hyde KD (2006) Ribosomal and RPB2 DNA sequence analyses suggest that *Sporidesmium* and morphologically similar genera are polyphyletic. Mycological Research 110(8): 916–928. https://doi.org/10.1016/j.mycres.2006.06.004

Shoemaker RA, White GP (1985) *Lasiosphaeria caesariata* with *Sporidesmium hormiscioides* and *L. triseptata* with *S. adscendens.* Sydowia 38: 278–283.

Song HY, Sheikha AF, Zhai ZJ, Zhou JP, Chen MH, Huo GH, Huang XG, Hu DM (2020) *Distoseptispora longispora* sp. nov. from freshwater habitats in China. Mycotaxon 135(3): 513–523. https://doi.org/10.5248/135.513

Stamatakis A (2014) RAxML version 8: A tool for phylogenetic analysis and post-analysis of large phylogenies. Bioinformatics (Oxford, England) 30(9): 1312–1313. https://doi.org/10.1093/bioinformatics/btu033

Su HY, Hyde KD, Maharachchikumbura SSN, Ariyawansa HA, Luo ZL, Promputtha I, Tian Q, Lin CG, Shang QJ, Zhao YC, Chai HM, Liu XY, Bahkali AH, Bhat JD, McKeenzie EHC, Zhou DQ (2016) The families Distoseptisporaceae fam. nov., Kirschsteiniotheliaceae, Sporormiaceae and Torulaceae, with new species from freshwater in Yunnan Province, China. Fungal Diversity 80(1): 375–409. https://doi.org/10.1007/s13225-016-0362-0

Subramanian CV (1992) A reassessment of *Sporidesmium* (hyphomycetes) and some related taxa. Proceedings of the Indian National Science Academy B58: 179–190.

Sun YR, Goonasekara ID, Thambugala KM, Jayawardena RS, Wang Y, Hyde KD (2020) *Distoseptispora bambusae* sp. nov. (Distoseptisporaceae) on bamboo from China and Thailand. Biodiversity Data Journal 8: e53678. https://doi.org/10.3897/BDJ.8.e53678

Tibpromma S, Hyde KD, McKenzie EHC, Bhat DJ, Phillips AJL, Wanasinghe DN, Samarakoon MC, Jayawardena RS, Dissanayake AJ, Tennakoon DS, Doilom M, Phookamsak R, Tang AMC, Xu JC, Mortimer PE, Promputtha I, Maharachchikumbura SSN, Khan S, Karunarathna SC (2018) Fungal diversity notes 840–928: Micro-fungi associated with Pandanaceae. Fungal Diversity 93(1): 1–160. https://doi.org/10.1007/s13225-018-0408-6

White TJ, Bruns TD, Lee SB, Taylor JW, Innis MA, Gelfand DH, Sninsky JJ (1990) Amplification and direct sequencing of fungal ribosomal RNA genes for phylogenetics. In: Innis MA, Gelfand DH, Sninsky JJ, White TJ (Eds) PCR protocols: a guide to methods and applications. Academic, San Diego, 315–322. https://doi.org/10.1016/B978-0-12-372180-8.50042-1

Wong KMK, Goh TK, Hodgkiss IJ, Hyde KD, Ranghoo VM, Tsui CKM, Ho WH, Wong SW, Yuen TK (1998) Role of fungi in freshwater ecosystems. Biodiversity and Conservation 7(9): 1187–1206. https://doi.org/10.1023/A:1008883716975

Xia JW, Ma YR, Li Z, Zhang XG (2017) Acrodictys-like wood decay fungi from southern China, with two new families Acrodictyaceae and Junewangiaceae. Scientific Reports 7(1): e7888. https://doi.org/10.1038/s41598-017-08318-x

Yang J, Maharachchikumbura SSN, Liu JK, Hyde KD, Jones EBG, Al-Sadi AM, Liu ZY (2018) *Pseudostanjehughesia aquitropica* gen. et sp. nov. and *Sporidesmium* sensu lato species from freshwater habitats. Mycological Progress 17(5): 591–616. https://doi.org/10.1007/s11557-017-1339-4

MycoKeys 88: 55–78 (2022)
doi: 10.3897/mycokeys.88.73951
https://mycokeys.pensoft.net

RESEARCH ARTICLE

A peer-reviewed open-access journal
MycoKeys
Launched to accelerate biodiversity research

Hemiaustroboletus, a new genus in the subfamily Austroboletoideae (Boletaceae, Boletales)

Olivia Ayala-Vásquez[1], Jesús García-Jiménez[1], Elvira Aguirre-Acosta[2], Rigoberto Castro-Rivera[3], Rodolfo Enrique Ángeles-Argáiz[2], Ángel Emmanuel Saldivar[4], Roberto Garibay-Orijel[2]

1 *Tecnológico Nacional de México, Instituto Tecnológico de Ciudad Victoria, Blvd. Emilio Portes Gil #1301 Pte., Ciudad Victoria, Tamaulipas, CP 87010, Mexico* **2** *Instituto de Biología, Universidad Nacional Autónoma de México, Circuito exterior s/n Ciudad Universitaria, Ciudad de México, CP 04510, Mexico* **3** *CIBA, Instituto Politécnico Nacional, Tlaxcala, CP 90700, Mexico* **4** *Departamento de Botánica y Zoología, Universidad de Guadalajara, Zapopan, Jalisco, CP 45101, Mexico*

Corresponding author: Roberto Garibay-Orijel (rgaribay@ib.unam.mx)

Academic editor: Olivier Raspé | Received 4 September 2021 | Accepted 9 March 2022 | Published 30 March 2022

Citation: Ayala-Vásquez O, García-Jiménez J, Aguirre-Acosta E, Castro-Rivera R, Ángeles-Argáiz RE, Saldivar AE, Garibay-Orijel R (2022) *Hemiaustroboletus*, a new genus in the subfamily Austroboletoideae (Boletaceae, Boletales). MycoKeys 88: 55–78. https://doi.org/10.3897/mycokeys.88.73951

Abstract

The present study describes *Hemiaustroboletus* **gen. nov.** in the subfamily Austroboletoideae (Boletaceae). *Hemiaustroboletus* is supported by morphological and molecular data using LSU and RPB2 regions. Additionally, its geographic distribution and intraspecific variation were inferred using ITS sequences. The genus is characterised by pileate-stipitate basidiomata; purple, brown, reddish-brown, orange-brown to dark brown vinaceous pileus; whitish or lilac to vinaceous context and a subclavate stipe. Microscopically, it is characterised by ornamented, slightly verrucose, cracked to perforated brown basidiospores. Two species are described within the genus, *Hemiaustroboletus vinaceobrunneus* **sp. nov.** and *H. vinaceus* **sp. nov.** *Hemiaustroboletus vinaceus* **sp. nov.** is morphologically similar to *Austroboletus gracilis*, which suggests they may have been confused in the past. This study presents the phylogenetic placement, microscopic structures, detailed morphological descriptions and illustrations of both new species.

Keywords

Mexico, mycodiversity, neotropics, new taxa

Introduction

Boletaceae is the most diverse family within the Boletales; it has a wide distribution in both temperate and tropical regions (Binder and Hibbett 2006; Wu et al. 2014). Most species of this family are ectomycorrhizal with members of Betulaceae, Casuarinaceae, Dipterocarpaceae, Ericaceae, Fabaceae, Fagaceae, Mimosaceae, Myrtaceae, Pinaceae, Polygonaceae, and Salicaceae (Tedersoo et al. 2010; Smith et al. 2013; Wu et al. 2016). Currently, 98 genera are recognised in this family (He et al. 2019; Vadthanarat et al. 2019; Hosen and Yang 2021). Its members are characterised by fleshy, epigeous pileate-stipitate basidiomata or hypogeous to subhypogeous gastroid basidiomata, with tubular or lamellar hymenophore; elliptical, cylindrical, fusoid, subfusoid, ovoid, subglobose to globose, smooth or ornamented basidiospores; spore ornamentation ranging from striated, reticulate, echinulate, filiform and perforated to verrucose (Singer et al. 1991; Wu et al. 2014; Halling et al. 2015; Ayala-Vásquez et al. 2018).

Wu et al. (2014) proposed six subfamilies for Boletaceae, of which Austroboletoideae includes *Austroboletus* (Corner) Wolfe, *Fistulinella* Henn., *Mucilopilus* Wolfe and *Veloporphyrellus* L.D. Gómez & Singer, with *Austroboletus* as the type genus. This subfamily is distinguished by pileate-stipitate basidiomes; smooth, furfuraceous, tomentose, dry or viscous pileus, with or without a marginal veil and whitish context that does not change colour when cut. The hymenophore is tubular, whitish or pink with purple tinge, immutable or rarely brown when cut. The stipe is smooth, reticulate or squamose with a whitish basal mycelium. The basidiospores are smooth or ornamented, perforated, verrucose to smooth, grey-violet, yellowish, yellow brown, ochraceous in potassium hydroxide (KOH) and yellow-brown, yellow-cinnamon to ochraceous in Melzer's reagent. The pileipellis is formed by a trichoderm or ixotrichoderm. The hymenophoral trama is boletoid. Austroboletoideae species are mainly associated with Fagaceae and Pinaceae hosts in temperate, subtropical to tropical regions.

In recent years, various authors (Wu et al. 2014; Wu et al. 2016; Gelardi et al. 2020; Kuo and Ortiz-Santana 2020) have recognised the polyphyly of *Austroboletus*, which is divided into the *Austroboletus* s.s., *Austroboletus* s.l. and the *A. gracilis* s.l. independent clades. This study focuses on the phylogenetic placement and taxonomy of the *A. gracilis* s.l. clade, placing it in the new genus *Hemiaustroboletus* with two new species, *Hemiaustroboletus vinaceobrunneus* and *H. vinaceus.*

Materials and methods

To resolve the systematics and taxonomy of the new genus *Hemiaustroboletus*, we conducted an exhaustive sampling of an area with high bolete diversity according to García-Jiménez et al. (2013). The sampling was carried out over the last 10 years including the different biogeographic areas of Mexico: Nearctic, Neovolcanic Axis and Neotropic. The collection trips were conducted in the States of Chiapas, Chihuahua,

Estado de Mexico, Jalisco, Michoacan and Oaxaca, in six vegetation types in temperate and subtropical forests during the rainy season from June to October from 2010 to 2019. The samples were characterised at macro- and micromorphological level and three genetic markers were sequenced and analysed.

Morphological study

Morphological characters were described according to Largent (1986) and Lodge et al. (2004). Chemical reactions with KOH and ammonium hydroxide (NH_4OH) were characterised. Photographs of basidiomata were taken *in situ*, as well as data on the botanical composition of the sites. The colours for taxonomic descriptions were based on Kornerup and Wanscher (1978). Microscopic characters of 30 basidiospores, basidia, pleurocystidia, cheilocystidia, pileipellis cells and stipitipellis were measured by optical microscopy (Carl Zeiss GmbH 37081, Germany). The Q index (length/width) was estimated for the basidiospores. Ornamentation of basidiospores was observed by scanning electron microscopy (SEM) (Hitachi Su 1510, Hitachi, Japan). The specimens were deposited at the "Herbario Nacional de México" of the "Instituto de Biología, Universidad Nacional Autónoma de México" (MEXU), at the "Herbario José Castillo Tovar del Tecnológico de Ciudad Victoria" (ITCV) and at the "Herbario del Instituto de Botánica, Universidad de Guadalajara" (IBUG).

DNA Extraction, PCR and Sequencing

Samples of dehydrated basidiomata were used for DNA extraction. The DNA was extracted using the DNeasy Power-Soil kit (QIAGEN). Cell lysis was performed by grinding samples in mortar with liquid nitrogen. Three nuclear loci (ITS, LSU and RPB2) were amplified with Platinum Taq DNA Polymerase (Invitrogen-Thermo Fisher Scientific) and Taq & Load PCR Mastermix (MP Biomedicals) in a thermocycler (BIO-RAD). The PCR parameters were as follows: 95 °C initial denaturation for 4 min; 35 cycles of denaturation at 94 °C for 60 s, alignment at 54 °C for 60 s, extension at 72 °C for 60 s and a final extension at 72 °C for 10 min. The primers ITS1/ITS4 (White et al. 1990) were used for the ITS region; LROR/LR5 (Vilgalys and Hester 1990) for LSU; and RPB2-B-F2/RPB2-B-R (Wu et al. 2014) for the partial RPB2 gene. The amplification was examined by 1% agarose gel electrophoresis; gels were stained with GelRed (Biotium) and observed under an UVP Multidoc-It transilluminator (Analytikjena). Only PCR products generated with Taq-Platinum required LB loading buffer. PCR products with successful amplification were cleaned with ExoSAP-IT (Thermo Fisher Scientific) diluted 1:1 with ddH_2O and incubated at 37 °C for 45 min and 80 °C for 15 min. Sanger sequencing was performed at the "Laboratorio de secuenciación genómica de la biodiversidad y la salud, Instituto de Biología, Universidad Nacional Autónoma de México". Samples were sequenced in both directions with PCR primers using BigDye Terminator v.3.1 (Thermo Fisher Scientific).

Phylogenetic analyses

Hemiaustroboletus species produce scarce fruit bodies; from 606 Boletales specimens collected, just eight (1.32%) belonged to this genus. Three materials corresponded to *H. vinaceus*, four to *H. vinaceobrunneus* and two were determined as *Hemiaustroboletus* sp. The three loci of the holotype of *H. vinaceus* (IBUG-AES334) and one more collection (ITCV-AV524, MEXU-30103) were sequenced; we only recovered ITS and RPB2 loci from a third specimen (IBUG-AES364) (Table 1). The three loci of the holotype of *H. vinaceobrunneus* (ITCV-AV868, MEXU-30051) and one additional material (ITCV-AV845, MEXU-30052) were sequenced; only the ITS and RPB2 loci were sequenced for a third collection (ITCV-AV1168, MEXU-30053). ITS locus was also sequenced for one *Hemiaustroboletus* sp. collection (ITCV-AK_3508) (Table 1).

We conducted two sets of phylogenetic analyses, the first one to reconstruct the phylogenetic relationships of *Hemiaustroboletus* gen. nov. and the second one to complement its taxonomic concept with biogeographic and ecological information. The first analysis used the LSU and RPB2 markers in a concatenated matrix, while the second used ITS in order to leverage GenBank data.

Individual LSU and RPB2 alignments were concatenated into a single matrix (83 taxa, 1335 characters) with GENEIOUS PRIME V.2019.0.4 (Biomatters Ltd). Alignments and concatenation were performed with the MAFFT algorithm (Katoh et al. 2002) using GENEIOUS PRIME V.2019.0.4. Sequences representing the subfamilies Austroboletoideae, Boletoideae and Xerocomoideae came from: 83 LSU sequences, 56 rpb2 sequences, 30 ITS sequences from published works and unpublished sequences available in GenBank (Table 1).

The best-fit evolutionary model was estimated with JMODELTEST 2 (Darriba et al. 2012) using CIPRES SCIENCE GATEWAY V. 3.3 (Miller et al. 2010) for each marker separately. For all three markers, the best model was GTR+G+I. We used the LSU-RPB2 dataset to make evolutionary inferences within Austroboletoideae and the ITS dataset to make biogeographic/ecological inferences for *Hemiaustroboletus*.

The phylogenetic hypotheses (LSU-RPB2) were constructed with Bayesian Inference (BI) and Maximum Likelihood (ML) on a partitioned alignment with same evolutionary model for both markers. Bayesian posterior probability phylogeny was performed using MrBayes algorithm (Ronquist et al. 2012) using two separate Monte Carlo four chains starting from random trees for 10 million generations each (final standard deviation $\pm$ 0.224), trees were sampled every 100 generations. The first 25% of samples were discarded as burn-in. ML analyses were performed using the RAxML algorithm (Stamatakis 2014) with 1000 bootstrap replicates. For both analyses, members of subfamilies Boletoideae and Xerocomoideae were used as outgroup. The second analysis (ITS) was performed with the same parameters including *Veloporphyrellus* and *Austroboletus* without outgroup. The resulting phylogenetic trees were edited with FIGTREE V.1.4.3 (Rambaut 2009).

Average intrageneric and intergeneric nucleotide similarities between the genera within Austroboletoidae were obtained separately for RPB2, LSU and ITS alignments

as follows. For each alignment a nucleotide similarity matrix was computed in GENEIOUS 10.2.6 (Biomatters Ltd). Sequences belonging to genera outside Austroboletoidae were removed and then the mean nucleotide similarity was calculated amongst all pairwise comparisons between sequences of each pair of genera.

Table 1. List of species, geographic origin and GenBank accession numbers of ITS, LSU and RPB2 sequences used in the phylogenetic analyses.

Taxa	Voucher	Country	ITS	LSU	RPB2	Reference
Aureoboletus betula		USA		MK601736	MK766298	Kuo and Ortiz-Santana (2020)
A. garciae	MEXU:29006	Mexico		MH337251	MT228983	Haelewaters et al. (2020)
Austroboletus amazonicus	1839_ AMV	Colombia	KF937307	KF714508		Vasco-Palacios et al. (2014)
A. amazonicus	1914_ AMV	Colombia	KF937308	KF714509		Vasco-Palacios et al. (2014)
A. austrovirens	BRI:AQ0795791	Australia	KP242211	KP242225	KP242133	Fechner et al. (2017)
A. austrovirens	BRI:AQ0794622	Australia	KP242210			Fechner et al. (2017)
A. austrovirens	MEL:2382920a	Australia		KP242284	KP242113	Fechner et al. (2017)
A. austrovirens	BRI:AQ0794609	Australia		KP242226	KP242131	Fechner et al. (2017)
A. austrovirens	BRI:AQ0794171	Australia		KP242227	KP242133	Fechner et al. (2017)
A. eburneus	REH9487	Australia		JX889668		Vasco-Palacios et al. (2014)
A. dictyotus	HKAS59804	China		JX901138		Hosen et al. (2013)
A. fusisporus	HKAS75207	China	JX889719	JX889720		Hosen et al. (2013)
A. fusisporus	JXSB0351	China		MK765810		GenBank
A. gracilis	112-96	USA		DQ534624		Binder and Hibbett (2006)
A. gracilis	TM03_434	Canada		EU522815		Porter et al. (2008)
A. gracilis var. *gracilis*	CFMR BOS-547	USA		MK601715	MK766277	Kuo and Ortiz-Santana (2020)
A. gracilis var. *flavipes*	CFMR BOS-562	USA		MK601714		Kuo and Ortiz-Santana (2020)
A. gracilis	ACAD11344F	Canada	MH465078			Young et al. (2019)
A. gracilis	SFC20140823-02	South Korea	MN794901			GenBank
A. gracilis	NAMA 2017-106	USA	MH979242			GenBank
A. gracilis	310751	México	MH167935			GenBank
A. gracilis	CNV35	USA	MT345212			Victoroff (2020)
A. cf. *gracilis*	JLF6600	USA	MN174796			GenBank
A. lacunosus	REH9146	Australia		JX889669		Vasco-Palacios et al. (2014)
A. lacunosus	MEL2233764	Australia		KC552056		GenBank
A. mucosus	TH6300	Guyana		AY612798		Drehmel et al. (2008)
A. mutabilis	BRI:AQ0795793	Australia	KP242169	KP242263	KP242098	Fechner et al. (2017)
A. mutabilis	BRI:AQ0669270	Australia		KP242266	KP242097	Fechner et al. (2017)
A. mutabilis	BRI:AQ0796266	Australia		KP242262	KP242099	Fechner et al. (2017)
A. niveus	312	New Zealand		DQ534622		Binder and Hibbett (2006)
A. niveus	MEL2053830	Australia	KC552016	KC552058		Orihara et al. (2016)
A. novae-zelandiae	PDD:72542	New Zealand	HM060327			GenBank
A. rarus	BRI:AQ0794045	Australia	KP242197	KP242236	KP242086	Fechner et al. (2017)
A. rostrupii	TH8189	Guyana	JN168683			Smith et al. (2011)
Austroboletus sp.	BRI:AQ0794156	Australia		KP242235	KP242115	GenBank
Austroboletus sp.	BRI:AQ0794222	Australia		KP242234	KP242106	GenBank
Austroboletus sp.	BRI:AQ0794271	Australia		KP242259	KP242102	GenBank
Austroboletus sp.	HKAS 57756	China		KF112383	KF112764	Wu et al. (2014)
Austroboletus sp.	HKAS 59624	China		KF112485	KF112765	Wu et al. (2014)
Austroboletus sp.	HKAS 74743	China		KT990527	KT990367	Wu et al. (2014)
Austroboletus sp.	PERTH6658407	Australia		KP242277	KP242126	GenBank
Austroboletus sp.	BRI:AQ0794242	Australia			KP242087	GenBank
Austroboletus sp.	OR0891	Thailand			MH614753	Vadthanarat et al. (2019)

Taxa	Voucher	Country	ITS	LSU	RPB2	Reference
Austroboletus sp.	OTA-FUNNZ2013434	New Zealand			KP191670	GenBank
A. subflavidus	JBSD130771	Dominican Republic		MT580902	MT590754	Gelardi et al. (2020)
A. subflavidus	JBSD130772	Dominican Republic		MT580903	MT590755	Gelardi et al. (2020)
A. subflavidus	CFMR BZ-3178	Belize		MK601716	MK766278	Kuo and Ortiz-Santana (2020)
A. subvirens	KPM-NC-0017836	Japan		JN378518		Orihara et al. (2012)
A. viscidoviridis	Perth 7588682	Australia		KP242282	KP242128	Fechner et al. (2017)
Boletellus indistinctus	HKAS77623	China		KT990531	KT990371	Wu et al. (2016)
Boletellus sp.	HKAS80554			KT990535	KT990374	Wu et al. (2016)
Boletus harrisonii	MICH: KUO-09071204	USA		MK601718	MK766280	Kuo and Ortiz-Santana (2020)
Boletus sp.	dd08055	China	FJ810161			GenBank
Boletus sp.	MHM165	Mexico	EU569243			Morris et al. (2008)
Boletales sp.	B0229	Canada	KY825985			GenBank
Fistulinella campinaranae var. *scrobiculata*	AMV1980	Colombia		KF714520		Vasco-Palacios et al. (2014)
F. gloeocarpa	JBSD130769	Dominican Republic		MT580906	MT590756	Gelardi et al. (2020)
F. gloeocarpa	CFMR:B4	Bahamas		MT580904		Gelardi et al. (2020)
F. gloeocarpa	CFMR:B10	Bahamas		MT580905		Gelardi et al. (2020)
F. prunicolor	REH9502	Australia		JX889648	MG212630	Halling et al. (2012)
F. olivaceoalba	HKAS 53432	Vietnam		MH745969		GenBank
F. olivaceoalba	LE312004	Vietnam		MH718396		GenBank
F. ruschii	CORT:TJB-8329	USA		MT580907		Gelardi et al. (2020)
F. viscida	238 25S	New Zealand		AF456826		Vasco-Palacios et al. (2014)
F. cinereoalba	TH8471	Guyana		GQ477439	KT339237	GenBank
Hemiaustroboletus vinaceobrunneus	**MEXU_30051 Holotype**	**Mexico**	**MN178797**	**MN200222**	**MT887617**	**This study**
H. vinaceobrunneus	**MEXU_30052 Isotype**	**Mexico**	**MN178798**	**MN200223**	**MT887618**	**This study**
H. vinaceobrunneus	**MEXU_30053 Isotype**	**Mexico**	**MN178799**		**MT887619**	**This study**
H. vinaceus	**AV524 Paratype**	**Mexico**	**MN178802**	**MN200225**	**MT887622**	**This study**
H. vinaceus	**AES334 Holotype**	**Mexico**	**MN178800**	**MN200224**	**MT887620**	**This study**
H. vinaceus	**AES364 Isotype**	**Mexico**	**MN178801**		**MT887621**	**This study**
***Hemiaustroboletus* sp.**	**AK_3508**	**Mexico**	**MN178803**			**This study**
Hemileccinum subglabripes	MICH: KUO-08301402	USA		MK601739	MK766301	Kuo and Ortiz-Santana (2020)
Hortiboletus rubellus	MICH: KUO-06081002	USA		MK601741	MK766303	Kuo and Ortiz-Santana (2020)
H. amygdalinus	HKAS54166	China		KT990581	KT990416	Wu et al. (2016)
Hourangia cheoi	Tang572	China		KP136953	KP136985	Zhu et al. (2015)
Imleria badia	MICH: KUO-09110404	USA		MK601743	MK766305	Kuo and Ortiz-Santana (2020)
Mucilopilus castaneiceps	HKAS 75045	China		KF112382	KF112735	Wu et al. (2016)
M. castaneiceps	HKAS50338	China		KT990555	KT990391	Wu et al. (2016)
M. castaneiceps	HKAS71039	China		KT990547	KT990385	Wu et al. (2016)
Parvixerocomus pseudoaokii	HKAS 80480	China		KP658468	KP658470	Wu et al. (2016)
Porphyrellus castaneus	HKAS52554	China		KT990697	KT990502	Wu et al. (2016)
P. porphyrosporus	MB97-023	Germany		DQ534643	GU187800	Binder and Hibbett (2006)
P. orientifumosipes	HKAS53372	China		KT990629	KT990461	Wu et al. (2016)
Tengioboletus sp.	HKAS 77869	China		KT990658	KT990483	Wu et al. (2016)

Taxa	Voucher	Country	ITS	LSU	RPB2	Reference
Strobilomyces confusus	CFMR:DR-3024	Dominican Republic		MK601809	MK766365	Kuo and Ortiz-Santana (2020)
Tylopilus felleus	CFMR: BOS-780	USA		MK601814	MK766370	Kuo and Ortiz-Santana (2020)
T. sordidus	MICH: KUO-06240801			MK601815	MK766371	Kuo and Ortiz-Santana (2020)
Tylopilus sp.	HKAS 50229	China		KF112423	KF112734	Wu et al. (2014)
Uncultured mycorrhizal	BOLETE1	USA	AY656925			Walker et al. (2005)
Uncultured mycorrhizal	clon N_1	South Korea	AB571507			Obase et al. (2012)
Uncultured *Boletus*	isolate: YM490	Japan	LC175482			Miyamoto et al. (2018)
Uncultured *Boletus*	Clon ZE2	China	GU391428			Ma et al. (2010)
Veloporphyrellus alpinus	KUN:HKAS68301	China		JX984537		Li et al. (2014)
V. pseudovelatus	KUN: HKAS59444	China		JX984542		Li et al. (2014)
V. pseudovelatus	KUN:HKAS52244	China		JX984531		Li et al. (2014)
V. conicus	CFMR:BZ1670	Belize		JX984543		Li et al. (2014)
V. conicus	CFMR:BZ1705	Belize		JX984544		Li et al. (2014)
V. pantoleucus	F:Gomez21232	Costa Rica		JX984548		Li et al. (2014)
V. velatus	KUN: HKAS63668	China		JX984546		Li et al. (2014)
V. aff. *velatus*	HKAS 57490	China		KF112380	KF112733	Wu et al. (2014)
V. vulpinus	LE315544	Vietnam	MN511177	MN511170		GenBank
V. vulpinus	LE315549	Vietnam	MN511180			GenBank
V. vulpinus	LE315546	Vietnam	MN511179			GenBank
V. vulpinus		Vietnam	MN511178			GenBank
Xerocomellus chrysenteron	HKAS:56494	China		KF112357	KF112685	Wu et al. (2014)

Results

Phylogenetic analyses of LSU-RPB2 concatenated alignment showed that *Hemiaustroboletus* is a supported monophyletic group, belonging to the Austroboletoideae (BPP = 0.98, MLB = 47%). Additionally, *H. vinaceobrunneus* (BPP = 1, MLB = 100%) and *H. vinaceus* (BPP = 1, MLB = 96%) were supported monophyletic species (Fig. 1). The ITS analyses showed that *Hemiaustroboletus* forms ectomycorrhizae with Fagaceae, particularly *Quercus* and also with *Pinus* in temperate, subtropical and tropical forests. It distributes in North America (Mexico, USA and Canada) and Asia (China, Japan and Korea) (Fig. 2). These analyses also showed that *Austroboletus gracilis* s.l. is a widely-used name mainly applied to designate *Hemiaustroboletus* species.

Taxonomy

***Hemiaustroboletus* Ayala-Vásquez, García-Jiménez & Garibay-Orijel, gen. nov.**
MycoBank No: 838460

Diagnosis. *Hemiaustroboletus* is characterised by small and medium basidiomata with slightly ornamented pileus surface, stipe fibrillose to striated without veil, slightly verrucose or cracked to pitted basidiospores and pileipellis formed by an ixotrichoderm or trichoderm.

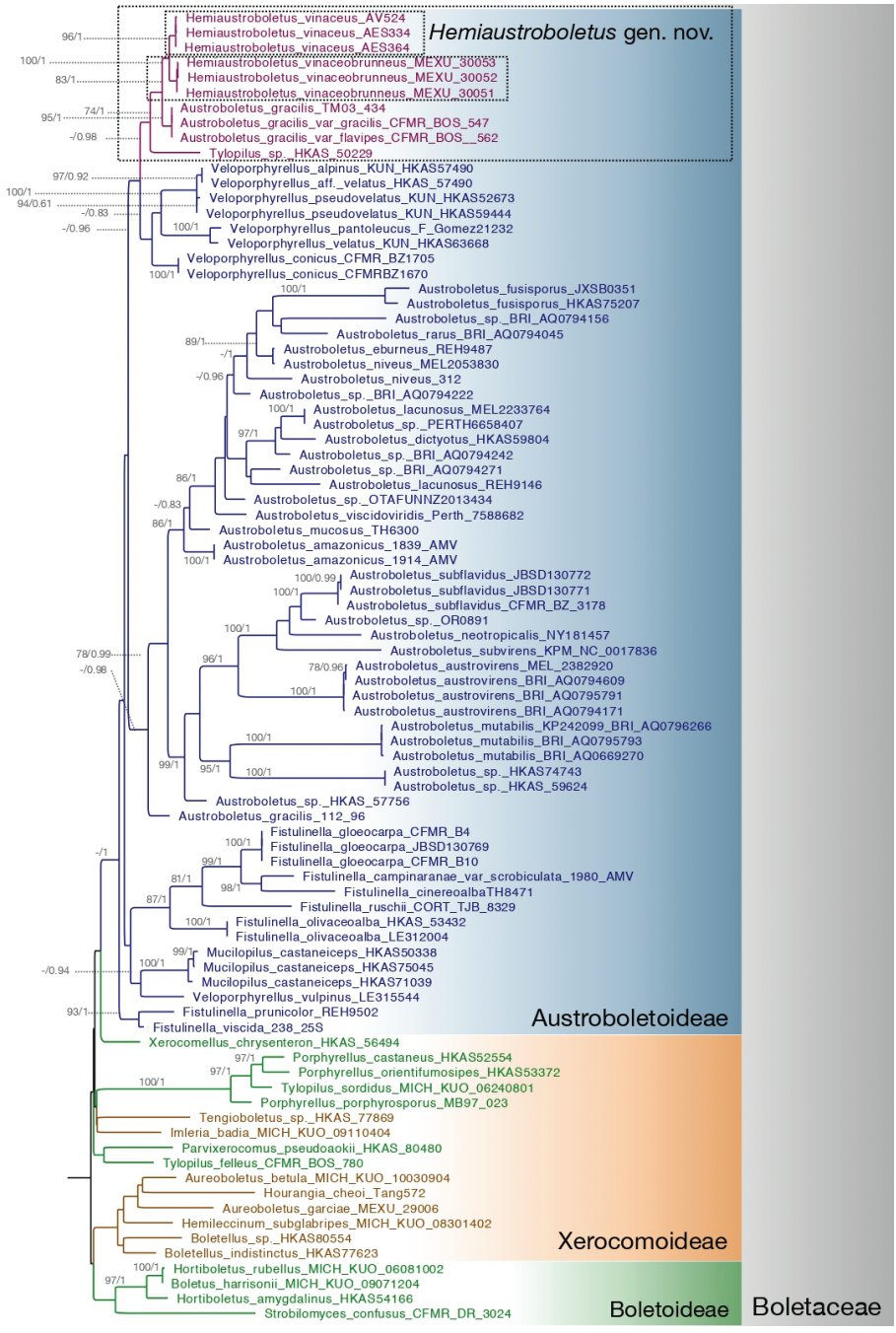

Figure 1. Phylogenetic placement of *Hemiaustroboletus* gen. nov. in the Austroboletoideae subfamily (Boletaceae) using LSU and RPB2 markers in a concatenated and partitioned matrix. The tree shows the topology of Bayesian analysis, with both MLB (≥ 70%) and BPP (≥ 0.7) clade support given. New genera and new species are indicated in the rectangles; taxa and/or branches in purple correspond to *Hemiaustroboletus* gen. nov.; remaining Austroboletoideae (blue); Boletoideae (green); Xerocomoideae (mustard). Background colours correspond to subfamilies; grey bars correspond to families.

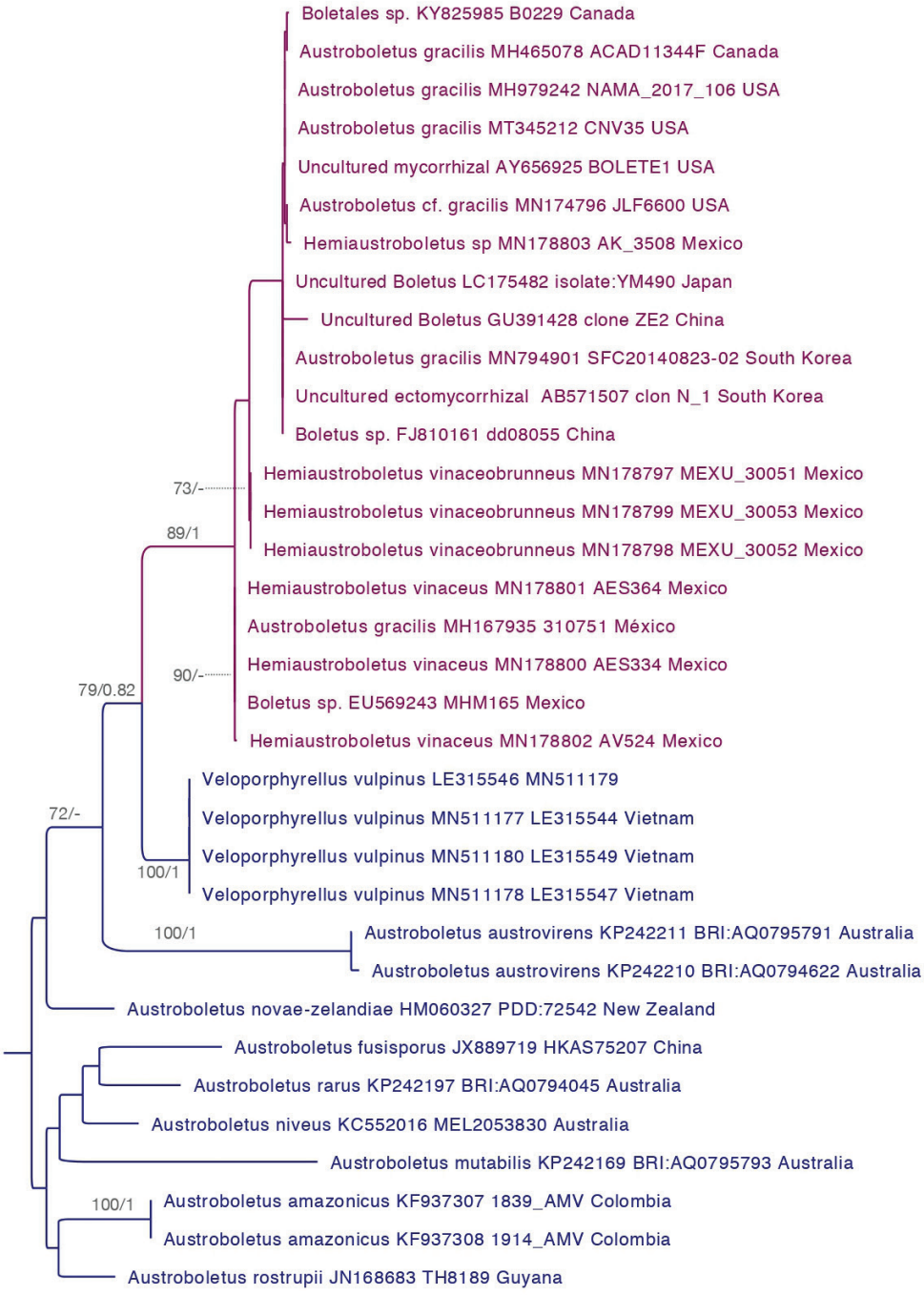

Figure 2. Phylogenetic tree of *Hemiaustroboletus* displaying geographic distribution using voucher and environmental ITS nrDNA sequences. The tree shows the topology of Bayesian analysis, with both MLB (≥ 70%) and BPP (≥ 0.7) clade support given. Taxa and branches in purple correspond to *Hemiaustroboletus* gen. nov. and those in blue to *Veloporphyrellus* and *Austroboletus*.

Etymology. From the Latin *hemi* "almost or half", *Austroboletus* the generic epithet refers to the morphological affinities with this genus.

Generic type. *Hemiaustroboletus vinaceobrunneus* Ayala-Vásquez, García-Jiménez & Garibay-Orijel sp. nov.

Generic Description. Epigeous, stipitate-pileate basidiomata. **Pileus** reddish-brown, violet-brown, dark violet, reddish-brown, orange-brown, yellow-brown, cinnamon, dry surface, finely velvety, velutinous, rivulose, granular-tomentose, subtomentose, minutely areolate. **Hymenophore** tubular, circular to angular pores, whitish, pink-purple, lilac, magenta-grey, brown-violet to pinkish-brown, with or without change brown when cut. **Context** whitish to pale red. **Stipe** subclavate, tomentose, pruinose, granular furfuraceous, striate surface, longitudinally fibrous, very finely reticulated in tapering towards apex. Whitish basal mycelium. **Basidiospores** ornamented, slightly verrucose, cracked to pits, fusoid, oval-elliptical, cylindrical to subfusoid, oblong, ovoid-oblong. **Cystidia** clavate, sphaeropedunculate, subfusoid. **Pileipellis** an ixotrichoderm or trichoderm; terminal cells cylindrical, fusoid, ventricose-rostrate with or without encrustations in the wall. **Caulocystidia** fusoid, cylindrical to subclavate and tetrasporic caulobasidia.

Distribution. Canada, China, Japan, Mexico, South Korea and United States.

Ecology. Temperate and subtropical forests, with conifers and broadleaf trees (*Abies* spp., *Quercus* spp., *Pinus* spp.) from 2000 to 3000 m alt.

***Hemiaustroboletus vinaceobrunneus* Ayala-Vásquez, García-Jiménez & Garibay-Orijel, sp. nov.**

MycoBank No: 838461

Figs 3, 4, 5B, D

Diagnosis. Pileus vinaceous to brown, pores whitish to pinkish at maturity, vinaceous context; longitudinally fribrillose stipe; basidiospores (10) 11–17 (–21) × 4–5 (–7) µm, slightly verrucose to cracked, fusoid to cylindrical; pleurocystidia ventricose-rostrate to fusoid, cheilocystidia sphaeropedunculate.

Holotype. Mexico. Oaxaca State, Santa Catarina Ixtepeji Municipality, La Cumbre Town, Peña Prieta site, 17°11'11.34"N, 96°38'00"W (DMS), 2800 m alt., 19 July 2017, Ayala-Vásquez (MEXU-30051; isotype ITCV-AV868).

Etymology. The name refers to the colour of the pileus, from the Latin "*vinosus*" vinaceous when young and "*brunneus*" brown when mature.

Description. Basidiomata stipitate-pileate. **Pileus** 36–40 mm diameter, convex when young becoming plano-convex, reddish-vinaceous (13B6) when young, orange brown (7C8), reddish-brown (8D8-8E8) to dark brown (7F8) with some ruby tones (12E8) at maturity, dry surface, subtomentose, rivulose to areolate, whitish context, decurved margin. **Hymenophore** slightly depressed around the stipe to subadnate, pores 1–1.2 mm diameter, circular to subangular, whitish when young, pink to red-whitish (11A3-11A2) at maturity, tubes 6 mm length, of pores concolorous, unchanging when

cut or touched, tubes detachable from the context. **Context** 4–8 mm thick, whitish, with some shades of pale red, vinaceous at the edge of the pileus and at the apex of the stipe at maturity. **Stipe** 45–65 × 8–10 mm, subclavate, reddish-vinaceous (13B6), orange-brown (7C8) to brown (7D8 -7E8) at the apex and part of the base, orange in the middle area (6B8) to orange-brown (6C8), rest of the base whitish; surface furfuraceous, longitudinally fibrillose. Whitish mycelium. **Chemical reactions** pileus negative in KOH, the context and the hymenophore slightly become pale violet (16A2) and the stipe becomes pale brown (6D4). When ammonium hydroxide (NH_4OH) is applied, the pileus becomes brown-violet (11F8-11F7), the hymenophore and context pale orange (5A2) and the stipe pale violet (16A2).

Basidiospores 10–15 (–20) × 4–5 (–7) µm, X = 14.04 × 4.96 µm, std = 3.46 × 0.99 µm, (n = 30, Q = (2.2) 2.4–2.5 (2.8), (holotype); (10–) 11–15 (–21) × 4.5–7 (–8) µm, X = 13.78 × 6.07 µm, std = 3.74 × 1.3 µm, Q = (2.2) 2.4–2.6 (2.8) (paratype MEXU-30052); (10–) 11–15 (–17) × (4–) 4.5–5.5 (–6) µm,

Figure 3. *Hemiaustroboletus vinaceobrunneus* **A, C** basidiomata (MEXU-30052 Holotype) **B, D** pileus (MEXU-30053, MEXU-30051, Isotype) **E** hymenophore (MEXU-30052 Holotype) **F, G** context (MEXU-30052 Holotype). Scale bar: 10 mm (**A–G**).

X = 13.15 × 4 µm, std = 2.62 × 0.64 µm, Q = (2.2) 2.6–2.9 (3) µm, (paratype ITCV-AV1121), cylindrical to subfusoid, slightly verrucose to cracked, brown-orange in KOH, inamyloid in Melzer's reagent. **Basidia** 30–33 (–49) × 9–11 (–12) µm, clavate, hyaline in KOH, pale yellow in Melzer's reagent, with granular content, tetrasporic. **Pleurocystidia** 31–45 × 8–11 µm, ventricose to fusoid, some mammillate, hyaline in KOH, yellowish in Melzer's reagent, thick walled (1–1.5 µm). **Cheilocystidia** 42–70 (–86) × 9–15 (–17) µm, clavate with septa (1–2 µm thick), sphaeropedunculate, some mammillate, hyaline in KOH, yellowish in Melzer's reagent, thick-walled (1–1.5 µm).

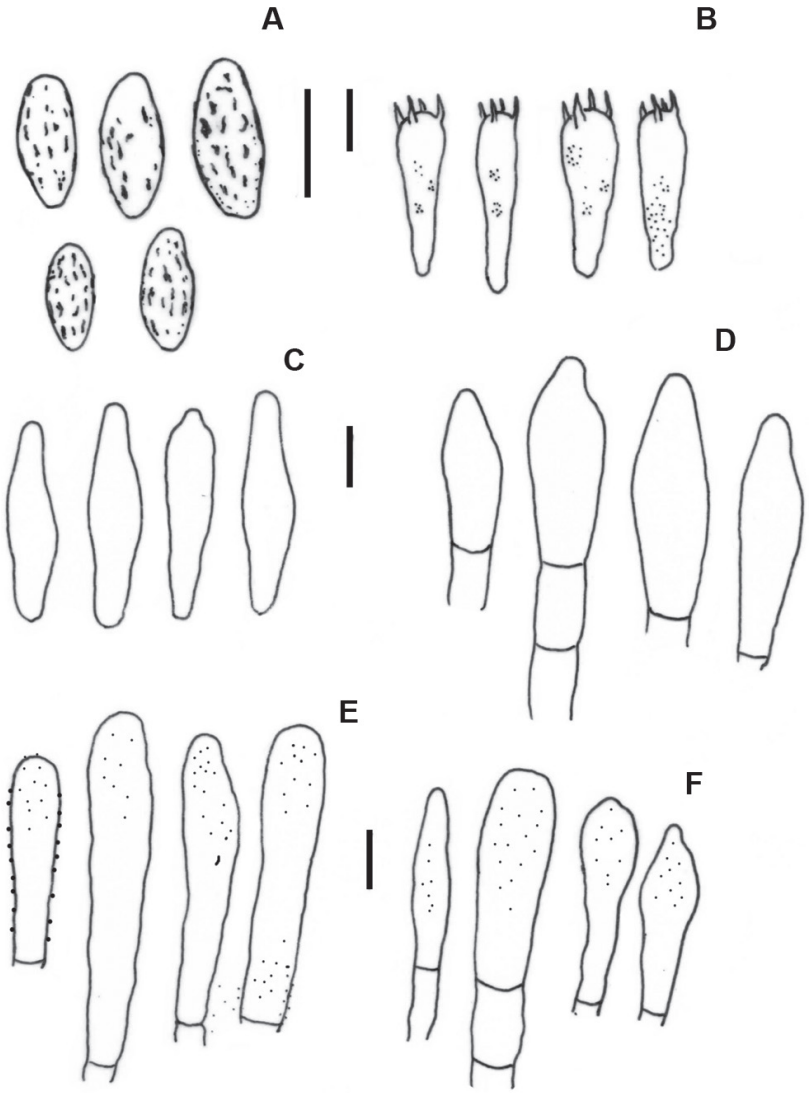

Figure 4. *Hemiaustroboletus vinaceobrunneus* (AV845-ITCV, MEXU-30052 Holotype) **A** basidiospores **B** basidia **C** pleurocystidia **D** cheilocystidia **E** pileipellis **F** caulocystidia. Scale bars: 10 µm (**A–F**).

Hymenophoral trama boletoid; hyphae cylindrical 3–15 µm diameter, with gelatinous wall some with smooth walls, hyaline to yellowish in KOH and Melzer's reagent. **Pileipellis** a trichoderm with terminal cells (22–) 35–75 (–105) × 8–14 (–21) µm, cylindrical to subclavate, hyaline in KOH, yellowish in Melzer's reagent, embedded in a gelatinous substance and with visible contents in Melzer's reagent, thick-walled (1–1.5 µm). **Caulocystidia** 20–64 (–140) × 6–14 (–16) µm, fusoid, cylindrical to sphaeropedunculate with one to two septa, hyaline to yellowish KOH with visible contents visible in Melzer's reagent. **Caulobasidia** 25–30 × 7–8 µm tetrasporic, concolorous with the caulocystidia. **Clamp connections** absent.

Habit and habitat. Solitary, in *Abies guatemalensis*, *Pinus pseudostrobus* and *Quercus laurina* mixed forest, putatively associated with *Quercus laurina*, from 2800 to 3000 m alt.

Known distribution. Currently only known from Oaxaca State, southeast Mexico.

Additional materials examined. Mexico, Oaxaca State, Santa Catarina Ixtepeji Municipality, La Cumbre Town, East of cottage site, 17°11'30"N, 96°38'18"W (DMS), 2903 m alt., 18 July 2017, Ayala-Vásquez (MEXU-30052; ITCV-AV845); Cabeza de Vaca site, 17°11'10"N, 96°38'28"W (DMS), 3038 m alt., 18 July 2017, Ayala-Vásquez (ITCV-AV1121), Cabeza de Vaca site, 15 August 2018, Ayala-Vásquez (MEXU-30053; ITCV-AV1168).

Remarks. *Hemiaustroboletus vinaceobrunneus* differs from *H. vinaceus* by its context with vinaceous tones especially at maturity and a whitish-pink to pale red hymenophore; the stipe is orange-brown; basidiospores are 10–15 (–20) × 4–5 (–7) µm, finely verrucose to cracked, lodged to sphaeropedunculate cheilocystidia, caulocystidia fusoid, cylindrical to sphaeropedunculate with a septum. In contrast, *H. vinaceus* has a whitish context with slight yellowish-brown tones near the epicutis, has shorter basidiospores (9–) 10–14.4 (–16) × 4–5(–8) µm, cylindrical to clavate queilocystidia and caulocystidia fusoid or clavate. In the field, the former can be mistaken for *Gyroporus purpurinus* because of the colours and size of the basidiomata, but *G. purpurinus* has a hollow stipe (Davoodian and Halling 2013), while *H. vinaceobrunneus* has a compact context.

***Hemiaustroboletus vinaceus* Ayala-Vásquez, García-Jiménez & Saldivar, sp. nov.**
MycoBank No: 838462
Figs 5A, C, 6, 7

Diagnosis. Pileus dark violet to dark brown, whitish context; hymenophore pink-purple to violet-brown; stipe surface tomentose to longitudinally fribrillose; basidiospores 9–13 × 4–5 µm, surface with cylindrical pits; pleurocystidia and cheilocystidia fusiform-ventricose to lanceolate.

Holotype. Mexico, Jalisco State, Tequila Municipality, Tequila Volcano site, between 11 and 12 km on the road uphill to the antenna station, 20°48'35"N, 103°51'46"W (DMS), 2144 m alt., 18 August 2019, Á.E. Saldivar (IBUG-AES334).

Etymology. The name refers to the colour of the pileus from the Latin "*vinosus*" vinaceous.

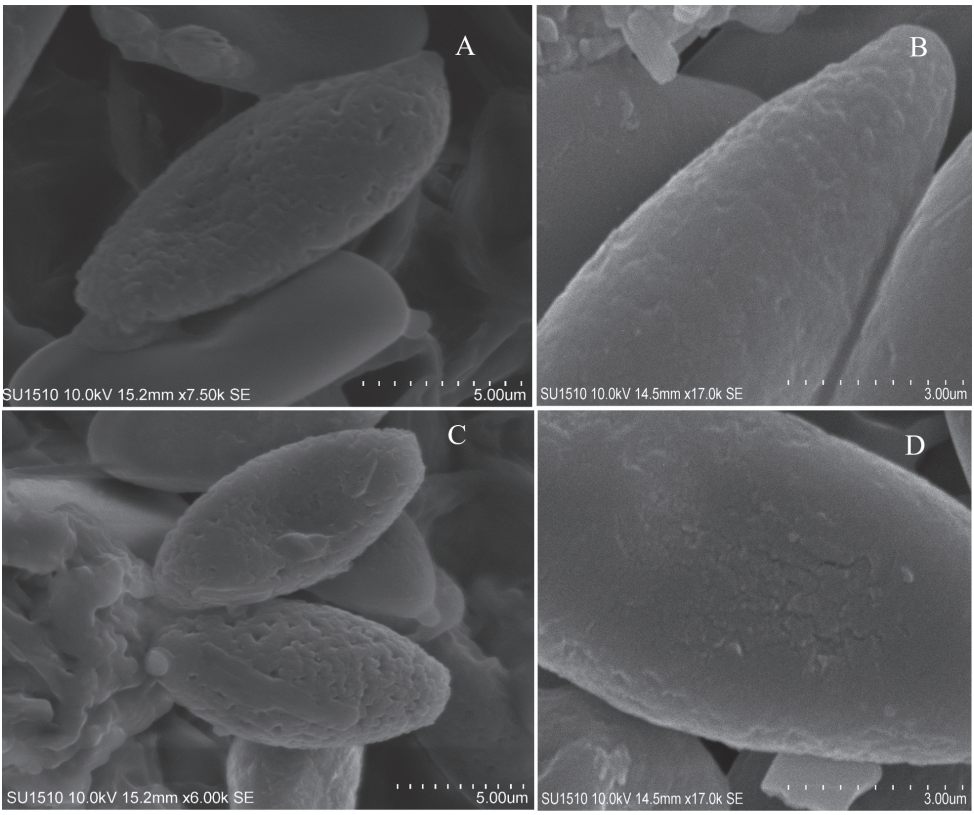

Figure 5. Basidiospore ornamentation of *Hemiaustroboletus* revealed by SEM **A, C** *Hemiaustroboletus vinaceus* (AV868-ITCV, MEXU-30051, Holotype) **B, D** *Hemiaustroboletus vinaceobrunneus* (AV1168-ITCV, MEXU-30053 Isotype).

Description. Pileus 35–70 mm in diameter, convex when young, becoming plano-convex with age, dark violet (16F6-16F4), violet-brown (11F5-11F8), orange-brown (5E7), with lighter shades of dark brown (6F5-6F8) lighter towards margin, whole edge, straight, dry surface, finely scamose, slightly areolate at the centre. **Hymenophore** adnate, slightly depressed, pores 0.5–2 mm in diameter, subangular to angular, pink-purple (14A4), lilac (14B4–14C4), magenta-grey (14C4–14D4), ruby-grey (12C4–12D4), colour unchanging when injured, tubes 7–10 mm, concolorous with the pores. **Context** 7–12 mm thick, solid, whitish, with slight yellowish-brown tones near the epicutis. **Stipe** 62–77 × 8–9 mm, central, cylindrical, with wider base, surface with longitudinal striations, whitish at the apex, yellowish-brown (5D5-5E5), orange-brown (5C5) shades in the middle, base with yellowish (5B6) to whitish shades; whitish context, unchanged when cut. Whitish basal mycelium. **Odour** pleasant. **Taste** slightly acidic. **Chemical reactions:** KOH reddish-brown in pileus, brown in hymenophore, slightly pinkish in context, yellowish-brown in stipe. NH_4OH orange with violet tones on pileus, yellow in hymenophore, pale yellow in context, red-orange in stipe.

Figure 6. *Hemiaustroboletus vinaceus* (AES334-IBUG, Holotype) **A, B** basidiomata **C** hymenophore **D** context **E** pileus surface. Scale bar: 10 mm (**A–E**).

Basidiospores 9–13 (–14.5) × 4–5 (–8) µm, X = 12.14 × 5.2 µm, std = 2.08 × 1.36 µm, (n = 35), Q = (1.8) 2.1–2.2 (2.5) (holotype); (10–) 12–14 × 4–5 (–7) µm, X = 11.94 × 5.14 µm, std = 1.60 × 1.13 µm, (n = 35), Q = (2.2) 2.3–2.4 (2.5), (paratype MEXU-30103); (10–) 14–15 (–16) × (4–) 5–6 (–7) µm, X = 14.29 × 5.8 µm, std = 1.69 × 0.76 µm, (n = 40), Q = (2.2) 2.3–2.5 (2.6), (paratype colpos-CP5); subfusiform to cylindrical, slightly rough or dotted, apex rounded to subacute, with suprahilar depression, yellowish. **Basidia** 27–34 × 7–15.2 µm, claviform, bisporic, tetrasporic, with sterigma 2–4 × 0.5–1 µm, thin-walled, hyaline in KOH, yellow in Melzer's reagent. **Pleurocystidia** 28–50 × 6.4–11 µm, fusoid-ventricose, slightly lanceolate, with content hyaline in KOH, yellow in Melzer's reagent, with walls 0.5 µm thick. **Cheilocystidia** 25–61 × 6.4–11 µm, subclavate, hyaline in KOH, yellow in Melzer's reagent, thin-walled. **Hymenophoral trama** divergent, with central and lateral hyphae tubular, 2–6 µm wide, hyaline in KOH, yellow in Melzer's reagent, thin-walled; septa without clamp connections. **Pileipellis** a trichoderm with terminal cells 32–92 × 5–11 µm, cylindrical to subclaviform, hyaline in KOH, yellow in Melzer's reagent, thin-walled. **Caulocystidia** 29–95 × 14–17 (–19) µm, subclaviform to claviform, thin-walled, with yellow visible contents in Melzer's reagent, hyaline in KOH.

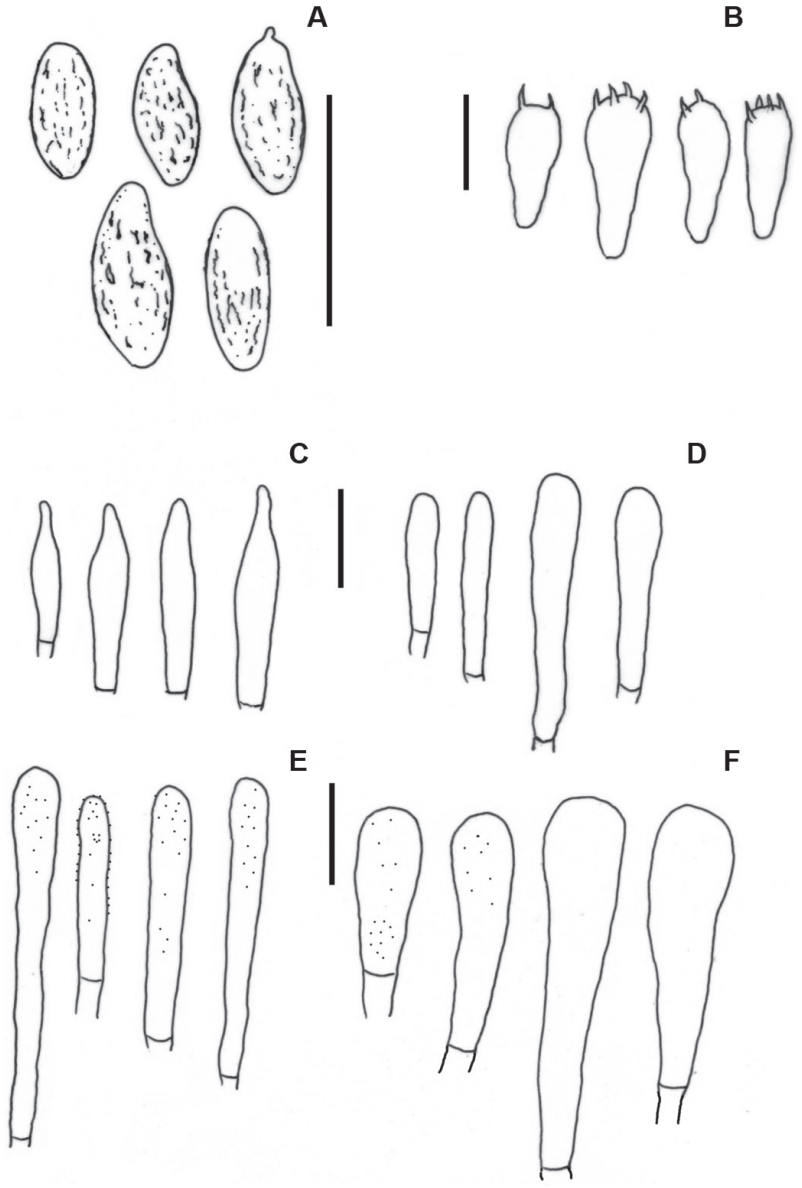

Figure 7. *Hemiaustroboletus vinaceus* (AES334-IBUG, Holotype) **A** basidiospores **B** basidia **C** pleurocystidia **D** cheilocystidia **E** pileipellis **F** caulocystidia. Scale bars: 10 μm (**A–F**).

Habit and habitat. *Pinus-Quercus* forests and *Quercus* forests, associated with *Q. liebmanii* and other *Quercus* spp.

Known distribution. Currently only known from Neovolcanic Axis and Sierra Madre del Sur, Mexico.

Additional material examined. Mexico, Jalisco State, Tequila Municipality, Tequila Volcano site, km 11–12 on the road uphill to the antenna station, 20°48'14"N,

103°51'37"W (DMS), 2144 m alt., 18 September 2019, A.E. Saldivar (IBUG-AE364); Oaxaca State, San Antonio de la Cal Municipality, Las Peñas site, 17°01'11"N, 96°40'33"W (DMS), 2160 m alt., 4 October 2014, Ayala-Vásquez (MEXU-30103; ITCV-AV524, duplicated ENCB); Michoacan State, Road Morelia, Ciudad Hidalgo Town, km 40, 21 July 1983, García-Jiménez (ITCV-3662), Mil Cumbres Town, 9 August 1969, R. Singer M8993 (F). Estado de México State, Ocuilan, San Juan Atzingo Town, mixed forest, 15 July 2021, mycoredes (Colpos- CP5).

Remarks. *Hemiaustroboletus vinaceus* differs from *H. vinaceobrunneus* due to its dark violet pileus, lilac to violet hymenophore, yellow stipe in the basal area and whitish apex. It has short, perforated basidiospores 9–13 (–14.4) × 4–5 (–8) µm, caulocystidia clavate to fusoid and pileipellis formed by a trichoderm with terminal cell cylindrical or subclavate, thin-walled. In contrast, *H. vinaceobrunneus* has a pileipellis formed by a trichoderm with encrustations. *Hemiaustroboletus vinaceus* is easily confused with *Austroboletus gracilis sensu* Wolfe (1979), because of its macroscopic characteristics and basidiospore ornamentation, but *A. gracilis* differs by pileus red-brown, brown-orange, having a total or partial reticulum on the stipe surface; longer basidiospores 10–19.5 × 4.5–9 µm, rugulose-punctate, elliptical to ovoid-elliptical. *Austroboletus* var. *gracilis* (Peck) Wolfe differs from *H. vinaceus* by pileus surface dry, finely velvety, when young, sometime rimose, reddish-brown, cinnamon or yellow-brown; stipe surface anastomosing lines, narrow reticulation overall or at least on the upper half; basidiospores 10–17 × 5–8 µm, narrowly ovoid to subelliptical. *Austroboletus gracilis* var. *laevipes* is distinguished by the smooth stipe, pileus yellow-ochraceous to yellow-brown, stipe subclavate, striate, finely pruinose, neither ribs nor reticulated surface, pale yellow or yellow-brown, basidiospores 11.2–14 × 5–8µm, oval-elliptical in face view, inequilateral in profile (Bessette et al. 2000). *Austroboletus gracilis* var. *pulcherripes* Both & Bessette differs from *H. vinaceus* by a white hymenium when young, becoming pinkish to pale cocoa at maturity; stipe clavate, surface dry, coarsely reticulated on the upper two- thirds, reticulated, finely tomentose; basidiospores 13–19 × 5–8 µm, smooth to rugose-punctate, ovoid-elliptical, narrowly ovoid, inequilateral profile.

Discussion

According the phylogenetic analysis, our collections are nested within the Austroboletoideae close to *Veloporphyrellus*. Recognising the *Hemiaustroboletus* genus contributes to solving the systematics within Austroboletoideae since previous works have shown that *Austroboletus* and *Veloporphyrellus*, as currently morphologically circumscribed, are polyphyletic (Wu et al. 2016; Gelardi et al. 2020; Kuo and Ortiz-Santana 2020). For example, Wu et al. (2016) found two clades of *Austroboletus*, *Austroboletus*. s.s. and a second clade where *Austroboletus gracilis* s.l. (strain, 112/96) is nested with *Veloporphyrellus gracilioides*, this species being separated from the *Veloporphyrellus* s.s. clade. Gelardi et al. (2020) also recovered *Austroboletus* as polyphyletic with *Austroboletus* s.s. containing most of the species and other samples divided into four more clades. Particularly, in their analyses, most *A. gracilis* samples nested close to *Veloporphyrellus*; this is the clade we are erecting now as *Hemiaustroboletus*.

Our analyses show that *Hemiaustroboletus* is related to *Veloporphyrellus* (Fig. 1). This is supported by previous analyses (Gelardi et al. 2020; Kuo and Ortiz-Santana, 2020); indeed, they differ in several morphological characteristics. *Veloporphyrellus* has a veil which often embraces the apex of the stipe in younger basidiomata; hymenophoral surface white when young becoming pinkish to pink when mature; basidiospores smooth subfusiform to oblong. In contrast, *Hemiaustroboletus* has furfuraceous, tomentose to minutely areolate pileus surface; whitish, pink-purple, lilac, magenta-grey to brown-violet hymenophoral surface; and slightly verrucose, cracked to pitted ornamented basidiospores (Table 2). Even while the phylogenetic relations between both genera are not statistically supported, nucleotide similarity demonstrated that

Table 2. Comparative table of Austroboletoidae genera, based on Wolfe (1979) and Wu et al. (2016).

Genera	Basidiomata	Basidiospores	Cystidia	Pileipellis
Austroboletus	Pileus margin which embraces the stipe when young. Stipe surface distinctly reticulate, alveolate-lacunose	Ornamented, elongate to amygdaliform, with warts, reticulate ridges or shallow to irregularly furrowed pits	Cylindrical, clavate, fusoid	Trichoderm with filamentous interwoven hyphae, sometimes strongly gelatinous
Fistulinella	Stipitate-pileate to occasionally sequestrate, with or without veil, usually viscid to strongly glutinous pileus	Smooth, elongate fusoid, inamyloid to dextrinoid	Fusiform to ventricose fusiform or lageniform	Trichoderm, ixotrichoderm or ixocutis
Hemiaustroboletus	Pileus surface furfuraceous, tomentose, minutely areolate, stipe surface longitudinally fibrillose to striate	Slightly verrucose, cracked to pitted	Clavate, Rope-dunculate, subfusoid	Ixotrichoderm or trichoderm, terminal cells cylindrical, fusoid, ventricose-rostrate
Mucilopilus	Viscid pileus, stipe without colour change, white to pinkish or pink hymenophore	Smooth, subfusiform to oblong	Fusoid, ventricose to subfusiform	Ixotrichoderm, composed of strongly gelatinous filamentous hyphae
Veloporphyrellus	Pileus margin with distinct membranous veil or appendiculate, stipe nearly glabrous or fibrillose	Smooth, subfusiform to oblong	Subfusiform to ventricose	Trichoderm composed of filamentous interwoven hyphae

Table 3. Average nucleotide similarity amongst genera of Austroboletoidae.

Genus 1	Genus 2	Average nucleotide similarity (ITS) %	Average nucleotide similarity (LSU) %	Average nucleotide similarity (RPB2) %
Hemiaustroboletus	***Hemiaustroboletus***	**95.49**	**98.93**	**97.96**
Hemiaustroboletus	***Mucilopilus***		**92.51**	**91.25**
Hemiaustroboletus	***Austroboletus***	**71.27**	**85.94**	**87.75**
Hemiaustroboletus	***Fistulinella***		**88.58**	**89.76**
Hemiaustroboletus	***Veloporphyrellus***	**74.75**	**94.01**	**93.45**
Veloporphyrellus	*Veloporphyrellus*		95.49	100
Veloporphyrellus	*Austroboletus*		85.64	86.66
Veloporphyrellus	*Mucilopilus*		91.45	89.73
Veloporphyrellus	*Fistulinella*		88.06	89.5
Fistulinella	*Fistulinella*		90.48	89.5
Fistulinella	*Mucilopilus*		87.61	89.5
Fistulinella	*Austroboletus*		83.03	86.87
Austroboletus	*Austroboletus*		86	92.06
Austroboletus	*Mucilopilus*		85.05	87.88
Mucilopilus	*Mucilopilus*		98.5	99.4

they are the closest genera within Austroboletoidae. The overall nucleotide similarity between genera in Austroboletoidae in RPB2 is 89.23%, in LSU it is 88.19%, and in ITS it is 72.55%. Between *Hemiaustroboletus* and *Veloporphyrellus*, the average nucleotide similarity is 93.45% in RPB2, 94.01% in LSU and 74.75 in ITS (Table 3). These amounts of variation in the three markers also support the conclusion of recognising both genera.

Hemiaustroboletus gen. nov. accomplishes the guidelines for the establishment of new genera proposed by Vellinga et al. (2015). It is a monophyletic group supported by morphological data and phylogenetic analyses (BPP = 0.98) (Fig. 1). When *Hemiaustroboletus* is recognised, the related clade *Austroboletus* s.s. (the clade including *A. dictyotus*, the genus type) becomes monophyletic. Additionally, the DNA sequence sampling is broad in taxonomic and geographic terms and uses ribosomal markers and protein coding genes. Indeed, holotypes for both species described are represented with the three markers included in the phylogenetic analyses.

Hemiaustroboletus is proposed as a new genus with two species *H. vinaceobrunneus* and *H. vinaceus*, including several of the revised material being previously identified as *A. gracilis* by Singer et al. (1991), Ayala-Vásquez et al. (2018) and Saldivar et al. (2021). The genus has at least one more known clade (Fig. 1) containing samples originally identified as *A. gracilis* (TM03-434) from Canada, *A. gracilis* var. *gracilis* (CFMR BOS-547) and *A. gracilis* var. *flavipes* (CFMR BOS-562) from USA. As found in our analyses and previous works (Wu et al. 2016; Gelardi et al. 2020; Kuo and Ortiz-Santana 2020), *A. gracilis* is a name widely applied to several clades. In our analysis, the sample *A. gracilis* 112/96 belongs to *Austroboletus* (maybe because it lacks RPB2 locus), while the rest of the sequences with this epithet belong to *Hemiaustroboletus*. As this species is polyphyletic, establishing the true identity of *A. gracilis* s.s. requires the sequencing of its type specimen, a task beyond the objectives of this study.

Hemiaustroboletus differs morphologically from *Austroboletus* sect. *Austroboletus sensu* Wu et al. (2016) (*Austroboletus* s.s. in this study) because the species of the latter have clearly reticulated to costate stipe, elongate, fusoid or amygdaliform basidiospores with warts, reticulate ridges, irregularly furrowed pits or shallow ornamentation and a subrepent to trichoderm pileipellis, composed of filamentous interwoven hyphae, sometimes strongly gelatinous. In contrast, *Hemiaustroboletus* is characterised by a subclavate, tomentose, pruinose, granular furfuraceous, striate surface, longitudinally fibrous, very finely reticulated stipe, oval-elliptical, cylindrical to subfusoid, oblong, ovoid-oblong basidiospores with slightly verrucose, cracked to pitted surface, its pilleipellis is an ixotrichoderm or trichoderm with terminal cells cylindrical, fusoid or ventricose-rostrate with or without incrustations in the wall.

Finally, *A. gracilis*, described by Ortiz-Santana et al. (2007) from Central America, is probably *Hemiaustroboletus vinaceus* or a close species, because they match the description presented here. Further analysis of these collections and others, labelled as *A. gracilis* in subtropical regions of Central America and eastern Asia, are needed to fully understand the diversity and distribution of *Hemiaustroboletus*.

Acknowledgements

Ayala-Vásquez acknowledges financial support from the Mexican Council of Science and Technology CONACYT 449637 for financial support (Scholarship); the MEXBOL network project CONACYT 280896, the CONACYT-PRONACES FOP07-2021-03 Project 316198; Javier Isaac de la Fuente, César Martínez-González for technical support, Laura Margarita Marquez Valdelamar, Head of the Sequencing facility at IB-UNAM; Lidia Irene Cabrera Martínez Head of the Molecular Biology Laboratory of the Botany Department of IB-UNAM; María Berenit Mendoza-Garfias, Head of the Laboratory of Scanning Electron Microscopy facility at IB-UNAM; García-Jiménez thanks CONACYT for financial support and the Technological Institute of Mexico.

References

Ayala-Vásquez O, Valenzuela R, Aguirre-Acosta E, Raymundo T, García-Jiménez J (2018) Species of Boletaceae (Boletales, Basidiomycota) with ornamented spores from temperate forests at the State of Oaxaca, Mexico. Studies in Fungi 3(1): 271–292. https://doi.org/10.5943/sif/3/1/28

Bessette A, Roody WC, Bessette AR (2000) North American boletes: a color guide to the fleshy pored mushrooms. Syracuse University Press, New York, 20–320.

Binder M, Hibbett DS (2006) Molecular systematics and biological diversification of Boletales. Mycologia 98(6): 971–983. https://doi.org/10.1080/15572536.2006.11832626

Darriba D, Taboada GL, Doallo R, Posada D (2012) JModelTest 2: More models, new heuristics and parallel computing. Nature Methods 9(8): 772–772. https://doi.org/10.1038/nmeth.2109

Davoodian N, Halling RE (2013) Validation and typification of *Gyroporus purpurinus.* Mycotaxon 125(1): 103–105. https://doi.org/10.5248/125.103

Drehmel D, James T, Vilgalys R (2008) Molecular phylogeny and biodiversity of the boletes. Fungi 1: 17–23.

Fechner N, Bonito G, Bougher NL, Lebel T, Halling RE (2017) New species of *Austroboletus* (Boletaceae) in Australia. Mycological Progress 16(8): 769–775. https://doi.org/10.1007/s11557-017-1314-0

García-Jiménez J, Singer R, Estrada E, Garza-Ocañas F, Valenzuela R (2013) Dos especies nuevas del género *Boletus* (Boletales: Agaricomycetes) en México. Revista mexicana de biodiversidad 84: 152–162. https://doi.org/10.7550/rmb.31988

Gelardi M, Angelini C, Costanzo F, Ercole E, Ortiz-Santana B, Vizzini A (2020) Outstanding pinkish brown-spored Neotropical Boletes: *Austroboletus subflavidus* and *Fistulinella gloeocarpa* (Boletaceae, Boletales) from the Dominican Republic. Mycobiology.

Haelewaters D, Dima B, Abdel-Hafiz BII, Abdel-Wahab MA, Abul-Ezz SR, Acar I, Aguirre-Acosta E, Aime MC, Al Demir S, Ali M, Ayala-Vásquez O, Bakhit MS, Bashir H, Battistin E, Bendiksen E, CastroRivera R, Çolak ÖF, De Kesel A, de la Fuente JI, Dizkırıcı A, Hussain S, Jansen GM, Kaygusuz O, Khalid AN, Khan J, Kiyashko AA, Larsson E,

Martínez González CR, Morozova OV, Niazi AR, Noordeloos ME, Pham THG, Popov ES, Psurtseva NV, Schoutteten N, Sher H, Türkekul I, Verbeken A, Ahmad H, Afshan NS, Christe P, Fiaz M, Glaizot O, Liu J, Majeed J, Markotter W, Nagy A, Nawaz H, Papp V, Péter Á, Pfliegler WP, Qasim T, Riaz M, Sándor AD, Szentiványi T, Voglmayr H, Yousaf N, Krisai-Greilhuber I (2020) Fungal Systematics and Evolution 6. Sydowia 72: 271–296.

Halling RE, Nuhn M, Osmundson T, Fechner N, Trappe JM, Soytong K, Arora D, Hibbett DS, Binder M (2012) Affinities of the *Boletus chromapes* group to *Royoungia* and the description of two new genera, *Harrya* and *Australopilus.* Australian Systematic Botany 25(6): 418–431. https://doi.org/10.1071/SB12028

Halling R, Fechner N, Nuhn M, Osmundson T, Soytong K, Arora D, Binder M, Hibbett D (2015) Evolutionary relationships of *Heimioporus* and *Boletellus* (Boletales) with an emphasis on Australian taxa including new species and new combinations in *Aureoboletus*, *Hemileccinum* and *Xerocomus.* Australian Systematic Botany 28(1): 1–22. https://doi.org/10.1071/SB14049

He MQ, Zhao RL, Hyde KD, Begerow D, Kemler M, Yurkov A, McKenzie EHC, Raspé O, Kakishima M, Sánchez-Ramírez S, Vellinga EC, Halling R, Papp V, Zmitrovich IV, Buyck B, Ertz D, Wijayawardene NN, Cui B-K, Schoutteten N, Liu X-Z, Li T-H, Yao Y-J, Zhu X-Y, Liu A-Q, Li G-J, Zhang M-Z, Ling Z-L, Cao B, Antonín V, Boekhout T, da Silva BDB, De Crop E, Decock C, Dima B, Dutta AK, Fell JW, Geml J, Ghobad-Nejhad M, Giachini AJ, Gibertoni TB, Gorjón SP, Haelewaters D, He S-H, Hodkinson BP, Horak E, Hoshino T, Justo A, Lim YW, Menolli Jr N, Mešić A, Moncalvo J-M, Mueller GM, Nagy LG, Nilsson RH, Noordeloos M, Nuytinck J, Orihara T, Ratchadawan C, Rajchenberg M, Silva-Filho AGS, Sulzbacher MA, Tkalčec Z, Valenzuela R, Verbeken A, Vizzini A, Wartchow F, Wei T-Z, Weiß M, Zhao C-L, Kirk PM (2019) Notes, outline and divergence times of Basidiomycota. Fungal Diversity 99(1): 105–367. https://doi.org/10.1007/s13225-019-00435-4

Hosen MI, Feng B, Wu G, Zhu XT, Li YC, Yang ZL (2013) *Borofutus*, a new genus of Boletaceae from tropical Asia: Phylogeny, morphology, and taxonomy. Fungal Diversity 58(1): 215–226. https://doi.org/10.1007/s13225-012-0211-8

Hosen MI, Yang ZL (2021) *Kaziboletus*, a new boletoid genus of Boletaceae associated with *Shorea robusta* in Bangladesh. Mycological Progress, 20: 1145–1156. https://doi.org/10.1007/s11557-021-01723-7

Katoh K, Misawa K, Kuma K, Miyata T (2002) MAFFT: A novel method for rapid multiple sequence alignment based on fast Fourier transform. Nucleic Acids Research 30(14): 3059–3066. https://doi.org/10.1093/nar/gkf436

Kornerup A, Wanscher JH (1978) Methuen Handbook of Color, 31st edn. Eyre Methuen Ltd. London, 227 pp.

Kuo M, Ortiz-Santana B (2020) Revision of leccinoid fungi, with emphasis on North American taxa, based on molecular and morphological data. Mycologia 112(1): 197–211. https://doi.org/10.1080/00275514.2019.1685351

Largent DL (1986) How to identify mushrooms to genus I: macroscopic features. I, 2nd edn. Mad River Press Inc., Eureka, 166 pp.

Li YC, Ortiz-Santana B, Zeng NK, Yang BFZL (2014) Molecular phylogeny and taxonomy of the genus *Veloporphyrellus.* Mycologia 106(2): 291–306. https://doi.org/10.3852/106.2.291

Lodge DJ, Ammirati JF, O'Dell TE, Müller G (2004) Collecting and describing macrofungi. In: Muller G, Bills G, Foster M (Eds) Biodiversity of fungi inventory and monitoring methods. California: Elsevier Academic Press, 128–158. https://www.fpl.fs.fed.us/documnts/pdf2004/fpl_2004_lodge001.pdf

Ma D, Yang G, Mu L (2010) Morphological and molecular analyses of ectomycorrhizal diversity in *Pinus densiflora* seedlings. Symbiosis 51(3): 233–238. https://doi.org/10.1007/s13199-010-0079-x

Miller MA, Pfeiffer W, Schwartz T (2010) Creating the CIPRES Science Gateway for inference of large phylogenetic trees. Proceedings of the Gateway Computing Environments Workshop (GCE). New Orleans, LA, 1–8. https://doi.org/10.1109/GCE.2010.5676129

Miyamoto Y, Narimatsu M, Nara K (2018) Effects of climate, distance, and a geographic barrier on ectomycorrhizal fungal communities in Japan: A comparison across Blakiston's Line. Fungal Ecology 33: 125–133. https://doi.org/10.1016/j.funeco.2018.01.007

Morris MH, Perez-Perez MA, Smith ME, Bledsoe CS (2008) Multiple species of ectomycorrhizal fungi are frequently detected on individual oak root tips in a tropical cloud forest. Mycorrhiza 18(8): 375–383. https://doi.org/10.1007/s00572-008-0186-1

Obase K, Cha JY, Lee JK, Lee SY, Chun KW (2012) Ectomycorrhizal fungal community associated with naturally regenerating *Pinus densiflora* Sieb. et Zucc. seedlings on exposed granite slopes along woodland paths. Journal of Forest Research 17(4): 388–392. https://doi.org/10.1007/s10310-011-0301-6

Orihara T, Smith ME, Shimomura N, Iwase K, Maekawa N (2012) Diversity and systematics of the sequestrate genus *Octaviania* in Japan: Two new subgenera and eleven new species. Persoonia 28(1): 85–112. https://doi.org/10.3767/003158512X650121

Orihara T, Lebel T, Ge ZW, Smith ME, Maekawa N (2016) Evolutionary history of the sequestrate genus *Rossbeevera* (Boletaceae) reveals a new genus *Turmalinea* and highlights the utility of ITS minisatellite-like insertions for molecular identification. Persoonia 37(1): 173–198. https://doi.org/10.3767/003158516X691212

Ortiz-Santana B, Lodge DJ, Baroni TJ, Both EE (2007) Boletes from Belize and the Dominican Republic. Fungal Diversity 27: 247–416.

Porter TM, Skillman JE, Moncalvo JM (2008) Fruiting body and soil rDNA sampling detects complementary assemblage of Agaricomycotina (Basidiomycota, Fungi) in a hemlock-dominated forest plot in southern Ontario. Molecular Ecology 17(13): 3037–3050. https://doi.org/10.1111/j.1365-294X.2008.03813.x

Rambaut A (2009) FigTree. Tree figure drawing tool. http://tree.bio.ed.ac.uk/software/figtree/

Ronquist F, Teslenko M, Van der Mark P, Ayres DL, Darling A, Höhna S, Larget B, Liu L, Suchard MA, Huelsenbeck JP (2012) MrBayes 3.2: Efficient Bayesian phylogenetic inference and model choice across a large model space. Systematic Biology 61(3): 539–542. https://doi.org/10.1093/sysbio/sys029

Saldivar ÁE, García Jiménez J, Herrera Fonseca MJ, Rodríguez Alcántar O (2021) Listado actualizado y nuevos registros de Boletaceae (Fungi, Basidiomycota, Boletales) en Jalisco, México. Polibotánica 0(52): 25–49. https://doi.org/10.18387/polibotanica.52.3

Singer R, García J, Gómez LD (1991) The Boletineae of Mexico and Central America. III. Nova Hedwigia. Beiheft 98: 1–72.

Smith ME, Henkel TW, Catherine AM, Fremier AK, Vilgalys R (2011) Ectomycorrhizal fungal diversity and community structure on three co-occurring leguminous canopy tree species in a Neotropical rainforest. The New Phytologist 192(3): 699–712. https://doi.org/10.1111/j.1469-8137.2011.03844.x

Smith ME, Henkel TW, Uehling JK, Fremier AK, Clarke HD, Vilgalys R (2013) The Ectomycorrhizal fungal community in a Neotropical forest dominated by the endemic *Dipterocarp Pakaraimaea* Dipterocarpacea. PLoS ONE 8(1): e55160. https://doi.org/10.1371/journal.pone.0055160

Stamatakis A (2014) RAxML version 8: A tool for phylogenetic analysis and post-analysis of large phylogenies. Bioinformatics (Oxford, England) 30(9): 1312–1313. https://doi.org/10.1093/bioinformatics/btu033

Tedersoo L, May TW, Smith ME (2010) Ectomycorrhizal lifestyle in fungi: Global diversity, distribution, and evolution of phylogenetic lineages. Mycorrhiza 20(4): 217–263. https://doi.org/10.1007/s00572-009-0274-x

Vadthanarat S, Lumyong S, Raspé O (2019) Cacaoporus, a new Boletaceae genus, with two new species from Thailand. MycoKeys 54: 1–29. https://doi.org/10.3897/mycokeys.54.35018

Vasco-Palacios AM, López-Quintero C, Franco-Molano AE, Boekhout T (2014) *Austroboletus amazonicus* sp. nov. and *Fistulinella campinaranaevar. scrobiculata*, two commonly occurring boletes from a forest dominated by *Pseudomonotes tropenbosii* (Dipterocarpaceae) in Colombian Amazonia. Mycologia 106(5): 1004–1014. https://doi.org/10.3852/13-324

Vellinga EC, Kuyper TW, Ammirati J, Desjardin DE, Halling RE, Justo A, Læssøe T, Lebel T, Lodge DJ, Matheny PB, Methven AS, Moreau PA, Mueller GM, Noordeloos ME, Nuytinck J, Ovrebo CL, Verbeken A (2015) Six simple guidelines for introducing new genera of fungi. IMA Fungus 6(2): 65–68. https://doi.org/10.1007/BF03449356

Victoroff C (2020) Response of ectomycorrhizal fungal fruiting to nitrogen and phosphorus additions in Bartlett Experimental Forest, New Hampshire. Dissertations and Theses. PhD Thesis, New Hampshire, USA 167: 1–104. https://digitalcommons.esf.edu/etds/167

Vilgalys R, Hester M (1990) Rapid genetic identification and mapping of enzymatically amplified ribosomal DNA from several *Cryptococcus* species. Journal of Bacteriology 172(8): 4238–4246. https://doi.org/10.1128/jb.172.8.4238-4246.1990

Walker JF, Miller OK, Horton JL (2005) Hyperdiversity of ectomycorrhizal fungus assemblages on oak seedlings in mixed forests in the Southern Appalachian Mountains. Molecular Ecology 14: 829–838. https://doi.org/10.1111/j.1365-294X.2005.02455.x

White TJ, Bruns T, Lee S, Taylor J (1990) Amplification and direct sequencing of fungal ribosomal RNA genes for phylogenies. In: Innis MA, Gelfand DH, Sninsky JJ, White TJ (Eds) PCR protocols: a guide to methods and applications. San Diego, Academic Press, 315–322. https://doi.org/10.1016/B978-0-12-372180-8.50042-1

Wolfe Jr CB (1979) *Austroboletus* and *Tylopilus* subgenus *Porphyrellus* with emphasis on North American taxa. J Cramer. Bibliotheca Mycologica, 69 pp.

Wu G, Feng B, Xu J, Zhu XT, Li YC, Zeng NK, Hosen MI, Yang ZL (2014) Molecular phylogenetic analyses re-define seven major clades and reveal 22 new generic clades in the fungal family Boletaceae. Fungal Diversity 69(1): 93–115. https://doi.org/10.1007/s13225-014-0283-8

Wu G, Li YC, Zhu XT, Zhao K, Han LH, Cui YY, Li F, Xu JP, Yang ZL (2016) One hundred noteworthy boletes from China. Fungal Diversity 81(1): 25–188. https://doi.org/10.1007/s13225-016-0375-8

Young AP, Evans RC, Newell R, Walker AK (2019) Development of a DNA barcoding protocol for fungal specimens from the E.C. Smith Herbarium (ACAD). Northeastern Naturalist 26(3): 465–483. https://doi.org/10.1656/045.026.0302

Zhu XT, Wu G, Zhao K, Halling RE, Yang ZL (2015) *Hourangia*, a new genus of Boletaceae to accommodate *Xerocomus cheoi* and its allied species. Mycological Progress 14(6): e37. https://doi.org/10.1007/s11557-015-1060-0

MycoKeys 88: 79–108 (2022)
doi: 10.3897/mycokeys.88.79266
https://mycokeys.pensoft.net

RESEARCH ARTICLE

A peer-reviewed open-access journal
MycoKeys
Launched to accelerate biodiversity research

Taxonomic study of *Collybiopsis* (Omphalotaceae, Agaricales) in the Republic of Korea with seven new species

Ji Seon Kim[1], Yoonhee Cho[1], Ki Hyeong Park[1], Ji Hyun Park[2], Minkyeong Kim[3], Chang Sun Kim[4], Young Woon Lim[1]

1 *School of Biological Sciences and Institute of Microbiology, Seoul National University, Seoul 08826, Republic of Korea* **2** *Water Supply and Sewerage Research Division, National Institute of Environmental Research, Incheon 22689, Republic of Korea* **3** *Microorganism Resources Division, National Institute of Biological Resources, Incheon, Republic of Korea* **4** *Forest Biodiversity Division, Korea National Arboretum, Pocheon-si 11186, Republic of Korea*

Corresponding author: Young Woon Lim (ywlim@snu.ac.kr)

Academic editor: Bao-Kai Cui | Received 13 December 2021 | Accepted 4 March 2022 | Published 30 March 2022

Citation: Kim JS, Cho Y, Park KH, Park JH, Kim M, Kim CS, Lim YW (2022) Taxonomic study of *Collybiopsis* (Omphalotaceae, Agaricales) in the Republic of Korea with seven new species. MycoKeys 88: 79–108. https://doi.org/10.3897/mycokeys.88.79266

Abstract

Collybiopsis is a genus of the gymnopoid/marasmioid complex of the family Omphalotaceae. The classification system of *Collybiopsis* has recently undergone large changes through molecular approaches. The new classification system has not been applied for *Collybiopsis* in the Republic of Korea, and general research on this genus was also lacking. In this study, we analyzed the *Collybiopsis* species in the Republic of Korea by assessing all gymnopoid/marasmioid specimens collected nationwide for ten years by combining morphological approaches and multilocus (ITS + nrLSU) phylogenetic analysis. We thus confirmed that 16 species of *Collybiopsis* are present in the Republic of Korea, including two previously unreported species (*Co. nonnulla* and *Co. dichroa*) and seven new species (*Co. albicantipes* **sp. nov.**, *Co. clavicystidiata* **sp. nov.**, *Co. fulva* **sp. nov.**, *Co. orientisubnuda* **sp. nov.**, *Co. subumbilicata* **sp. nov.**, *Co. undulata* **sp. nov.**, and *Co. vellerea* **sp. nov.**). A thorough examination of the *Collybiopsis* suggested that it is difficult to distinguish or identify the species based on morphological characteristics only; a combined molecular approach is needed for accurate identification. The *Collybiopsis* database of the Republic of Korea is updated, and information on the new species is provided. Five new combinations from *Marasmiellus* to *Collybiopsis* are also proposed (*Co. istanbulensis* **comb. nov.**, *Co. koreana* **comb. nov.**, *Co. omphalodes* **comb. nov.**, *Co. pseudomphalodes* **comb. nov.**, and *Co. ramuliciola* **comb. nov.**).

Keywords

Collybia, gymnopoid, *Gymnopus*, ITS, *Marasmiellus*, marasmioid, nrLSU

Introduction

Collybiopsis Earle (1909) is a genus of gymnopoid/marasmioid mushrooms belonging to the family Omphalotaceae Bresinsky (Earle 1909; Petersen and Hughes 2021). Species of *Collybiopsis* are characterized by collybioid, gymnopoid, marasmielloid, omphalioid, and pleurotoid basidiomata; free to decurrent lamellae; a central to eccentric, insititious to subinsititious stipe; ellipsoid to oblong, inamyloid, and hyaline basidiospores with white sporeprints; presence of caulocystidia; and coralloid or diverticulate terminal elements of pileipellis (Murrill 1915; Singer 1973; Antonín and Noordeloos 1993; Retnowati 2018; Oliveira et al. 2019). Owing to its relatively uncharacteristic basidiocarp and little variation in morphological characteristics, most gymnopoid/marasmioid species were previously placed within the genus *Collybia* Staude (1857) and *Marasmius* Fr. (1835) before molecular identification was introduced actively to taxonomy. However, recent molecular studies have clarified the phylogenetic relationship of gymnopoid/marasmioid species belonging to the family Omphalotaceae and family Marasmiaceae Roze ex Kühner (Wilson and Desjardin 2005; Oliveira et al. 2019).

Initial molecular studies have segregated *Collybia* and *Marasmius* and some species of both genera transferred into several genera such as *Gymnopus* Roussel, *Marasmiellus* Murril, *Rhodocollybia* Singer, etc. (Moncalvo et al. 2002; Mata et al. 2004b; Mata et al. 2004c; Wilson and Desjardin 2005; Hughes et al. 2010; Oliveira et al. 2019; Petersen and Hughes 2017, 2021). Five *Collybia* sections (*Iocephalae* Halling, *Levipedes* Quél, *Striipedes* Quél, *Subfumosae* Singer, and *Vestipedes* Quél) were subsumed into *Gymnopus* sensu lato (s.l.) (Mata et. al., 2004c). However, *Gymnopus* s. l. is polyphyletic, and there has been much debate on the delimitation of this genus (Mata et al, 2004c; Wilson and Desjardin 2005; Mata et al. 2006; Oliveira et al. 2019; Petersen and Hughes 2016). Prior to this debate, a monophyletic genus, *Marasmiellus* sensu stricto (s. str.), was proposed (Wilson and Desjardin 2005), with *Marasmiellus juniperinus* Murrill as the monotype species (Wilson and Desjardin 2005; Sandoval-Leiva et al. 2016; Oliveira et al. 2019). A recent study showed that if judged congeneric, *Collybiopsis* Earle (1909) has priority over *Marasmiellus* Murrill (1915) based on the nomenclature rule (Petersen and Hughes 2021). Hereupon, *Collybiopsis* has been redefined based on the type species, *Collybiopsis ramealis* Earle, with at least 44 closely related species (Petersen and Hughes 2021). All species of *Collybiopsis* and some species of *Gymnopus* sect. *Vestipedes*, as well as some species of *Marasmiellus*, are included in the genus *Collybiopsis* (Petersen and Hughes 2021).

Collybiopsis is morphologically similar and phylogenetically close to *Gymnopus* (Desjardin et al. 1999; Mata 2002; Dutta et al. 2015). Both genera are reported to be distinguishable through like types of the terminal element of pileipellis, attachment of lamellae, the character of stipe, basidiospores, and cheilocystidia. However, as the characteristics of each genus cannot be seen as absolute because exceptions exist, and some characteristics overlap, it is difficult to distinguish *Collybiopsis* from *Gymnopus* solely on morphology. Furthermore, the morphological characteristics of their basidiomata vary greatly depending on the environment and developmental stage. Therefore,

molecular data play an important role in distinguishing these genera (Antonín and Herink 1999; Hughes et al. 2014; Hughes and Petersen 2015).

Although there have been many taxonomic changes for gymnopoid/marasmioid species, these changes have not been reflected in the gymnopoid/marasmioid species in the Republic of Korea. Since the first report of *Collybiopsis confluens* (Pers.) R.H. Petersen, as its previous name *Collybia confluens* Fr. (Kaburagi 1940), nine current *Collybiopsis* species have been reported until recently (National list of species of Korea 2020). However, they were identified and classified as *Collybia*, *Gymnopus*, and *Marasmiellus* based on their macroscopic morphological features. Owing to the uncertain placement of previous morphologically identified collybioid collections, it was necessary to re-examine Korean collections of collybioids and marasmioids based on molecular data. In this study, we investigated gymnopoid/marasmioid specimens collected over 10 years and deposited in three Korean herbaria based on their molecular analysis. As a result, we provide a list of *Collybiopsis* species in the Republic of Korea with seven new species.

Methods

Collections of specimens

A total of 372 specimens deposited in three Korean fungal herbarium – Seoul National University Fungus Collection (**SFC**), Korea National Arboretum (**KA**), and the National Institute of Biological Resources (**NIBR**) – were used in this study. The specimens were collected from 2012 to 2021 and stored in dried condition. All specimens were identified based on their morphological characteristics by each herbarium. The collection information (e.g. collection date, collection site, collector, etc.) and the notes of fresh basidiomata of each specimen were provided from each herbarium.

Molecular analysis

Genomic DNA was extracted from each specimen using a modified CTAB DNA extraction protocol (Rogers and Bendich 1994). The primer set ITS1F/ITS4B (Gardes and Bruns 1993) was used to amplify the internal transcribed spacer (ITS) region for all specimens, and the primer set LR0R/LR5 (Vilgalys and Hester 1990; Rehner and Samuels 1994) was used to amplify the nuclear large subunit ribosomal RNA (nrLSU) region. PCR was conducted by a C1000 thermal cycler (Bio-Rad, Richmond, CA, USA) using AccuPower PCR master premix (Bioneer Co., Daejeon, the Republic of Korea). PCR conditions for ITS and nrLSU region were: 5 min initial denaturation at 95 °C followed by 35 cycles of 40 s at 95 °C, 40 s at 55 °C and 60 s at 72 °C with a final extension step for 7 min at 72 °C. The amplifications of the PCR products were verified by visualization using 1% agarose gels with EcoDye DNA staining solution (SolGent Co., Daejeon, the Republic of Korea). The PCR products were purified using the ExpinTM PCR Purification Kit (GeneAll Biotechnology, Seoul, the Republic

of Korea) following the manufacturer's instructions. The purified PCR amplicons were sequenced using an ABI Prism 3700 Genetic Analyzer (Life Technologies, Gaithersburg, MD, USA) at Macrogen (Seoul, the Republic of Korea).

All sequences generated in this study were proofread using MEGA version 7 (Kumar et al. 2016). The sequences used for analyses were deposited in GenBank (Table 1). We then selected the closely related sequences from NCBI databases mainly referred to Oliveira et al. (2019) and Petersen and Hughes (2021). After retrieving all published ITS and nrLSU sequences of all *Collybiopsis* species in GenBank, phylogenetic analyses were performed together with new sequences generated from specimens. The sequences were respectively aligned for each loci using Multiple Alignment Fast Fourier Transform (MAFFT ver. 7) with the L-NSI-I option algorithm (Katoh and Standley 2013). The aligned sequence data were manually checked and edited. The final sequence of each specimen was created as a concatemer by manually attaching the aligned sequences of the two loci. Maximum likelihood (ML) phylogenetic tree was constructed on the CIPRES Science Gateway (Miller et al. 2012) using the GTR+GAMMA model with 1000 bootstrap replicates. *Rhodocollybia butyraceae* Lennox (TFB14382), *Rhodocollybia dotae* JL Mata and Halling (REH7007), and *Rhodocollybia maculate* Singer (TFB13989) were used as outgroups (Oliveira et al. 2019). Bootstraps higher than 70% were considered to support a clade and are shown in the tree (Figure 1).

Morphological observation

All specimens were preliminarily observed and macro/micro-structures of two to four representative specimens, which were in the best condition among the specimens, were presented in figures. Photographs and notes of fresh basidiomata taken at the time of collection were used for macro-morphological description. For micro-morphological observations, tissues of dried specimens were rehydrated in 5% (w/v) KOH and mounted in Congo red solution (Clémençon 1973) and Melzer's reagent. The observation was performed by using a Nikon Eclipse 80i optical microscope (Nikon, Tokyo, Japan) at 20 × to 1000 × magnification. More than thirty basidiospores and more than twenty other microstructures (e.g., basidia, cheilocystidia, etc.) were measured to analyze the microstructures based on the microscopic pictures of specimens stained with Congo red. The Methuen Handbook of Colour (Kornerup and Wanscher 1978) was used for color indications. The following abbreviations and acronyms were used: ***Co*** = *Collybiopsis*; ***G*** = *Gymnopus*; ***Ma*** = *Marasmiellus*; **L** = the number of complete lamellae; **l** = the number of lamellulae tiers between neighboring complete lamellae; and **Q** = the values of the length divided by the width of basidiospores (Petersen and Hughes 2021; Ryoo et al. 2020).

Results

Through ITS sequence analysis of 372 gymnopoid/marasmioid specimens, 201 specimens were confirmed to belong to *Collybiopsis*. The remaining 160 specimens were

Table 1. Information about the *Collybiopsis* specimens and published *Collybiopsis* sequences used in phylogenetic analysis. Species with an asterisk are those proposed as new species. Sequences newly produced in this study are presented in bold.

Organisms	Specimen	Collection Date	Location	GenBank Accession Number	
				ITS	nrLSU
Collybiopsis albicantipes*	**SFC20170725-35**	25.7.2017	Yeosu-si, Jeollanam-do, the Republic of Korea	**OL467272**	**OL462811**
	SFC20180704-86	4.7.2018	Jindo-gun, Jeollanam-do, the Republic of Korea	**OL467273**	**OL462812**
Co. biformis	TFB14251		USA: Tennessee, GSMNP	KJ416245	KJ189567
	TFB13890		USA: North Carolina	KJ416248	KJ189570
	TFB13814		USA: Tennessee	KJ416249	KJ189569
	KA14-0526	15.7.2014	Suncheon, Jeollanam-do, the Republic of Korea	**OL467227**	**OL462784**
	KA16-0526	13.7.2016	Sinan-gun, Jeollanam-do, the Republic of Korea	**OL467228**	**OL462785**
	SFC20180704-36	4.7.2018	Wando-gun, Jeollanam-do, the Republic of Korea	**OL467229**	**OL462789**
	SFC20180831-16	31.8.2018	Jindo-gun, Jeollanam-do, the Republic of Korea	**OL467230**	**OL462790**
Co. brunneigracilis	AWW01		Java/Bali	AY263434	AY639412
Co. californica	TFB5787		Canada: British Columbia	MN413338	
Co. clavicystidiata*	**SFC20180705-26**	5.7.2018	Haenam-gun, Jeollanam-do, the Republic of Korea	**OL467250**	**OL462816**
	SFC20180705-84	5.7.2018	Jindo-gun, Jeollanam-do, the Republic of Korea	**OL467252**	**OL462817**
	SFC20180705-92	5.7.2018	Jindo-gun, Jeollanam-do, the Republic of Korea	**OL467253**	**OL462818**
	SFC20180713-09	13.7.2018	Gwanak-gu, Seoul, the Republic of Korea	**OL467251**	**OL462819**
Co. confluens	**SFC20190731-06**	31.7.2019	Taebaek-si, Gangwon-do, the Republic of Korea	**OL467237**	**OL462797**
	SFC20190731-48	31.7.2019	Taebaek-si, Gangwon-do, the Republic of Korea	**OL467238**	**OL462798**
	TFB14115		Germany, Thuringia	KP710292	KJ189578
	110116MFBPL0425		China	MW554401	
	HMAS 290186		China	MK966541	
Co. confluens ssp. *americana*	TFB14409		Canada: New Brunswick	KP710278	KJ189585
	TFB14075		USA: North Carolina	KP710281	KJ189581
Co. dichroa	**KA14-0969**	19.8.2014	Hwasun-gun, Jeollanam-do, the Republic of Korea	**OL467254**	**OL462799**
	KA18-0389	10.7.2018	Cheongdo-gun, Gyeongsangbuk-do, the Republic of Korea	**OL467255**	**OL546541**
	SFC20180712-16	12.7.2018	Gwangju, Gyeonggi-do, the Republic of Korea	**OL467256**	**OL462800**
	TFB9623		USA: North Carolina	MW396865	MW396865
	TENN60014c2		USA: Tennessee, GSMNP	JF313671	
	TFB7920		USA	DQ450007	
	TENN61624c1a		USA: Tennessee, GSMNP	JF313678	
	TFB2028		USA	DQ450008	
	TENN61624c9		USA: Tennessee, GSMNP	JF313692	
Co. disjuncta	TFB14339		USA: Connecticut	NR_137865	
	TFB14281		USA: Mississippi	KJ416253	KY019643
Co. eneficola	09-09-26AV13		Canada: Newfoundland	NR_137613	NG_059502
	MICH:PK6975		Alaska	KP710270	KP710304
Co. fibrosipes	FB9699		Costa Rica	AF505763	
Co. filamentipes	TFB13962		USA: Tennessee	MN897832	MN897832
Co. foliiphila	CUH AM090		India	NR_154176	NG_060320
	CUM AM101		India	KP317638	KP317636
Co. fulva*	**KA13-0216**	19.6.2013	Geochang-gun, Gyeongsangnam-do, the Republic of Korea	**OL467257**	**OL462793**
	KA13-0333	10.7.2013	Pocheon-si, Gyeonggi-do, the Republic of Korea	**OL467258**	**OL462794**
	KA15-0210	21.7.2015	Pocheon-si, Gyeonggi-do, the Republic of Korea	**OL467259**	**OL462795**
Co. furtiva	TFB4796		USA: Georgia	MN413343	MW396879
Co. gibbosa	MEL:2382838		Australia	KP012713	KP012713
	URM 90012		Brazil	KY061202	KY061202
Co. hasanskyensis	TFB11846		Russia: Kedrovaya	MN897829	
	TFB11847		Russia	MN897830	

Organisms	Specimen	Collection Date	Location	GenBank Accession Number	
				ITS	nrLSU
Co. indoctus	AWW04		Unknown	AY263439	
Co. istanbulensis	KATO Fungi 3596		Turkey	KX184795	KX184796
	BRNM 781163		Turkey	KY250435	
Co. juniperina	TFB9889		USA: Louisiana	AY256708	KY019637
	TFB10782		Argentina: Missiones	KY026661	KY026661
Co. koreana	**SFC20120821-84**	21.8.2012	Boryeong-si, Chungcheongnam-do, the Republic of Korea	**OL467269**	**OL546545**
	SFC20130711-05	11.7.2013	Pyeongchang-gun, Gangwon-do, the Republic of Korea	**OL467270**	**OL462801**
	SFC20150721-10	21.7.2015	Inje-gun, Gangwon-do, the Republic of Korea	**OL467271**	**OL462802**
	BRNM 714972		Korea	GU319113	GU319117
	BRNM 718782		Korea	GU319114	GU319118
Co. luxurians	**NIBRFG0000502888**	4.9.2018	Ongjin-gun, Incheon, the Republic of Korea	**OL467248**	**OL462803**
	SFC20190731-18	31.7.2019	Taebaek-si, Gangwon-do, the Republic of Korea	**OL467249**	**OL462804**
	TFB10350		USA: North Carolina	AY256709	AY256709
	ZD16102301		China	MN523270	
	TFB9121		USA: Louisiana	KY026649	KY026649
Co. melanopus	AWW54		Java/Bali	NR_137539	NG_060624
	CUH AM093		India	KM896875	KP100305
Co. menehune	**SFC20150811-29**	11.8.2015	Guri-si, Gyeonggi-do, the Republic of Korea	**OL467235**	**OL462805**
	SFC20180905-33	5.9.2018	Anyang City, Gyeonggi Province, the Republic of Korea	**OL467236**	**OL462806**
	SFSU: DED5866		Hawaii	AY263426	
	CUH:AM074		India	KJ778753	KP100302
	SFSU-AWW15		Java/Bali	AY263443	AY639424
Co. mesoamericana	TFB11005		Costa Rica	DQ450035	KY019632
	REH7379		Costa Rica	AF505768	
Co. micromphaleoides	TENN 68165				
	TFB14282				
Co. minor	TFB11930		USA: Tennessee, GSMNP	MN413334	MW396880
	TFB5434		USA: South Carolina	MW396872	MW396872
Co. neotropica	TFB10416		Costa Rica	AF505769	
Co. nonnulla	**KA13-0254**	20.6.2013	Geochang-gun, Gyeongsangnam-do, the Republic of Korea	**OL467242**	**OL462820**
	KA13-0741	21.8.2013	Geochang-gun, Gyeongsangnam-do, the Republic of Korea	**OL467243**	**OL462807**
	KA15-0129	14.7.2015	Gangneung-si, Gangwon-do, the Republic of Korea	**OL467244**	**OL462808**
	TFB14492		USA: Mississippi	KY026699	KY026699
	TFB14278		USA: Mississippi	KY026701	KY026701
Co. nonnulla var. *attenuatus*	AWW05		Java/Bali	AY263445	AY639426
	AWW55		Java/Bali	AY263446	
	RAK369.2		Cameroon	MN930621	
	RAK372.2		Cameroon	MN930622	
Co. obscuroides	GB-0150514		Norway: Svalbard	KX958399	KX958399
Co. omphalodes	FB11021		Costa Rica	AF505761	
	TFB 10427		Costa Rica	DQ450011	
	TFB 10022		Costa Rica	AY256700	
Co. orientisubnuda*	**NIBRFG0000500990**	19.7.2016	Ulleung-gun, Gyeongsangbuk-do, the Republic of Korea	**OL467262**	**OL546546**
	SFC20170823-39	23.8.2017	Hapcheon-gun, Gyeongsangnam-do, the Republic of Korea	**OL467263**	**OL546547**
	SFC20180830-29	30.8.2018	Hapcheon-gun, Gyeongsangnam-do, the Republic of Korea	**OL467264**	**OL462796**
(as *Gymnopus subnudus*)	KUC20150911-19		Korea	KX513748	
Co. parvula	TFB10419		Costa Rica	DQ450060	
	TFB10422		Costa Rica	AF505774	

Organisms	Specimen	Collection Date	Location	GenBank Accession Number	
				ITS	nrLSU
Co. peronata	TFB13743		Belgium	KY026677	KY026677
	LE-Bin1364		Russia	KY026755	KY026755
	CBS 223.37		unknown	MH855896	MH867405
Co. polygramma	**SFC20170807-35**	7.8.2017	Hapcheon-gun, Gyeongsangnam-do, the Republic of Korea	**OL467245**	**OL546542**
	SFC20180905-63	5.9.2018	Gwanak-gu, Seoul, the Republic of Korea	**OL467246**	**OL546544**
	SFC20210629-01	29.6.2021	Gwanak-gu, Seoul, the Republic of Korea	**OL467247**	**OL546543**
	PR2542TN		Puerto Rico	DQ450028	
	CUH:AM082		India	KJ778752	KP100303
	URM 90015		Brazil: Amapa	KY074640	KY088275
	MHHNU 30912		China	MK214392	
	TFB9628		Puerto Rico	DQ450028	
	SFC20120821-64		Korea	KJ609162	
	HFJAU 0425		China: Jiangxi	MN258643	
(as *Gymnopus iocephalus*)	KUC20140804-02		Korea	KX513745	
Co. pseudoluxurians	TFB14290		USA: Mississippi	NR_137863	
Co. pseudomphalodes	REH7348		Costa Rica	AF505762	
	PR24TN		Puerto Rico	AY842957	
Co. quercophila	TFB14570		Slovakia	KY026728	KY026728
	TFB14615		USA: California	KY026736	KY026736
Co. ramealis	**NIBRFG0000508888**	29.7.2020	Jeongseon-gun, Gangwon-do, the Republic of Korea	**OL467260**	**OL546549**
	TFB13769		Belgium: Couvin	MN413345	MN413345
	TFB13770		Belgium: Couvin	MN413346	MW396882
	DED4425		USA: North Carolina	DQ450031	AF042650
	TFB14555		Slovakia	MW405779	MW396884
	BR 72_41		Belgium	MW396875	MW396875
Co. ramulicola	GDGM 43884		China	KU057798	
	GDGM 44256		China	KU321529	
	GDGM 50060		China	KU321530	
Co. readiae	TFB7571		New Zealand	DQ450034	
	PDD:95844		New Zealand	HQ533036	
Co. stenophylla	TFB13998		USA: Tennessee,	MN413331	MW396886
	TFB4798		USA: Georgia	MN413330	MW396887
Co. subcyathiformis	TFB9629				
	URM 90023		Brazil: Para	KY404982	KY404982
	URM 90022		Brazil: Para	KY404983	KY404983
Co. subnuda	TFB12577		USA: Tennessee, GSMNP	KY026667	FJ750262
	WRW 08-462		USA: West Virginia	KY026765	KY026765
	TFB14043		USA: North Carolina	MW396876	MW396876
Co. subpruinosus	BRNM781138		Portugal: Madeira	MK646034	
	TFB11063		USA	DQ450025	
Co. subumbilicata*	**SFC20120802-03**	2.8.2012	Goseong-gun, Gangwon-do, the Republic of Korea	**OL467231**	**OL462786**
	SFC20140701-03	1.7.2014	Inje-gun, Gangwon-do, the Republic of Korea	**OL467232**	**OL462787**
	SFC20150902-50	2.9.2015	Ulleung-gun, Gyeongsangbuk-do, the Republic of Korea	**OL467234**	**OL546540**
	SFC20170822-14	22.8.2017	Ulleung-gun, Gyeongsangbuk-do, the Republic of Korea	**OL467233**	**OL462788**
Co. trogioides	AWW51		Indonesia	AY263428	AY639431
Co. undulata*	**SFC20120821-04**	21.8.2012	Boryeong-si, Chungcheongnam-do, the Republic of Korea	**OL467239**	**OL462813**
	SFC20130808-08	8.8.2013	Sangju-si, Gyeongsangbuk-do, the Republic of Korea	**OL467240**	**OL462814**
	SFC20150813-04	13.8.2015	Goyang-si, Gyeonggi-do, the Republic of Korea	**OL467241**	**OL462815**

Organisms	Specimen	Collection Date	Location	GenBank Accession Number	
				ITS	nrLSU
Co. utriformis	TFB14334h1		USA: Connecticut	KY026708	KY026708
	WRW05-1170		USA: West Virginia	KY026764	KY026764
Co. vellerea*	**NIBRFG0000502858**	4.9.2018	Ongjin-gun, Incheon, the Republic of Korea	**OL467265**	**OL462791**
	SFC20120708-02	8.7.2012	Seosan-si, Chungcheongnam-do, the Republic of Korea	**OL467266**	**OL462809**
	SFC20140821-29	21.8.2014	Gwanak-gu, Seoul, the Republic of Korea	**OL467267**	**OL462810**
	SFC20180705-90	5.7.2018	Jindo-gun, Jeollanam-do, the Republic of Korea	**OL467268**	**OL462792**
Co. vallianti	TFB13739		USA: Tennessee, GSMNP	KY026676	KY026676
Co. villosipes	TFB9539		USA	DQ450058	
	TFB12836		New Zealand: Fiordland	KJ416255	FJ750264
Collybiopsis cf. *ramealis*	**SFC20180829-20**	29.8.2018	Shinan-gun, Jeollanam-do, the Republic of Korea	**OL467261**	**OL546548**
Rhodocollybia butyracea	TFB 14382		Canada: New Brunswick	KY026716	KY026716
Rhodocollybia dotae	REH7007		Costa Rica	AF505758	
Rhodocollybia maculata	TFB 13989		USA: Mississippi	KY026688	KY026688

identified as members of the following genera: *Gymnopus*, *Marasmius*, or *Rhodocollybia* and were excluded from this study. A total of 201 specimens were segregated into 16 putative taxa based on ITS phylogenetic analyses (Table 2). To confirm the species' identity and to infer the phylogenetic relationships within *Collybiopsis*, the nrLSU region was amplified and sequenced from 47 representative specimens of 16 taxa (Table 1). The final phylogenetic analyses were conducted with datasets of two loci from 16 *Collybiopsis* species (Table 1). In ML analysis, 178 multigene sequences (110 for ITS and 68 for nrLSU) were retrieved from GenBank and used. The adjusted alignments comprised 535 to 794 bases for ITS and 324 to 904 bases for nrLSU. The phylogenetic analysis results of the two combined loci revealed that *Collybiopsis* specimens from the Republic of Korea were identified as 16 taxa (Fig. 1).

Of the 16 putative taxa, nine matched with previously described species – *Co. biformis* (Peck) R.H. Petersen, *Co. confluens*, *Co. dichroa* (Berk. & M.A. Curtis) Earle, *Co. luxurians* (Peck) R.H. Petersen, *Co. menehune* (Desjardin, Halling & Hemmes) R.H. Petersen, *Co. nonnulla* (Corner) R.H. Petersen, *Co. polygramma* (Mont.) R.H. Petersen, *Co. ramealis* (Bull.) Earle, and *Marasmiellus koreanus* Antonín, Ryoo & H.D. Pictures of basidiomata are shown in Fig. 2. The other seven taxa formed distinct clades and did not correspond to any known *Collybiopsis* species. Furthermore, based on the comparison with other *Collybiopsis* species, these seven species have distinct morphological characteristics, confirming that they were new to science – *Co. albicantipes* sp. nov., *Co. clavicystidiata* sp. nov., *Co. fulva* sp. nov., *Co. orientisubnuda* sp. nov., *Co. subumbilicata* sp. nov., *Co. undulata* sp. nov., and *Co. vellerea* sp. nov. Illustrations of basidiomata and micro-morphological features are shown in Figs 3 and 4.

Five species (*G. omphalodes* Halling & J.L. Mata, *G. pseudomphalodes* J.L. Mata, *G. ramulicola* T.H. Li & S.F. Deng, *Ma. istanbulensis* E. Sesli, Antonín and E.Aytaç, and *Ma. koreanus*), previously placed in *Gymnopus* section *Vestipedes*, were confirmed to be-

Table 2. Identification information of Korean *Collybiopsis* specimens confirmed in the study. Scientific names in bold indicate new species.

Species	Specimen Number				
Co. albicantipes	SFC20170725-35	SFC20180704-86			
Co. biformis	NIBRFG0000502789	KA14-0259	KA14-0526	KA14-0917	KA14-0924
	KA16-0307	KA16-0371	KA16-0526	KA18-0657	KA18-0673
	SFC20140724-41	SFC20160719-42	SFC20180704-36	SFC20180706-05	SFC20180831-13
	SFC20180831-16				
Co. clavicystidiata	KA14-0667	KA14-0724	KA15-0211	KA17-0287	KA17-0369
	KA18-0282	KA18-0353	SFC20180705-84	SFC20180705-92	SFC20180706-04
	SFC20180713-09				
Co. confluens	NIBRFG0000508913	NIBRFG0000508991	KA16-0696	KA18-0338	SFC20150626-26
	SFC20190731-06	SFC20190731-32	SFC20190731-34	SFC20190731-48	
Co. dichroa	KA14-0969	KA17-0344	SFC20180706-60	SFC20180712-16	
Co. fulva	KA13-0215	KA13-0216	KA13-0333	KA13-0357	KA14-0168
	KA14-0386	KA14-0666	KA14-0691	KA15-0210	KA16-0425
	KA16-0428	KA17-0388	KA17-0596	KA18-0233	KA18-0241
Co. koreana	SFC20120821-84	SFC20150702-25	SFC20170713-06	SFC20180704-17	
Co. luxurians	NIBRFG0000502888	SFC20190731-18	SFC20190731-08	SFC20190730-36	SFC20180907-105
	SFC20180905-86	SFC20180905-43	KA18-0321	KA14-0579	
Co. menehune	NIBRFG0000502876	KA13-0887	KA14-0494	KA14-0510	SFC20150811-29
	SFC20160719-15	SFC20180905-33			
Co. nonnulla	KA13-0254	KA13-0741	KA15-0129		
Co. orientisubnuda	SFC20170823-39	SFC20170708-14	SFC20150902-01	SFC20150820-59	SFC20150820-01
	SFC20150811-48	SFC20150701-100	QM20200911-57	QM20200911-52	KA17-0787
	KA17-0600	KA16-1154	KA16-0925	KA16-0902	KA16-0780
	KA16-0724	KA15-0179	KA14-0985	KA13-1225	F20200730-24
	F20200701-11	F20200630-30	F20180904KCM21	F20160719-12	
Co. polygramma	KA13-0506	KA13-0956	KA13-1101	KA13-1333	KA14-0904
	KA14-1089	KA14-1092	KA18-0115	KA18-0724	QM20200721-07
	NIBRFG0000508098	NIBRFG0000508059	NIBRFG0000508089	SFC20170712-08	SFC20170807-35
	SFC20170822-66	SFC20180905-49	SFC20180905-63		
Co. ramealis	SFC20130711-05				
Co. subumbilicata	KA13-1214	KA15-0173	KA15-0185	KA15-0787	SFC20120802-03
	SFC20140701-03	SFC20150902-50	SFC20170822-14	SFC20210623-03	
Co. undulata	KA17-0335	KA18-0651	KA18-0651	SFC20120821-04	SFC20130808-08
	SFC20150715-24	SFC20150813-04			
Co. vellerea	KA14-0132	KA14-0163	KA14-0196	KA14-0245	KA14-0397
	KA14-0412	KA14-0446	KA14-0447	KA14-0474	KA14-0725
	KA14-0734	KA14-0735	KA14-0774	KA14-0787	KA14-1005
	KA14-1061	KA14-1147	KA14-1349	KA14-1426	KA14-1475
	KA14-1555	KA14-1558	KA15-0213	KA15-0215	KA15-0473
	KA15-0485	KA15-0502	KA15-0527	KA15-0568	KA16-0191
	KA16-0252	KA16-0485	KA16-0783	KA16-0982	KA16-0985
	KA16-0986	KA16-0992	KA17-0368	KA17-0586	KA17-0742
	KA17-1074	KA18-0089	KA18-0139	KA18-0151	KA18-0152
	KA18-0348	KA18-0795	KA18-0836	KA18-0987	KA18-1027
	KA19-0125	SFC20120708-02	SFC20120820-02	SFC20140821-29	SFC20150630-38
	SFC20150714-01	SFC20170705-06	SFC20180705-90	SFC20180829-30	SFC20180901-01
Collybiopsis cf. *ramealis*	F20200729-14				

long to the genus *Collybiopsis*, and we thus propose to reclassify them as *Co. omphalodes* comb. nov., *Co. pseudomphalodes* comb. nov., *Co. ramulicola* comb. nov., *Co. istanbulensis* comb. nov., and *Co. koreana* comb. nov. respectively.

Figure 1. Phylogenetic tree based on maximum likelihood analysis using combined sequence data of ITS and nrLSU. ML bootstrap values greater than 70% are indicated at the nodes. *Collybiopsis* species that were newly sequenced in this study are represented in bold. Species with an asterisk are those proposed as new species.

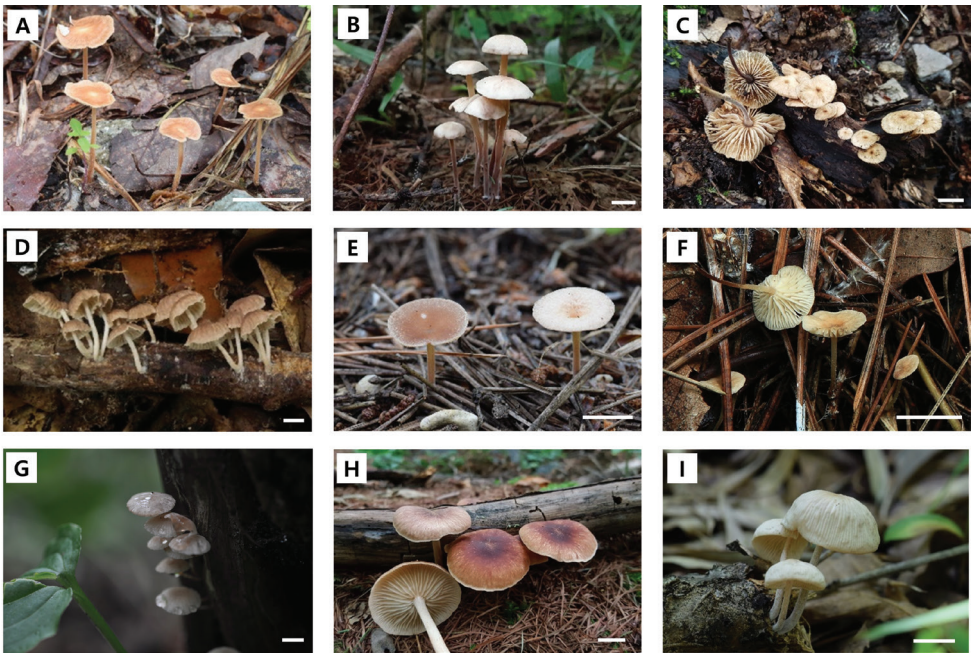

Figure 2. Basidiomata of the described *Collybiopsis* species in the Republic of Korea **A** *Co. biformis* (SFC20180706–05) **B** *Co. confluens* (SFC20190731–06) **C** *Co. dichroa* (KA18–0389) **D** *Co. koreana* (SFC20180704–17) **E** *Co. luxurians* (SFC20190731–18) **F** *Co. menehune* (SFC20150811–29) **G** *Co. nonnulla* (KA13–0254) **H** *Co. polygramma* (SFC20170712–08) **I** *Co. ramealis* (SFC20180829–20). Scale bar: 1 cm (**A–I**).

Taxonomy

Collybiopsis albicantipes **J.S. Kim & Y.W. Lim, sp. nov.**
MycoBank No: 842053
Fig. 3A–B, Suppl. material 1: Fig. S1A

Etymology. Epithet "*albicantipes*" refers to having a whitish base of the stipe.

Holotype. The Republic of Korea, Jeollanam-do: Yeosu-si, Dolsan-eup, Hyangiram, 34°35'27"N, 127°47'55"E, alt. 183 m, 25 July 2017, Jae Young Park, Komsit Wisitrassameewong, SFC20170725–35 (GenBank accession no. ITS: OL467272; nrLSU: OL462811).

Diagnosis. This species notably has hemispherical to convex, 4–23 mm pileus, distant lamellae, central to eccentric, tomentose, 5–15 × 0.5−1.5 mm stipe with a white base; ellipsoid to ovoid, 5.8–7.4 × 2.8–4 µm basidiospores, clavate (often constricted), 25.5–34.8 × 4.8–6.7 µm basidia, broadly clavate, irregular, sometimes lobed, 26–49 × 5.4–10.6 µm cheilocystidia, and a habit of fruiting on branches.

Description. Pileus: 4−23 mm, eccentric, convex to hemispherical when young, becoming depressed and undulating with age; Surface smooth, brownish orange (5C3 to 6D4) at the center, becoming paler to the margin (4A3 to 3A2). Lamellae: distant,

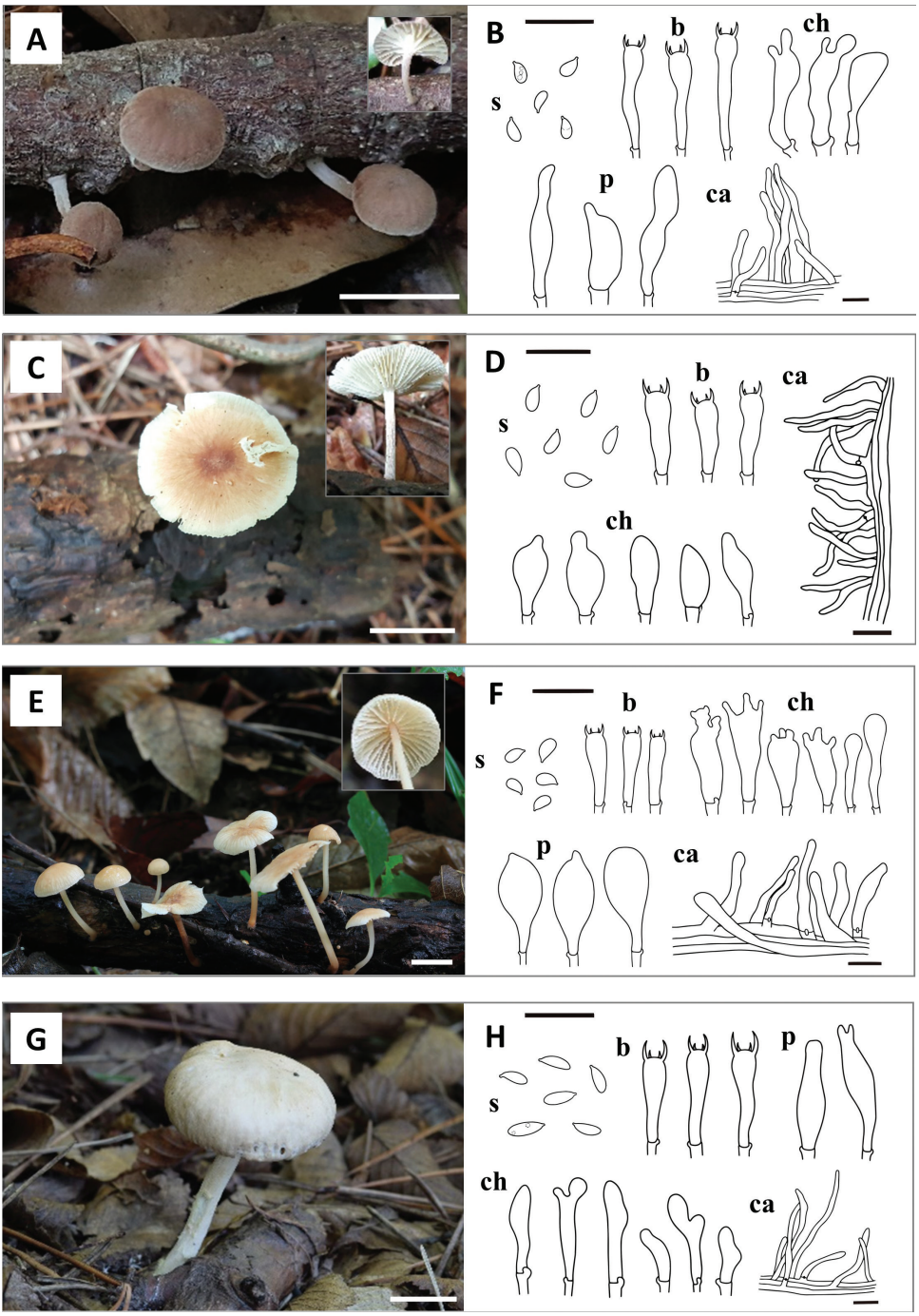

Figure 3. Basidiomata and microscopic characters of the four new *Collybiopsis* species **A, B** *Co. albicantipes* (SFC20170725–35) **C, D** *Co. clavicystidiata* (SFC20180705–84) **E, F** *Co. fulva* (KA15–0210) **G, H** *Co. orientisubnuda* (NIBRFG0000502862). Scale bars: 1cm (A, C, E, G); 20 *μm* (**B, D, F, H**). Abbreviations: **s** basidiospores; **b** basidia; **ch** cheilocystidia; **p** pleurocystidia; **ca** caulocystidia.

L = 10–16, l = 3–7, adnate, whitish to yellowish white (3A2). Stipe: 5–15 × 0.5−1.5 mm, central to eccentric, cylindrical, tomentose, apex brownish orange (5C3) to light brown (6D4), gradually becoming paler downwards (5B2 to 6C2), with whitish basal tomentum. Basidiospores: 5.8–7.4 × 2.8–4 μm (average 5.5 × 3.2 μm), *Q* = 1.6–2.1 (mean = 1.97), ellipsoid to ovoid, amygdaliform, smooth, hyaline, non-dextrinoid, with drops. Basidia: (23) 25.5–34.8 × 4.8–6.7 (7) μm, 4-spored, clavate, often constricted. Cheilocystidia: 26–49 × 5.4–10.6 (14) μm, broadly clavate, irregular, sometimes lobed. Pleurocystidia: 25.8–56.4 (62) × 6.2–12.5 μm, clavate, subulate, sometimes lobed. Trama hyphae: cylindrical, often sub-inflated, smooth, non-dextrinoid 1.7–9 (12) μm wide. Pileipellis: a cutis made up of cylindrical, often sub-inflated, with weak annular ornamentation, 2.0−7.5 μm wide hyphae; terminal elements adpressed, cylindrical, clavate, sometimes constricted or curved, 2.0−5 μm wide. Stipitipellis: a cutis of cylindrical, smooth, 2.7−9.7 (11) μm wide hyphae. Caulocystidia: 21.7–90 × 3.9–11.7 μm, cylindrical, flexuose, sometimes curved. Clamp connections: present in all tissues.

Other specimens examined. The Republic of Korea, Jeollanam-do: Jindo-gun, Maenggoldo island, 34°12'21"N, 125°51'41"E, alt. 24 m, 4 July 2018, Jae Young Park, SFC20180704–86.

Habit and habitat. Scattered to gregarious on the branch in mixed forest dominated by *Camellia japonica* Linne, in summer.

Distribution. The Republic of Korea.

Remark. *Collybiopsis albicantipes* is similar to *Co. ramulicola* and *Co. koreana* when comparing macro-morphological characteristics. *Collybiopsis ramulicola* is distinguishable from *Co. albicantipes* by a reddish pileus, fewer and buff lamellulae (1–4), a shorter and thinner stipe (12–23 × 2–3 mm), shorter and slightly elongated basidiospores (6.6–8.4 × 3.5–4.5 μm), shorter basidia (23–27 × 3.8–5.5 μm), and shorter cheilocystidia (23–27 × 3–6 μm) (Deng et al. 2016). *Collybiopsis koreana* differs from *Co. albicantipes* by having a larger pileus (27–60 mm), more lamellae (15–20) and lamellulae (2–3), longer and thicker stipe (14–70 × 2–3.5 μm), bigger and elongated basidiospores (7.5–10 × 4–5 μm), cheilocystidia with different shapes and sizes (25–55 × 4–10 μm), and incrustation dark brown in KOH (Antonín et al. 2010).

***Collybiopsis clavicystidiata* J.S. Kim & Y.W. Lim, sp. nov.**

MycoBank No: 842054

Fig. 3C–D, Suppl. material 1: Fig. S1B

Etymology. Epithet "*clavicystidiata*" indicates that the new species has clavate cheilocystidia.

Holotype. The Republic of Korea, Jeollanam-do: Jindo-gun, Jodo-myeon, Donggeocha island, 34°23'34"N, 125°93'84"E, alt. 70 m, 05 July 2018, Jae Young Park, Tae Heon Kim, SFC20180705–84, (GenBank accession no. ITS: OL467252; nrLSU: OL462817).

Diagnosis. The prominent features of this species include a greyish orange to brownish, 6–45 mm pileus, whitish lamellae, a subinstitious, tomentose, whitish, 15–

26 × 1.2−1.6 mm stipe, oblong to subcylindrical, 6.7−9.4 × 3.1−4.6 μm basidiospores, utriform, clavate, 20.1–37.5 × 6.8–12.2 μm cheilocystidia, and cylindrical, flexuose, irregular, 17–50 × 3.5–7 μm caulocystidia.

Description. Pileus: 6–45 mm, convex to hemispherical, becoming plano-convex to flat with an uplifted margin with age; Surface smooth, dull, hygrophanous, greyish orange (6B3) to brownish (7D8 to E8) at the center, being whitish at the margin (4A2 to 6C8), being paler with age. Lamellae: subdistant, L = 20–32, l = 1–7, adnexed, white. Stipe: 15–26 × 1.2−1.6 mm, cylindrical, tomentose, subinsititious, whitish to reddish grey (9B2). Basidiospores: 6.7−9.4 × 3.1−4.6 μm, average 8.13 × 3.62 μm, Q = 2–2.4 (mean = 2.26), oblong to cylindrical, smooth, hyaline, non-dextrinoid, with drops. Basidia: 18.3–30 × 4.1–8.8 μm, 4-spored, narrowly clavate, narrowly utriform, often curved. Cheilocystidia: 20.1–37.5 × 6.8–12.2 μm, utriform, clavate, sometimes with mucronate apex. Pleurocystidia: absent. Trama hyphae: cylindrical, often subinflated, smooth, branched, non-dextrinoid, 2−12 μm wide. Pileipellis: transition between cutis and trichoderm, composed of cylindrical, with heavy annular ornamentation, 4−12 μm wide hyphae; terminal elements adpressed to suberect, cylindrical, clavate, often incrusted (often incrusted), thin-walled, 3−6 μm wide. Stipitipellis: a cutis of cylindrical, smooth, 2−7 μm wide hyphae. Caulocystidia: 17–50 × 3.5–7 μm, cylindrical, flexuose, irregular or curved. Clamp connections: present in all tissues.

Other specimens examined. The Republic of Korea, Jeollanam-do: Haenam-gun, Mt. Duryun, 34°29'6"N, 126°38'54"E, alt. 169 m, 5 July 2018, Young Woon Lim, Abel Severin Lupala, Jun Won Lee, SFC20180705–26. The Republic of Korea, Seoul: Gwanak-gu, Gwanak-ro 1, Seoul National University, 37° 27' 37"N, 126° 56' 59"E, alt. 80m, 13 July 2018, Jae Young Park, SFC20180713–09.

Habit and habitat. Solitary to scattered on dead wood debris of conifers, in summer.

Distribution. The Republic of Korea

Remark. *Collybiopsis clavicystidiata* is morphologically similar to *G. omphalodes* and *Co. menehune*. *Collybiopsis omphalodes* differs in their larger pileus (2–30 mm), a darker colored stipe, smaller basidiospores (5–6 × 2.5–3 μm), and thinner hyphae in the pileipellis (5–8 μm wide). *Collybiopsis menehune* can be distinguished from *Co. clavicystidiata* by its larger pileus (8–30 mm), buff lamellae, longer stipe (15–60 mm), longer basidiospores (7.5–9.5 × 3.5–4.2 μm, Q = 2.2), and longer caulocystidia (16–67 × 3–5 μm) (Desjardin et al. 1999). *Co. clavicystidiata* is phylogenetically close to *Co. pseudomphalodes*. *Collybiopsis pseudomphalodes* has relatively few references for comparison, but differences can be found in the lengths of the stipe (3–4 mm) and cheilocystidia (40 × 3 μm) when compared with *Co. clavicystidiata* (Dennis 1961).

Collybiopsis fulva **J.S. Kim & Y.W. Lim, sp. nov.**

MycoBank No: 842055

Fig. 3E–F, Suppl. material 1: Fig. S1C

Diagnosis. This species has a pale orange to brownish-colored, 4–20 mm pileus, an orange white colored to light brownish colored, 7–30 × 0.7–1 mm stipe with pubescence,

spheropedunculate, pleurocystidia, oblong to subcylindrical, 6.8–9.2 × 3.1–4.9 µm basidiospore, lobed, clavate with rostrate apex, 24.8–38.4 × 6.5–11.8 µm cheilocystidia.

Etymology. Epithet "*fulva*" referring to fox-colored pileus.

Holotype. The Republic of Korea, Gyeonggi-do: Pocheon-si, Soheul-eup, Gwangneungsumogwon-ro 415, 37°45'17"N, 127°9'59"E, alt. 101 m, Sang Kook Han, 21 July 2015, KA15–0210 (GenBank accession no. ITS: OL467259; nrLSU: OL462795).

Description. Pileus: 4–20mm, hemispherical, convex to plane, sometimes concave with slightly reflexed, wavy margin, hygrophanous, pale orange (6A3) to greyish orange, becoming more brownish to the center (5B4 to 7C4). Lamellae: distant, L = 16–28, l = 1–5, sinuate, broad, whitish to yellowish white (4A2) to brownish orange (6C4 to 7C4). Stipe: 7–30 × 0.7–1 mm, cylindrical, gradually widened towards the base, tomentose, apex orange white (5A2) to brownish orange (6C6), becoming dense downwards (6D8), covered with pubescence. Basidiospores: 6.8–9.2 × 3.1–4.9 µm (average 7.47 × 3.69 µm), Q = 2.05, oblong to cylindrical, smooth, colorless, non-dextrinoid, with drops. Basidia: 20.4–29.4 × 4.7–7.8 µm, 4-spored, narrowly clavate, sometimes constricted or curved. Cheilocystidia: (20.5) 24.8–38.4 × 6.5–11.8 µm, lobed, clavate, sometimes with rostrate apex. Pleurocystidia: 31.5–46.9 × 12–20.6 µm, spheropedunculate, obovoid, sometimes with mucronate apex. Trama hyphae: cylindrical to subinflated, irregular, thin-walled, smooth, branched, non-dextrinoid, 2.0−15 µm wide. Pileipellis: a cutis of cylindrical, thin-walled, 4–15 µm wide hyphae; terminal elements adpressed to suberect, narrowly clavate, thin-walled, with heavy annular ornamentation, 3–8 µm wide. Stipitipellis: a cutis of cylindrical, thin-walled, smooth, 5−15 µm wide hyphae. Caulocystidia: 45.6–108.3 (131) × 6.8–14.8 µm, cylindrical, irregular, curved. Clamp connections: present in all tissues.

Other specimens examined. The Republic of Korea, Gyeonggi-do: Pocheon-si, Soheul-eup, Gwangneung forest exhibition hall, 37°45'19"N, 127°9'58"E, alt. 99 m, 8 July 2016, Sang Kook Han, KA16–0428. The Republic of Korea, Gyeongsangnam-do: Geochang-gun, Mt. Gibaek, 35°43'6"N, 127°45'49"E, alt. 1095 m, 19 June 2013, Sang Kook Han, KA13–0216.

Habit and habitat. Scattered or gregarious on the bark of deciduous trees or on the rotting branch of both broadleaf trees and conifers, in summer.

Distribution. The Republic of Korea.

Remark. *Collybiopsis fulva* morphologically resembles *Co. menehune* and *Co. ramealis*. They can be distinguished based on several morphological differences. *Collybiopsis menehune* has a longer stipe (15–60 mm length), denser lamellae, and larger basidiospores (7.5–9.5 × 3.5–4.2 µm) (Desjardin et al. 1999). *Collybiopsis ramealis* has a smaller basidiocarp (2–20 mm), shorter basidiospores (7.8–11 × 2.5–4 mm) and different type of pileipellis (*Rameales*-structure) (Noordeloos 1983; Desjardin et al. 1997). Phylogenetically, *Co. fulva* is closely related to *Co. ramulicola*. *Collybiopsis ramulicola* differs in having a more yellowish pileus, fewer lamellae (9–12) that are brighter in color, a more reddish and thicker stipe (2–3 mm), and smaller sized cheilocystidia (23–27 × 3–6 mm) (Deng et al. 2016).

Collybiopsis orientisubnuda **J.S. Kim & Y.W. Lim, sp. nov.**
MycoBank No: 842056
Fig. 3G–H, Suppl. material 1: Fig. S1D

Etymology. Epithet "*orientisubnuda*" meaning the new species has originated from the East and is morphologically similar to *Co. subnuda*.

Holotype. The Republic of Korea, Gyeongsangbuk-do: Ulleung-gun, 37°31'21"N, 130°53'14"E, alt. 757 m, 19 July 2016, Changmu Kim, Jinsung Lee, Jae Young Park, NIBRFG0000500990 (GenBank accession no. ITS: OL467262; nrLSU: OL546546).

Diagnosis. It features a brownish, 15−50 mm pileus, orangish cream-colored lamellae, greyish to brownish orange, tomentose, 20–80 × 2.5−6 mm stipe, subcylindrical to fusoid, 6.7–8.6 × 1.8–3.2 µm basidiospores, and cylindrical, flexuose, sometimes irregular or curved, 26.3–52 (63) × 3.5–6.5 µm caulocystidia. This species is morphologically similar to *Co. subnuda*.

Description. Pileus: 15−50 mm, convex to plano-convex, sometimes subumbonate; Surface smooth, brownish orange (6C5 to 7C4), becoming paler to the margin (5A2). Lamellae: distant, L = 16–28, l = 3–7, adnexed, pale yellow (4A3) to orange white (5A2). Stipe: 20–80 (100) × 2.5−6 mm, central to eccentric, cylindrical, tomentose, often twisted, greyish orange (6B4) to brownish orange(7C4), becoming paler and thinner to the base. Basidiospores: 6.7–8.6 × 1.8–3.2 µm (average 7.5 × 2.5 µm), *Q* = 2.5–3.2 (mean = 2.92), cylindrical to fusoid, smooth, hyaline, non-dextrinoid, with drops. Basidia: (17) 19.8–28.7 (29) × 3.7–7.3 µm, 4-spored, narrowly clavate, often constricted. Cheilocystidia: variable in shape and size, 21–33.3 × 4.7–8.2 µm, lobed, clavate, slightly sphaeropendunculate, sometimes constricted or with rostrate apex. Pleurocystidia: 24.7–52.3 × 5.1–9.1 µm, narrowly utriform, clavate, sometimes clavate with rostrate apex. Trama hyphae: cylindrical, often subinflated, smooth, branched, non-dextrinoid, 2.0–7.0 µm wide. Pileipellis: a cutis made up of cylindrical, 2−8 µm wide hyphae; terminal elements adpressed, cylindrical, often subinflated, with weak annular ornamentation, 3−6 µm wide. Stipitipellis: a cutis of cylindrical, smooth, 2.5–7 µm wide hyphae. Caulocystidia: 26.3–52 (63) × 3.5–6.5 µm, cylindrical, flexuose, sometimes irregular or curved. Clamp connections: present in all tissues.

Other specimens examined. The Republic of Korea, Chungcheongnam-do: Yesan-gun, Mt. Gaya, 35°48'14"N, 128°5'49"E, alt. 863 m, 23 August 2017, Hae Jin Cho, Ki Hyeong Park, SFC20170823–39. The Republic of Korea, Gangwon-do: Pyeongchang-gun, Mt. Odae, 37°43'54"N, 128°35'42"E, alt. 683 m, 8 July 2017, Nam Kyu Kim, SFC20170708–14. The Republic of Korea, Gyeongsangbuk-do: Ulleung-gun, 37°31'30"N, 130°52'21"E, alt. 718 m, 2 September 2015, Jae Young Park, SFC20150902-01.

Habit and habitat. Scattered to gregarious on the ground covered with dead and decaying leaves of broadleaf forest, from summer to autumn.

Distribution. The Republic of Korea.

Remark. *Collybiopsis orientisubnuda* is morphologically similar to *Co. peronata* (Bolton) R.H. Petersen and *Co. subnuda* (Ellis ex Peck) R.H. Petersen. *Collybiopsis peronata* can be distinguished from *Co. orientisubnuda* by fewer and buff lamellulae (1–3), a thicker stipe (3–8 mm), smaller Q value (2.3), longer basidia (20–40 µm), and longer cheilocystidia (25–90 × 5–10 µm) (Noordeloos et al. 1999). *Collybiopsis subnuda* differs from *Co. orientisubnuda* with thinner stipe (~3 mm), larger basidiospores (8–11 × 3–4.5 µm) and the absence of pleurocystidia (Tekpınar and Acar 2020).

***Collybiopsis subumbilicata* J.S. Kim & Y.W. Lim, sp. nov.**
MycoBank No: 842057
Fig. 4A, B, Suppl. material 1: Fig. S1E

Etymology. Epithet "*subumbilicata*" referring to having a small depressed center in pileus.

Holotype. The Republic of Korea, Seoul, Gwanak-gu, Mt. Gwanak, 37°12'39"N, 128°19"E, alt. 877 m, 01 July 2014, Young Woon Lim, SFC20140701–03 (GenBank accession no. ITS: OL467232; nrLSU: OL462787).

Diagnosis. The distinctive features include a brownish, 10–35 mm pileus, white colored lamellae, a brownish, 25–60 × 1−3 mm stipe covered with pubescence, ellipsoid to oblong basidiospores, narrowly clavate and cylindrical, 17–24.3 × 3.5–5.1 µm basidia, and cylindrical, flexuose, sometimes curved, 12.6–38.2 × 2.4–6.6 µm caulocystidia.

Description. Pileus: 10–35 mm, plano-convex to plano-concave, subumbilicate, becoming undulate and uplifted in age; Surface smooth, greyish orange (5B3) to brown (6E5). Lamellae: subdistant, L = 22–38, l = 3–7, free to adnexed, white. Stipe: 25–60 × 1−3 mm, cylindrical, tomentose, hollow, light brown (7D4) to dark brown (9F8), becoming paler to the apex, covered with pubescence. Basidiospores: 5.5−7.5 × 2.5−3.6 µm (average 6.47 × 3.0 µm), *Q* = 1.8–2.2 (mean = 2), oblong to fusiform, smooth, hyaline, non-dextrinoid, with drops. Basidia: (15.6) 17–24.3 (27.6) × 3.5–5.1 (5.9) µm, 4-spored, narrowly clavate, cylindrical. Cheilocystidia: 17.6–38.4 × 5–7.8 µm, various in shape, lobed. Pleurocystidia: 20.3−30.7 × 6.8−9.5 µm, clavate, fusiform, slightly sphaeropedunculate. Trama hyphae: cylindrical, subinflated, branched, smooth, non-dextrinoid, 1.5−8 µm wide. Pileipellis: a cutis made up of cylindrical, often incrusted, with heavy annular ornamentation, 5.0−15 µm wide hyphae; terminal elements adpressed to suberect, fusoid, clavate, 6.0−16 µm wide. Stipitipellis: a cutis of cylindrical, smooth, thin-walled, 2.0−6.0 µm wide hyphae. Caulocystidia: 12.6–38.2 × 2.4–6.6 µm, cylindrical, flexuose, sometimes irregular or curved. Clamp connections: present in all tissues.

Other specimens examined. The Republic of Korea, Gangwon-do: Goseong-gun, Hwajinpo, Hwajinpo Condominium, 38°28'24"N, 128°26'30"E, alt. 7 m, 2 August 2012, Young Woon Lim, SFC20120802–03. The Republic of Korea, Gyeongsangbuk-do: Ulleung-gun, Ulleung island, 37°30'38"N, 130°51'44"E, alt. 429 m, 22 August 2017, Jae Young Park, Nam Kyu Kim, SFC20170822–14.

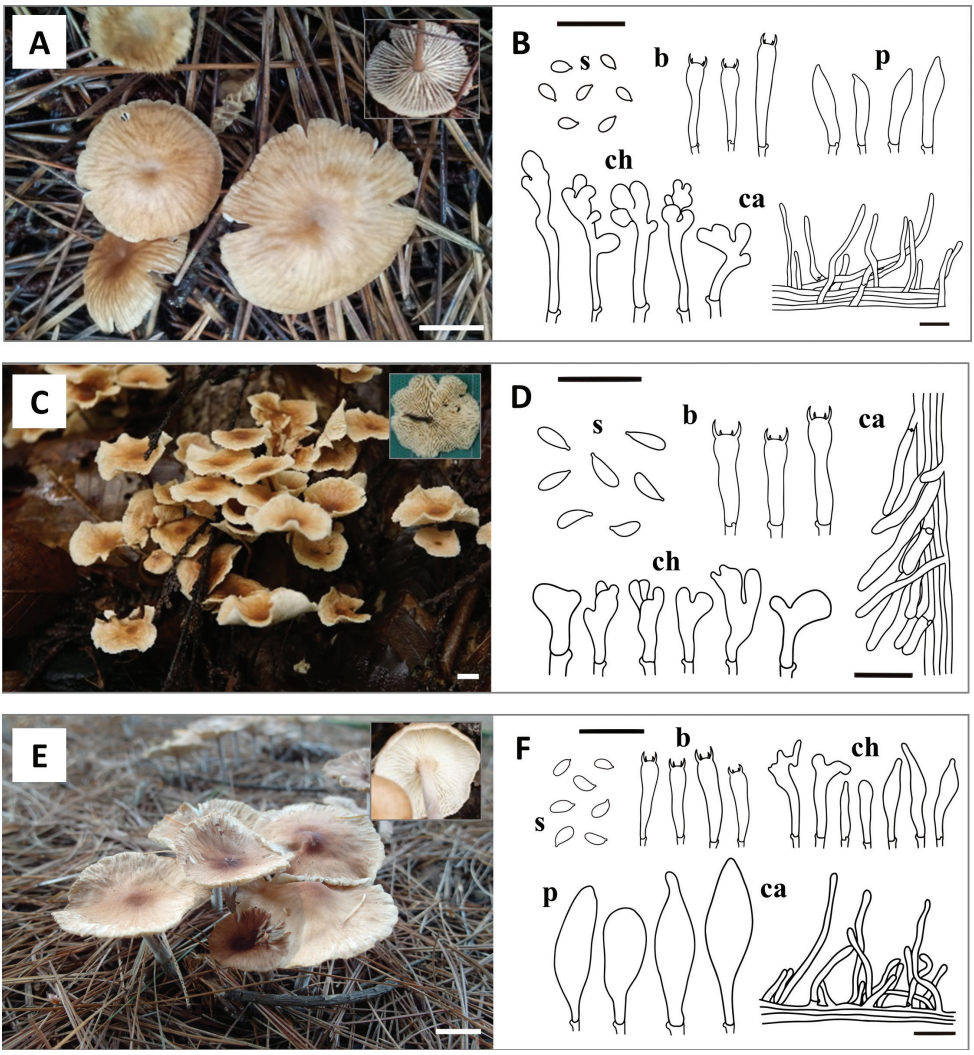

Figure 4. Basidiomata and microscopic characters of the three new *Collybiopsis* species **A, B** *Co. subumbilicata* (SFC20120802–03) **C, D** *Co. undulata* (SFC20150813–04) **E, F** *Co. vellerea* (SFC20140821–29). Scale bars: 1cm (**A, C, E**); 20 *μm* (**B, D, F**). Abbreviations: **s** basidiospores; **b** basidia; **ch** cheilocystidia; **p** pleurocystidia; **ca** caulocystidia.

Habit and habitat. Scattered to gregarious on the ground covered with dead leaves in temperate mixed forests, from summer to autumn.

Distribution. The Republic of Korea.

Remark. *Collybiopsis subumbilicata* appears similar to *Co. villosipes* (Cleland) R.H. Petersen. *Collybiopsis villosipes* is distinguished from *Co. subumbilicata* by fewer and brownish lamellae (also lamellulae), a noninsititious, light-colored stipe, larger basidiospores (6.5−10.5 × 3.5−4.5 μm) and basidia (25−34 × 6.5−7.5 μm) (Desjardin et al.

1997). Furthermore, *Co. subumbilicata* is phylogenetically close to *Co. biformis* and *Co. disjuncta* (R.H. Petersen & K.W. Hughes) R.H. Petersen & K.W. Hughes. *Collybiopsis biformis* is morphologically similar to *Co. subumbilicata* but can be distinguished by elongated basidiospores (6.4–9.2 × 2.4–4.8 μm), thicker basidia (6–7 μm thick) and cheilocystidia (6–12 μm thick) (Morgan 1905; Mata 2002). *Collybiopsis disjuncta* can be distinguished from *Co. subumbilicata* by a smaller pileus (7–12 mm) with olivaceous tint, pinkish lamellae, slender stipe (0.5–1 mm thick), bigger basidiospores (6–7.5 × 3–3.5 μm), bigger basidia (22–34 × 5–7 μm), and a seldom incrusted pileipellis (Petersen and Hughes 2014).

Collybiopsis undulata **J.S. Kim & Y.W. Lim, sp. nov.**
MycoBank No: 842058
Fig. 4C–D, Suppl. material 1: Fig. S1F

Etymology. Epithet "*undulata*" referring to having an undulate margin of pileus.

Holotype. The Republic of Korea, Chungcheongnam-do, Boryeong-si, recreation forest of Mt Sungju, 36°20'4"N, 126°39'50"E, alt. 241 m, 21 August 2012, Jae Young Park, SFC20120821–04 (GenBank accession no. ITS: OL467239; nrLSU: OL462813).

Diagnosis. It is characterized by having 10–23 mm sized pileus that is particularly brown in the middle with a wavy margin, subdistant and creamy lamellae, a dark brown, 35–55 × 0.8–2 mm stipe that becomes lighter to the apex, subcylindrical, broadly clavate or irregular, sometimes lobed, 16.7–28 × 4.8–8 μm cheilocystidia, and 27–60 × 3.5–6 μm sized caulocysitida which has a morphology similar to cheilocystidia and sometimes grows in bundles.

Description. Pileus: 10–23 mm, convex to concave, margin becoming undulate with age; Surface smooth, hygrophanous, brown (7D2 to 7E6) in the center, becoming paler to the margin (5A2–5B3 to 7B2). Lamellae: subdistant, L = 15–30, l = 3–9, adnexed, cream. Stipe: 35–55 × 0.8–2 mm, cylindrical, tomentose, dark brown (7F5 to 8F8), gradually becoming paler to apex (7B2 to 7C2). Basidiospores: 5.6–9.5 × 2–3.4 μm (average 7.3 × 2.8 μm), Q = 2–3.1 (mean = 2.58), cylindrical, smooth, hyaline, non-dextrinoid, with drops. Basidia: 15–22.3 × 3.6–6.8 μm, 4-spored, cylindrical, narrowly clavate to utriform, often curved. Cheilocystidia: 16.7–28 × 4.8–8 μm, subcylindrical, broadly clavate or irregular, sometimes lobed. Pleurocystidia: absent. Trama hyphae: cylindrical, sometimes subinflated, smooth, branched, non-dextrinoid, 2–8 μm wide. Pileipellis: a cutis made up of cylindrical, often incrusted, slightly brownish, with heavy annular ornamentation, 2.4–7 μm wide hyphae; terminal elements adpressed to suberect, cylindrical to clavate, 3–6 μm wide. Stipitipellis: a cutis of cylindrical, smooth, 2.0–3.5 μm wide hyphae. Caulocystidia: 27–60 × 3.5–6 μm, irregularly cylindrical, narrowly utriform, seldom apically lobed, sometimes gathered in a bunch. Clamp connections: present in all tissues.

Other specimens examined. The Republic of Korea, Gyeonggi-do: Goyang-si, Deogyang-gu, Seooreung, 37°37'26"N, 126°54'4"E, alt. 35 m, 13 August 2015, Jae Young Park,

SFC20150813–04. The Republic of Korea, Gyeongsangbuk-do, Sangju-si, Mt Noheum, 36°26'20"N, 128°5'48"E, alt. 695 m, 8 August 2013, Jae Young Park, SFC20130808–08.

Habit and habitat. Scattered to gregarious on leaf litter in mixed forest dominated with broadleaf trees, in summer.

Distribution. The Republic of Korea.

Remark. *Collybiopsis undulata* is morphologically similar to *Co. subpruinosa* (Murrill) R.H. Petersen. *Collybiopsis subpruinosa* has differences in having small central papilla on pileus, fewer lamellulae (3–4 series), vivid colored lamellae, thicker basidiospores (4.5–5.2 μm wide), larger basidia (30–36 × 7.5–8.5 μm) and cheilocystidia (25–80 × 5–16 μm), thick-walled trama hyphae (0.5–1 μm), caulocystidia with a wider size range, and a habit of growing solitary on rotten twigs or logs (Desjardin et al. 1999). *Collybiopsis undulata* is phylogenetically close to *Co. villosipes* but *Co. villosipes* can be differentiated by having fewer lamelluale (2–3 series), vivid colored lamellae, thicker stipe (1.5–4.0 mm), slightly thicker basidiospores (3.5–4.5 μm wide), and basidia (25–34 × 6.5–7.5 μm) (Desjardin et al. 1997).

Collybiopsis vellerea **J.S. Kim & Y.W. Lim, sp. nov.**
MycoBank No: 842059
Fig. 4E–F, Suppl. material 1: Fig. S1G

Etymology. Epithet "*vellerea*" refers to having a velvety stipe.

Holotype. The Republic of Korea, Seoul: Gwanak-gu, Mt. Gwanak, 37°27'32"N, 126°56'49"E, alt. 90 m, 21 August 2014, Young Woon Lim, SFC20140821–29 (GenBank accession no. ITS: OL467267; nrLSU: OL462810).

Diagnosis. It has a dull, greyish orange, 18−45 mm pileus with darker center, a tomentose (like velvet), insititious, orangish, 15–55 × 3−5 mm stipe, sphaeropendunculate, subovoid, 23.4–49 × 7.5–13.4 μm pleurocystidia, oblong to subcylindrical basidiospores, narrowly clavate with rostrate apex, sometimes lobed, 7.7–49.7 × 3.8–14.6 μm cheilocystidia.

Description. Pileus: 18−45 mm, hemispherical, appendiculate to convex, subumbonate with an uplifted margin when old; Surface smooth, dull, hygrophanous, orange white (5A2) to greyish orange (6E8 to 7F8) on the center, gradually becoming paler to the edge (5A1 to 5B2). Lamellae: crowded to close, L = 38−52, l = 3−7, furcate, white. Stipe: 15–55 × 3−5 mm, cylindrical, finely tomentose, insititious, pale orange (5A3) to reddish grey (7B2), becoming darker to the base (6A2 to 7C2). Basidiospores: 5.2−7 × 2.5−3.8 μm (average 6.17 × 3.06 μm), Q = 1.8–2.4 (mean = 2.03), oblong to subcylindrical, smooth, hyaline, non-dextrinoid, with drops. Basidia: 16.2–24.8 × 3.3–5.3 μm, 4-spored, (narrowly) clavate, often curved or constricted. Cheilocystidia: 7.7–49.7 × 3.8–14.6 μm, narrowly clavate with rostrate apex, sometimes lobed. Pleurocystidia: 23.4–49 × 7.5–13.4 μm, sphaeropendunculate, subovoid. Trama hyphae: cylindrical, often subinflated, thin-walled, smooth, branched, non-dextrinoid, 2−5 μm wide. Pileipellis: a cutis made up of cylindrical, thin-walled, with weak annular ornamentation, 3−10 μm wide hyphae; terminal elements adpressed to suberect, cylindrical, fusoid, clavate, 5−11 μm wide. Stipitipellis: a cutis of cylindrical, thin-walled, smooth,

2.0−6.0 μm wide hyphae. Caulocystidia: 12–38 × 2.4–6.6 μm, cylindrical, narrowly utriform, sometimes irregular, or curved. Clamp connections: present in all tissues.

Other specimens examined. The Republic of Korea, Chungcheongnam-do: Seosan-si, Mt. Gaya, 36°41'0"N, 126°35'19"E, alt. 260 m, 20 August 2012, Jae Young Park, SFC20120820–02. The Republic of Korea, Incheon: Ongjin-gun, 37°13'10"N, 126°10'4"E, alt. 6 m, 4 September 2018, Changmu Kim, Jin Sung Lee, NIBRFG0000502858. The Republic of Korea, Jeollanam-do: Jindo-gun, Seogeocha island, 34°15'22"N, 125°55'11"E, alt. 38 m, 5 July 2018, Jae Young Park, Tae Heon Kim, SFC20180705–90.

Habit and habitat. Scattered to gregarious on the ground covered with dead and decaying conifer needles, from summer to autumn.

Distribution. The Republic of Korea.

Remark. *Collybiopsis vellerea* is morphologically similar to *Co. menehune* and *G. spongiosus* Halling. *Collybiopsis menehune* has a paler stipe, a smaller pileus (8–30 mm), and fewer lamellulae (4–6 series) (Desjardin et al. 1999). *Gymnopus spongiosus* has a smaller pileus (8–20 mm) and longer stipe (20–55 mm). Micromorphologically, *Co. menehune* has larger basidiospores, basidia, and caulocystidia (Desjardin et al. 1999). *Gymnopus spongiosus* differs from *Co. vellerea* in that its pileipellis is a *Dryophila*-type cutis and its color changes in alkalies. Furthermore, its basidia (18–25 × 6–9 μm) and trama hyphae (3.5–17 μm) are thicker and its caulocystidia (3.5–10.5 μm broad) are smaller (Halling 1996). *Collybiopsis vellerea* is phylogenetically close to *Co. omphalodes*. *Collybiopsis omphalodes* differs in having smaller basidiomata (20–30 mm) and its habit on logs (Dennis 1951).

Proposal for *Collybiopsis* recombination

In this study, many epithets were found that required an additional transfer of species from *Marasmiellus* to *Collybiopsis* apart from the study done by Petersen and Hughes (2021). Oliveira et al. (2019) had previously suggested to replace these species from *Gymnopus* to *Marasmiellus* s. str., but this study suggests that these species should be further transferred from *Marasmiellus* s. str. to *Collybiopsis*.

Collybiopsis istanbulensis **(E.Sesli, Antonín & E.Aytaç) J.S. Kim & Y.W. Lim, comb. nov.**
MycoBank No: 842060

Basionym. *Marasmiellus istanbulensis* E. Sesli, Antonín & E.Aytaç. Pl. Biosystems 152(4): 669. 2018.

Collybiopsis koreana **(Antonín, Ryoo & H.D.Shin) J.S. Kim & Y.W. Lim, comb. nov.**
MycoBank No: 842061

Basionym. *Marasmiellus koreanus* Antonín, Ryoo and H.D.Shin. Mycotaxon 112: 190. 2010.

Collybiopsis omphalodes **(Berk.) J.S. Kim & Y.W. Lim, comb. nov.**
MycoBank No: 842062

Chamaeceras omphalodes (Berk.) Kuntze, Revis. gen. pl. (Leipzig) 3(3): 456. 1898.
Collybia omphalodes (Berk.) Dennis, Trans. Br. mycol. Soc. 34(4): 443. 1951.
Marasmiellus omphalodes (Berk.) Singer. Sydowia 9(1–6): 385. 1955.
Gymnopus omphalodes (Berk.) Halling & J.L. Mata, in Mata, Halling, and Petersen, Fungal Diversity 16: 122. 2004.

Basionym. *Marasmius omphalodes* Berk., Hooker's J. Bot. Kew Gard. Misc. 8: 138. 1856.

Collybiopsis pseudomphalodes **(Dennis) J.S. Kim & Y.W. Lim, comb. nov.**
MycoBank No: 842063

Gymnopus pseudomphalodes (Dennis) J.L. Mata, in Mata, Hughes, and Petersen, Sydowia 58(2): 289. 2006, as "pseudo-omphalodes".
Marasmiellus pseudomphalodes (Dennis) J.S. Oliveira, in Oliveira, Vargas-Isla, Cabral, Rodrigues and Ishikawa, Mycol. Progr. 18(5): 735. 2019, as "pseudomphalioides".

Basionym. *Collybia pseudomphalodes* Dennis, Kew Bull. 15(1): 74 (1961).

Collybiopsis ramulicola **(T.H. Li & S.F. Deng) J.S. Kim & Y.W. Lim, comb. nov.**
MycoBank No: 842064

Basionym. *Gymnopus ramulicola* T.H. Li & S.F. Deng, in Deng, Li, Jiang and Song, Mycotaxon 131(3): 665. 2016.

Taxonomic key to *Collybiopsis* in Korea

1	Pileus < 25 mm diam	**2**
–	Pileus > 25 mm diam	**11**
2	Lamellae subdistant to distant (10–30)	**3**
–	Lamellae close to crowded (> 30)	**9**
3	Basidiomes on bark, branch, or woody debris	**4**
–	Basidiomes on duff or on soil	**8**
4	Pleurocystidia present	**5**
–	Pleurocystidia absent	**7**
5	Stipe base covered with dense whitish basal tomentum	***Co. albicantipes***
–	Stipe base not covered with whitish basal tomentum	**6**
6	Pileipellis composed of a coarse *Rameales*-structure hyphae	***Co. ramealis***
–	Pileipellis composed of a cylindrical, often sub-inflated hyphae, not a *Rameales*-structure	***Co. fulva***

7	Pileus distinctly sulcate. Stipe base covered with dense whitish basal tomentum	***Co. koreana***
–	Pileus slightly sulcate. Stipe base covered with weak whitish basal tomentum	***Co. nonulla***
8	Stipe < 2 cm long. Q value of basidiospores 1.6–2.2	***Co. dichroa***
–	Stipe > 2 cm long. Q value of basidiospores 2.0–3.1	***Co. undulata***
9	Lamellae crowded (> 100)	***Co. confluens***
–	Lamellae close to crowded (< 100)	**10**
10	Basidia > 22 µm long	***Co. menehune***
–	Basidia < 22 µm long	***Co. biformis***
11	Lamellae subdistant to distant (10–38)	**12**
–	Lamellae close (> 38)	**15**
12	Pleurocystidia present	**13**
–	Pleurocystidia absent	**14**
13	Q value of basidiospores > 2.2	***Co. orientisubnuda***
–	Q value of basidiospores < 2.2	***Co. subumbilicata***
14	Pileus convex, hemispherical, plano-convex to flat. Cheilocystidia utriform and clavate	***Co. clavicystidiata***
–	Pileus convex to broad-convex. Cheilocystidia narrowly clavate	***Co. polygramma***
15	Pleurocystidia present	***Co. vellerea***
–	Pleurocystidia absent	***Co. luxurians***

Discussion

Of the 372 gymnopoid/marasmioid specimens, we confirmed 201 specimens (54%) to belong to *Collybiopsis*. These results indicate that the species of *Collybiopsis* can be confused with those of similar genera as well as with other *Collybiopsis* members when identification is based solely on morphological information. This is because some characteristics are overlapped between species (Suppl. material 2: Fig. S2) and the characteristics can be different depending on developmental stage or environmental conditions. Further, the high misidentification ratio may be caused by the slow rate of adoption of the current names. Sequence-based taxonomy has introduced rapid changes in the classification of gymnopoid/marasmioid species (Mata 2002; Mata et al. 2004a; Mata et al. 2004c; Hughes et al. 2010; Oliveira et al. 2019; Petersen and Hughes 2017, 2021). As such, taxonomic confusion has been resolved in taxa that have been well researched based on molecular data (Desjardin et al. 1999; Mata 2002; Lee et al. 2019).

Nine of the sixteen *Collybiopsis* species were identified as already known species. Of the nine described species, seven species were identified as the species previously recorded in the Republic of Korea: *Collybiopsis biformis*, *Co. confluens*, *Co. koreana*, *Co. luxurians*, *Co. menehune*, *Co. polygramma*, and *Co. ramealis*. Two species, *Co. dichroa* and *Co. nonnulla*, were reported for the first time in the Republic of Korea. Most of the nine described species formed a monophyletic clade with each corresponding species. However, sequence

variations by continent were detected in *Co. biformis*, *Co. confluens*, *Co. dichroa*, and *Co. nonnulla*. Asian samples, including our specimens, were clearly separated from those of Europe, North America, and Africa. These results have also been reported in previous studies on *Collybiopsis biformis* (Mata 2002; Petersen and Hughes 2014; Razaq et al. 2020) and *Co. confluens* (Hughes and Petersen 2015). Especially, *Co. confluens* is known as a representative example of intra-specific variation between continents. Percent ITS sequence divergence of this species was reported to be 3.25% when comparing the sequences of the North America and Europe (Hughes and Petersen 2015). We confirmed that percent ITS sequence divergence of Asian *Co. confluens* (our Korean samples and Chinese sequences) were each about 3% when compared to American and European sequences.

Similarly, *Co. dichroa* showed sequence variations that were previously reported in association with intraspecific hybridization and dramatic sequence variations including frequent nucleotide substitutions of Adenine and Guanine (Hughes et al. 2015). The Korean *Co. dichroa* was closely related to *Co. dichroa* taxa 2 mentioned in Hughes et al. 2015. Similarly, the intraspecific genetic variation depending on environmental conditions or geographical distribution has been reported in many other fungal species (Manian et al. 2001; Kauserud et al. 2007; Seierstad et al. 2013). For the last, Korean *Co. nonnulla* showed high intra-specific divergence when matching with sequences of *Co. nonnulla* of America and Cameroon. According to the phylogenetic analysis results, there is a slight sequence variation, but it forms a clade supported by a high bootstrap and morphologically almost coincides with the reference. Therefore, we view this sequence variation as due to different environments by continent and identify the specimens as *Co. nonnulla*. Nevertheless, compared to the fact that it was reported as a new species a long time ago, only seven sequences were deposited in the NCBI, so further study on this species is necessary.

Morphologically, the morphological characteristics of the seven described species were also in agreement with the previous descriptions (Suppl. material 2: Fig. S2). However, *Co. luxurians* and *Co. polygramma* found in the Republic of Korea showed few differences compared to the Western descriptions in the previous literature (Mata 2003; Noordeloos et al. 1999). In the case of the *Co. luxurians*, Korean sequences formed a slightly distinct clade in the phylogenetic tree, along with the Chinese sequence (ZD16102301), from European sequences. In this study, direct morphological comparison studies with European and Chinese samples were difficult and there was no significant morphological difference from the references. For these reasons, we identified Korean specimens as *Co. luxurians*, but further studies are needed with more samples from other countries for this species.

Seven new species have common characteristics of *Collybiopsis* such as insititious to subinsititious stipe, ellipsoid to oblong, inamyloid basidiospores, and presence of caulocystidia. However, it is difficult to distinguish them from other *Collybiopsis* species based on morphological characteristics alone. Upon molecular phylogenetic analyses, each of them clearly formed a distinct clade clearly in the ML phylogenetic tree (Fig. 1). Their morphological features may or may not be distinguished from their phylogenetically close relatives. The morphological differences between new species and morphologically similar or phylogenetically close species are discussed in the remarks for each species.

Two species previously reported in the Republic of Korea, *Co. peronata* (Cho & Lee, 1979) and *Co. subnuda* (National list of species of Korea 2020), were not confirmed in this study. *Co. peronata* and *Co. subnuda*, which are typical collybioid mushrooms, have been reported in Asia based on their morphological characteristics (Cho and Lee 1979; Kim et al. 1991; Park and Cho 1992; Yoshida and Muramatsu 1998; Tolgor and Yu 2000). Molecular analyses showed that none of the Korean specimens examined in this study could be identified as *Co. peronata* nor *Co. subnuda*. Instead, the specimens labelled as *Co. peronata* or *Co. subnuda* were identified as different species – *Gymnopus similis* Antonín, Ryoo & Ka and *Co. orientisubnuda*. *Collybiopsis peronata* were originally mostly reported from Europe and America and *Co. subnuda* were originally reported from America (Desjardin et al. 1999; Mata et al. 2006). Furthermore, there have been no recent sequence uploads to GenBank or reports of *Co. peronata* and *Co. subnuda* from Asia, making it difficult to confirm whether they exist in the Republic of Korea. Although *Co. orientisubnuda* is closely related to *Co. peronata* and *Co. subnuda*, there are clear differences in the ITS regions of these three species (Suppl. material 3: Fig. S3). Morphologically, *Co. orientisubnuda* is highly similar to *Co. subnuda* and considerably different from *Co. peronata*. The detailed comparisons of the morphological features are provided in the remarks for each species.

In conclusion, we identified 16 *Collybiopsis* species in the Republic of Korea through morphological and molecular analyses and we update the Korean inventory of *Collybiopsis*. Our study showed that the identification of *Collybiopsis* species requires both morphological and molecular analyses. Further, this study has the following significance as in the previous study conducted by Petersen and Hughes (2021): additional combinations of *Marasmiellus* species under *Collybiopsis*, detailed morphological characterization of *Collybiopsis* species in the Republic of Korea along with photographs and drawings, and specific approaches to species differentiation and identification through morphological and molecular analyses. Furthermore, we believe that this study will be helpful for further studies such as research of *Collybiopsis* distribution worldwide as it provides additional molecular information about *Collybiopsis* in the Republic of Korea and proposes seven new species identified from the Republic of Korea. These data will be useful for the identification and taxonomic arrangement of gymnopoid/marasmioid mushrooms.

Acknowledgements

We greatly appreciate Prof. R.H. Petersen for his valuable comments on this manuscript. This study was supported by the National Institute of Biological Resources (NIBR202203112) and the Korea National Arboretum (KNA1-1-25, 19-2).

References

Antonín V, Herink J (1999) Notes on the variability of *Gymnopus luxurians* (Tricholomataceae). Czech Mycology 52(1): 41–49. https://doi.org/10.33585/cmy.52103

Antonín V, Noordeloos ME (1993) A Monograph of *Marasmius*, *Collybia*, and Related Genera in Europe: *Marasmius*, *Setulipes*, and *Marasmiellus*. Libri botanici 8: 1–229.

Antonín V, Ryoo R, Shin HD (2010) Two new marasmielloid fungi widely distributed in the Republic of Korea. Mycotaxon 112(1): 189–199. https://doi.org/10.5248/112.189

Cho DH, Lee JY (1979) Higher fungi in the Northern area of Kyungsangbuk-do. The Korean Journal of Mycology 7: 1–7.

Clémençon H (1973) Zwei verbesserte Präparierlösungen für die mikroskopische Untersuchung von Pilzen Z. Pilzkunde 38: 49–53.

Deng SF, Li TH, Jiang ZD, Song B (2016) *Gymnopus ramulicola* sp. nov., a pinkish species from southern China. Mycotaxon 131(3): 663–670. https://doi.org/10.5248/131.663

Dennis R (1951) Some Agaricaceae of Trinidad and Venezuela. Leucosporae: Part I. Transactions of the British Mycological Society 34(4): 411–482. https://doi.org/10.1016/S0007-1536(51)80030-5

Dennis R (1961) Fungi venezuelani: IV. Agaricales. Kew Bulletin 15(1): 67–156[+ii]. https://doi.org/10.2307/4115784

Desjardin DE, Halling RE, Perry BA (1997) *Gymnopus villosipes*-a common collybioid agaric from California. Mycotaxon 64: 141–148.

Desjardin DE, Halling RE, Hemmes DE (1999) Agaricales of the Hawaiian Islands. 5. The genera *Rhodocollybia* and *Gymnopus*. Mycologia 91(1): 166–176. https://doi.org/10.2307/3761206

Dutta AK, Wilson AW, Antonín V, Acharya K (2015) Taxonomic and phylogenetic study on gymnopoid fungi from Eastern India. I. Mycological Progress 14(10): 1–18. https://doi.org/10.1007/s11557-015-1094-3

Earle FS (1909) The genera of the North American gill fungi. Bulletin of the New York Botanical Garden 5: 373–451.

Gardes M, Bruns TD (1993) ITS primers with enhanced specificity for basidiomycetes-application to the identification of mycorrhizae and rusts. Molecular Ecology 2(2): 113–118. https://doi.org/10.1111/j.1365-294X.1993.tb00005.x

Halling RE (1996) Notes on Collybia V. *Gymnopus* section *Levipedes* in tropical South America with comments on Collybia. Brittonia 48(4): 487–494. https://doi.org/10.2307/2807862

Hughes K, Petersen RH (2015) Transatlantic disjunction in fleshy fungi III: *Gymnopus confluens*. MycoKeys 9: 37–63. https://doi.org/10.3897/mycokeys.9.4700

Hughes KW, Mather DA, Petersen RH (2010) A new genus to accommodate *Gymnopus acervatus* (Agaricales). Mycologia 102(6): 1463–1478. https://doi.org/10.3852/09-318

Hughes KW, Segovia AR, Petersen RH (2014) Transatlantic disjunction in fleshy fungi. I. The Sparassis crispa complex. Mycological Progress 13(2): 407–427. https://doi.org/10.1007/s11557-013-0927-1

Hughes K, Morris SD, Reboredo-Segovia AL (2015) Cloning of ribosomal ITS PCR products creates frequent, non-random chimeric sequences – A test involving heterozygotes between *Gymnopus dichrous* taxa I and II. MycoKeys 10: 45–56. https://doi.org/10.3897/mycokeys.10.5126

Kaburagi Y (1940) Korean and Manchurian practical manual of forest. Korea Forest Experiment Station, Tokyo, 339–367.

Katoh K, Standley DM (2013) MAFFT multiple sequence alignment software version 7: Improvements in performance and usability. Molecular Biology and Evolution 30(4): 772–780. https://doi.org/10.1093/molbev/mst010

Kauserud H, Hofton TH, Saetre GP (2007) Pronounced ecological separation between two closely related lineages of the polyporous fungus *Gloeoporus taxicola*. Mycological Research 111(7): 778–786. https://doi.org/10.1016/j.mycres.2007.03.005

Kim KS, Park WH, Min KH (1991) The higher fungal Flora in the areas of Mt. Daesung and Mt. Daeduck. The Korean Journal of Mycology 19: 167–174.

Kornerup A, Wanscher JH (1978) Methuen handbook of colour. 3rd edn. Methuen, London.

Kumar S, Stecher G, Tamura K (2016) MEGA7: Molecular Evolutionary Genetics Analysis version 7.0 for bigger datasets. Molecular Biology and Evolution 33(7): 1870–1874. https://doi.org/10.1093/molbev/msw054

Lee H, Wissitrassameewong K, Park MS, Verbeken A, Eimes J, Lim YW (2019) Taxonomic revision of the genus *Lactarius* (Russulales, Basidiomycota) in Korea. Fungal Diversity 95(1): 275–335. https://doi.org/10.1007/s13225-019-00425-6

Manian S, Sreenivasaprasad S, Bending G, Mills P (2001) Genetic diversity and interrelationships among common European *Suillus* species based on ribosomal DNA sequences. FEMS Microbiology Letters 204(1): 117–121. https://doi.org/10.1111/j.1574-6968.2001.tb10873.x

Mata JL (2002) Taxonomy and systematics of *Lentinula*, *Gymnopus* and *Rhodocollybia* (Agaricales, Fungi) with emphasis on oak forests of southern Costa Rica. PhD Thesis, University of Tennessee, Knoxville.

Mata JL (2003) Type studies of neotropical *Collybia* species. Mycotaxon 86: 303–316.

Mata JL, Halling RE, Hughes KW, Petersen RH (2004a) *Rhodocollybia* in neotropical montane forests. Mycological Progress 3(4): 337–352. https://doi.org/10.1007/s11557-006-0104-x

Mata JL, Halling RE, Petersen RH (2004b) New species and mating system reports in *Gymnopus* (Agaricales) from Costa Rica. Fungal Diversity 16: 113–129.

Mata JL, Hughes KW, Petersen RH (2004c) Phylogenetic placement of *Marasmiellus juniperinus*. Mycoscience 45(3): 214–221. https://doi.org/10.1007/S10267-004-0170-3

Mata JL, Hughes KW, Petersen RH (2006) An investigation of/omphalotaceae (Fungi: Euagarics) with emphasis on the genus *Gymnopus*. Sydowia 58: 191–289.

Miller MA, Pfeiffer W, Schwartz T (2012) The CIPRES science gateway: enabling high-impact science for phylogenetics researchers with limited resources. Proceedings of the 1st Conference of the Extreme Science and Engineering Discovery Environment: Bridging from the extreme to the campus and beyond. https://doi.org/10.1145/2335755.2335836

Moncalvo JM, Vilgalys R, Redhead SA, Johnson JE, James TY, Aime MC, Hofstetter V, Verduin SJ, Larsson E, Baroni TJ (2002) One hundred and seventeen clades of euagarics. Molecular Phylogenetics and Evolution 23(3): 357–400. https://doi.org/10.1016/S1055-7903(02)00027-1

Morgan AP (1905) North American species of Marasmius. Journal of Mycology 11(5): 201–212. https://doi.org/10.2307/3752425

Murrill W (1915) Agaricaceae (pars). Flora of North America 9: 286–296.

National list of species of Korea (2020) National Institute of Biological Resources. http://kbr.go.kr [Accessed on 14.10.2021]

Noordeloos ME (1983) Notulae as Floram agaricinam neerlandicam – I–III. *Marasmiellus*, *Macrocystidia* and *Rhodocybe*. Persoonia-Molecular Phylogeny and Evolution of Fungi 12: 31–49.

Noordeloos ME, Kuyper TW, Vellinga E (1999) Flora Agaricina Neerlandica Vol 4. CRC Press, Florida.

Oliveira JJ, Vargas-Isla R, Cabral TS, Rodrigues DP, Ishikawa NK (2019) Progress on the phylogeny of the Omphalotaceae: *Gymnopus* s. str., *Marasmiellus* s. str., *Paragymnopus* gen. nov. and *Pusillomyces* gen. nov. Mycological Progress 18(5): 713–739. https://doi.org/10.1007/s11557-019-01483-5

Park SS, Cho DH (1992) The Mycoflora of Higher Fungi in Mt. Paekdu and Adjacent Areas (I). The Korean Journal of Mycology 20: 11–28.

Petersen R, Hughes K (2014) New North American species of *Gymnopus*. North American Fungi 9(0): 1–22. https://doi.org/10.2509/naf2014.009.003

Petersen RH, Hughes KW (2016) *Micromphale* sect. *Perforantia* (Agaricales, Basidiomycetes); expansion and phylogenetic placement. MycoKeys 18: 1–122. https://doi.org/10.3897/mycokeys.18.10007

Petersen RH, Hughes KW (2017) An investigation on *Mycetinis* (Euagarics, Basidiomycota). MycoKeys 24: 1–139. https://doi.org/10.3897/mycokeys.24.12846

Petersen RH, Hughes KW (2021) *Collybiopsis* and its type species, *Co. ramealis*. Mycotaxon 136(2): 263–349. https://doi.org/10.5248/136.263

Razaq A, Ilyas S, Khalid AN (2020) Molecular systematics and evolutionary relationships of some inland gilled basidiomycetes from the Himalayan moist temperate forests of Pakistan based on rDNA marker. Pakistan Journal of Botany 52(3): 1055–1063. https://doi.org/10.30848/PJB2020-3(3)

Rehner SA, Samuels GJ (1994) Taxonomy and phylogeny of *Gliocladium* analysed from nuclear large subunit ribosomal DNA sequences. Mycological Research 98(6): 625–634. https://doi.org/10.1016/S0953-7562(09)80409-7

Retnowati A (2018) The species of *Marasmiellus* (Agaricales: Omphalotaceae) from Java and Bali. Gardens'. Bull, Singapore 70(1): 191–258. https://doi.org/10.26492/gbs70(1).2018-17

Rogers SO, Bendich AJ (1994) Extraction of total cellular DNA from plants, algae, and fungi. In: Plant molecular biology manual. Springer, 183–190. 10.1007/978-94-011-0511-8_12

Ryoo R, Antonín V, Ka KH (2020) Marasmioid and Gymnopoid Fungi of the Republic of Korea. 8. *Gymnopus* Section *Levipedes*. Mycobiology 48(4): 252–262. https://doi.org/10.1080/12298093.2020.1769541

Sandoval-Leiva PA, McDonald JV, Thorn RG (2016) *Gymnopanella nothofagi*, a new genus and species of gymnopoid fungi (Omphalotaceae) from Chilean *Nothofagus* forest. Mycologia 108(4): 820–827. https://doi.org/10.3852/15-303

Seierstad KS, Carlsen T, Sætre GP, Miettinen O, Hofton TH, Kauserud H (2013) A phylogeographic survey of a circumboreal polypore indicates introgression among ecologically differentiated cryptic lineages. Fungal Ecology 6(1): 119–128. https://doi.org/10.1016/j.funeco.2012.09.001

Singer R (1973) The genera *Marasmiellus*, *Crepidotus* and *Simocybe* in the neotropics. Nova Beih Nova Hedwigia 44: 1–517. https://doi.org/10.2307/3758379

Staude F (1857) Die Schwämme Mitteldeutschlands, insbesondere des Herzogthums Coburg. Dietz, Coburg.

Tekpınar A, Acar İ (2020) Fungal Systematics and Evolution: FUSE 6. Sydowia: 231–356. https://doi.org/10.12905/0380.sydowia72-2020-0271

Tolgor LI, Yu LI (2000) Study on fungal flora diversity in Daqinggou Nature Reserve. Shengwu Duoyangxing 8(1): 73–80. https://doi.org/10.17520/biods.2000010

Vilgalys R, Hester M (1990) Rapid genetic identification and mapping of enzymatically amplified ribosomal DNA from several *Cryptococcus* species. Journal of Bacteriology 172(8): 4238–4246. https://doi.org/10.1128/jb.172.8.4238-4246.1990

Wilson AW, Desjardin DE (2005) Phylogenetic relationships in the gymnopoid and marasmioid fungi (Basidiomycetes, euagarics clade). Mycologia 97(3): 667–679. https://doi.org/10.1080/15572536.2006.11832797

Yoshida S, Muramatsu Y (1998) Concentrations of alkali and alkaline earth elements in mushrooms and plants collected in a Japanese pine forest, and their relationship with 137Cs. Journal of Environmental Radioactivity 41(2): 183–205. https://doi.org/10.1016/S0265-931X(97)00098-2

Supplementary material 1

Figure S1

Authors: Ji Seon Kim, Yoonhee Cho, Ki Hyeong Park, Ji Hyun Park, Minkyeong Kim, Chang Sun Kim, Young Woon Lim

Data type: Jpg file.

Explanation note: Pileipellis elements of seven new species. **A** *Collybiopsis albicantipes* **B** *Co. clavicystidiata* **C** *Co. fulva* **D** *Co. orientisubnuda* **E** *Collybiopsis subumbilicata* **F** *Co. undulata* **G** *Co. vellerea*. Scale bars: 10 *μm*.

Link: https://doi.org/10.3897/mycokeys.88.79266.suppl1

Supplementary material 2

Figure S2

Authors: Ji Seon Kim, Yoonhee Cho, Ki Hyeong Park, Ji Hyun Park, Minkyeong Kim, Chang Sun Kim, Young Woon Lim

Data type: Jpg file.

Explanation note: Comparison of the morphological characters of 16 Korean *Collybiopsis* species.

Link: https://doi.org/10.3897/mycokeys.88.79266.suppl2

Supplementary material 3

Figure S3

Authors: Ji Seon Kim, Yoonhee Cho, Ki Hyeong Park, Ji Hyun Park, Minkyeong Kim, Chang Sun Kim, Young Woon Lim

Data type: Jpg file.

Explanation note: Sequence difference between the three species in the ITS region.

Link: https://doi.org/10.3897/mycokeys.88.79266.suppl3

MycoKeys 88: 109–122 (2022)
doi: 10.3897/mycokeys.88.81437
https://mycokeys.pensoft.net

RESEARCH ARTICLE

A peer-reviewed open-access journal
MycoKeys
Launched to accelerate biodiversity research

Three new species of *Candolleomyces* (Agaricomycetes, Agaricales, Psathyrellaceae) from the Yanshan Mountains in China

Hao Zhou[1], GuiQiang Cheng[1], XiMei Sun[1], RuiYi Cheng[2], HongLiang Zhang[2], YanMin Dong[2], ChengLin Hou[1]

1 *College of Life Science, Capital Normal University, Beijing, 100048, China* **2** *Beijing Songshan National Nature Reserve Management Office, Beijing 102115, China*

Corresponding author: ChengLin Hou (chenglin-hou@cnu.edu.cn)

Academic editor: María P. Martín | Received 30 January 2022 | Accepted 30 March 2022 | Published 13 April 2022

Citation: Zhou H, Cheng GQ, Sun XM, Cheng RY, Zhang HL, Dong YM, Hou CL (2022) Three new species of *Candolleomyces* (Agaricomycetes, Agaricales, Psathyrellaceae) from the Yanshan Mountains in China. MycoKeys 88: 109–121. https://doi.org/10.3897/mycokeys.88.81437

Abstract

Three new species, *Candolleomyces incanus*, *C. subcandolleanus* and *C. yanshanensis*, were found and described from Yanshan Mountains in China. The identification is based on morphological observation combined with phylogenetic analysis of ITS-LSU-*Tef1a*-*TUB2*. This study enriched the species diversity of *Candolleomyces* in Yanshan Mountains and provided important data support for the systematic study of *Candolleomyces* in the future.

Keywords

molecular systematics, new taxon, *Psathyrellaceae*, taxonomy

Introduction

Candolleomyces Wächter & A. Melzer was established in 2020, belonging to Basidiomycota, Agaricomycetes, Agaricales, Psathyrellaceae (Wächter and Melzer 2020). In a previous study, this genus was subordinate to *Psathyrella* (Fr.) Quél. (1872) and molecular sequence data have improved understanding of relationships of *Psathyrella* species (Hopple and Vilgalys 1999; Moncalvo et al. 2002; Matheny et al. 2006). However, the combination analysis of the ITS and LSU regions showed that the delimitation of some species within *Psathyrella* are still unclear (Larsson and Örstadius 2008). In more

recent studies, multi-gene loci (for example, ITS, LSU, *Tef1a* and *TUB2*) became the main methods for identification of *Psathyrella* (Wang and Bau 2014; Yan and Bau 2017, 2018a, 2018b, 2021; Yan 2018; Yan et al. 2019).

In previous studies of *Psathyrella*, there are approximately 100 taxa lacking pleurocystidia, but this feature has not been used as a key distinguishing feature (Fries 1838; Smith 1972; Kits van Waveren 1985; Örstadius and Kundsen 2012; Battistin et al. 2014). Based on extensive specimen collection, morphological studies and phylogenetic analyses, *Candolleomyces* has been separated from *Psathyrella* as a new genus and it differs from *Psathyrella* s.s. in lacking pleurocystidia. (Wächter and Melzer 2020).

Currently, there are 25 recognised species in *Candolleomyces* in the Index Fungorum website (http://www.indexfungorum.org, until Jan. 2022) and 10 species were reported in China (Yan 2018; Bau and Yan 2021).

Yanshan Mountains are located in North China and have a warm temperate continental monsoon climate, with higher plant diversity. The dominant plants include *Quercus* spp., *Betula* spp., *Abies* spp. and *Pinus tabuliformis* Carr. et al. (Wang et al. 2021). There is no information about *Candolleomyces* as yet. In this study, based on morphological characters and the phylogenetic analyses, three new species of *Candolleomyces* from Yanshan Mountains in China are described.

Materials and methods

Morphological studies

Collections were obtained and photographed in the field from Yanshan Mountains in China from 2017 to 2020. The collected specimens were dehydrated with a dryer (Dorrex) at 50 °C and the specimens were deposited in the Herbarium of the College of Life Science, Capital Normal University, Beijing, China (**BJTC**). Macroscopic characters were recorded from specimens. Microscopic characters were observed in thin sections of specimens mounted in 3% potassium hydroxide (KOH) or sterilised water. The shape and size of microscopic structures were observed and noted using a light microscope [Olympus DP71, Tokyo, Japan]. The measurements and Q values are given as (a)b–c(d), in which "a" is the lowest value, "b–c" covers a minimum of 90% of the values and "d" is the highest value. Q stands for the ratio of length and width of a spore (Bau and Yan 2021). Nomenclatural details were submitted to the MycoBank. In this study, the morphological colour comparison was compared to the reference website colorhexa (https://www.colorhexa.com).

DNA extraction PCR amplification and sequencing

DNA extraction was achieved by the M5 Plant Genomic DNA Kit [Mei5 Biotechnology, Co., Ltd, China]. The purified DNA was dissolved in 1 × TE buffer and stored at – 20 °C for later use. The PCR amplifications were performed in Bio-Rad S1000 TM

Thermal Cycler [Bio-Rad Laboratories, Inc, USA]. The primer sets ITS1/ITS4 (White et al. 1990) were used to amplify the rDNA ITS region, LR5/LR0R (Vilgalys and Hester 1990) were used to amplify the large subunit nuclear ribosomal DNA (nuLSU rDNA) region and EF983F/EF2218R (Örstadius et al. 2015) were used to amplify the translation elongation factor subunit 1 alpha (*Tef1a*) region. The primer sets B36f and B12r (Nagy et al. 2011) were used to amplify the β-tubulin gene (*TUB2*) region. PCRs were performed in a volume of 25 μl consisted of 2 μl of DNA template; 1 μl of (10 μM) per primer; 12.5 μl 2 × Master Mix [Mei5 Biotechnology, Co., Ltd, China]. PCR amplification conditions refer to Bau and Yan (2021). DNA sequences were sequenced by Zhongkexilin Biotechnology, Co., Ltd, Beijing, China.

Molecular data analyses

The generated raw reads of the DNA sequences were used to obtain consensus sequences using SeqMan v.7.1.0 in the DNASTAR Lasergene Core Suite software (DNASTAR Inc., Madison, WI, USA). All sequences were aligned using MAFFT v.6 (Katoh and Toh 2010) and trimmed manually using MEGA 6 (Tamura et al. 2013). For phylogenetic analyses, newly-obtained sequences and additional reference sequences of *Candolleomyces* species were included in the dataset of combined ITS-LSU-*Tef1a*-*TUB2* muti-locus DNA (Table 1), with *Psathyrella multipedata* (Peck) A.H. Sm. (LÖ237-04) used as outgroup. Phylogenetic analyses were performed using PAUP v.4.0b10 for Maximum Parsimony (MP) analysis (Swofford 2003) and MrBayes v.3.1.2 for Bayesian Inference (BI) analysis (Ronquist and Huelsenbeck 2003). ML gene-trees were estimated using the software RAxML 7.4.2 Black Box (Stamatakis 2006; Stamatakis et al. 2008; Zhou and Hou 2019; Zhou et al. 2021).

Maximum Parsimony analysis was performed by a heuristic search option of 1000 random-addition sequences with a tree bisection and reconnection (TBR) algorithm. Maxtrees were set to 1000, branches of zero length were collapsed and all equally parsimonious trees were saved. Other calculated parsimony scores were tree length (TL), consistency index (CI), retention index (RI) and rescaled consistency (RC) (Zhou and Hou 2019).

Maximum Likelihood analysis was performed with a GTR site substitution model (Guindon et al. 2010). Branch support was calculated with a bootstrapping (BS) method of 1000 replicates (Hillis and Bull 1993). Bayesian Inference (BI) analysis, using a Markov Chain Monte Carlo (MCMC) algorithm, was performed (Rannala and Yang 1996). MrModeltest v. 2.3 was used to estimate the best model. Two MCMC chains were run from random trees for 10,000,000 generations and stopped when the average standard deviation of split frequencies fell below 0.01. Trees were saved for each 1000 generations. The first 25% of trees were discarded as the burn-in phase of each analysis. Branches with significant Bayesian posterior probabilities (BPP) were estimated in the remaining trees (Posada and Crandall 1998).

The combined alignment and phylogenetic tree were submitted on TreeBASE (www.treebase.org, study 29579).

Table 1. Sequences information used in the phylogenetic analysis in this study.

Taxa	Voucher	Locality	ITS	LSU	*β-Tub*	*tef-1α*
Candolleomyces aberdarensis	GLM-F116094	Kenya	MH880928	–	–	–
C. albipes	DED8340	Sao Tome	KX017209	–	–	–
C. badhyzensis	79478 (TAA) Type	Turkmenistan	KC992883	KC992883	–	–
C. badiophyllus	SZMC-NL-2347	–	FN430699	FM876268	FN396261	FM897252
C. cacao	SFSU DED 8339	Sao Tome	NR148106	–	–	–
C. cacao	FP1R4	USA	KU847452	–	–	–
C. cacao	MP2R2	USA	KU847436	–	–	–
C. candolleanus	LAS73030 Neotype	Sweden	KM030175	KM030175	–	–
C. cladii-marisci	CLUF302 Type	Italy	MK080112			
C. efflorescens	Pegler2133 (K)	Sri Lanka	KC992941	–	–	–
C. eurysporus	GLM-F126263 Type	Germany	MT651560	MT651560	–	–
C. incanus	**BJTC Z777 Type**	**China: Beijing**	**ON042759**	**ON042766**	**ON098513**	**ON098508**
C. incanus	**BJTC S173**	**China: Beijing**	**ON042760**	**ON042767**	**ON098514**	**ON098509**
C. leucotephrus	LÖ138-01 (UPS)	Sweden	KC992885	KC992885	KJ664865	KJ732775
C. luteopallidus	Sharp20863 (MICH) Type	USA	KC992884	KC992884	–	–
C. luteopallidus	HMJAU5148	China: Jilin	MG734736	MW301084	MW314056	MW314073
C. secotioides	UES2918 Type	Mexico	KR003281	KR003282	–	KR003283
C. singeri	HMJUA37867	China: Jilin	MG734718	MW301088	MW314059	MW314077
C. singeri	HMJAU37877	China: Chongqing	MW301073	MW301091	MW314062	MW314080
C. subcacao	HMJAU37807 Type	China: Henan	MW301064	MW301092	MW314063	MW314081
C. subcacao	HMJAU37808	China: Henan	MW301065	MW301093	MW314064	MW314082
C. subcacao	HFJAU1014	China: Jiangxi	MW559218	–	–	–
C. subcacao	HFJAU1274	China: Jiangxi	MW559219	–	–	–
C. subcacao	HFJAU1488	China:Anhui	MW559220	–	–	–
C. subcandolleanus	**BJTC Z239 Type**	**China: Tianjin**	**ON042755**	**ON042762**	**ON098510**	**ON098505**
C. subcandolleanus	**BJTC Z232**	**China: Tianjin**	**ON042756**	**ON042763**	–	–
C. subminutisporus	HMJAU37801 Type	China: Hubei	MW301066	MW301094	MW314065	MW314083
C. subminutisporus	HMJAU37916	China: Henan	MW301067	MW301095	MW314066	MW314084
C. subsingeri	HMJAU37811 Type	China: Jilin	MG734715	MW301097	MW314067	MW314085
C. subsingeri	HMJAU37913	China: Jilin	MG734725	MW301098	MW314068	MW314086
C. sulcatotuberculosus	GB:LO55-12	–	KJ138422	KJ138422	–	–
C. sulcatotuberculosus	HFJAU1515	China: Fujian	MW375696	–	MW382967	MW382965
C. sulcatotuberculosus	Chiarello 07-10-2013	–	KJ138423	–	–	–
C. trinitatensis	TL9035 (C)	Ecuador	KC992882	KC992882	KJ664863	–
C. trinitatensis	ADK4162 (BR)	Togo	KC992886	KC992886	–	–
C. yanshanensis	**BJTC Z783**	**China: Beijing**	**ON042757**	**ON042764**	**ON098511**	**ON098506**
C. yanshanensis	**BJTC Z110 Type**	**China: Beijing**	**ON042758**	**ON042765**	**ON098512**	**ON098507**
Candolleomyces sp.	BAB-4773	India	KP686450	–	–	–
Candolleomyces sp.	BAB-5172	India	KR349656	–	–	–
Candolleomyces sp.	BAB-4748	India	KR154977	–	–	–
Candolleomyces sp.	BAB-4747	India	KR154976	–	–	–
Candolleomyces sp.	BAB-5202	India	KT188611	–	–	–
Psathyrella multipedata	LÖ237-04	Sweden	KC992888	KC992888	KJ664867	KJ732777

Notes: The new generated sequences are emphasised in bold.

Result

Phylogenetic analyses

For the ITS-LSU- *Tef1a-TUB2* sequence dataset, a total of 3459 characters including gaps (694 for ITS, 1316 for LSU, 1023 for *Tef1a*, and 426 for *TUB2*) were included in the

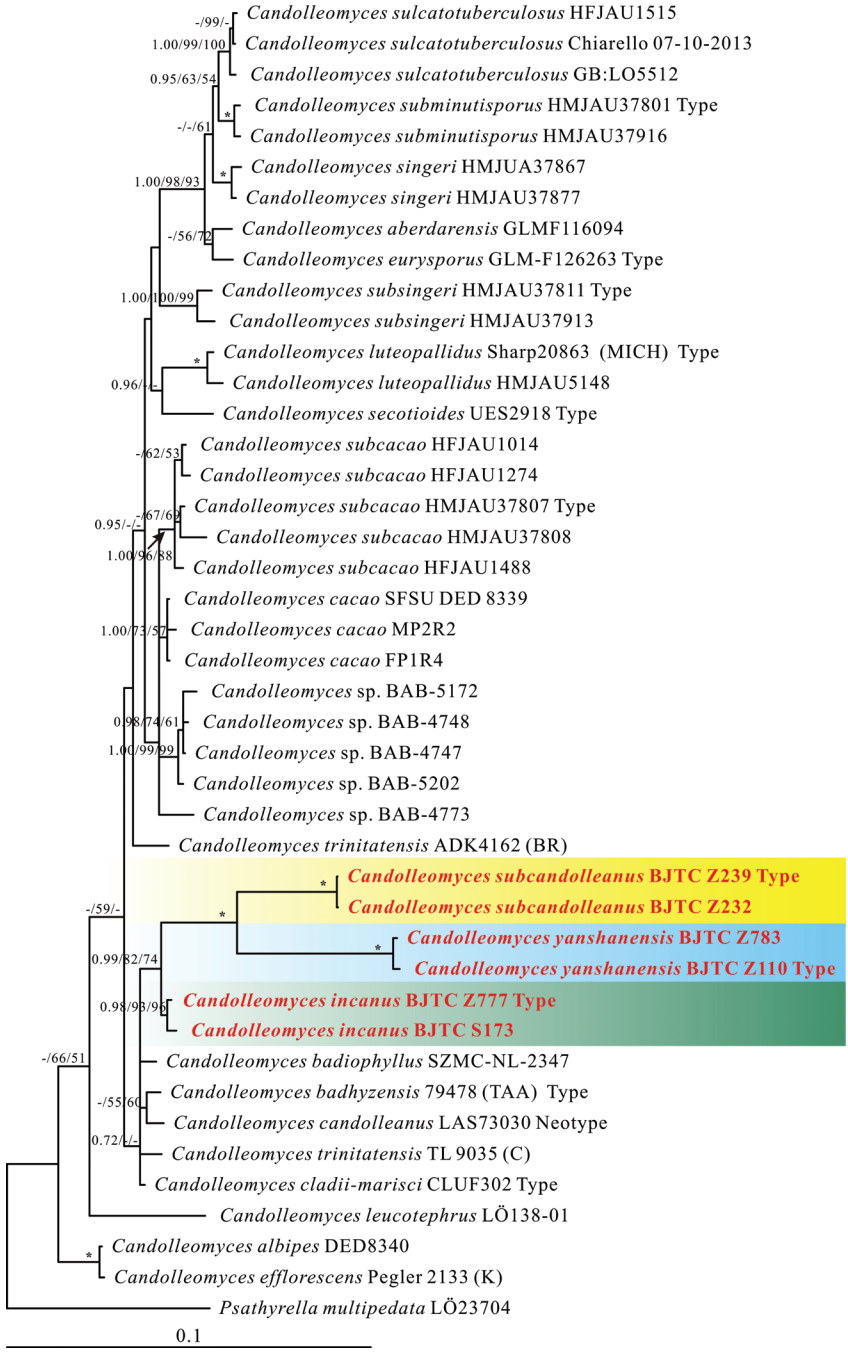

Figure 1. Multi-gene phylogenetic tree obtained from the Bayesian analysis. Numbers above branches are Bayesian posterior probability (pp) values, Maximum Likelihood bootstrap (MLB) and Maximum parsimony bootstrap (MP) values. Asterisks (*) denote branches with pp = 1.00, MLb = 100% and MPb = 100%. Numbers above branches represent strongly and moderately support (pp ≥ 0.95, MLb ≥ 50% and MPb ≥ 50%). The red font indicates the position of the new species.

phylogenetic analysis. Using RAxML, MrBayes and PAUP to construct ML, Bayesian and MP phylogenetic trees, the results show that the topology and branching order were similar and the Bayesian tree is shown in this paper (Fig. 1). The Maximum likelihood analysed was performed with a GTR model. For the Bayesian analyses, the GTR + I + G models were recommended by MrModeltest. The heuristic search using Maximum Parsimony (MP) generated 1000 parsimonious trees (TL = 1168, CI = 0.768, RI = 0.815, RC = 0.232) and branches of zero length were collapsed and all multiple parsimonious trees were saved.

Based on the results, six specimens were assigned to three branches and were described as three new species. The three new species (*Candolleomyces yanshanensis*, *C. subcandolleanus*, *C. incanus*) and a known species (*Candolleomyces badiophyllus* (Romagn.) D. Wächt. & A. Melzer etc.) clustered together in the phylogenetic tree. The three new species clustered into together (pp = 0.99, MLbs = 82%,MPbs = 74%), but three new species separately formed three subclades with high support value. *Candolleomyces yanshanensis*, *C. subcandolleanus* and *C. incanus* can be distinguished by the phylogenetic tree, sequence base differences and morphological characteristics.

Taxonomy

Candolleomyces yanshanensis **C. L. Hou & H. Zhou, sp. nov.**
MycoBank No: 843464
Fig. 2

Etymology. *yanshanensis* referred to the locality where the type specimen was collected.

Type. China, Beijing, Changping District, Beitaizi Village, 40.272906°N, 116.4203°E, alt. 149 m, 14 Aug 2019, coll. X.Y. Shen, H Zhou and R.T. Zhang, BJTC Z110.

Diagnosis. *Candolleomyces yanshanensis*, pileus 20–60 mm, flabellate, flattening with age, hygrophanous. Basidiospores 5.8–8.2 × 3.3–5.4 μm, often with germ pore. Subglobose cell, irregular oval, (18) 20–27μm broad.

Description. Pileus 20–60 mm, flabellate, flattening with age, hygrophanous, slightly dirty white (#e3dac9) to pale brown (#deb887). Veil white (#ffffff), fibrils in young, evanescent. Context 1.0–2.0 mm broad at centre, same colour as pileus. Lamellae sparsely to moderately, adnate, slightly dirty white (#e3dac9) to champagne (#fad6a5), edge white (#ffffff) as spores mature. Stipes 50–130 × 3–6 mm, smooth, fibrils on the base, cornsilk (#f0ead6) to white (#ffffff).

Basidiospores 5.8–8.2 × 3.3–5.4 μm, Q = 1.4–2.0, ellipsoid to long ellipsoid, ovoid to ellipsoid, partly triangular at base, dark brown (#b8860b) to brown (#b06500) in water, smooth, abundant, multi-guttules, often with germ pore. Basidia 17–31 × 5.8–7.5 μm, short clavate, hyaline, 4-spored. Cheilocystidia 22–35 (40) × 8–11 (15) μm, irregular utriform or claviform, apex obtuse or broadly obtuse or often subcapitate, rarely with deposits. Pileipellis consists of 2–3 cells deep layer of irregular subglobose cell, irregular oval, (18) 20–27μm broad.

Habit and habitat. Clumped on the ground with rich humus in broad-leaved forests or broad-leaved shrubs.

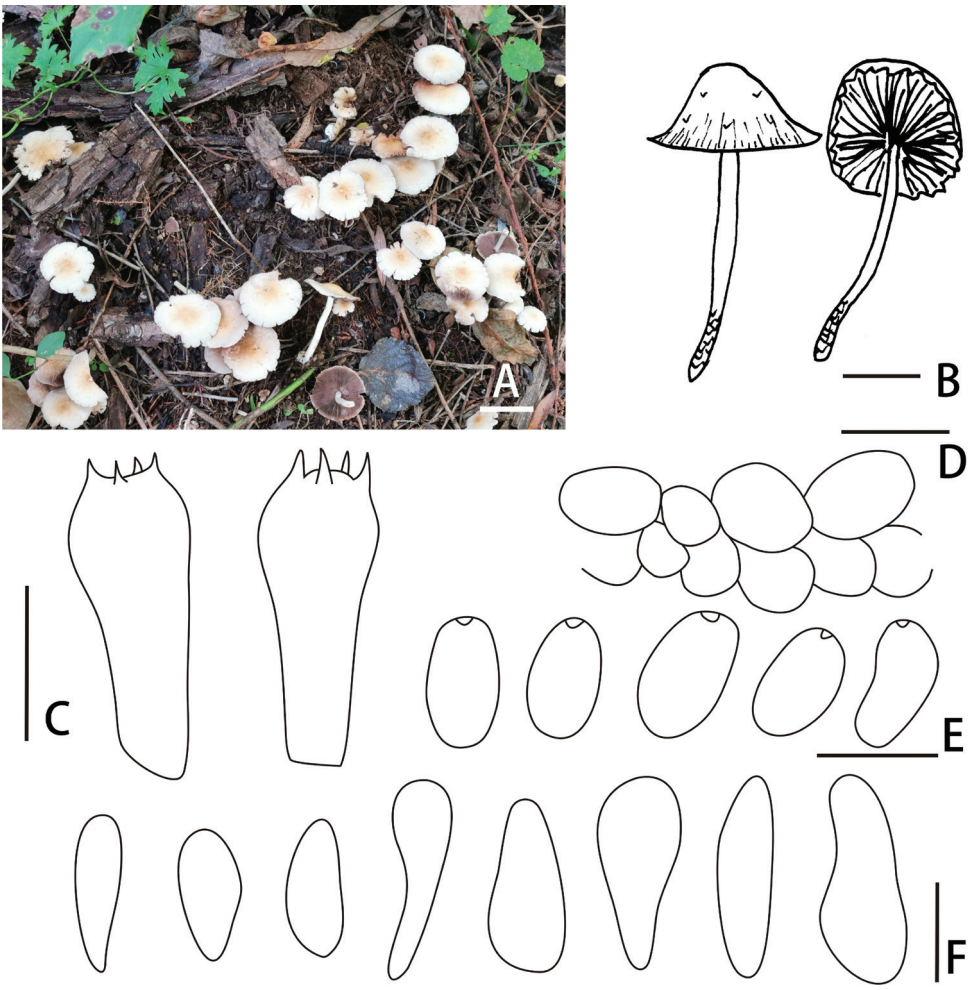

Figure 2. Basidiomata and microscopic features of *Candolleomyces yanshanensis* (BJTC Z110) **A, B** basidiomata **C** basidia **D** pileipellis **E** basidiospores **F** cheilocystidia. Scale bars: 20 mm (**A, B**); 10 μm (**C**); 20 μm (**D**); 5 μm (**E**); 20 μm (**F**).

Additional specimen examined. China, Beijing, Changping District, Tailing, 40.327397°N, 116.21916°E, alt. 172 m, 17 Aug 2020, coll. X.Y. Shen, H Zhou and X.B. Huang, BJTC Z783.

***Candolleomyces subcandolleanus* C. L. Hou & H. Zhou, sp. nov.**
MycoBank No: 843466
Fig. 3

Etymology. *subcandolleanus* referred to its morphological similarity to *Candolleomyces candolleanus* (Fr.) D. Wächt. & A. Melzer.

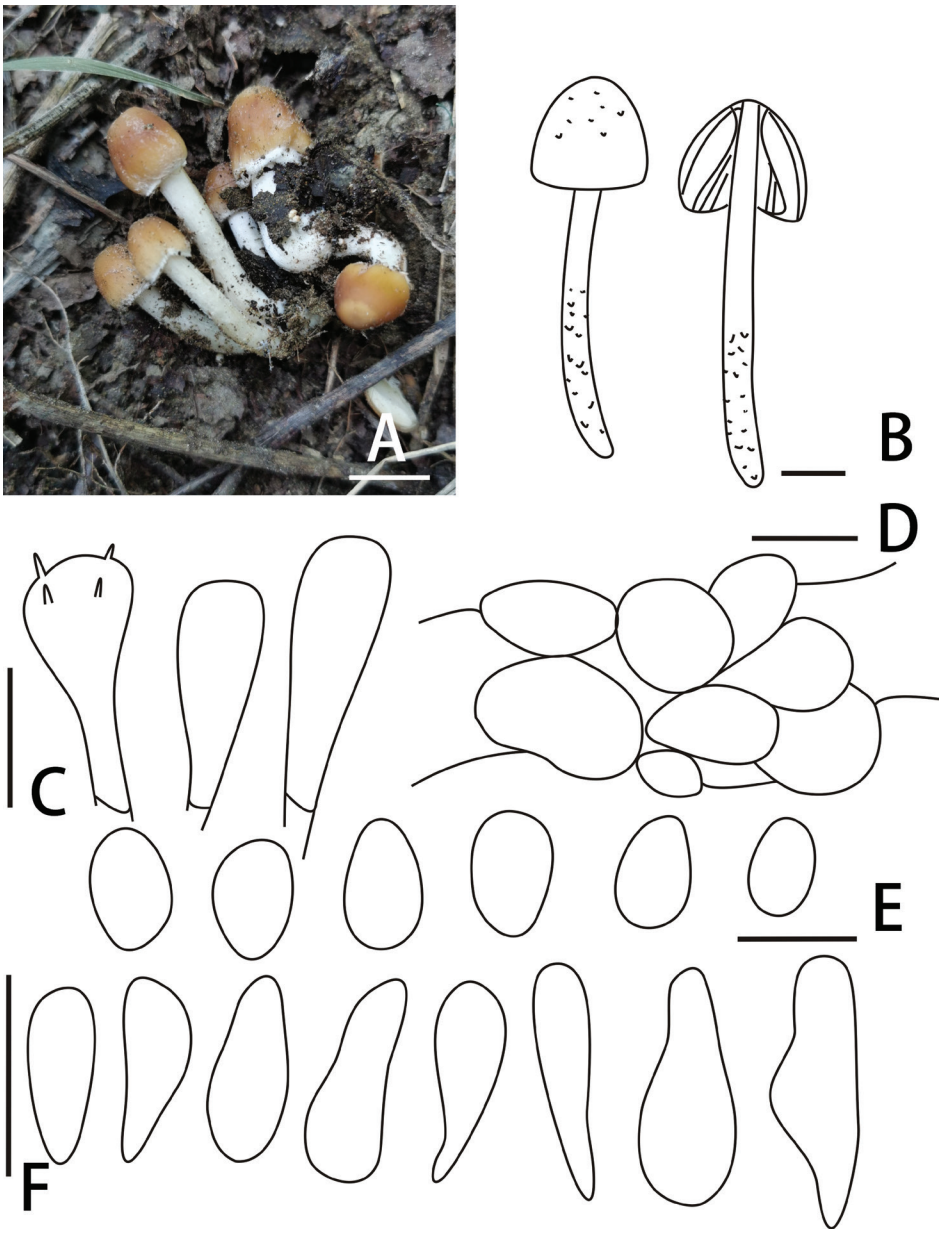

Figure 3. Basidiomata and microscopic features of *Candolleomyces subcandolleanus*. (BJTC Z239) **A, B** basidiomata **C** basidia **D** pileipellis **E** basidiospores **F** cheilocystidia. Scale bars: 10 mm (**A, B**); 10 μm (**C**); 20 μm (**D**); 5 μm (**E**); 20 μm (**F**).

Type. China, Tianjin, Jizhou District, Sanjiebei, 40.227984°N, 117.43354°E, alt. 235 m, 17 Aug 2019, coll. X.Y. Shen, H. Zhou and R.T. Zhang, BJTC Z239.

Diagnosis. *Candolleomyces subcandolleanus*, pileus 5–20 mm. Basidiospores 5.5–6.7 × 3.2–4.5 μm, germ pore absent. Cheilocystidia 21–28 (30) × 8–12 (15) μm. Subglobose cell, irregular oval or long oval, (13) 16–25 μm broad.

Description. Pileus 5–20 mm, campanulate to conical, smooth, fibrils in young, evanescent, brown (#b06500) to golden brown (#996515). Veil white (#ffffff), fibrils in young, evanescent. Context 0.2–0.5 mm broad at centre, same colour as pileus. Lamellae moderately to normally, adnate, slightly dirty white (#e3dac9) to white (#ffffff), edge white (#ffffff) as spores mature. Stipes 20–60 × 1–3 mm, smooth, fibrils on the base, cornsilk (#f0ead6) to white (#ffffff).

Basidiospores 5.5–6.7 × 3.2–4.5 μm, Q = 1.4–2.0, ellipsoid to ovoid, pale cream (#fffff0) to pale lemon (#fffacd) in water, smooth, multi-guttules, germ pore absent. Basidia 18–27 × 5–10 μm, short clavate, hyaline, 4-spored. Cheilocystidia 21–28 (30) × 8–12 (15) μm, utriform or claviform, apex obtuse or broadly obtuse or often subcapitate, rarely with deposits. Trama of gills irregular. Pileipellis consists of irregular subglobose cell, irregular oval or long oval, (13) 16–25 μm broad.

Habit and habitat. Clumped on the ground with rich humus in broad-leaved forests or broad-leaved shrubs.

Additional specimen examined. China, Tianjin, Jizhou District, Huangyaguan Great Wall, 40.245615°N, 117.44047°E, alt. 235 m, 17 Aug 2019, coll. X.Y. Shen, H. Zhou and R.T. Zhang, BJTC Z232.

Candolleomyces incanus **C. L. Hou & H. Zhou, sp. nov.**
MycoBank No: 843465
Fig. 4

Etymology. *incanus* referred to the basidiomata appears incanus.

Type. China, Beijing, Changping District, Sidaohe Village, 40.246374°N, 116.4406°E, alt. 114 m, 16 Aug 2020, coll. X.Y. Shen, H Zhou and X.B. Huang, BJTC Z777.

Diagnosis. *Candolleomyces incanus*, pileus 5–25 mm, hemispherical to conical. Basidiospores 6.0–7.0 × 3.2–4.5 μm. Stipe 40–70×4–6 mm, smooth, germ pore absent. Subglobose cell, irregular oval or long oval, (22) 25–32 μm broad.

Description. Pileus 5–25 mm, hemispherical to conical, hygrophanous, incanus (#f2f3f4) to nude (#fdf5e6). Veil white (#ffffff), fibrils in young, evanescent. Context 0.5–1.0 mm broad at centre, same colour as pileus. Lamellae moderately to normally, adnate, off-white (#f2f3f4) to white (#ffffff), edge white (#ffffff) as spores mature. Stipes 40–70 × 4–6 mm, smooth, hygrophanous, cornsilk (#f0ead6) to white (#ffffff).

Basidiospores 6.0–7.0 × 3.2–4.5 μm, Q = 1.4–1.9, ellipsoid, floral white (#fffaf0) to dark yellow (#eedc82) in water, smooth, abundant, multi-guttules, germ pore absent. Basidia 15–20 × 5–8 μm, short clavate, hyaline, 4-spored. Cheilocystidia 17–27 (31) × 7–11 (13) μm, utriform, apex obtuse or broadly obtuse or often subcapitate, rarely with deposits. Trama of gills irregular. Pileipellis consisted of irregular subglobose cell, irregular oval or long oval, (22) 25–32 μm broad.

Habit and habitat. Clumped on the ground with rich humus in deciduous broad-leaved or deciduous coniferous forests.

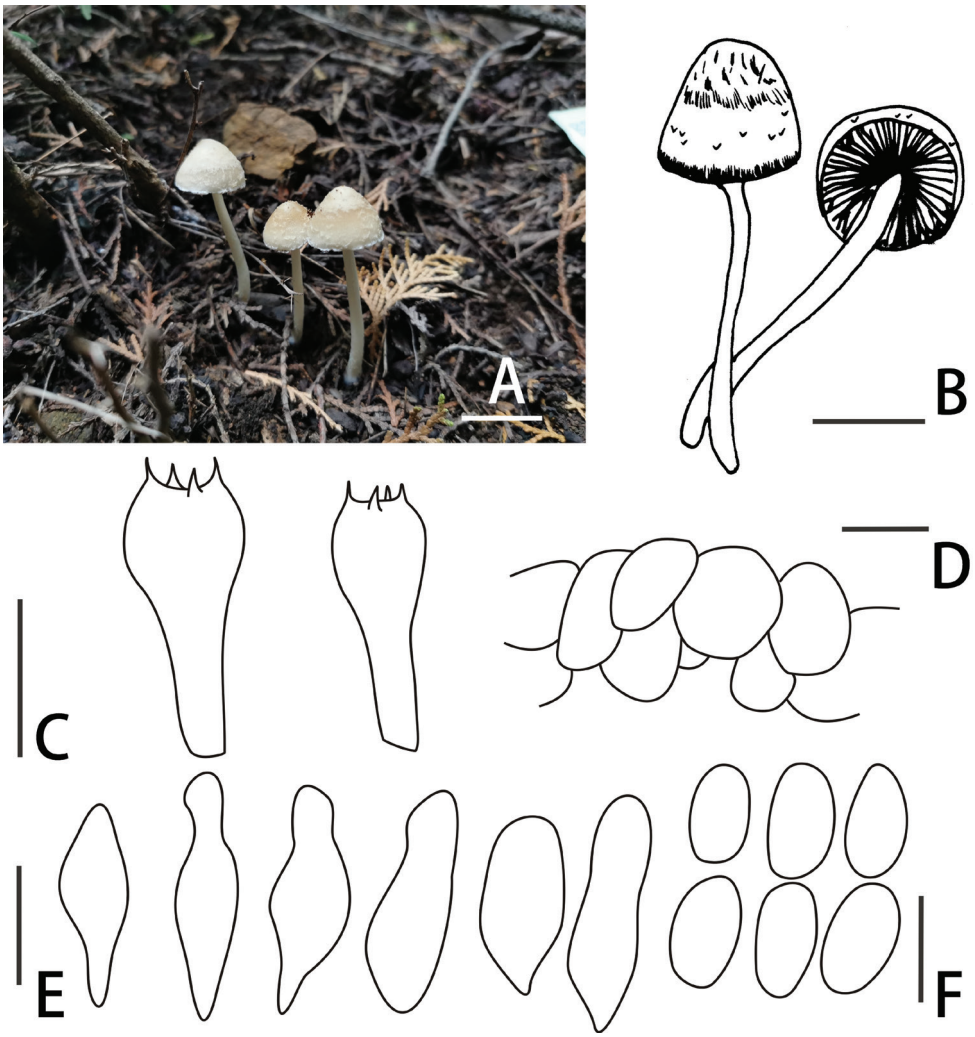

Figure 4. Basidiomata and microscopic features of *Candolleomyces incanus* (BJTC Z777) **A, B** basidiomata **C** basidia **D** pileipellis **E** cheilocystidia **F** basidiospores. Scale bars: 20 mm (**A, B**); 10 μm (**C**); 20 μm (**D, E, F**).

Additional specimen examined. China, Beijing, Yanqing District, Yudu Mountain, 40.54399°N, 115.893984°E, alt. 860 m, 12 Sep 2018, coll. C.L. Hou, H Zhou and J.Q. Li, BJTC 646.

Discussion

In this study, three new species were identified by morphology and phylogeny. It is very interesting that the three new species *C. yanshanensis*, *C. subcandolleanus* and *C. incanus* formed a stronger supported clade and they clustered with *Candolleomyces badiophyllus* (Romagn.) D. Wächt. & A. Melze, *Candolleomyces candolleanus*,

Candolleomyces badhyzensis (Kalamees) D. Wächt. & A. Melzer, *Candolleomyces trinitatensis* (R.E.D. Baker & W.T. Dale) D. Wächt. & A. Melzer and *Candolleomyces cladii-marisci* (Sicoli, N.G. Passal., De Giuseppe, Palermo & Pellegrino) J.Q. Yan together in the phylogenetic tree. In addition, three new species were weakly sister to the known species *C. badiophyllus* in the phylogenetic tree.

Candolleomyces yanshanensis and *C. subcandolleanus* are different in macroscopic morphology of basidiomata. *Candolleomyces yanshanensis* is lighter in pileus colour and *C. yanshanensis* has larger spores (5.8–8.2 × 3.3–5.4 vs. 5.5–6.7×3.2–4.5 μm) and longer cheilocystidia (22–35 × 8–11 vs. 21–28 × 8–12 μm) than those of *C. subcandolleanus*. Moreover, *C. yanshanensis* spores often have a germ pore. *Candolleomyces subcandolleanus* is very easily confused with *C. candolleanus* in the field because of their similar macroscopic characteristics. In particular, two species in these sections possess the combined characteristics of small basidiomata. *C. candolleanus* is the type species of *Candolleomyces*, with early studies on this species being based on the number of pleats and other characteristics, but this also led to confusion in the identification of this species. *Candolleomyces subcandolleanus* can be distinguished from *C. candolleanus* by the smaller spores (5.5–6.7 × 3.2–4.5 vs. 7–9 × 4–5 μm) (Kits van Waveren 1980; Breitenbach and Kränzlin 1995; Mifsud 2017).

Candolleomyces incanum, *C. badiophyllus*, *C. candolleanus* and *C. badhyzensis* are close to each other in the phylogenetic tree. However, the four species show significant differences in morphology. These species can be distinguished as follows: *C. incanus* has smaller and narrower spores (6.0–7.0 × 3.2–4.5 μm), whereas *C. candolleanus*, *C. badhyzensis* and *C. badiophyllus* have larger spores (Spores of *C. candolleanus* were 7.0–9.0 × 4.0–5.0 μm, spores of *C. badhyzensis* were 10.2–11.5 × 5.5–6.5 μm, spores of *C. badiophyllus* were 10–14 × 5–6 μm). In addition, *C. incanus* has smaller cheilocystidia (17–27 × 7–11 vs. 34–51 × 10–15 μm) than those of *C. badhyzensis* (Kalamees 1981; Kasik et al. 2004; Wächter and Melzer 2020).

Except for morphological differences, the three new species in this study can also be distinguished by sequence similarity. *Candolleomyces yanshanensis* (BJTC Z110) can be distinguished, based on nucleotide differences in ITS, LSU, *Tef1a* and *TUB2* loci from *C. subcandolleanus* (BJTC Z239) (sequence base similarity 93% in ITS, 100% in LSU, 99% in *Tef1a* and 98% in *TUB2*); *C. yanshanensis* (BJTC Z110) can be distinguished, based on nucleotide differences from *C. incanus* (BJTC Z777) (sequence base similarity 80% in ITS, 99% in LSU, 99% in *Tef1a* and 96% in *TUB2*); *C. subcandolleanus* (BJTC Z239) can be distinguished, based on nucleotide differences from *C. incanus* (BJTC Z777) (sequence base similarity 81% in ITS, 99% in LSU, 99% in *Tef1a* and 98% in *TUB2*). It can also be found that the ITS loci have a greater degree of differentiation for the species in *Candolleomyces*, Nevertheless, LSU and *Tef1a* were more conservative for the genus.

According to the research of Wächter and Melzer (2020), the species of *Candolleomyces* may be more abundant than previously thought and better delimitation of species boundaries is required. While the boundaries of some species are disputed, the number of new taxa is steadily increasing (Sicoli et al. 2019; Büttner et al. 2020; Bau and Yan 2021). However, the continued discovery of clear boundaries in new taxa like this study enhances our comprehension of species in this genus.

It is considered that the natural growth of *Candolleomyces* may be related to precipitation. However, the investigation and specimen collection in this study were carried out in the rainy season in July to August, with no collection in other periods. Therefore, more species of *Candolleomyces* might be expected in Yanshan Mountains.

Acknowledgements

This study was supported by the Biodiversity Survey and Assessment Project of the Ministry of Ecology and Environment, China. (2019HJ2096001006) and National Natural Science Foundation of China (No. 31870629).

Reference

Battistin E, Chiarello O, Vizzini A, Örstadius L, Larsson E (2014) Morphological characterization and phylogenetic placement of the very rare species *Psathyrella* sulcatotuberculosa. Sydowia 66(2): 171–181. https://doi.org/10.12905/0380.sydowia66(2)2014-0171

Bau T, Yan JQ (2021) Two new rare species of *Candolleomyces* with pale spores from China. MycoKeys 80: 149–161. https://doi.org/10.3897/mycokeys.80.67166

Breitenbach J, Kränzlin F (1995) Pilze der Schweiz 4. Mykologia, Luzern.

Büttner E, Karich A, Nghi DH, Lange M, Liers C, Kellner H, Hofrichter M, Ullrich R (2020) *Candolleomyces eurysporus*, a new *Psathyrellaceae* (*Agaricales*) species from the tropical Cúc Phương National Park, Vietnam. Asian Journal of Mycology 28: 79–92. https://doi.org/10.21203/rs.3.rs-57408/v1

Fries E (1838) Epicrisis Systematis Mycologici. seu synopsis Hymenomycetum. Uppsala 4: 44–45.

Guindon S, Dufayard JF, Lefort V, Anisimova M, Hordijk W, Gascuel O (2010) New algorithms and methods to estimate maximum likelihood phylogenies: Assessing the performance of PhyML 3.0. Systematic Biology 59(3): 307–321. https://doi.org/10.1093/sysbio/syq010

Hillis DM, Bull JJ (1993) An empirical test of bootstrapping as a method for assessing confidence in phylogenetic analysis. Systematic Biology 42(2): 182–192. https://doi.org/10.1093/sysbio/42.2.182

Hopple Jr JS, Vilgalys R (1999) Phylogenetic relationships in the mushroom genus *Coprinus* and dark-spored allies based on sequence data from the nuclear gene coding for the large ribosomal subunit RNA: Divergent domains, outgroups, and monophyly. Molecular Phylogenetics and Evolution 13(1): 1–19. https://doi.org/10.1006/mpev.1999.0634

Kalamees K (1981) Agaric fungi of Badhyz Nature Reserve. Folia Cryptogamica Estonica 15: 5–8.

Kasik G, Dogan HH, Öztürk C, Aktas S (2004) New records in *Coprinaceae* and *Bolbitaceae* from Mut (Mersin) District. Turkish Journal of Botany 28: 449–455.

Katoh K, Toh H (2010) Parallelization of the MAFFT multiple sequence alignment program. Bioinformatics (Oxford, England) 26(15): 1899–1900. https://doi.org/10.1093/bioinformatics/btq224

Kits van Waveren E (1980) Checklist of synonyms, varieties and forms of *Psathyrella candolleana*. Transactions of the British Mycological Society 75(3): 429–437. https://doi.org/10.1016/S0007-1536(80)80123-9

Kits van Waveren E (1985) The Dutch. French and British species of *Psathyrella*. Persoonia 2: 1–284.

Larsson E, Örstadius L (2008) Fourteen coprophilous species of *Psathyrella* identified in the Nordic countries using morphology and nuclear rDNA sequence data. Mycological Research 112(10): 1165–1185. https://doi.org/10.1016/j.mycres.2008.04.003

Matheny PB, Curtis JC, Hofstetter V, Aime MC, Moncalvo JM, Ge ZW, Yang ZL, Slot JC, Ammirati JF, Baroni TJ, Bougher NL, Hughes KW, Lodge DJ, Kerrigan RW, Seidl MT, Aanen DK, DeNitis M, Danielle G, Desjardin DE, Kropp BR, Norvell LL, Parker A, Vellinga EC, Vilgalys R, Hibbett DS (2006) Major clades of Agaricales: A multi-locus phylogenetic overview. Mycologia 98(6): 982–995. https://doi.org/10.1080/15572536.2006.11832627

Mifsud S (2017) Contribution to the Mycobiota and Myxogastria of the Maltese islands. Part I (2014–2016). Micologia e Vegetazione Mediterranea 32(1): 3–58.

Moncalvo JM, Vilgalys R, Redhead SA, Johnson JE, James TY, Aime MC, Hofstetter V, Verduin SJW, Larsson E, Baroni TJ, Thorn RG, Jacobsson S, Clèmencon H, Miller OK (2002) One hundred and seventeen clades of euagarics. Molecular Phylogenetics and Evolution 23(3): 357–400. https://doi.org/10.1016/S1055-7903(02)00027-1

Nagy LG, Walther G, Házi J, Vágvölgyi C, Papp T (2011) Understanding the evolutionary processes of fungal fruiting bodies: Correlated evolution and divergence times in the Psathyrellaceae. Systematic Biology 60(3): 303–317. https://doi.org/10.1093/sysbio/syr005

Örstadius L, Kundsen H (2012) *Psathyrella* (Fr.) Quél. In: Knudsen H, Vesterholt J (Eds) Funga Nordica. Agaricoid, boletoid, cyphelloid and gasteroid genera. Nordsvamp, Copenhagen, 586–623.

Örstadius L, Ryberg M, Larsson E (2015) Molecular phylogenetics and taxonomy in Psathyrellaceae (Agaricales) with focus on psathyrelloid species: Introduction of three new genera and 18 new species. Mycological Progress 14(5): 1–42. https://doi.org/10.1007/s11557-015-1047-x

Posada D, Crandall KA (1998) Modeltest: Testing the model of DNA substitution. Bioinformatics (Oxford, England) 14(9): 817–818. https://doi.org/10.1093/bioinformatics/14.9.817

Rannala B, Yang Z (1996) Probability distribution of molecular evolutionary trees: A new method of phylogenetic inference. Journal of Molecular Evolution 43(3): 304–311. https://doi.org/10.1007/BF02338839

Ronquist F, Huelsenbeck JP (2003) MrBayes 3: Bayesian phylogenetic inference under mixed models. Bioinformatics (Oxford, England) 19(12): 1572–1574. https://doi.org/10.1093/bioinformatics/btg180

Sicoli G, Passalacqua NG, De Giuseppe AB, Palermo AM, Pellegrino G (2019) A new species of *Psathyrella* (*Psathyrellaceae*, *Agaricales*) from Italy. MycoKeys 52: 89–102. https://doi.org/10.3897/mycokeys.52.31415

Smith AH (1972) The North America species of *Psathyrella*. The New York Botanical Garden 24: 1–633.

Stamatakis A (2006) RAxML-VI-HPC: Maximum likelihood-based phylogenetic analyses with thousands of taxa and mixed models. Bioinformatics (Oxford, England) 22(21): 2688–2690. https://doi.org/10.1093/bioinformatics/btl446

Stamatakis A, Hoover P, Rougemont J (2008) A rapid bootstrap algorithm for the RAxML web servers. Systematic Biology 57(5): 758–771. https://doi.org/10.1080/10635150802429642

Swofford DL (2003) PAUP*: Phylogenetic analysis using parsimony (* and other methods). Version 4.0b10. Sunderland, England.

Tamura K, Stecher G, Peterson D, Filipski A, Kumar S (2013) MEGA6: Molecular evolutionary genetics analysis version 6.0. Molecular Biology and Evolution 30(12): 2725–2729. https://doi.org/10.1093/molbev/mst197

Vilgalys R, Hester M (1990) Rapid genetic identification and mapping of enzymatically amplified ribosomal DNA from several Cryptococcus species. Journal of Bacteriology 172(8): 4238–4246. https://doi.org/10.1128/jb.172.8.4238-4246.1990

Wächter D, Melzer A (2020) Proposal for a subdivision of the family Psathyrellaceae based on a taxon-rich phylogenetic analysis with iterative multigene guide tree. Mycological Progress 19(11): 1151–1265. https://doi.org/10.1007/s11557-020-01606-3

Wang Y, Bau T (2014) Well-known Chinese species of *Psathyrella* and their distribution. Journal of Fungal Research 12(3): 133–141. https://doi.org/10.13341/j.jfr.2014.0053

Wang YT, Huang ZH, Wang J, Tong Z, Cui GF (2021) The population structure and dynamic characteristics of *Phellodendron amurense* in Yanshan Mountains. Acta Ecologica Sinica 47(7): 2826–2834. https://doi.org/10.5846/stxb202003300743

White TJ, Bruns T, Lee S, Taylor J (1990) Amplification and direct sequencing of fungal ribosomal RNA genes for phylogenetics. PCR Protocols: a Guide to Methods and Applications 18: 315–322. https://doi.org/10.1016/B978-0-12-372180-8.50042-1

Yan JQ (2018) Taxonomy and molecular phylogeny of *Psathyrella* and related genera in China. Dissertation. Jilin Agricultural University.

Yan JQ, Bau T (2017) New and newly recorded species of *Psathyrella* (Psathyrellaceae, Agaricales) from northeast China. Phytotaxa 321(1): 139–150. https://doi.org/10.11646/phytotaxa.321.1.7

Yan JQ, Bau T (2018a) The northeast Chinese species of *Psathyrella* (*Agaricales*, *Psathyrellaceae*). MycoKeys 33: 85–102. https://doi.org/10.3897/mycokeys.33.24704

Yan JQ, Bau T (2018b) *Psathyrella alpina* sp. nov. (*Psathyrellaceae*, *Agaricales*), a new species from China. Phytotaxa 349(1): 85–91. https://doi.org/10.11646/phytotaxa.349.1.11

Yan JQ, Bau T (2021) A new and two newly recorded species in the /pygmaea clade of *Psathyrella* (*Psathyrellaceae*, *Agaricomycetes*) from China. Junwu Xuebao 40(3): 462–472. https://doi.org/10.13346/j.mycosystema.200350

Yan JQ, Ge Y, Hu D, Zhou J, Huo GH (2019) *Psathyrella tintinnabula* sp. nov. (*Psathyrellaceae*, *Agaricales*), a new species from southwest China. Phytotaxa 400(2): 64–70. https://doi.org/10.11646/phytotaxa.400.2.2

Zhou H, Hou CL (2019) Three new species of Diaporthe from China based on morphological characters and DNA sequence data analyses. Phytotaxa 422(2): 157–174. https://doi.org/10.11646/phytotaxa.422.2.3

Zhou H, Wang QT, Tong X, Hou CL (2021) Phylogenetic analysis of *Engleromyces sinensis* and identification of cytochalasin D from culture. Mycological Progress 20(10): 1343–1352. https://doi.org/10.1007/s11557-021-01739-z

MycoKeys 88: 123–149 (2022)
doi: 10.3897/mycokeys.88.79475
https://mycokeys.pensoft.net

RESEARCH ARTICLE

A peer-reviewed open-access journal
MycoKeys
Launched to accelerate biodiversity research

Morpho-molecular characterisation of *Arecophila*, with *A. australis* and *A. clypeata* sp. nov. and *A. miscanthi* comb. nov.

Qi Rui Li[1,2], Xu Zhang[2], Yan Lin[2], Milan C. Samarakoon[3], Kevin David Hyde[4], Xiang Chun Shen[2], Wan Qing Liao[5], Anuruddha Karunarathna[4], Si Han Long[2], Ying Qian Kang[6], Ji Chuan Kang[1]

1 *The Engineering and Research Center for Southwest Bio-Pharmaceutical Resources of National Education Ministry of China, Guizhou University, Guizhou, China* **2** *The High Efficacy Application of Natural Medicinal Resources Engineering Center of Guizhou Province (The Key Laboratory of Optimal Utilization of Natural Medicine Resources), School of Pharmaceutical Sciences, Guizhou Medical University, University Town, Guian New District, Guizhou, China* **3** *Department of Entomology and Plant Pathology, Faculty of Agriculture, Chiang Mai University, Chiang Mai 50200, Thailand* **4** *Center of Excellence in Fungal Research, Mae Fah Luang University, Chiang Rai 57100, Thailand* **5** *Shanghai Key Laboratory of Molecular Medical Mycology, Department of Dermatology and Venereology, Changzheng Hospital, Shanghai, China* **6** *Department of Microbiology, Guizhou Medical University, University Town, Guian New District, Guizhou, China*

Corresponding authors: Ying Qian Kang (joycekangtokyo@gmail.com), Ji Chuan Kang (jckang@gzu.edu.cn)

Academic editor: S. Maharachchikumbura | Received 17 December 2021 | Accepted 16 March 2022 | Published 13 April 2022

Citation: Li QR, Zhang X, Lin Y, Samarakoon MC, Hyde KD, Shen XC, Liao WQ, Karunarathna A, Long SH, Kang YQ, Kang JC (2022) Morpho-molecular characterisation of *Arecophila*, with *A. australis* and *A. clypeata* sp. nov. and *A. miscanthi* comb. nov.. MycoKeys 88: 123–149. https://doi.org/10.3897/mycokeys.88.79475

Abstract

Three arecophila-like fungal samples were collected on dead culms of gramineous plants in China. Morphological studies of our new collections and the herbarium specimen of *Arecophila gulubiicola* (generic type) were conducted and the morphological affinity of our new collections with *Arecophila* was confirmed. Maximum likelihood and Bayesian analyses using combined ITS, LSU, *rpb2* and β-tubulin data from our collections revealed the phylogeny of *Cainiaceae.* The monospecific genus *Alishanica* (type species *Al. miscanthi*), which had been accepted in *Cainiaceae*, is revisited and synonymised under *Arecophila*. Based on morphology and phylogeny, *Arecophila australis* sp. nov. and *A. clypeata* sp. nov. are introduced as new species, while *A. miscanthi* is a new record for China. All the new collections are illustrated and described.

Keywords

Cainiaceae, gramineous plants, phylogeny, taxonomy

Introduction

The current study is a part of a series of papers on *Xylariales* (*Sordariomycetes*) from China (Long et al. 2019; Xie et al. 2019, 2020; Pi et al. 2020). *Arecophila* K.D. Hyde, which is typified by *A. gulubiicola* K.D. Hyde, was introduced by Hyde (1996) with five species. *Arecophila* is characterised by immersed, subglobose to lenticular ascomata, peridium with *textura angularis* cells, non- or poorly-developed clypeus, asci with a wedge-shaped, apical ring, J+ in Melzer's reagent and 2-celled, brown ascospores with wall striations, surrounded by a mucilaginous sheath. Thanks to subsequently undertaken morphological studies of holotypes, several species have been transferred to *Arecophila* from genera such as *Amphisphaeria* Ces. & De Not., *Cainia* Arx & E. Müll., *Didymosphaeria* Fuckel and *Schizostoma* Ehrenb. ex Lév. (Hyde 1996; Umali et al. 1999; Wang et al. 2004).

Currently, there are 15 *Arecophila* epithets in Index Fungorum (http://www.indexfungorum.org/Names/Names.asp, May 2021), which have been introduced, based on morphology and lack sequence data (e.g. Hyde 1996; Umali et al. 1999; Wang et al. 2004). After searching for *Arecophila* in NCBI, there were only five hits of LSU, SSU and metagenomic sequences of *A. bambusae* and *Arecophila* sp. HKUCC 6487 in GenBank.

Arecophila was introduced as a genus of *Amphisphaeriaceae* (Hyde 1996), based on its unitunicate, cylindrical asci with a J+ apical ring and brown, 2-celled ascospores. Kang et al. (1999) reviewed the genus and accepted it in *Cainiaceae* and the occurrence on monocotyledons (palms and bamboo). The single and combined molecular analyses of LSU and SSU genes resulted in *Arecophila* grouping with *Cainia* in *Xylariales* (Smith et al. 2003). Based on analyses of partial LSU gene sequences, the generic placement of *Arecophila* within the *Cainiaceae* has been verified (Jeewon et al. 2003; Senanayake et al. 2015; Hyde et al. 2020; Wijayawardene et al. 2020). However, the available molecular data do not provide strong evidence of the phylogenetic affinity of *Arecophila* and related taxa.

During our continuous collecting of xylarialean taxa in China, we found some specimens that share a morphology resembling *Arecophila*. In this paper, two new species and a new record of *Arecophila* are provided with descriptions and illustrations. Furthermore, *Alishanica* is synonymised under *Arecophila*, based on morphology and phylogeny.

Materials and methods

Collection, isolation and morphology

Fresh samples were collected in Guizhou and Yunnan Provinces in China during the rainy season and taken to the laboratory in paper bags. Single-spore isolations were obtained following the method described in Chomnunti et al. (2014). The cultures on

potato dextrose agar (**PDA**) were transferred to 2 ml screw cap centrifuge tubes filled with 10% glycerol and sterile water to deposit at –20 °C and 4 °C, respectively. Herbarium materials were deposited at the Herbarium of Guizhou Agricultural College (**GACP**) and the Herbarium of Guizhou University (**GZUH**). Cultures were deposited at the Culture Collection of Guizhou University (**GZUCC**).

The morphological examination of fresh and herbarium specimens was carried out as described by Hyde (1996). Macro-morphological characters were examined and photographed using a digital camera (Canon 700D) fitted to the Olympus SZ61 stereomicroscope. Materials mounted in water, Melzer's reagent and Indian ink were examined. At least 30 ascospores, 30 asci and 20 apical rings were measured for each taxa with Tarosoft (R) Image Frame Work (v. 0.9.0.7) and photographed using a digital camera (Nikon 700D) fitted to a light microscope (Nikon Ni).

DNA extraction, polymerase chain reaction (PCR) amplification and sequencing

Total genomic DNA was extracted from fresh mycelium scraped off from pure cultures with the BIOMIGA fungus genomic DNA extraction kit (GD2416) (Wijayawardene et al. 2013) following the manufacturer's instructions. Primers, LR0R/LR5 (Vilgalys and Hester 1990), ITS4/ITS5 (White et al. 1990), RPB2-5F/RPB2-7cR (Liu et al. 1999), Bt2a/Bt2b and ACT-512F/ACT-783R (Hsieh et al. 2005) were used for amplifying partial large-subunit ribosomal RNA (LSU), internal transcribed spacer (ITS), partial second-largest subunit of the RNA polymerase II (*rpb*2), β-tubulin (*tub*) and α-actin gene (Hsieh et al. 2005). The amplification conditions were carried out according to Liu et al. (2011) and Hsieh et al. (2005). Amplified products were examined and sent to the sequencing company, Sangon Biotech, Shanghai, China. The obtained sequences were checked, assembled and uploaded to GenBank.

Sequence alignment and phylogenetic analyses

Following the NCBI BLAST results and literature (e.g. Jeewon et al. 2003; Senanayake et al. 2015), relevant sequences from all families of Xylariomycetidae were downloaded from GenBank for the phylogenetic analyses (Table 1). Sequences of each segment were aligned using MAFFT (http://mafft.cbrc.jp/alignment/server/index.html, Katoh and Standley 2019) and improved manually in BioEdit 7.2.3 (Hall 1999). The combined alignment of ITS, LSU, *rpb*2 and β-tubulin was concatenated from individual datasets. Ambiguously aligned areas of each gene region were excluded and gaps were treated as missing data. The ALTER (http://sing.ei.uvigo.es/ALTER/) phylogeny website tool was used to obtain the phylip file for RAxML analysis and the nexus file for Bayesian analysis (Glez-Peña et al. 2010). Phylogenetic trees were visualised using FigTree v.1.4.0. and processed using Adobe Photoshop CS6 software (Adobe Systems, USA). The alignment for the tree in this paper was uploaded on the website (https://treebase.org/) with submission ID 26613.

Table 1. Sequences used for phylogenetic analyses in this study.

Species	Strain number	Status	GenBank accession numbers				References
			ITS	LSU	*rpb2*	β-tubulin	
Achaetomium macrosporum	CBS 532.94	–	KX976574	KX976699	KX976797	KX976915	Wang et al. (2016)
Amphibambusa bambusicola	MFLUCC 11-0617	HT	KP744433	KP744474	N/A	N/A	Senanayake et al. (2015)
Amphisphaeria acericola	MFLU 16-2479	HT	NR_171945	MK640424	N/A	N/A	Senanayake et al. (2019, submitted directly)
Amphisphaeria thailandica	MFLU 18-0794	HT	NR_168783	NG_068588	MK033640	MK033639	Samarakoon et al. (2019)
Amphisphaeria umbrina	AFTOL-ID 1229	AF009805	N/A	FJ176863	FJ238348	N/A	Schoch (2008, submitted directly)
Apiospora bambusae	ICMP 6889	–	N/A	DQ368630	DQ368649	N/A	Tang et al. (2007)
Apiospora hyphopodii	MFLUCC 15-0003	HT	KR069110	KY356093	N/A	N/A	Dai et al. (2016)
Apiospora setosa	ICMP 4207	–	N/A	DQ368631	DQ368650	DQ368620	Tang et al. (2007)
Apiospora yunnana	MFLUCC 15-0002	HT	KU940147	NG_057104	KU940177	MK291950	Dai et al. (2017)
Arecophila australis	GZUCC0112	HT	MT742126	MT742133	N/A	MT741734	This study
Arecophila australis	GZUCC0124	–	MT742125	MT742132	N/A	N/A	This study
Arecophila bambusae	HKUCC 4794	–	N/A	AF452038	N/A	N/A	Kang et al. (1999)
Arecophila clypeata	GZUCC0110	HT	MT742129	MT742136	MT741732	N/A	This study
Arecophila clypeata	GZUCC0127	–	MT742128	MT742135	N/A	N/A	This study
Arecophila miscanthi	GZUCC0122	–	MT742127	MT742134	N/A	N/A	This study
Arecophila miscanthi	MFLU 19-2333	HT	NR_171235	MK503827	N/A	N/A	Hyde et al. (2020)
Arecophila sp.	HKUCC 6487	–	N/A	AF452039	N/A	N/A	Jeewon et al. (2003)
Apiospora yunnana	MFLUCC 15-0002	HT	KU940147	NG_057104	KU940177	MK291950	Dai et al. (2017)
Atrotorquata spartii	MFLUCC 13-0444	HT	N/A	KP325443	N/A	N/A	Thambugala et al. (2015)
Bagadiella lunata	CBS 124762	HT	NR_132832	NG_058637	N/A	N/A	Cheewangkoon et al. (2009)
Barrmaelia rappazii	Cr2 = CBS 142771	HT	MF488989	MF488989	MF488998	MF489017	Voglmayr et al. (2018)
Barrmaelia rhamnicola	BR = CBS 142772	HT	MF488990	MF488990	MF488999	MF489018	Voglmayr et al. (2018)
Bartalinia pondoensis	CMW 31067	–	MH863602	MH875078	MH554904	MH554663	Vu et al. (2019)
Beltrania pseudorhombica	CBS 138003	HT	MH554124	NG_058667	MH555032	N/A	Liu et al. (2019)
Beltrania rhombica	CBS 123.58	T	MH857718	MH868082	MH554899	MH704631	Vu et al. (2019)
Beltraniopsis longiconidiophora	MFLUCC 17-2139	HT	NR_158353	NG_066200	N/A	N/A	Liu et al. (2017)
Biscogniauxia nummularia	MUCL 51395	ET	KY610382	KT281894	KY624236	KX271241	Senanayake et al. (2015)
Cainia anthoxanthis	MFLUCC 15-0539	HT	NR_138407	KR092777	N/A	N/A	Senanayake et al. (2015)
Cainia graminis	CBS 136.62	–	MH858123	AF431949	N/A	N/A	Vu et al. (2019)

Species	Strain number	Status	GenBank accession numbers				References
			ITS	LSU	*rpb2*	β-tubulin	
Cainia graminis	MFLUCC 15-0540	–	KR092793	KR092781	N/A	N/A	Senanayake et al. (2015)
Camillea obularia	ATCC 28093	–	KY610384	KY610429	KY624238	KX271243	Wendt et al. (2018)
Castanediella acaciae	CBS 139896	HT	NR_137985	NG_067293	N/A	N/A	Crous et al. (2015)
Castanediella couratarii	CBS 579.71	HT	NR_145250	NG_066249	N/A	N/A	Vu et al. (2019)
Castanediella eucalypticola	CPC 26539	HT	KX228266	KX228317	N/A	KX228382	Crous et al. (2013)
Chaetomium elatum	CBS 374.66	–	KC109758	KC109758	KF001820	KC109776	Wang et al. (2016)
Ciferriascosea fluctuatimura	MFLUCC 15-0541	HT	KR092789	KR092778	N/A	N/A	Senanayake et al. (2015)
Ciferriascosea rectimura	MFLUCC 15-0542	HT	NR_153905	KR092776	N/A	N/A	Senanayake et al. (2015)
Clypeophysalospora latitans	CBS 141463	ET	NR_153929	NG_058958	N/A	N/A	Giraldo et al. (2017)
Coniocessia maxima	CBS 593.74	HT	NR_137751	MH878275	N/A	N/A	Vu et al. (2019)
Coniocessia nodulisporioides	CBS 281.77	IT	MH861061	AJ875224	N/A	N/A	García et al. (2006)
Creosphaeria sassafras	STMA 14087	–	KY610411	KY610468	KY624265	KX271258	Wendt et al. (2018)
Cylindrium aeruginosum	CBS 693.83	–	KM231854	KM231734	KM232430	KM232124	Lombard et al (2014, submitted directly)
Cylindrium grande	CBS 145655	HT	NR_165557	NG_068656	MK876481	MK876502	Crous et al. (2019)
Cylindrium purgamentum	CPC 29580	HT	NR_155691	NG_067320	N/A	N/A	Koppel et al. (2017)
Daldinia concentrica	CBS 113277	–	AY616683	KT281895	KY624243	KC977274	Senanayake et al. (2015)
Delonicicola siamense	MFLUCC 15-0670	HT	MF167586	NG_059172	MF158346	N/A	Perera et al. (2017)
Diatrype palmicola	MFLUCC 11-0018	–	KP744439	KP744481	N/A	N/A	Liu et al. (2015)
Diatrype whitmanensis	ATCC MYA-4417	–	FJ746656	FJ430587	N/A	N/A	Igo et al. (2009, direct submission)
Entosordaria perfidiosa	EPE = CBS 142773	ET	MF488993	MF488993	MF489003	MF489021	Voglmayr et al. (2018)
Entosordaria quercina	RQ = CBS 142774	HT	MF488994	MF488994	MF489004	MF489022	Voglmayr et al. (2018)
Eutypa flavovirens	MFLUCC 13-0625	–	KR092798	KR092774	N/A	N/A	Senanayake et al. (2015)
Eutypa laevata	CBS 291.87	–	HM164737	N/A	HM164805	HM164771	Trouillas and Gubler (2010)
Eutypa lata	CBS 208.87	NT	MH862066	MH873755	KF453595	DQ006969	Vu et al. (2019)
Furfurella nigrescens	CBS 143622	HT	MK527844	MK527844	MK523275	MK523332	Voglmayr et al. (2019)
Furfurella stromatica	CBS 144409	HT	NR_164062	MK527846	MK523277	MK523334	Voglmayr et al. (2019)
Graphostroma platystomum	AFTOL-ID 1249	HT	HG934115	DQ836906	DQ836893	HG934108	Zhang et al. (2006)
Hyponectria buxi	UME 31430	–	-	AY083834	N/A	N/A	Smith et al. (2002, submitted directly)
Hypoxylon fragiforme	MUCL51264	ET	KM186294	KM186295	KM186296	KM186293	Daranagama et al. (2015)
Iodosphaeria honghensis	MFLU 19-0719	HT	MK737501	MK722172	MK791287	N/A	Marasinghe et al. (2019)
Iodosphaeria tongrenensis	MFLU 15-0393	HT	KR095282	KR095283	N/A	N/A	Li et al. (2015)

Species	Strain number	Status	GenBank accession numbers				References
			ITS	LSU	*rpb2*	β-tubulin	
Jackrogersella multiformis	CBS 119016	ET	KC477234	KT281893	KY624290	KX271262	Wendt et al. (2018)
Kretzschmaria deusta	CBS 163.93	–	KC477237	KT281896	KY624227	KX271251	Senanayake et al. (2015)
Lepteutypa fuckelii	CBS 140409	NT	NR_154123	KT949902	MK523280	MK523337	Jaklitsch et al. (2016)
Leptosillia pistaciae	CBS 128196	HT	NR_160064	MH798901	MH791334	MH791335	Voglmayr et al. (2019)
Leptosillia wienkampii	CBS 143630	ET	NR_164067	MK527865	MK523297	MK523353	Voglmayr et al. (2019)
Longiappendispora chromolaenae	MFLUCC 17-1485	HT	NR_169723	NG_068714	N/A	N/A	Mapook et al. (2020)
Lopadostoma americanum	LG8	HT	KC774568	KC774568	KC774525	N/A	Jaklitsch et al. (2014)
Lopadostoma dryophilum	LG21	ET	KC774570	KC774570	KC774526	MF489023	Jaklitsch et al. (2014)
Lopadostoma fagi	LF1	HT	KC774575	KC774575	KC774531	N/A	Jaklitsch et al. (2014)
Lopadostoma quercicola	LG27	HT	KC774610	KC774610	KC774558	N/A	Jaklitsch et al. (2014)
Lopadostoma turgidum	LT2	ET	KC774618	KC774618	KC774563	MF489024	Jaklitsch et al. (2014)
Melogramma campylosporum	MBU	–	JF440978	JF440978	N/A	N/A	Jaklitsch and Voglmayr (2012)
Neophysalospora eucalypti	CBS 111123	–	KP031107	KP031109	N/A	N/A	Crous et al. (2014)
Neophysalospora eucalypti	CBS 138864	HT	KP004462	MH878627	N/A	N/A	Crous et al. (2014)
Oxydothis metroxylicola	MFLUCC 15-0281	HT	KY206774	KY206763	KY206781	N/A	Konta et al. (2016)
Oxydothis palmicola	MFLUCC 15-0806	HT	KY206776	KY206765	KY206782	N/A	Konta et al. (2016)
Oxydothis phoenicis	MFLUCC 18-0269	HT	MK088065	MK088061	N/A	N/A	Hyde et al. (2020)
Phlogicylindrium uniforme	CBS 131312	HT	JQ044426	JQ044445	MH554910	MH704634	Crous et al. (2011)
Podosordaria tulasnei	CBS 128.80	–	KT281902	KT281897	N/A	N/A	Senanayake et al. (2015)
Poronia punctata	CBS 656.78	HT	KT281904	KY610496	KY624278	KX271281	Wendt et al. (2018)
Pseudomassaria chondrospora	MFLUCC 15-0545	–	KR092790	KR092779	N/A	N/A	Senanayake et al. (2015)
Pseudomassaria sepincoliformis	CBS 129022	–	JF440984	JF440984	N/A	N/A	Jaklitsch and Voglmayr (2012)
Pseudosporidesmium knawiae	CBS 123529	HT	MH863299	MH874823	N/A	N/A	Crous et al. (2017, submitted directly)
Pseudosporidesmium lambertiae	CBS 143169	HT	NR_156656	NG_058506	N/A	N/A	Crous et al. (2017)
Pseudotruncatella arezzoensis	MFLUCC 14-0988	HT	NR_157489	NG_070426	N/A	N/A	Perera et al. (2018)
Pseudotruncatella bolusanthi	CBS 145532	HT	NR_165575	MK876448	N/A	N/A	Crous et al. (2019)
Robillarda roystoneae	CBS 115445	HT	NR_145251	NG_069287	MH554880	KR873317	Liu et al. (2019)
Sarcoxylon compunctum	CBS 359.61	–	MH858083	KY610462	KY624230	KX271255	Wendt et al.(2018)
Seiridium marginatum	CBS 140403	ET	NR_156602	MH554223	LT853149	MT853249	Liu et al. (2019)
Seynesia erumpens	SMH 1291	–	N/A	AF279410	AY641073	N/A	Bhattacharya et al. (2000)
Sordaria fimicola	CBS 723.96	–	MH862606	MH874231	DQ368647	DQ368618	Vu et al. (2019)

Species	Strain number	Status	GenBank accession numbers				References
			ITS	LSU	*rpb2*	β-tubulin	
Sporocadus rotundatus	CBS 616.83	HT	NR_161091	NG_069584	MH554974	MH554737	Liu et al. (2019)
Subsessila turbinata	MFLUCC 15-0831	HT	NR_148122	NG_059724	N/A	N/A	Lin et al. (2017)
Vialaea insculpta	DAOM 240257	–	JX139726	JX139726	N/A	N/A	Hambleton et al. (2010, submitted directly)
Vialaea mangiferae	MFLUCC 12-0808	HT	NR_171903	NG_073594	N/A	N/A	Senanayake et al. (2021, submitted directly)
Vialaea minutella	BRIP 56959	–	KC181926	KC181924	N/A	N/A	McTaggart et al. (2013)
Xyladictyochaeta lusitanica	CBS 143502	–	MH107926	MH107972	N/A	MH108053	Crous et al. (2013)
Xylaria hypoxylon	CBS 122620	ET	KY610407	KY610495	KY624231	KX271279	Wendt et al. (2018)
Xylaria obovata	MFLUCC 13-0115	–	KR049088	KR049089	N/A	N/A	Wendt et al. (2018)
Xylaria polymorpha	MUCL 49884	–	KY610408	KT281899	KY624288	KX271280	Wendt et al. (2018)

Note. Type specimens are labelled with HT (holotype), ET (epitype) and IT (isotype), T (Type). N/A: not available.

Maximum likelihood (ML) analysis was performed on the CIPRES Science Gateway v.3.3 (http://www.phylo.org/portal2; Miller et al. 2010) using RAxML v.8.2.8 as part of the 'RAxML-HPC BlackBox' tool (Stamatakis et al. 2008). All free model parameters were estimated by RAxML with ML estimates of 25 per-site rate categories. GTRGAMMA + I model was chosen for RAxML, based on the result of MrModeltest 2.2. The best-scoring tree was selected with a final likelihood value of –10720.566919.

A Bayesian analysis (BY) was performed using MrBayes v.3.2.2 (Ronquist et al. 2012). The best-fit model was selected with MrModeltest 2.2 (Nylander 2004). Posterior probabilities (PP) (Rannala and Yang 1996) were determined by Markov Chain Monte Carlo sampling (MCMC) (Ronquist and Huelsenbeck 2003). Six simultaneous Markov chains were initially run for 30×10^6 generations and for every 1000^{th} generation, a tree was sampled (resulting in 30,000 total trees). The MCMC heated chain was set with a 'temperature' value of 0.15. All sampled topologies beneath the asymptote (20%) were discarded. The remaining 24,000 trees were used to calculate the posterior probability (PP) values in the majority rule consensus tree (Liu et al. 2011).

Results

Phylogenetic analyses

The resulted trees from ML and BY were similar in topology. *Cainiaceae* is a monophyletic group (Fig. 1) with 100%/1.00 (PP/BS) support. *Arecophila* species form two clades. Clade 1 consists of *A. miscanthi* (≡ *Alishanica miscanthi*), *A. clypeata* and *A. australis*, with high statistical support (100%/1.00 PP). In Clade 2, *A. bambusae* (HKUCC 4794) and *Arecophila* sp. (HKUCC 6487) display a close relationship with *Amphibambusa bambusicola*.

Taxonomy

Arecophila **K.D. Hyde, Nova Hedwigia 63(1–2): 82 (1996)**
MycoBank No: 27653

≡ *Alishanica* Karun., C.H. Kuo & K.D. Hyde, in Hyde et al., Mycosphere 11(1): 460 (2020)

Sexual morph. *Ascomata* immersed, raised, blackened areas on the host surface, a central erumpent, short, cone-shaped or umbilicate papilla, subglobose to lenticular in vertical section. *Clypeus* present or not, comprising host cells and intracellular brown hyphae. *Peridium* comprising several layers of angular cells. *Paraphyses* hypha-like, filamentous, septate, hyaline. *Asci* 8-spored, unitunicate, cylindrical, with an apical ring bluing in Melzer's reagent or not. *Ascospores* ellipsoidal, 2-celled, constricted at the septum, brown, with longitudinal striations or a verrucose wall and surrounded by a wide mucilaginous sheath (Hyde 1996).

Asexual morph. Undetermined.

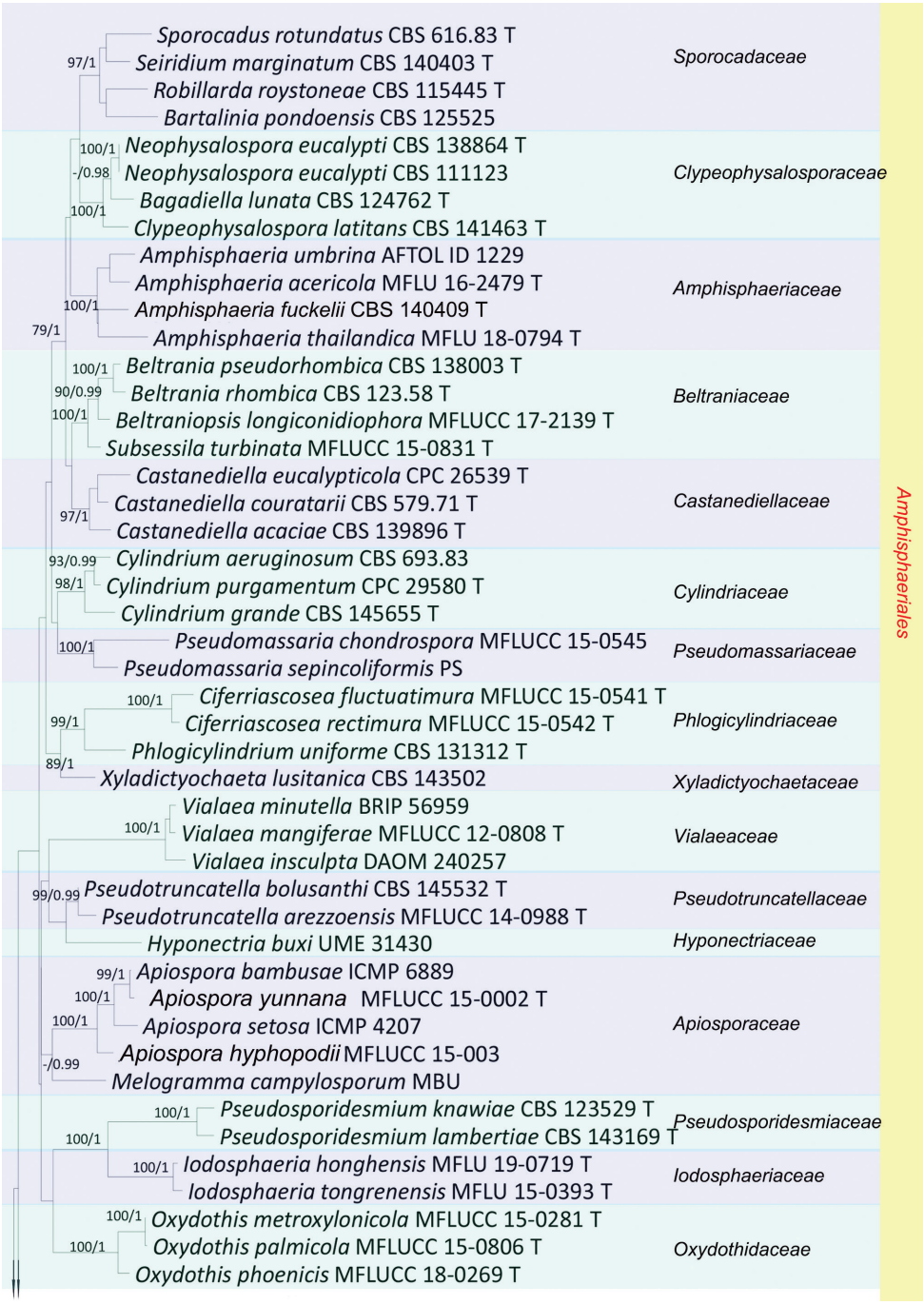

Figure 1. Phylogenetic tree, based on a combined ITS, LSU, *rpb2* and β-tubulin gene dataset. Numbers close to each node represent Maximum Likelihood bootstrap values (≥ 75%) and Bayesian posterior probabilities (≥ 0.95). The hyphen ("–") means a value lower than 75% (BS) or 0.95 (PP). New taxa are marked in red. Type materials are marked with T after the strains. The tree is rooted to *Achaetomium macrosporum* (CBS 532.94), *Chaetomium elatum* (CBS 374.66) and *Sordaria fimicola* (CBS 723.96).

Figure 1. Continued.

Arecophila australis **Q.R. Li, J.C. Kang & K.D. Hyde, sp. nov.**
MycoBank No: 836166
Fig. 2

Diagnosis. *Arecophila australis* differs from similar species by its dimension of ascospores (22.5–29 × 8–11 μm) covered by striations and ascomata with a disc area surrounding the ostioles.

Holotype. China, Guizhou Province, Guiyang City, Forest Park of Guiyang (26°32'55"N, 106°45'25"E), on dead culm of *Phragmites australis* (Cav.) Steud., 15 March 2014, Q.R. Li, GZ58 (GZUH0112, ***holotype***, **ex-type**: GZUCC0112; GACP QR0152, ***isotype***).

Additional sequences. ACT: MT741737

Etymology. In reference to the host, *Phragmites australis* (Cav.) Steud. *australis*

Description. Saprobic on dead culm of gramineous host. **Sexual morph**: *Ascomata* 420–560 × 290–380 μm ($\bar{x}$= 495 × 325 μm, n = 10), immersed under a clypeus, solitary, slightly raised, blackened, dome-shaped areas, scattered or gregarious, globose to subglobose, with a central, erumpent, cone-shaped papilla in vertical section. *Clypeus* black, comprising host cells and intracellular brown hyphae. *Ostioles* papillate, black. *Peridium* 15–25 μm ($\bar{x}$= 21 μm, n = 15) wide, comprising several layers, outer layer brown, thick-walled angular cells, inner layer hyaline. *Paraphyses* 3.3–5 μm ($\bar{x}$= 3.5 μm, n = 15) wide, hyaline, unbranched, septate. *Asci* 140–230 × 15.5–24 μm ($\bar{x}$= 183.5 × 19 μm, n = 30), 8-spored, unitunicate, long-cylindrical, short-pedicellate, apically rounded, with a 4–5 × 2.5–3 μm ($\bar{x}$= 4.5 × 2.7 μm, n = 20), trapezoidal, J+, apical ring. *Ascospores* 22.5–29 × 8–11 μm ($\bar{x}$= 25.5 × 9 μm, n = 30), overlapping uniseriate, 2-celled, light brown to brown, equilateral ellipsoidal, constricted at the septum, longitudinal with sulcate striations, along the entire spore length, surrounded by a mucilaginous sheath, lacking germ slits and appendages. **Asexual morph**: undetermined.

Culture characteristics. Colonies on PDA, reached 3 cm diam. after one week at 25 °C, white, cottony, flat, low, dense, with slightly wavy margin.

Known distribution. China

Additional material examined. China, Guizhou Province, Guiyang City, Leigongshan National Nature Reserve (26°21'39"N, 108°9'59"E), on dead culm of an unidentified gramineous plant, 13 June 2015, Q.R. Li, GY67 (GACP QR0124, GZUH 0136; living cultures, GZUCC0124).

Notes. *Arecophila australis* resembles *A. serrulata* (Ellis & Martin) K.D. Hyde and *A. calamicola* K.D. Hyde (Hyde 1996). However, *A. serrulata* has white ring surrounding ostioles of ascomata, narrower ascospores (17–26 × 7–9.5 μm vs. 22.5–29 × 8–11 μm), smaller asci and apical ring (3.2 × 2.4 μm vs. 4.5 × 2.7 μm) compared to *A. australis* (Hyde 1996). *Arecophila calamicola* differs from *A. australis* in lacking clypeus, ascospores covered by verrucose ornamentation and surrounding by a mucilaginous sheath attached at the poles. Molecular phylogeny, based on combined ITS, LSU, *rpb*2 and β-tubulin sequences, shows that *A. australis* clusters as a distinctive clade in *Arecophila* (Clade 1). Based on its distinct morphology and

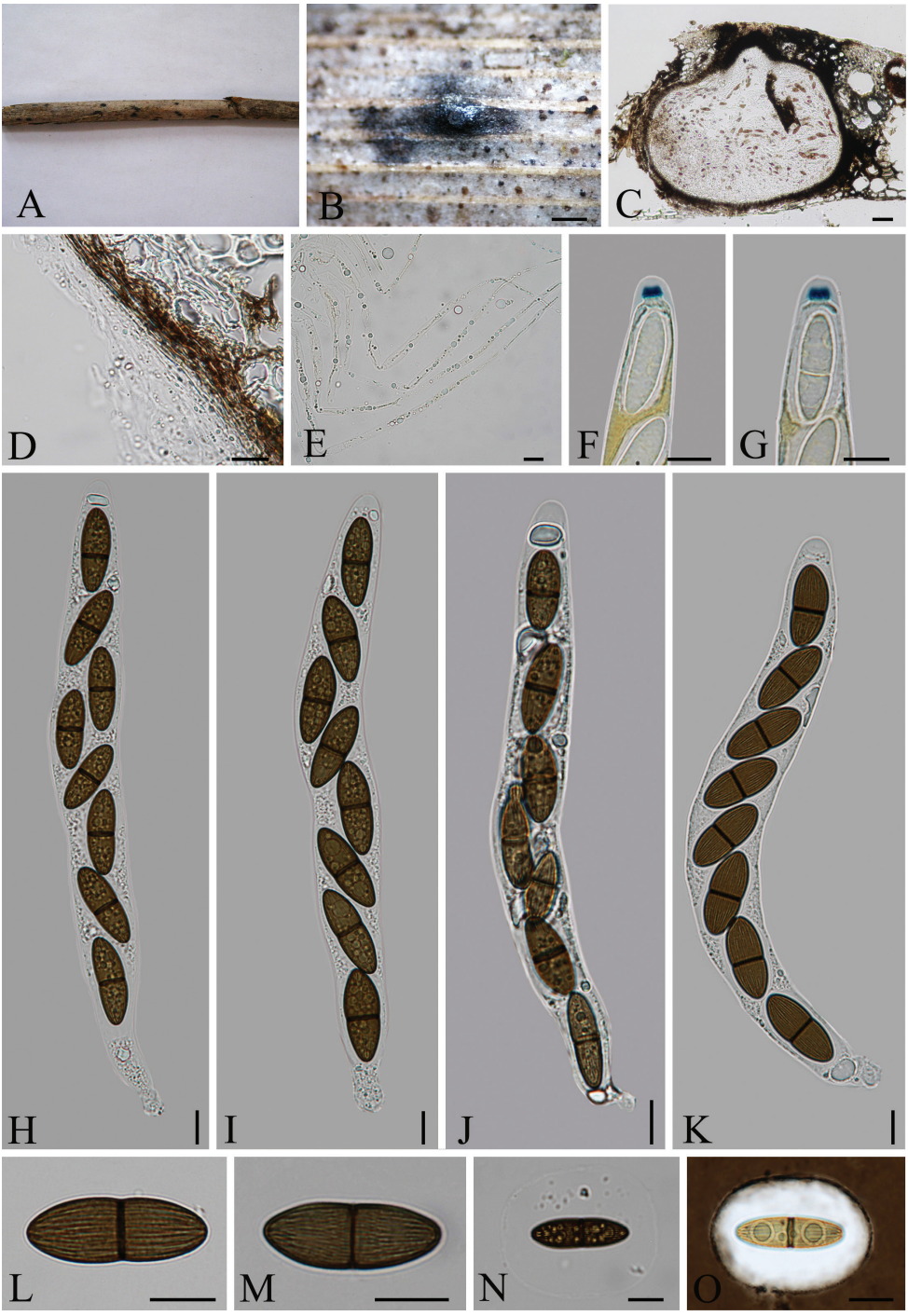

Figure 2. *Arecophila australis* (holotype) **A** material **B** ascoma on the surface of host **C** section of ascoma **D** peridium **E** paraphyses **F, G** ascus apex with a J+, apical ring (stained in Melzer's reagent) **H–K** asci with ascospores **L–O** ascospores surrounded by a wide mucilaginous sheath (O stained in India ink). Scale bars: 300 μm (**B**); 50 μm (**C**); 5 μm (**D–O**).

phylogeny, *A. australis* is introduced as a new species. Here, we need to explain the name of *A. serrulata*. Although Index Fungorum (02/07/2022) shows that the current name of *A. serrulata* is *Roussoella serrulata* (Ellis & G. Martin) K.D. Hyde & Aptroot, we have not found relevant literature. Hyde (1996) renamed *Didymosphaeria serrulota* Eltis & G. Martin and *Roussoella serrulata* as synonyms of *A. serrulata* (Ellis & G. Martin) K.D. Hyde. *Arecophila serrulata* was erected with the unitunicate asci with a blue-staining ring (Hyde 1996) which is clearly inconsistent with the morphological features of *Roussoella* Sacc. Therefore, we still compare with the original description of *A. serrulata* in this article.

Arecophila clypeata **Q.R. Li, J.C. Kang & K.D. Hyde, sp. nov.**
MycoBank No: 836167
Fig. 3

Diagnosis. *Arecophila clypeata* differs from similar species by its ascomata with clypeus and ascospores (18.5–22.5 × 6.5–9 μm).

Holotype. China, Yunnan Province, Kunming City, Kunming Botanical Garden (25°8'51"N, 102°44'57"E), on dead culm of gramineous plant, 20 March 2014, Q.R. Li, kib21 (***holotype***: GZUH0110; ***isotype*****:** GACP QR0173; **ex-type** living cultures: GZUCC0110).

Etymology. In reference to the clypeus.

Description. Saprobic on dead stem of a gramineous. **Sexual morph**: *Ascomata* 367–448 × 278–363 μm ($\bar{x}$= 403 × 323 μm, n = 8), immersed under a black clypeus, solitary, slightly raised, dome-shaped areas, scattered or gregarious, subglobose to globose, with a central, erumpent, cone-shaped papilla, in vertical section. *Ostioles* papillate on the centre, black. *Peridium* 15–30 μm ($\bar{x}$= 25 μm, n = 10) wide, comprising several layers, outer layer brown, thick-walled angular cells, inner layer hyaline. *Paraphyses* 3–5 μm ($\bar{x}$= 4 μm, n =15) wide, hyaline, unbranched, septate. *Asci* 180–245 × 10.5–14.5 μm ($\bar{x}$= 215.5 × 12 μm, n=20), 8-spored, unitunicate, long-cylindrical, short-pedicellate, apically rounded, with a square-shaped, J+, apical ring, 3–4 × 3–4 μm. *Ascospores* 18.5–22.5 × 6.5–9 μm ($\bar{x}$= 20.5 × 7.5 μm, n = 30), overlapping uniseriate, 2-celled, light brown to brown, equilateral ellipsoidal, constricted at the septum, longitudinal, sulcate along the entire spore length, faint, surrounded by a mucilaginous sheath, lacking germ slits and appendages. **Asexual morph**: undetermined.

Culture characteristics. Colonies on PDA, reached 3 cm diam. after one week at 25 °C, white, cottony, flat, low, dense, with slightly wavy margin; fructifications were not observed in culture.

Known distribution. China

Additional material examined. China, Guizhou Province, Buyi and Miao Autonomous Prefecture in southern Guizhou Province, Maolan National Nature Reserve (25°17'17"N, 107°59'1"E), on dead culm of an unidentified gramineous plant, 12 June 2015, Q.R. Li, GZ120 (GACP QR0129; GZUH0127; living cultures, GZUCC0127).

Additional sequences. ACT: MT741737

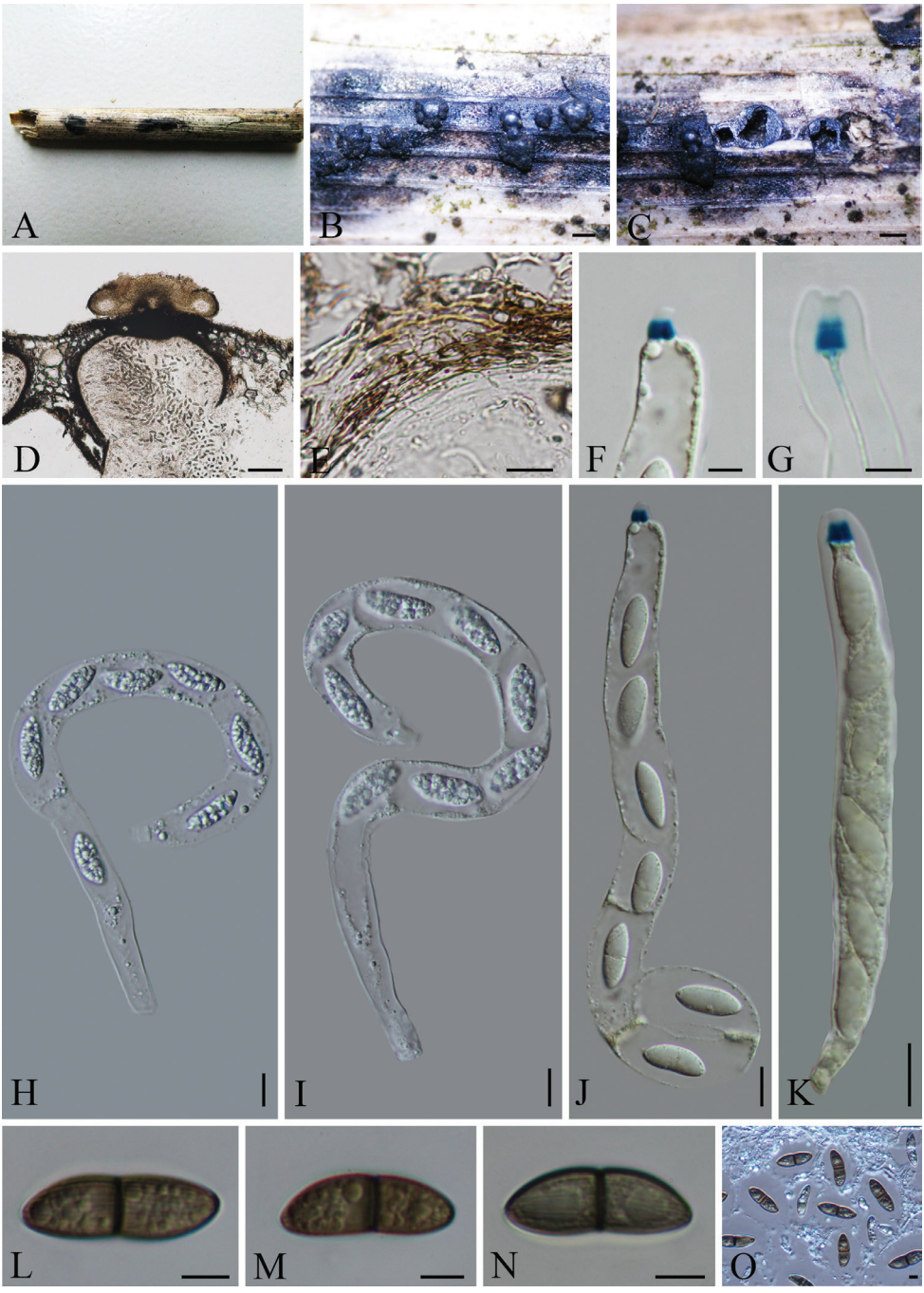

Figure 3. *Arecophila clypeata* (holotype) **A** material **B** ascomata on the surface of host **C, D** section of ascomata **E** peridium **F, G** ascus apex with a J+, apical ring (stained in Melzer's reagent) **H–K** asci with ascospores **L–O** ascospores. Scale bars: 500 μm (**B, C**); 100 μm (**D**); 10 μm (**E, H–K**); 5 μm (**F, G, L–O**).

Notes. *Arecophila clypeata* has long and weakly striate ascospores similar to *A. coronata* (Rehm) Umali & K.D. Hyde, *A. serrulata* (Ellis & G. Martin) K.D. Hyde and *A. bambusae* (Hyde 1996; Umali et al. 1999). However, *A. coronata* does not have a prominent clypeus and has longer and fusiform ascospores. *Arecophila clypeata* differs from *A. serrulata* by the ascomata without a central papilla surrounded by a circle of white tissue, further in having ascospores with wide sheaths (Hyde 1996). *Arecophila clypeata* is similar to *A. bambusae* which, however, has narrower ascospores (19–22.5 × 5.5–7 μm) covered by the strong striations and has ascomata without a central papilla surrounded by a black corolla protuberance (Umali et al. 1999).

Arecophila gulubiicola **K.D. Hyde, Nova Hedwigia 63(1–2): 91 (1996)**
MycoBank No: 416041
Fig. 4

Description. *Saprobic* on dead trunk of *Gulubia costata* (Becc.) Becc. **Sexual morph:** *Ascomata* 290–400 × 140–190 μm ($\overline{x}$ = 336 × 167 μm, n = 8), immersed under a clypeus, solitary or clustered, in vertical section, lenticular, with a central ostiole. *Clypeus* raised, oval, blackened areas on the host surface, dome-shaped, well-developed and black. *Peridium* 25–35 μm wide, dense, compressed layers of brown-walled, *angular* cells, tightly adhered to the host tissues. *Paraphyses* 2–2.5 μm wide, filamentous, hyaline, septate, branched, tapering distally. *Asci* 107–145 × 11–13.5 μm ($\overline{x}$ = 114.3 × 12.4 μm, n = 15), 8-spored, unitunicate, cylindrical, short-pedicellate, apically rounded, wedge-shaped, J+, subapical ring, 3–4 × 1–2 μm ($\overline{x}$ =3.5 × 1.5 μm, n = 15). *Ascospores* 14.5–18.5 × 6–9 μm ($\overline{x}$ = 17.4 × 6.5 μm, n = 25), overlapping uniseriate, ellipsoidal, brown, 2-celled, septate at the centre, constricted at the septum, longitudinal, sulcate striations along the entire spore length, surrounded by a mucilaginous sheath. **Asexual morph**: Undetermined.

Material examined. Papua New Guinea, Central Province, 08°30'00"N, 147°24'35"E, on dead trunk of *G. costate* (Becc.) Becc. (*Arecaceae*), May 1992, K.D. Hyde, (BRIP 23002a, ***holotype***).

Notes. *Arecophila gulubiicola* has deeply immersed, subglobose to lenticular ascomata with a small or lacking clypeus, cylindrical, short-pedicellate asci with a wedge-shaped, conical, apical ring and ellipsoidal, brown ascospores with wall striations and surrounded by a mucilaginous sheath (Hyde 1996). *Alishanica* has been introduced as a monospecific genus with the type species *Al. miscanthi* Karun. et al. on dead sheaths of *Miscanthus sinensis* (Poaceae) from Taiwan (Hyde et al. 2020). We re-examined both *A. gulubiicola* and *Al. miscanthi* herbarium specimens and observed that they are congeneric. *Alishanica miscanthi* has characters that immersed ascoma under a clypeus, unitunicate, cylindrical asci with a J+ apical ring and brown, 2-celled ascospores with longitudinal wall striations and a mucilaginous sheath which are consistent with the generic characteristics of *Arecophila*. The phylogeny of *Al. miscanthi* was mainly considered by the *A. bambusae* (HKUCC 4794) sequences (Hyde et al.

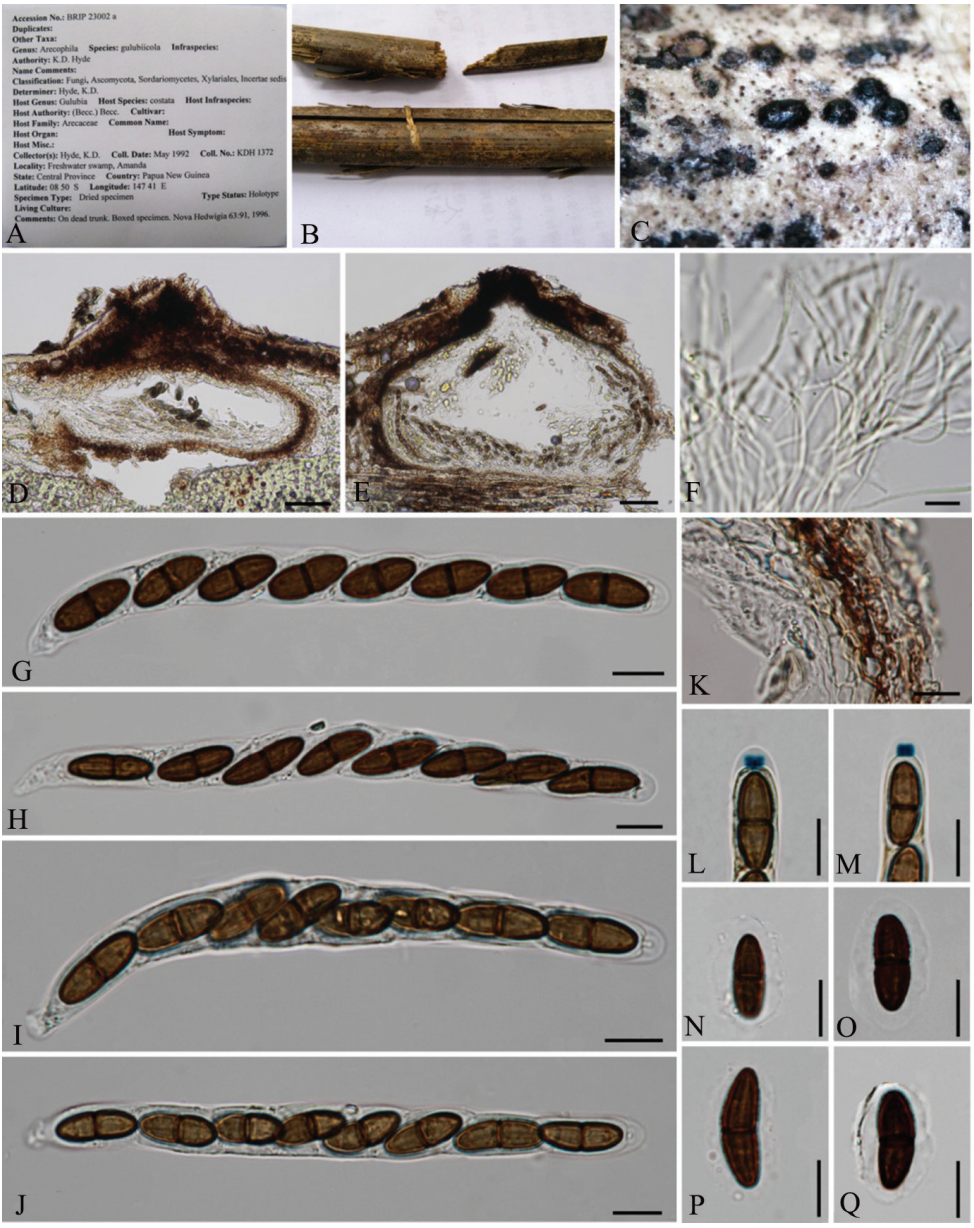

Figure 4. *Arecophila gulubiicola* (BRIP 23002a, holotype) **A, B** herbarium material with label **C** ascomata on the host **D, E** sections of ascomata **F** paraphyses **G–J** asci **K** peridium **L, M** wedge-shaped, J+ apical ring bluing in Melzer's reagent **N–Q** ascospores. Scale bars: 50 µm (**D, E**); 5 µm (**F–Q**).

2020). However, HKUCC 4794 is not the type material of *Arecophila* and cannot be used to represent *Arecophila*. In our phylogeny, HKUCC 4794 forms a distinct clade (Fig. 1; Clade 2) from the *Arecophila* representing the clade. Based on morphology and

phylogeny, we synonymise *Alishanica* under *Arecophila* and *Al. miscanthi* is accepted as an *Arecophila* species. Furthermore, *A. bambusae* needs to be recollected and provided with the phylogenetic affinity in future studies.

***Arecophila miscanthi* (Karun., C.H. Kuo & K.D. Hyde) Q.R Li & J.C. Kang, comb. nov.**
MycoBank No: 839706

≡ *Alishanica miscanthi* Karun., C.H. Kuo & K.D. Hyde [as 'miscanthii'], in Hyde et al., Mycosphere 11(1): 461 (2020)

Description (MFLU 19-2333). *Saprobic* on dead sheaths of *Miscanthus sinensis* (Poaceae). **Sexual morph**: *Ascomata* 272–277 × 283–296 µm ($\bar{x}$ = 275 × 291.5 µm, n = 8), immersed beneath blackened aggregated *clypeus* of the surface of dead sheath, loosely aggregated or rarely solitary; dark brown to black, globose to subglobose, slightly depressed, uniloculate. *Ostiole* 92–110 µm long, 52–56 µm diameter ($\bar{x}$ = 101 × 54 µm, n = 5), centrally erumpent, with periphyses, surrounded by distinct shiny black flanges, the tissue spreading down along the papilla. *Peridium* 51–60 µm wide, comprising 4–5 cell layers of thin-walled, brown cells of *textura angularis*, inwardly lighter. *Paraphyses* filamentous, distinctly septate, embedded in a hyaline gelatinous matrix. *Asci* 147–189 × 10–13 µm ($\bar{x}$ = 167 × 11 µm, n = 30), 8-spored, unitunicate, cylindrical, short pedicellate, slightly truncate at the apex, with a wedge-shaped J+, subapical ring, 3.5–4 µm broad, 2–2.5 µm high. *Ascospores* 20–24 × 6–8 µm ($\bar{x}$ = 22 × 7 µm, n = 40), overlapping, uniseriate, ellipsoidal, slightly tapering at the ends, equally 2-celled and guttulate at both cells, constricted at the septum, brown with striations, surrounded by a thick, hyaline mucilaginous sheath, subglobose, parallel to the margin of the spore. **Asexual morph**: Undetermined.

Material examined. China, Taiwan, Chiayi Province, Ali Mountain, Kwang Hwa, on dead sheaths of *Miscanthus sinensis* (Poaceae), 5 May 2018, A. Karunarathna, AKTW 44 (**MFLU 19-2333**, ***holotype***)

Additional material. China, Yunnan Province, Kunming City, Kunming Botanical Garden (25°8'45"N, 102°44'59"E), on dead culm of monocotyledon, 20 March 2014, Q.R. Li, GZ43 (GZUH0122, GACP QR0201; living cultures, GZUCC0122).

Note. The characteristics of the holotype specimen *Arecophila miscanthi* (≡ *Alishanica miscanthi*) were revised, re-measured and described. *Alishanica miscanthi* is similar to *A. muroiana* and *A. serrulata* (Wang et al. 2004, Hyde et al. 2020). However, no clypeus was observed for *A. muroiana*. *Arecophila serrulata* has larger ascomata (480–560 × 280–320 µm) with a central papilla surrounded by a circle of white tissue (Hyde 1996) which differs from those of *A. miscanthi*. One new collection (GZUH0122, Fig. 5) shows the same traits of *A. miscanthi* (MFLU 19-2333) in having immersed ascomata with clypeus, a wedge-shaped J+, ascus subapical ring, same dimensions of ascospores and here we provide it as a new geographical record from China.

Figure 5. *Arecophila miscanthi* (GZUH0122) **A, B** ascomata on the surface of host **C** paraphyses and asci **D** section of ascoma **E** peridium **F, G** apical rings **H–K** asci with ascospores **M–P** ascospores. Scale bars: 50 μm (**C, D**); 10 μm (**E, F–K**); 5 μm (**L–P**).

Table 2. Synopsis of the species of *Arecophila*.

Species	Host	Clypeus	Ascomata	Asci	Ascal ring	Ascospores	Distribution
A. australis	*Phragmites australis*	Present	420–560 × 290–380 µm, globose to subglobose	140–230 × 15.5–24 µm	4–5 × 2.5–3 µm, trapezoidal, J+	22.5–29 × 8–11 µm, wall striate, mucilaginous sheath	China (Guizhou)
A. bambusae	*Bambusa* sp.	Absent	500–560 × 294–350 µm, globose to subglobose	132.5–140 × 7.5–8 µm	2.5–3 µm in diam., ca. 2.5 µm high, wedge-shaped, J+	19–22.5 × 5.5–7 µm, slightly tapering at the ends, wall striate, mucilaginous sheath	Hong Kong
A. calamicola	*Calamus* sp.	Absent	520 × 390 µm, subglobose	160–190 × 14–20 µm	4-4.8 µm diam., 3.2-4 µm high, wedge-shaped, J+	24–33 × 5.5–9 µm, wall striate, verrucose, mucilaginous sheath	Brunel, Indonesia
A. chamaeropis	*Chamaerops humilis*	Minute	400–700 × 300–400 µm, subglobose	150–190 × 9–10 µm	3.5–4.5 diam., 1.5–2 µm high, wedge-shaped, J+	15–23 × 5.5–7 µm, wall striate, covered by pronounced verrucose ornamentation, mucilaginous sheath	Spain
A. coronata	*Gigantochloa scribneriana*, *Bambusa* sp.	Present	90–100 × 42–105 µm, subglobose or ellipsoidal	132.5–157.5 × 7.5–9 µm	3.5–4 µm in diam., 2–2.5 µm high, wedge-shaped, J+, with a faint canal leading to the apex.	29–31 × 5–5.5 µm, wall faint striate, mucilaginous sheath	Philippines, Hong Kong
A. clypeata	A unknown gramineous plant	Present	367−448 × 278−363 µm, subglobose to globose	180–245 × 10.5–14.5 µm	3–4 × 3–4 µm, square-shaped, J+	18.5–22.5 × 6.5–9 µm, wall striate, mucilaginous sheath	China (Guizhou)
A. deutziae	*Deutziae stamineae*	Absent	400–600 µm diam., globose	180–240 × 16–19 µm	3.5–4. 5 µm diam., 1.5–2 µm high, wedge-shaped, J+	26–32 × 11–13 µm, wall striate	India
A. eugeissonae	*Eugeissona tristis*	Absent	460–520 × 180–260 µm, Subglobose or ellipsoidal	175–220 × 11–16.5 µm	3–4 µm diam., 1.5–2.0 µm high, discoid, J+	25-40 × 6.5–9 µm, wall weakly striate, verrucose, mucilaginous sheath	Malaysia
A. foveata	*Nolinae* sp.	Present	300–400 ×400–500 µm, globose or ovoid	130–150 × 14–15 µm	3–4 µm wide, 4–5 µm high, tubular, J+	16–20 × 8–10 µm, wall striate, foveate, surface aspect of numerous warts	USA
A. gulubiicola	*Gulubia costate*	Present	290–400 × 140–190 µm, subglobose or lenticular	107–145 × 11–13.5 µm	3.2–4 µm diam., 2.4–3.2 µm high, cylindrical, J+	14.5–18.5 × 6–9 µm with a minutely verrucose wall, mucilaginous sheath	Papua New Guinea
A. miscanthi	*Miscanthus sinensis*	Present	283–296 × 272–277 µm, globose to subglobose	147–189 × 10–13 µm	3.5–4 µm broad, 2–2.5 µm high, wedge-shaped, J+	20–24 × 6–8 µm, wall striate, mucilaginous sheath.	China (Taiwan, Yunnan)
A. muroiana	*Phyllostachys bambusoides*	Absent	350–460 × 320–400 µm, globose	125–165 × 10–12 µm	3.5–4 µm diam., 2–2.5 µm high, wedge-shaped, J+	20–25 × 6–7.5 µm, wall finely striate, mucilaginous sheath	Japan

Species	Host	Clypeus	Ascomata	Asci	Ascal ring	Ascospores	Distribution
A. notabilis	*Calamus*, *Bamboo*	Present	400 × 360 µm, subglobose	180–220 × 11–14 µm	4–4.45 µm diam., 3–4.5 µm high, wedge-shaped, J+	20–26 × 6–8 µm, wall striate, finely verrucose, mucilaginous sheath	Brunei, Hong Kong, Indonesia
A. nypae	*Nypa fruticans*	Absent	400–500 µm diam., subglobose	140–205 × 11–13 µm	4.5 µm diam., 2.5–4 µm high, wedge-shaped, J+	19–26 × 7–8 µm, wall striate, mucilaginous sheath	Malaysia
A. saccharicola	*Sacchari officinarum*	Absent	420–525 × 350–420 µm high	140–16 × 7–10 µm	Not blued by Melzer's reagent	20–24 × 6–8 µm, wall smooth or striated	Jamaica
A. serrulata	*Korthalsia* sp., *Sabal* sp., *Serenoa* sp.	Present	480–560 × 280–320 µm, conical with flattened base	110–112 × 10–12 µm,	3.2 µm diam., 2.4 µm high, wedge-shaped, J+	17–26 × 7–9.5 µm, wall striate, mucilaginous sheath	Brunei, USA, Florida

Discussion

Arecophila shares similar morphology to *Atrotorquata*, *Cainia* and *Seynesia* in having immersed ascomata and 2-celled ascospores (Hyde 1996). *Arecophila*, *Atrotorquata*, *Cainia* and *Seynesia* are accepted in *Cainiaceae* with newly-introduced genera, such as *Amphibambusa* and *Longiappendispora* (Mapook et al. 2020). *Cainia* has similar characteristics to *Arecophila* in its occurrence on monocotyledons, having asci with J+, apical rings and brown 2-celled ascospores (Kohlmeyer and Volkmann-Kohlmeyer 1993). The ascospores of *Cainia* are provided with several longitudinal germ slits and differ from those of *Arecophila*, where the ascospores are provided with ridges or a verrucose wall and lack germ slits. *Seynesia* produces ascospores that are smooth-walled and surrounded by mucilaginous sheaths that are drawn out at the poles with germ slits, which differ from *Arecophila* (Hyde 1995). *Amphibambusa* possesses hyaline ascospores pointed at both ends, which differs from that of *Arecophila* (Liu et al. 2015). The phylogenetic tree (Fig. 1) displays that *Arecophila miscanthi* (≡ *Alishanica miscanthi*) clusters in the *Arecophila* group with high support values (100%/1.00 PP). *Longiappendispora* possesses ascospores with longitudinal striations and bristle-like polar appendages at both ends, without a gelatinous sheath, which differentiates it from other genera in *Cainiaceae*. Ascospores of *Atrotorquata* are provided with several longitudinal germ slits and differ from those of *Arecophila* (Kohlmeyer and Volkmann-Kohlmeyer 1993). At present, 16 *Arecophila* species have been described and a summary of each species are given in the Table 2.

The combined ITS, LSU, *rpb*2 and β-tubulin phylogeny (Fig. 1) showed two clades of *Arecophila* as Clade 1 and Clade 2. The *Arecophila* differs from *Amphibambusa* and *Cainia* (see above). The sequence from the holotype of *Atrotorquata spartii* is noticeably clustered with *Coniocessia* spp. in *Coniocessiaceae* (Fig. 1). However, *Atrotorquata spartii* showed a close affinity with *Cainia* spp. in *Cainiaceae*, based on analysis of the combined LSU and ITS sequence alignment in Senanayake et al. (2015). *Atrotorquata* has similar characteristics to *Arecophila* and other genera of *Cainiaceae* (Hyde 1996). Hence, there should be more evidence to reassess *Atrotorquata* in the future. The unitunicate asci with a J+ apical ring in Melzer's regent and brown ascospores covered with longitudinal wall striations, without germ slits can clearly distinguish *Arecophila* from its similar genera. In addition, a table including synopsis of the species of *Arecophila* is provided.

Acknowledgements

We would like to thank the curator of BRIP for the loan of fungal material. This research was supported by the National Natural Science Foundation of China (32000009 and 31960005); the Open Fund Program of Engineering Research Center of Southwest Bio-Pharmaceutical Resources, Ministry of Education, Guizhou University No. GZUKEY20160; the Fund of the Science and Technology Foundation of Guizhou Province ([2020]1Y059); Guizhou Provincial Academician

Workstation of Microbiology and Health (No. [2020]4004); International Science and Technology Cooperation Base of Guizhou Province ([2020]4101); the Fund of High-Level Innovation Talents [No. 2015-4029], the Base of International Scientific and Technological Cooperation of Guizhou Province [No. [2017]5802].

References

Bhattacharya D, Lutzoni F, Reeb V, Simon D, Nason J, Fernandez F (2000) Widespread occurrence of spliceosomal introns in the rDNA genes of ascomycetes. Molecular Biology and Evolution 17(12): 1971–1984. https://doi.org/10.1093/oxfordjournals.molbev.a026298

Cheewangkoon R, Groenewald JZ, Summerell BA, Hyde KD, To-anun C, Crous PW (2009) *Myrtaceae*, a cache of fungal biodiversity. Persoonia - Molecular Phylogeny and Evolution of Fungi 23(23): 55–85. https://doi.org/10.3767/003158509X474752

Chomnunti P, Hongsanan S, Aguirre-Hudson B, Tian Q, Peršoh D, Dhami MK, Alisa AS, Xu JC, Liu XZ, Stadler M, Hyde KD (2014) The sooty moulds. Fungal Diversity 66(1): 1–36. https://doi.org/10.1007/s13225-014-0278-5

Crous PW, Summerell BA, Shivas RG, Romberg M, Mel'nik VA, Verkley GJM, Groenewald JZ (2011) Fungal Planet description sheets: 92–106. Persoonia. Molecular Phylogeny and Evolution of Fungi 27(1): 130–162. https://doi.org/10.3767/003158511X617561

Crous PW, Wingfield MJ, Guarro J, Cheewangkoon R, van der Bank M, Swart WJ, Stchigel AM, Cano-Lira JF, Roux J, Madrid H, Damm U, Wood AR, Shuttleworth LA, Hodges CS, Munster M, de Jesús Yáñez-Morales M, Zúñiga-Estrada L, Cruywagen EM, De Hoog GS, Silvera C, Najafzadeh J, Davison EM, Davison PJN, Barrett MD, Barrett RL, Manamgoda DS, Minnis AM, Kleczewski NM, Flory SL, Castlebury LA, Clay K, Hyde KD, Maússe-Sitoe SND, Chen S, Lechat C, Hairaud M, Lesage-Meessen L, Pawłowska J, Wilk M, Śliwińska-Wyrzychowska A, Mętrak M, Wrzosek M, Pavlic-Zupanc D, Maleme HM, Slippers B, Mac Cormack WP, Archuby DI, Grünwald NJ, Tellería MT, Dueñas M, Martín MP, Marincowitz S, de Beer ZW, Perez CA, Gené J, Marin-Felix Y, Groenewald JZ (2013) Fungal Planet description sheets: 154–213. Persoonia 31(4): 188–296. https://doi.org/10.3767/003158513X675925

Crous PW, Wingfield MJ, Schumacher RK, Summerell BA, Giraldo A, Gené J, Guarro J, Wanasinghe DN, Hyde KD, Camporesi E, Garethjones EB, Thambugala KM, Malysheva EF, Malysheva VF, Acharya K, Álvarez J, Alvarado P, Assefa A, Barnes CW, Bartlett JS, Blanchette RA, Burgess TI, Carlavilla JR, Coetzee MPA, Damm, U, Decock CA, Denbreeÿen A, Devries B, Dutta AK, Holdom DG, Rooney-Latham S, Manjón JL, Marincowitz S, Mirabolfathy M, Moreno G, Nakashima C, Papizadeh M, Shahzadehfazeli SA Amoozegar MA, Romberg MK Shivas RG, Stalpers JA, Stielow B, Stukely MJC, Swart WJ, Tan YP, Vanderbank M, Wood AR, Zhang Y, Groenewald JZ (2014) Fungal Planet description sheets: 281–319. Persoonia. Molecular Phylogeny and Evolution of Fungi 33(1): 212–289. https://doi.org/10.3767/003158514X685680

Crous PW, Wingfield MJ, Guarro J, Hernández-Restrepo M, Sutton DA, Acharya K, Barber PA, Boekhout T, Dimitrov RA, Dueñas M, Dutta AK, Gené J, Gouliamova

DE, Groenewald M, Lombard L, Morozova OV, Sarkar J, Smith MTH, Stchigel AM, Wiederhold NP, Alexandrova AV, Antelmi I, Armengol J, Barnes I, Cano-Lira JF, Ruiz RF, Castañeda Contu M, Courtecuisse PrR, da Silveira AL, Decock CA, de Goes A, Edathodu J, Ercole E, Firmino AC, Fourie A, Fournier J, Furtado EL, Geering ADW, Gershenzon J, Giraldo A, Gramaje D, Hammerbacher A, He X-L, Haryadi D, Khemmuk W, Kovalenko AE, Krawczynski R, Laich F, Lechat C, Lopes UP, Madrid H, Malysheva EF, Marín-Felix Y, Martín MP, Mostert L, Nigro F, Pereira OL, Picillo B, Pinho DB, Popov ES, Peláez CA, Rodas Rooney-Latham S, Sandoval-Denis M, Shivas RG, Silva V, Stoilova-Disheva MM, Telleria MT, Ullah C, Unsicker SB, van der Merwe NA, Vizzini A, Wagner HG, Wong PTW, Wood AR, Groenewald JZ (2015) Fungal Planet description sheets: 320–370. Persoonia Molecular Phylogeny and Evolution of Fungi 34(1): 167–266. https://doi.org/10.3767/003158515X688433

Crous PW, Wingfield MJ, Burgess TI, Carnegie AJ, St J Hardy GE, Smith D, Summerell BA, Cano-Lira JF, Guarro J, Houbraken J, Lombard L, Martín MP, Sandoval-Denis M, Alexandrova AV, Barnes CW, Baseia IG, Bezerra JDP, Guarnaccia V, May TW, Hernández-Restrepo M, Stchigel AM, Miller AN, Ordoñez ME, Abreu VP, Accioly T, Agnello C, Agustincolmán A, Albuquerque CC, Alfredo DS, Alvarado P, Araújo-Magalhães GR, Arauzo S, Atkinson T, Barili A, Barreto RW, Bezerra JL (2017) Fungal Planet description sheets: 625–715. Persoonia. Molecular Phylogeny and Evolution of Fungi 39: 270–467. https://doi.org/10.3767/persoonia.2017.39.11

Crous PW, Carnegie AJ, Wingfield MJ, Sharma R, Mughini G, Noordeloos ME, Santini A, Shouche YS, Bezerra JDP (2019) Fungal Planet description sheets: 868–950. Persoonia. Molecular Phylogeny and Evolution of Fungi 42: 291–473. https://doi.org/10.3767/persoonia.2019.42.11

Dai DQ, Jiang HB, Tang LZ, Bhat DJ (2016) Two new species of *Arthrinium* (*Apiosporaceae*, *Xylariales*) associated with bamboo from Yunnan, China. Mycosphere: Journal of Fungal Biology 7(9): 1332–1345. https://doi.org/10.5943/mycosphere/7/9/7

Dai DQ, Phookamsak R, Wijayawardene NN, Li WJ, Bhat DJ, Xu JC, Taylor JE, Hyde KD, Chukeatirote E (2017) Bambusicolous fungi. Fungal Diversity 82(1): 1–105. https://doi.org/10.1007/s13225-016-0367-8

Daranagama DA, Camporesi E, Tian Q, Liu XZ, Chamyuang S, Stadler M, Hyde KD (2015) *Anthostomella*, is polyphyletic comprising several genera in *Xylariaceae*. Fungal Diversity 73(1): 203–238. https://doi.org/10.1007/s13225-015-0329-6

García D, Stchigel AM, Cano J, Calduch M, Hawksworth D, Guarro J (2006) Molecular phylogeny of *Coniochaetales.* Mycological Progress 110(11): 1271–1289. https://doi.org/10.1016/j.mycres.2006.07.007

Giraldo A, Crous PW, Schumacher RK, Cheewangkoon R, Ghobad-Nejhad M, Langer E (2017) The Genera of Fungi-G3: *Aleurocystis*, *Blastacervulus*, *Clypeophysalospora*, *Licrostroma*, *Neohendersonia* and *Spumatoria.* Mycological Progress 16(4): 325–348. https://doi.org/10.1007/s11557-017-1270-8

Glez-Peña D, Gómez-Blanco D, Reboiro-Jato M, Fdez-Riverola F, Posada D (2010) ALTER: program-oriented conversion of DNA and protein alignments. Nucleic Acids Research 38 (suppl_2): W14–W18. https://doi.org/10.1093/nar/gkq321

Hall TA (1999) BioEdit: A user-friendly biological sequence alignment editor and analysis program for Windows 95/98/NT. Nucleic Acids Symposium Series 41: 95–98.

Hsieh HM, Ju YM, Rogers JD (2005) Molecular phylogeny of *Hypoxylon* and closely related genera. Mycologia 97(4): 914–923. https://doi.org/10.1080/15572536.2006.11832776

Hyde KD (1995) Fungi from palms. XXI. The genus *Seynesia.* Sydowia 47: 199–212.

Hyde KD (1996) Fungi from palms. XXIX. *Arecophila* gen. nov. (Amphisphaeriaceae, Ascomycota), with five new species and two new combinations. Nova Hedwigia 63(1/2): 81–100.

Hyde KD, Norphanphoun C, Maharachchikumbura SSN, Bhat DJ, Jones EBG, Bundhun D, Chen YJ, Bao DF, Boonmee S, Calabon MS, et al. (2020) Refined families of *Sordariomycetes.* Mycosphere 11(1): 305–1059. https://doi.org/10.5943/mycosphere/11/1/7

Jaklitsch WM, Voglmayr H (2012) Phylogenetic relationships of five genera of *Xylariales* and *Rosasphaeria* gen. nov. (*Hypocreales*). Fungal Diversity 52(1): 75–98. https://doi.org/10.1007/s13225-011-0104-2

Jaklitsch WM, Fournier J, Rogers JD, Voglmayr H (2014) Phylogenetic and taxonomic revision of *Lopadostoma.* Persoonia 32(2): 52–82. https://doi.org/10.3767/003158514X679272

Jaklitsch WM, Gardiennet A, Voglmayr H (2016) Resolution of morphology-based taxonomic delusions: *Acrocordiella*, *Basiseptospora*, *Blogiascospora*, *Clypeosphaeria*, *Hymenopleella*, *Lepteutypa*, *Pseudapiospora*, *Requienella*, *Seiridium* and *Strickeria.* Persoonia 37(1): 82–105. https://doi.org/10.3767/003158516X690475

Jeewon R, Liew ECY, Hyde KD (2003) Molecular systematics of the *Amphisphaeriaceae* based on cladistic analyses of partial LSU rDNA gene sequences. Mycological Research 107(12): 1392–1402. https://doi.org/10.1017/S095375620300875X

Kang JC, Hyde KD, Kong RYC (1999) Studies on *Amphisphaeriales*: The *Cainiaceae.* Mycological Research 103(12): 1621–1627. https://doi.org/10.1017/S0953756299001264

Katoh K, Rozewicki J, Yamada KD (2019) MAFFT online service: Multiple sequence alignment, interactive sequence choice and visualization. Briefings in Bioinformatics 20(4): 1160–1166. https://doi.org/10.1093/bib/bbx108

Kohlmeyer J, Volkmann-Kohlmeyer B (1993) *Atrotorquata* and *Loratospora*. New ascomycete genera on *Juncas roemeranus.* Systema Ascomycetum 12: 7–23.

Konta S, Hongsanan S, Tibpromma S, Thongbai B, Maharachchikumbura SSN, Bahkali AH, Hyde KD, Boonmee S (2016) An advance in the endophyte story: *Oxydothidaceae* fam. nov. with six new species of *Oxydothis.* Mycosphere 7(9): 1425–1446. https://doi.org/10.5943/mycosphere/7/9/15

Li QR, Kang JC, Hyde KD (2015) A multiple gene genealogy reveals the phylogenetic placement of *Iodosphaeria tongrenensis* sp nov in *Iodosphaeriaceae* (*Xylariales*). Phytotaxa 234(2): 121–132. https://doi.org/10.11646/phytotaxa.234.2.2

Lin CG, Hyde KD, Saisamorn L, Mckenzie HCE (2017) Beltrania-like taxa from Thailand. Cryptogamie. Mycologie 38(3): 301–319. https://doi.org/10.7872/crym/v38.iss3.2017.301

Liu YL, Whelen S, Hall BD (1999) Phylogenetic relationships among *ascomycetes*: Evidence from an RNA polymerase II subunit. Molecular Biology and Evolution 16(12): 1799–1808. https://doi.org/10.1093/oxfordjournals.molbev.a026092

Liu JK, Phookamsak R, Jones EBG, Zhang Y, Ko-Ko TW, Hu HL, Boonmee S, Doilom M, Chukeatirote E, Bahkali AH, Wang Y, Hyde KD (2011) *Astrosphaeriella* is polyphyletic,

with species in *Fissuroma* gen. nov., and *Neoastrosphaeriella* gen. nov. Fungal Diversity 51(1): 135–154. https://doi.org/10.1007/s13225-011-0142-9

Liu JK, Hyde KD, Jones EBG, Buyck B, Chethana KWT, Dai DQ, Dai YC, Daranagama DA, et al. (2015) Fungal diversity notes 1–110: Taxonomic and phylogenetic contributions to fungal species. Fungal Diversity 72(1): 1–197. https://doi.org/10.1007/s13225-015-0324-y

Liu F, Bonthond G, Groenewald JZ, Cai L, Crous PW (2019) *Sporocadaceae*, a family of coelomycetous fungi with appendage-bearing conidia. Studies in Mycology 92(1): 287–415. https://doi.org/10.1016/j.simyco.2018.11.001

Long QD, Liu LL, Zhang X, Wen TC, Kang JC, Hyde KD, Shen XC, Li QR (2019) Contributions to species of *Xylariales* in China-1. *Durotheca* species. Mycological Progress 18(3): 495–510. https://doi.org/10.1007/s11557-018-1458-6

Mapook A, Hyde KD, Mckenzie EHC, Jones GD, Bhat J, Jeewon R, Stadler M, Samarakoon MC, Malaithong M, Tanunchai B, Buscot F, Wubet T, Purahong W (2020) Taxonomic and phylogenetic contributions to fungi associated with the invasive weed *Chromolaena odorata* (Siam weed). Fungal Diversity 101(1): 1–175. https://doi.org/10.1007/s13225-020-00444-8

Marasinghe DS, Samarakoon MC, Hongsanan S, Boonmee S, Mchenzie EHC (2019) *Iodosphaeria honghense* sp. nov. (*Iodosphaeriaceae*, *Xylariales*) from Yunnan Province, China. Phytotaxa 420(4): 273–282. https://doi.org/10.11646/phytotaxa.420.4.3

McTaggart AR, Grice KR, Shivas RG (2013) First report of *Vialaea minutella* in Australia, its association with mango branch dieback and systematic placement of *Vialaea* in the *Xylariales.* Australasian Plant Disease Notes, Australasian Plant Pathology Society 8(1): 63–66. https://doi.org/10.1007/s13314-013-0096-8

Miller MA, Pfeiffer W, Schwartz T (2010) Creating the CIPRES Science Gateway for inference of large phylogenetic trees. In: Proceedings of the Gateway Computing Environments Workshop (GCE) 2010, New Orleans, Louisiana, 1–8. https://doi.org/10.1109/GCE.2010.5676129

Nylander JAA (2004) MrModeltest v.2. Program distributed by the author. Evolutionary Biology Centre. Uppsala University, Uppsala.

Perera RH, Maharachchikumbura SSN, Jones EBG, Bahkali AH, Elgorban AM, Liu JK, Liu ZY, Hyde KD (2017) *Delonicicola siamense* gen. & sp nov (*Delonicicolaceae* fam. nov. *Delonicicolales* ord. nov.), a saprobic species from *Delonix regia* seed pods. Cryptogamie. Mycologie 38(3): 321–340. https://doi.org/10.7872/crym/v38.iss3.2017.321

Perera RH, Maharachchikumbura SSN, Hyde KD, Bhat DJ, Camporesi E, Jones EBG, Senanayake IC, Ai-Sadi AM, Saichana N, Liu JK, Liu ZY (2018) An appendage-bearing coelomycete *Pseudotruncatella arezzoensis* gen. and sp. nov. (Amphisphaeriales genera incertae sedis) from Italy, with notes on *Monochaetinula.* Phytotaxa 338(2): 177–188. https://doi.org/10.11646/phytotaxa.338.2.2

Pi YH, Zhang X, Liu LL, Long QD, Shen XC, Kang YQ, Hyde KD, Boonmee S, Kang JC, Li QR (2020) Contributions to species of *Xylariales* in China–4. *Hypoxylon wujiangensis* sp. nov. Phytotaxa 455 (1): 021–030. https://doi.org/10.11646/phytotaxa.455.1.3

Rannala B, Yang Z (1996) Probability distribution of molecular evolutionary trees: A new method of phylogenetic inference. Journal of Molecular Evolution 43(3): 304–311. https://doi.org/10.1007/BF02338839

Ronquist F, Huelsenbeck JP (2003) MrBayes 3: Bayesian phylogenetic inference under mixed models. Bioinformatics (Oxford, England) 19(12): 1572–1574. https://doi.org/10.1093/bioinformatics/btg180

Ronquist F, Teslenko M, van der Mark P, Ayres DL, Darling A, Höhna S, Larget B, Liu L, Suchard MA, Huelsenbeck J (2012) MrBayes 3.2: Efficient Bayesian phylogenetic inference and model choice across a large model space. Systematic Biology 61(3): 539–542. https://doi.org/10.1093/sysbio/sys029

Samarakoon MC, Liu JK, Hyde KD, Promputtha I (2019) Two new species of *Amphisphaeria* (*Amphisphaeriaceae*) from northern Thailand. Phytotaxa 391(3): 207–217. https://doi.org/10.11646/phytotaxa.391.3.4

Senanayake IC, Maharachchikumbura SSN, Hyde KD, Bhat JD, Jones EBG, McKenzie EHC, Phookamsak R, Phukhamsakda C, Shenoy BD (2015) Towards unraveling relationships in *Xylariomycetidae* (*Sordariomycetes*). Fungal Diversity 73(1): 73–144. https://doi.org/10.1007/s13225-015-0340-y

Smith GJD, Liew ECY, Hyde KD (2003) The *Xylariales*: A monophyletic order containing 7 families. Fungal Diversity 13: 185–218.

Stamatakis A, Hoover P, Rougemont J (2008) A rapid bootstrap algorithm for the RAxML web servers. Systematic Biology 75(5): 758–771. https://doi.org/10.1080/10635150802429642

Tang AMC, Jeewon R, Hyde KD (2007) Phylogenetic utility of protein (RPB2, β-tubulin) and ribosomal (LSU, SSU) gene sequences in the systematics of *Sordariomycetes* (*Ascomycota*, *Fungi*). Antonie van Leeuwenhoek 91(4): 327–349. https://doi.org/10.1007/s10482-006-9120-8

Thambugala KM, Hyde KD, Tanaka K, Tian Q, Wanasinghe DN, Ariyawansa HA, Jayasiri SC, Boonmee S, Camporesi E, Hashimoto A, Hirayama K, Schumacher RK, Promputtha I, Liu ZY (2015) Towards a natural classification and backbone tree for *Lophiostomataceae*, *Floricolaceae*, and *Amorosiaceae* fam. nov. Fungal Diversity 74(1): 199–266. https://doi.org/10.1007/s13225-015-0348-3

Trouillas FP, Gubler WD (2010) Host range, biological variation, and phylogenetic diversity of *Eutypa lata* in California. Phytopathology 100(10): 1048–1056. https://doi.org/10.1094/PHYTO-02-10-0040

Umali TE, Hyde KD, Quimio TH (1999) *Arecophila bambusae* sp. nov. and *A. coronata* comb. nov., from dead culms of bamboo. Mycoscience 40(2): 185–188. https://doi.org/10.1007/BF02464296

Vilgalys R, Hester M (1990) Rapid genetic identification and mapping of enzymatically amplified ribosomal DNA from several *Cryptococcus* species. Journal of Bacteriology 172(8): 4238–4246. https://doi.org/10.1128/jb.172.8.4238-4246.1990

Voglmayr H, Friebes G, Gardiennet A, Jaklitsch WM (2018) *Barrmaeli*a, and *Entosordaria*, in *Barrmaeliaceae* (fam. nov. *Xylariales*) and critical notes on Anthostomella-like genera based on multigene phylogenies. Mycological Progress 17(1-2): 155–177. https://doi.org/10.1007/s11557-017-1329-6

Voglmayr H, Aguirre-Hudson MB, Wagner HG, Tello S, Jaklitsch WM (2019) Lichens or endophytes? The enigmatic genus *Leptosillia* in the *Leptosilliaceae* fam. nov. (*Xylariales*), and *Furfurella* gen. nov. (*Delonicicolaceae*). Persoonia 42(1): 228–260. https://doi.org/10.3767/persoonia.2019.42.09

Vu D, Groenewald M, de Vries M, Gehrmann T, Stielow B, Eberhardt U, Al-Hatmi A, Groenewald JZ, Cardinali G, Houbraken J, Boekhout T, Crous PW, Robert V, Verkley GJM (2019) Large-scale generation and analysis of filamentous fungal DNA barcodes boosts coverage for kingdom fungi and reveals thresholds for fungal species and higher taxon delimitation. Studies in Mycology 92(1): 135–154. https://doi.org/10.1016/j.simyco.2018.05.001

Wang YZ, Aptroot A, Hyde KD (2004) Revision of the genus *Amphisphaeria*. Hong Kong SAR, China. Fungal Diversity Research Series 13: 1–168.

Wang XW, Houbraken J, Groenewald JZ, Meijer M, Andersen B, Nielsen KF, Crous PW, Samson RA (2016) Diversity and taxonomy of *Chaetomium* and chaetomium-like fungi from indoor environments. Studies in Mycology 84(C): 145–224. https://doi.org/10.1016/j.simyco.2016.11.005

Wendt L, Benjamin E, Kuhnert SE, Heitkämper S, Lambert C, Hladki AI, Romero AI, Luangsa-ard JJ, Srikitikulchai P, Peršoh D, Stadler M (2018) Resurrection and emendation of the *Hypoxylaceae*, recognised from a multigene phylogeny of the *Xylariales.* Mycological Progress 17(1–2): 115–154. https://doi.org/10.1007/s11557-017-1311-3

White TJ, Bruns T, Lee S, Taylor JW (1990) Amplification and direct sequencing of fungal ribosomal RNA genes for phylogenetics. PCR protocols: a guide to methods and applications. Academic Press, San Diego, California, 315–322. https://doi.org/10.1016/B978-0-12-372180-8.50042-1

Wijayawardene DNN, Song Y, Bhat DJ, McKenzie EHC, Chukeatirote E, Wang Y, Hyde KD (2013) *Wojnowicia viburni* sp. nov. from China and its phylogenetic placement. Sydowia 65: 181–190.

Wijayawardene NN, Hyde KD, Al-Ani LKT, Tedersoo L, Haelewaters D, Rajeshkumar KC, Zhao RL, Aptroot A, Leontyev DV, Saxena RK, et al. (2020) Outline of Fungi and fungi-like taxa. Mycosphere 11(1): 1060–1456. https://doi.org/10.5943/mycosphere/11/1/8

Xie X, Liu LL, Zhang X, Long QD, Shen XC, Boonmee S, Kang JC, Li QR (2019) Contributions to species of *Xylariales* in China–2. *Rosellinia pervariabilis* and *R. tetrastigmae* spp. nov., and a new record of *R. caudata.* Mycotaxon 134(1): 183–196. https://doi.org/10.5248/134.183

Xie X, Liu LL, Shen XC, Kang YQ, Hyde KD, Kang JC, Li QR (2020) Contributions to species of *Xylariales* in China-3. *Collodiscula tubulosa* (*Xylariaceae*). Phytotaxa 428(2): 122–130. https://doi.org/10.11646/phytotaxa.428.2.6

Zhang N, Castlebury LA, Miller AN, Huhndorf SM, Schoch CL, Seifert KA, Rossman AY, Rogers JD, Kohlmeyer J, Volkmann-Kohlmeyer B, Sung G-H (2006) An overview of the systematics of the *Sordariomycetes* based on a four-gene phylogeny. Mycologia 98(6): 1076–1087. https://doi.org/10.1080/15572536.2006.11832635

MycoKeys 88: 151–170 (2022)
doi: 10.3897/mycokeys.88.80068
https://mycokeys.pensoft.net

RESEARCH ARTICLE

A peer-reviewed open-access journal
MycoKeys
Launched to accelerate biodiversity research

Two new *Clitocella* species from North China revealed by phylogenetic analyses and morphological characters

Ning Mao[1*], Jing-Chong Lv[1*], Yu-Yan Xu[1], Tao-Yu Zhao[1], Li Fan[1]

1 *College of Life Science, Capital Normal University, Xisanhuanbeilu 105, Haidian, Beijing 100048, China*

Corresponding author: Li Fan (fanli@mail.cnu.edu.cn)

Academic editor: Rui-Lin Zhao | Received 4 January 2022 | Accepted 2 April 2022 | Published 13 April 2022

Citation: Mao N, Lv J-C, Xu Y-Y, Zhao T-Y, Fan L (2022) Two new *Clitocella* species from North China revealed by phylogenetic analyses and morphological characters. MycoKeys 88: 151–170. https://doi.org/10.3897/mycokeys.88.80068

Abstract

Two new species of *Clitocella* are proposed based on morphological and phylogenetic investigations. *Clitocella borealichinensis* **sp. nov.** is closely related to *C. orientalis* but distinguished from the latter by its slightly smaller basidiospores and hyphae of pileipellis with pale brown to brown intracellular or parietal pigment. *Clitocella colorata* **sp. nov.** is closely related to *C. popinalis* and *C. mundula* in macromorphology but is differentiated from *C. popinalis* by its slightly smaller basidiospores and the difference in genetic profile, and from *C. mundula* by its relatively colorful pileus (white to yellowish white, grayish white to grayish brown, pink white). Phylogenetic analyses based on sequence data from five different loci (ITS, nrLSU, *tef1*, *rpb2* and *atp6*) support the taxonomic position of the two new species in the genus *Clitocella*. The illustrations and descriptions for the new taxa are provided.

Keywords

Entolomataceae, multigene, phylogeny, taxonomy

Introduction

The genus *Clitocella* Kluting, T.J. Baroni & Bergemann (Entolomataceae, *Agaricales*), with *C. popinalis* (Fr.) Kluting, T.J. Baroni & Bergemann as the type species, was established in 2014 (Kluting et al. 2014). The main characteristics of *Clitocella* are clitocyboid basidiomata, narrow and crowded, long-decurrent lamellae, central to eccentric stipe, thin-walled

* These authors contributed equally to this work.

(<0.5 μm) basidiospores with undulate pustules or minute bumps, clamp connections absent. (Baroni 1981; Kluting et al. 2014; Jian et al. 2020). Previous studies show that *Clitocella* is phylogenetically closely related to the genera *Clitopilus* (Fr. ex Rabenh.) P. Kumm. and *Clitopilopsis* Maire. *Clitopilus* differs from *Clitocella* in its longitudinally ridged basidiospore ornamentation, and *Clitopilopsis* in its basidiospores with thickened walls (0.5–0.9 μm) and obscure irregular rounded angles of the basidiospores in polar view (Kluting et al. 2014; Baroni et al. 2020; Jian et al. 2020). There are 10 accepted species in *Clitocella* (Index Fungorum, http://www.Indexfungorum.org/; accessed date: 19 November 2021).

In China, the species diversity of *Clitocella* is scarce and only two species are described (Jian et al. 2020). Recently, several specimens of *Clitocella* were collected when we investigated the macrofungi in Shanxi province, North China. The morphological examination and phylogenetic analysis for these collections revealed that they represented three taxa of *Clitocella*, including two new species. The aim of this paper is to describe the new species and provide the DNA data to confirm the presence in China of a previously described species.

Materials and methods

Morphological studies

Collections were obtained and photographed in the field from Shanxi regions in China, and then dried in a fruit drier at 40–50 °C and deposited in BJTC herbarium (Capital Normal University, Beijing, China). The sizes of basidiomata (pileal width) used in this study are as follows: small: <30 mm; medium-sized: 30–50 mm; large: >50 mm. Standardised color values were obtained from ColorHexa (http://www.colorhexa.com/). Microscopic characters were observed in sections obtained from dry specimens mounted in 3% KOH, Congo Red, or Melzer's reagent (Dring 1971). For scanning electron microscopy (SEM), basidiospores were scraped from the dried gleba, placed onto double-sided tape that was mounted directly on the SEM stub, coated with platinum-palladium film of 8 nm thick using an ion-sputter coater (HITACHI E-1010), and examined with a HITACHI S-4800 SEM. The term "[n/m/p]" means n basidiospores from m basidiomata of p collections. Dimensions of basidiospores are given using the following format '(a–)b–c(–d)', where the range 'b–c' represents at least 90% of the measured values, and 'a' and 'd' are the most extreme values. L_m and W_m indicate the average basidiospore length and width (± standard deviation) for the measured basidiospore, respectively. 'Q' refers to the length/width ratio of basidiospores in side-view; 'Q_{av}' refers to the average Q of all basidiospores ±standard deviation.

DNA extraction, PCR amplification and DNA sequencing

Dried basidiomata were crushed by shaking for 45 s at 30 Hz 2–4 times (Mixer Mill MM301, Retsch, Haan, Germany) in a 1.5 mL tube together with a 3 mm diam tungsten carbide ball. Total genomic DNA was extracted from the powdered basidiomata using

NuClean Plant Genomic DNA Kit (CWBIO, China), following the manufacturer's instructions. Primers ITS1F and ITS4 were employed for the ITS (White et al. 1990; Gardes and Bruns 1993), while LR0R and LR5 for nrLSU (Vilgalys and Hester 1990), EF1-983F and EF1-1953R for the *tef1* (Rehner 2001), bRPB2-6F and bRPB2-7R2 for the *rpb2* (Liu et al. 1999; Matheny 2005; Matheny et al. 2007), and ATP6-3 and ATP6-6r for the *atp6* (Kretzer and Bruns 1999; Binder and Hibbett 2003). Polymerase chain reactions (PCR) for ITS region, nrLSU region, *tef1* gene, *rpb2* gene and *atp6* gene were performed in 25 μL reaction containing 2 μL DNA template, 1 μL primer (10 μM) each, 12.5 μL of 2× Master Mix [Tiangen Biotech (Beijing) Co.], 8.5 μL ddH_2O.

PCR reactions were implemented as follows: an initial denaturation at 94 °C for 5 min, then to 35 cycles of the following denaturation at 94 °C for 30 s, annealing at 52 °C for 45 s (ITS), 60 s (nrLSU), 72 °C for 1 min; and a final extension at 72 °C for 10 min. Amplification of *rpb2* and *tef1* sequences followed Kluting et al. (2014), which entailed a touchdown protocol: an initial incubation of 94 °C for 5 min; 12 cycles of 94 °C for 1 min, 67 °C for 1 min, decreasing 1 °C each cycle, and 72 °C for 1.5 min; 36 cycles of 94 °C for 45 s, 55 °C for 1 min, and 72 °C for 1.5 min; and a final extension period at 72 °C for 7 min. Sequences of the *atp6* were amplified with a cycling protocol of 95 °C for 5 min, followed by 40 cycles at 95 °C for 30 s, 42 °C for 2 min, and 72 °C for 1 min, and a final extension at 72 °C for 10 min. The PCR products were sent to Beijing Zhongkexilin Biotechnology Co. Ltd. for purification, sequencing, and editing. Validated sequences were deposited in the NCBI database (http://www.ncbi.nlm.nih.gov/). Other sequences of *Clitocella* and related species were mainly selected from those used by previous studies (Kluting et al. 2014; Vizzini et al. 2016; Baroni et al. 2020; Jian et al. 2020). The accession numbers of all sequences employed are provided in Table 1.

Phylogenetic analyses

The combined nrLSU-*rpb2-tef1-atp6* dataset and ITS dataset were compiled to identify new species and to investigate their phylogenetic position in *Clitocella*. For the combined nrLSU-*rpb2-tef1-atp6* dataset, *Clitopilopsis albida* S.P. Jian & Zhu L. Yang was chosen as outgroups for individual (nrLSU, *rpb2*, *tef1*, *atp6*) or combined analyses (Jian et al. 2020). For ITS dataset *Mycena pura* (Pers.) P. Kumm. was selected as outgroup taxon (Baroni et al. 2020). The sequences of each marker (ITS, nrLSU, *rpb2*, *tef1*, *atp6*) were independently aligned in MAFFT v.7.110 (Katoh and Standley 2013) under default parameters. Ambiguously aligned sites were identified by Gblocks v.0.91b (Castresana 2000; using default options except "Allowed Gap Positions" = half) with default parameters (For ITS: 1137, nrLSU: 180, *rpb2*: 611, *tef1*: 166, *atp6*: 25 position were deleted). The software BioEdit 7.0.9 (Hall 1999) was used to manually check the aligned sequences. To examine the conflict among topologies with maximum likelihood (ML), separate single-gene analyses were conducted. Sequences were then concatenated. The ITS alignment can be found on Suppl. material 5. For the combined analyses, a partitioned mixed model was used by defining the sequences of nrLSU, *rpb2*, *tef1*, and *atp6* as four independent partitions and each gene was separately estimated by different model parameters. Maximum Likelihood (ML) and Bayesian Inference (BI) analyses were conducted on the resulting concatenated dataset.

Table 1. Specimens used in molecular phylogenetic studies and their GenBank accession numbers. Newly generated sequences are in bold.

Species	Voucher	Locality	GenBank accession No.				
			ITS	nrLSU	*rpb2*	*tef1*	*atp6*
Catathelasma ventricosum	DAOM221514	USA	KP255469	–	–	–	–
Clitocella colorata	**BJTC FM1593**	**China**	**OL966940**	–	–	–	–
Clitocella colorata	**BJTC FM1594**	**China**	**OL966941**	–	–	–	–
Clitocella colorata	**BJTC FM1891**	**China**	**OL966944**	**OL966955**	**OL989914**	**OL989918**	**OL989924**
Clitocella colorata	**BJTC FM1892**	**China**	**OL966945**	**OL966956**	**OL989915**	**OL989919**	**OL989925**
Clitocella colorata	**BJTC FM1952**	**China**	–	**OL966958**	**OL989916**	**OL989920**	**OL989926**
Clitocella fallax	CBS 605.79	–	AF357018	–	–	–	–
Clitocella fallax	CBS 129.63	–	AF357017	AF223166	EF421018	–	–
Clitocella fallax	K(M): 116541	Spain	–	–	KC816938	KC816847	KC816769
Clitocella fallax	O-F88953	Norway	–	–	KC816936	KC816845	KC816767
Clitocella fallax	25668OKM	USA	–	–	KC816937	KC816846	KC816768
Clitocella fallax	ME Noordeloos 1997173	Italy	–	GQ289209	GQ289275	–	–
Clitocella fallax	ME Noordeloos 200367	Slovakia	–	GQ289210	GQ289276	–	–
Clitocella mundula	7161 TJB	USA	–	–	KC816952	KC816862	KC816782
'*Clitocella mundula*'	O-F19454	Norway	–	–	KC816954	KC816864	KC816784
Clitocella mundula	O-F71544	Norway	–	–	KC816950	KC816860	KC816780
'*Clitocella mundula*'	AFTOL-ID 521	USA	–	–	KC816953	KC816863	KC816783
Clitocella mundula	7115 TJB	USA	–	–	KC816951	KC816861	KC816781
Clitocella mundula	K(M): 164736	UK	–	–	KC816949	KC816859	KC816779
'*Clitocella mundula*'	K(M): 49620	UK	–	–	KC816948	KC816858	KC816778
Clitocella mundula	HMJAU 7274	China	–	MN065724	MN148161	MN166272	MN133781
Clitocella mundula	HMJAU 7275	China	–	MN065723	MN148160	MN166271	MN133780
Clitocella mundula	HMJAU 27014	China	–	MN065722	MN148159	MN166270	MN133779
Clitocella borealichinensis	**BJTC FM1618**	**China**	**OL966942**	**OL966946**	**OL989912**	–	**OL989922**
Clitocella borealichinensis	**BJTC FM1781**	**China**	**OL966943**	**OL966957**	**OL989913**	**OL989917**	**OL989923**
Clitocella orientalis	HKAS 75548	China	MN061333	MN065727	MN148164	MN166275	MN133784
Clitocella orientalis	HKAS 75664	China	MN061332	MN065726	MN148163	MN166274	MN133783
Clitocella orientalis	HKAS 77899	China	–	MN065725	MN148162	MN166273	MN133782
Clitocella orientalis	HKAS 78876	China	MN061334	MN065729	MN148166	MN166277	MN133786
Clitocella orientalis (Holotype)	HKAS 78763	China	–	MN065728	MN148165	MN166276	MN133785
Clitocella orientalis	**BJTC FM1539**	**China**	–	**OL966947**	**OL989911**	**OL989921**	–
Clitocella popinalis	HBJU-550	India	KU561066	–	–	–	–
Clitocella popinalis	CBS 481.50	UK	FJ770397	–	–	–	–
Clitocella popinalis	KA12-1717	Korea	KR673647	–	–	–	–
Clitocella popinalis	RA802-3b	USA	MK217434	–	–	–	–
Clitocella popinalis	Smith-2018 iNaturalist # 17340579	USA	MK573922	–	–	–	–
Clitocella popinalis	K(M): 143166	UK	–	–	KC816971	KC816878	KC816796
Clitocella popinalis	K(M): 167017	UK	–	–	KC816972	KC816879	KC816797
Clitocella popinalis	O-F63376	Norway	–	–	KC816974	KC816880	KC816799
Clitocella popinalis	6378 TJB	Switzerland	–	–	KC816976	KC816882	KC816801
Clitocella popinalis	O-F105360	Norway	–	–	KC816975	KC816881	KC816800
Clitocella popinalis	K(M): 146162	UK	–	–	KC816970	KC816877	KC816795
'*Clitocella popinalis*'	MC2-TRENT	Italy	–	–	KC816973	–	KC816798
'*Clitocella popinalis*'	ME Noordeloos 9867	Austria	–	GQ289213	GQ289280	–	–
Clitocella popinalis	TB6378	USA	–	AF261285	GU384654	–	–
Clitocella. Mundula	HMJAU 7275	China	MN061331	–	–	–	–

Species	Voucher	Locality	GenBank accession No.				
			ITS	nrLSU	*rpb2*	*tef1*	*atp6*
Clitocella obscura	MK09051302	Czech Republic	KX271753	–	–	–	–
Clitocella prunulus	G.v. Zanen F96065	–	KC885965	–	–	–	–
Clitocella_termitophila	CORT014751	Dominican Republic	–	–	MN893319	–	–
Clitopilus brunneiceps (Holotype)	HKAS 104510	China	–	MN065684	MN148123	MN166234	MN133737
Clitopilus yunnanensis (Holotype)	HKAS 104518	China	–	MN065698	MN148136	MN166247	MN133752
Clitopilus. Amarus	A. d. Haan 98031	–	KC885963	–	–	–	–
Cltopilopsis albida (Holotype)	HKAS 104519	China	–	MN065730	MN148167	MN166278	MN133787
Lyophyllum decastes	Sundberg091007a	Japan	HM572548	–	–	–	–
Mycena pura	CBH371	Denmark	KF913023	–	–	–	–
Rhodocybe mellea	CORT013885	Dominican Republic	MN784992	–	–	–	–
Rhodocybe mellea	JBSD127402	Dominican Republic	MN784993	–	–	–	–
Rhodocybe mellea	CORT014470	Belize	MN784994	–	–	–	–
Rhodocybe mellea	NYBG815044	Costa Rica	MN784995	–	–	–	–

Maximum Likelihood (ML) was performed using RAxML 8.0.14 (Stamatakis et al. 2005; Stamatakis 2006, 2014) by running 1000 bootstrap replicates under the GTR-GAMMAI model (for all partitions). Bayesian Inference (BI) analysis was performed with MrBayes v3.1.2 (Ronquist and Huelsenbeck 2003) based on the best substitution models (GTR+I+G for ITS, GTR+I for nrLSU, SYM+G for *rpb2*, SYM+I+G for *tef1*, and GTR+G for *atp6*) determined by MrModeltest 2.3 (Nylander 2004). Two independent runs with four Markov chains were conducted for 10 M generations under the default settings. Average standard deviations of split frequency (ASDSF) values were far lower than 0.01 at the end of the runs. Trees were sampled every 100 generations after burn-in (25% of trees were discarded as the burn-in phase of the analyses, set up well after convergence), and a 70% majority-rule consensus tree was constructed.

Trees were visualized with TreeView32 (Page 2001). Bootstrap values (BS) ≥ 70% and Bayesian Posterior Probability values (BPP) ≥ 0.95 were considered significant (Hillis and Bull 1993; Alfaro et al. 2003).

Results

Phylogenetic analysis

Twenty-eight sequences were newly generated from our six collections in this study. Two datasets, nrLSU-*rpb2-tef1-atp6* combined dataset and ITS dataset were compiled to investigate the phylogenetic position of these *Clitocella* species. For the combined dataset, the phylogenetic trees based on individual loci (including nrLSU, *rpb2*, *tef1*, *atp6*) showed

the almost same major clades (Suppl. material 1–4: Figs S1–S4) as that of the combined dataset (Fig. 1). There was no strongly supported conflict between single gene phylogenies, except for the nrLSU phylogeny does not resolve *Clitocella mundula* and *C. popinalis*, while the *atp6* phylogeny does not resolve *C. orientalis* and the new species *C. colorata*. So here the

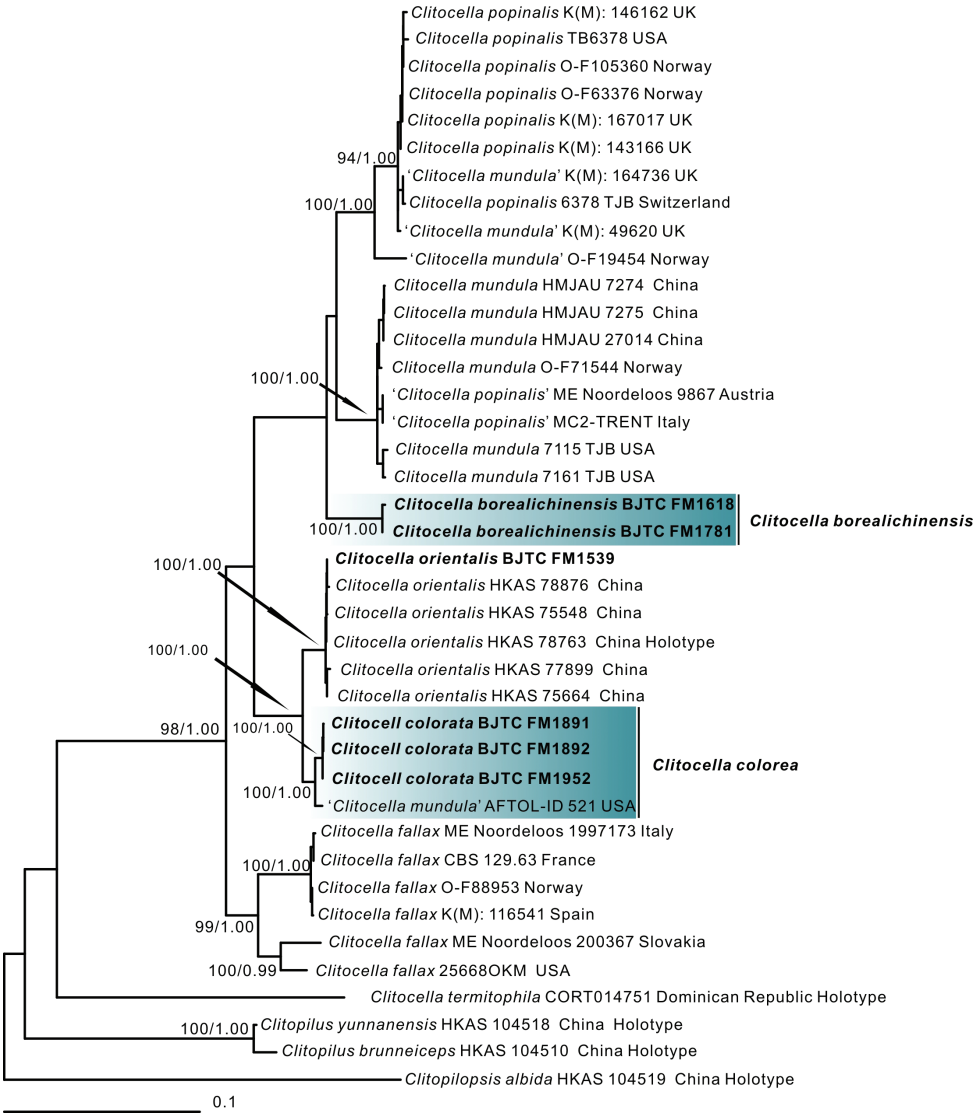

Figure 1. Phylogeny derived from Maximum Likelihood analysis of the combined nrLSU-*rpb2-tef1-atp6* dataset of *Clitocella* and related genera in the family Entolomataceae. *Clitopilopsis albida* was employed to root the tree as an outgroup. Numbers representing likelihood bootstrap support (BS≥ 70%, left) and significant Bayesian posterior probability (BPP≥ 0.95, right) are indicated above the nodes. New sequences are highlighted in bold.

combined dataset was used to infer the phylogenetic placement of *Clitocella* species. The final combined nrLSU-*rpb2-tef1-atp6* dataset contained 2963 total characters (905 from nrLSU, 599 from *rpb2*, 1010 from *tef1*, 449 from *atp6*, gaps included) and included 40 samples of 11 taxa. The topologies of ML and BI phylogenetic trees obtained in this study were practically the same, therefore only the tree inferred from the ML analysis is shown (Fig. 1). Except for the species *Clitocella termitophila* T.J. Baroni & Angelini, members of *Clitocella* in the dataset formed a monophyletic lineage with strong support (MLB = 98%, BPP = 1.00). *Clitocella termitophila* was sister to all other species of *Clitocella* but without strong support. Of our six collections, the sequences of a collection (BJTC FM1539) grouped in the clade *C. orientalis* S.P. Jian & Zhu L. Yang, indicating it is identity with this species. The remaining specimens fell in two strongly supported clades, one comprised of two collections was described as the new species *C. borealichinensis* and another comprised of three collections was described as the new species *C. colorata* together with a collection from USA (AFTOL-ID 521) originally labelled as *C. mundula*. *Clitocella colorata* was sister to *C. orientalis* with strong support, implying *C. colorata* is closely related to *C. orientalis*. *Clitocella borealichinensis* further clustered with *C. mundula* and *C. popinalis* (Fr.) Kluting, T.J. Baroni & Bergemann. One collection from Norway (O-F19454), which is labelled as *Clitocella mundula*, formed an independent clade.

The ITS dataset comprised 27 samples of 11 taxa and 662 characters. The topology of phylogenetic trees based on the ITS dataset generated from ML and BI analyses were almost identical and only the tree inferred from the ML analysis is shown (Fig. 2). The sequences of the new species *C. borealichinensis* formed an independent and strong support branch, like that of multilocus phylogeny (Fig. 1), supporting it is a distinct species. The sequences of the new species *C. colorata* together with five sequences labelled as *C. popinalis* from India, South Korea, UK and USA formed an independent and strong support branch, indicating they represented a distinct species.

Taxonomy

Clitocella borealichinensis **L. Fan & N. Mao, sp. nov.**
MycoBank No: 843689
Figs 3a, 4, 6a, b

Etymology. *borealichinensis*, referring to north China as the place of origin.

Holotype. China. Shanxi Province, Qinshui County, Lishan Mountain, 35°36.49'N, 112°11.7'E, alt. 1150m, 26 July 2021, on the ground in broad-leaved forest dominated by *Quercus* sp., N. Mao MNM340 (BJTC FM1781).

Diagnosis. *Clitocella borealichinensis* is characterized by its clitocyboid basidiomata, globose to subglobose, occasionally broadly ellipsoid basidiospores, the absence of hymenial cystidia and clamp connection, and usually growing in broad-leaved forests. It is most similar to *C. orientalis* but differs from it by the slightly smaller basidiospores, non-gelatinized hyphae of pileipellis and stipitipellis with pale brown to brown intracellular or parietal pigment.

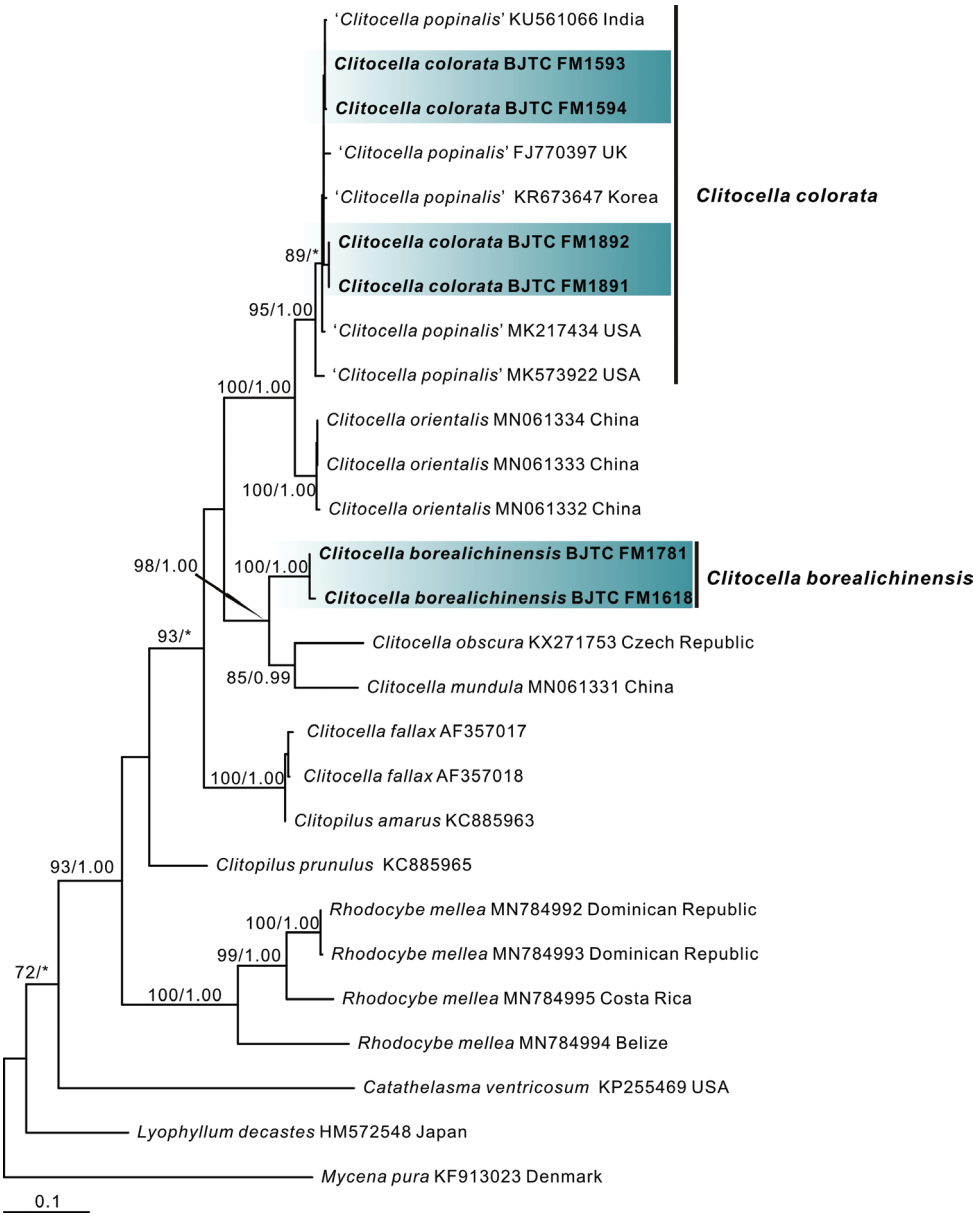

Figure 2. Phylogeny derived from Maximum Likelihood analysis of the ITS sequences from *Clitocella* and related genera in the family Entolomataceae. *Mycena pura* was employed to root the tree as an outgroup. Numbers representing likelihood bootstrap support (BS≥ 70%, left) and significant Bayesian posterior probability (BPP≥ 0.95, right) are indicated above the nodes. New sequences are highlighted in bold.

Description. Basidiomata clitocyboid, small to medium-sized. Pileus 13–50 mm wide, low convex to plane convex when young, then slightly depressed at center; surface smooth, grayish white (#f2f2f2) to pale white (#ffffff), yellowish white (#ffcd9a);

Figure 3. Basidiomata of *Clitocella* **a** *Clitocella borealichinensis* (BJTC FM1781, holotype) **b-d** *Clitocella colorata* (**b** BJTC FM1593 **c** BJTC FM1952 **d** BJTC FM1891, holotype) Scale bars: 10 mm (**a–d**). Photos by JingZhong Cao

margin incurved, non-striate; context thin pale white, 1.0–1.2 mm thick. Lamellae decurrent, grayish white (#f2f2f2), pale yellow (#fff3e7), crowded, edges smooth, thin and fragile, lamellulae numerous and concolorous with lamellae. Stipe 20–32 × 2–8 mm, central to eccentric, occasionally lateral, cylindrical to subcylindrical, equal or sometimes slightly tapering at base, pale white (#ffffff), smooth or tomentose, usually with white rhizomorphs. Odor unrecorded. Taste not recorded. Chemical color reaction: not reacting with KOH 3% at pileus of dried specimens.

Basidiospores [60/2/2] (3.8–)4–5(–5.5) × 3.8–4.5 µm, L_m × W_m = 4.61 (± 0.42) × 4.06 (± 0.18), Q = 0.95–1.25 (Q_{av} = 1.13 ± 0.10), hyaline, globose to subglobose, occasionally broadly ellipsoid in profile view, slightly angled in polar or face view with obscure minute pustules or bumps. Basidia 17–25 × 5–6(–7) µm, clavate, hyaline, four spored, rarely two spored; sterigmata 2–4 µm long. Lamellar trama more or less regular, composed of 3–8 µm wide hyaline hyphae, subhymenium consisting of filamentous hyphal segments. Lamellae edges fertile. Pleurocystidia and cheilocystidia absent. Pileipellis a cutis composed of more or less radially, loosely arranged, non-gelatinized, smooth, cylindrical hyphae, 2–6 µm wide and with pale brown to brown intracellular or parietal pigment; terminal hyphae subcylindric, narrowly clavate, occasionally irregular, 3–5 µm wide; subcutis made up of subparallel, compactly arranged, thin-walled, hyaline, smooth, cylindrical hyphae, 3–6 µm wide; pileal trama composed of interwoven, cylindrical hyphae, 2.5–10 µm wide. Stipitipellis a cutis composed of

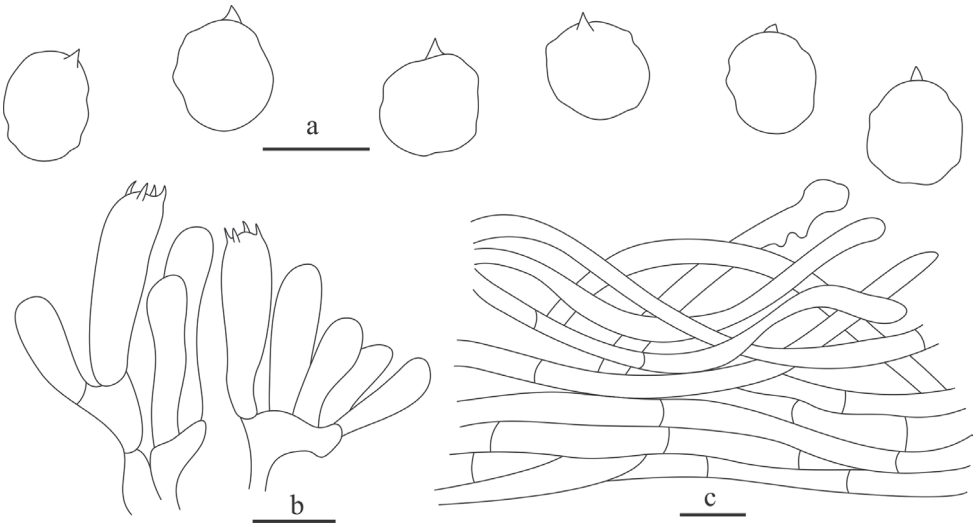

Figure 4. Microscopy of *Clitocella borealichinensis* **a** basidiospores **b** basidia **c** pileipellis. Scale bars: 5 μm (**a**); 10 μm (**b, c**). Drawings by Ning Mao.

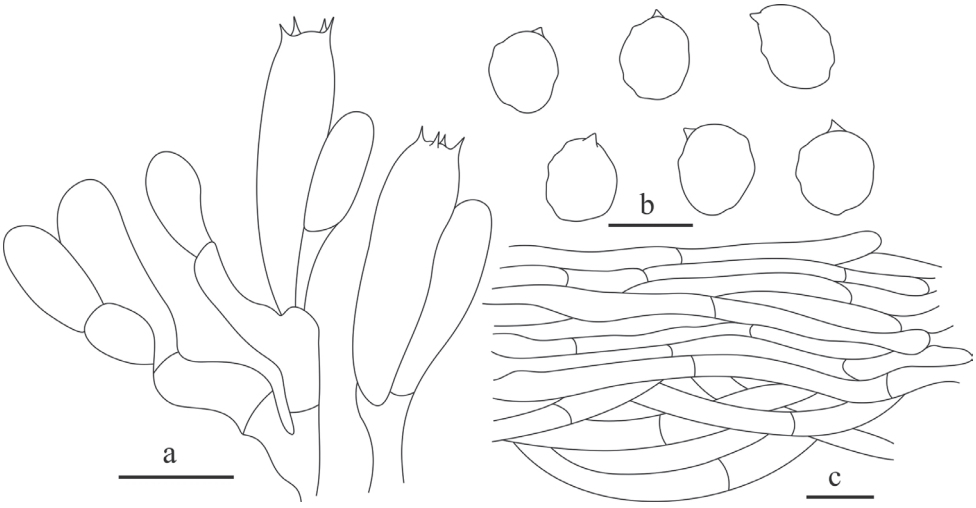

Figure 5. Microscopy of *Clitocella colorata* **a** basidiospores **b** basidia **c** pileipellis. Scale bars: 10 μm (**a, c**); 5 μm (**b**). Drawings by Ning Mao.

parallel, compactly arranged, thin-walled, non-gelatinized, hyaline hyphae, 2.5–6 μm wide. Stipititrama composed of interwoven, hyaline, cylindrical hyphae, 3–10 μm wide. Caulocystidia absent. Clamp connections absent.

Habit. Scattered or in groups on soil in broad-leaved (*Quercus*) forest, Shanxi province, China.

Additional specimens examined. China. Shanxi province, Xia County, alt. 970m, 7 October 2020, N. Mao MNM172 (BJTC FM1618).

Note. *Clitocella borealichinensis* is easily confused with *C. orientalis*, *C. obscura* (Pilát) Vizzini *et al.* and *C. pallescens* Silva-Filho & Cortez in morphology because they are all have white to grayish white pileus and decurrent lamellae. However, *C. orientalis* differs from *C. borealichinensis* by its viscid pileus and stipe when wet, gelatinized pileipellis and stipitipellis, and slightly larger basidiospores of (4–)4.5–6 × 4–5 µm (Jian et al. 2020). *Clitocella obscura* produce a distinctly reddish reaction when 3% KOH is placed on the pileus surface (Baroni 1981; as *Rhodocybe*) while *C. borealichinensis* has not that kind of reaction. *Clitocella pallescens* differs *C. borealichinensis* by its pale grey to yellowish white stipe (Silva-Filho et al. 2018; Jian et al. 2020).

Clitocella mundula and *C. popinalis* clustered with *C. borealichinensis* in our multilocus phylogeny (Fig. 1), indicating they are phylogenetically closely related to each other. Morphologically, *C. mundula* differs from *C. borealichinensis* by its yellowish gray or brown to dark smoke gray pileus and slightly larger basidiospores of (4–)4.5–6(–6.5) × 4–5 µm (Jian et al. 2020), *C. popinalis* by its brown to grayish brown pileus, bigger basidiospores of 5.5–7–5–5.5 µm, and its pileus surface produces a reddish reaction in 3% KOH (Baroni 1981; as *Rhodocybe*). Moreover, DNA analysis also revealed that *C. borealichinensis* shared less than 91.10% similarity in *tef1* sequence with *C. mundula* and 91.20% similarity with *C. popinalis*, supporting their separation.

***Clitocella colorata* L. Fan & N. Mao, sp. nov.**
MycoBank No: 843690
Figs 3b–d, 5, 6c, d

Etymology. *colorata*, referring to the colorful pileus.

Holotype. China. Shanxi Province, Pu County, Wulushan Mountain, 36°33.2'N, 111°11.58'E, alt. 1740 m, 28 July 2021, on the ground in coniferous forest dominated by *Pinus armandii* Franch., N. Mao MNM292 (BJTC FM1891).

Diagnosis. *Clitocella colorata* is characterized by its clitocyboid basidiomata, relatively colorful pileus (white to yellowish white, grayish white to grayish brown, pink white), globose or subglobose to broadly ellipsoid basidiospores, hyphae of pileipellis with pale yellow to yellowish brown intracellular or parietal pigment, the absence of hymenial cystidia and clamp connection. It is most similar to *C. popinalis* and *C. mundula* but differs from *C. popinalis* by its slightly smaller basidiospores, only appearing in the forest and genetic profile, and from *C. mundula* by its colorful pileus (white to yellowish white, grayish white to grayish brown, pink white).

Description. Basidiomata clitocyboid, small to large. Pileus 20–62 mm wide, dry,convex to plano-convex, sometimes infundibuliform, with a shallow depression at the center; margin not striate, often enrolled or flat, sometimes slightly uplifted; surface white (#ffffff) to yellowish white (#ffffe7), grayish white (#f2f2f2) to grayish brown (#dba773), pink white (#fff3f5); context white (#ffffff) to grayish white (#f2f2f2), 1.0–1.5 mm thick. Lamellae decurrent, white (#ffffff) to yellowish white(#fff3e7), becoming yellowish brown (#e0b487) on drying, crowded, 1.0–2.0 mm deep, edges entire and concolorous, thin and fragile, lamellulae in 2–4 tiers

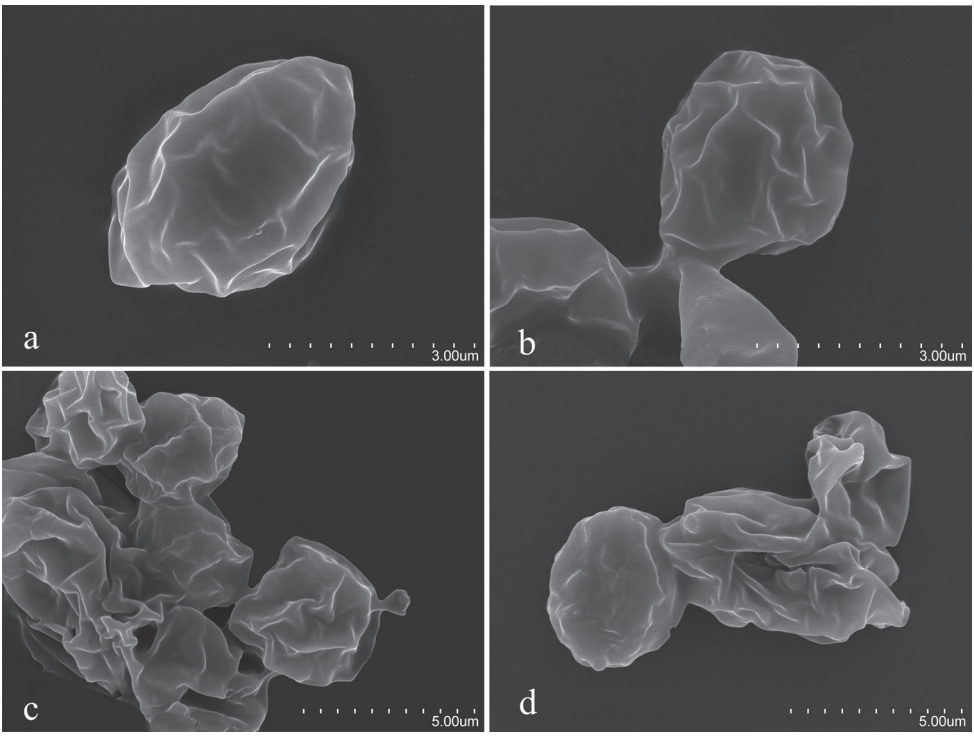

Figure 6. Basidiospores of species in *Clitocella*. *Clitocella* revealed by SEM **a, b** *Clitocella borealichinensis* **c, d** *Clitocella colorata* Scale bars: 3 μm (**a, b**); 5 μm (**c, d**). Photos by Li Fan.

of varying lengths. Stipe 22–42 × 4–10 mm, central, cylindrical, equal, pale white (#ffffff) to yellowish brown (#e0b487), smooth, usually with white rhizomorphs. Odor unrecorded. Taste not recorded. Chemical color reaction: pileal surface of dried samples negative with 3% KOH.

Basidiospores [100/5/2] (3.8–)4.5–5.5(–6.0) × (3.5–)4–4.8(–5.0) μm; $L_m \times W_m$ = 4.90 (± 0.44) × 4.29 (± 0.35), Q = 1.00–1.25 (Q_{av} = 1.14 ± 0.09); hyaline, globose or subglobose to broadly ellipsoid in profile view, slightly angled in polar or face view with obscure minute pustules or bumps. Basidia 20–30 × (4.5–)5–6.5 μm, clavate, hyaline, with four spored, rarely two spored; sterigmata 2–3.5 μm long. Lamellar trama composed of subparallel, hyaline, cylindrical hyphae, 2.5–6 μm wide, subhymenium consisting of filamentous hyphal segments, 2–3.5 μm wide. Lamellae edges fertile. Pleurocystidia and cheilocystidia absent. Pileipellis a cutis composed of parallel, compactly arranged, non-gelatinized, smooth, cylindrical hyphae, 2–5 μm wide, with pale yellow to yellowish brown intracellular or parietal pigment; subcutis made up of interwoven, slightly loosely arranged, hyaline, smooth, cylindrical hyphae, 3–6.5 μm wide; pileal trama composed of parallel, compactly arranged, hyaline, cylindrical hyphae, 3–10 μm wide. Stipitipellis a cutis composed of parallel, compactly arranged, thin-walled, non-gelatinized, cylindrical hyphae, 2–5 μm wide, heavily

or moderately encrusted with brown pigment. Stipititrama composed of parallel, compactly arranged, hyaline, cylindrical hyphae, 3–7 μm wide. Caulocystidia absent. Clamp connections absent.

Habit. Scattered or in groups on soil or rotten wood in coniferous (*Pinus*) or broad-leaved (*Quercus*) forest, Shanxi province, China.

Additional specimens examined. China. Shanxi province, Pu County, Wulushan Mountains, alt. 1750m, 28 July 2021, N. Mao MNM293 (BJTC FM1892); Wenshui County, alt. 1760m, 30 July 2021, L. Fan CF1219 (BJTC FM1952); Xia County, alt. 931m, 6 October 2020, N. Mao MNM102 (BJTC FM1593); Xia County, alt. 931m, 6 October 2020, N. Mao MNM103 (BJTC FM1594).

Notes. Morphologically, *Clitocella colorata* is easily confused with *C. mundula* and *C. popinalis*. However, according to Baroni (1981; as *Rhodocybe*), the pileus surface in *C. mundula* and *C. popinalis* can produce a reddish reaction in 3% KOH, whereas that is not exhibited in *Clitocella colorata*. The basidiospores of *C. popinalis*, 5.5–7 × 5–5.5 μm (Baroni 1981; Kluting et al. 2014; Jian et al. 2020), are broader and longer than those of *C. colorata* (4.5–5.5 ×4–4.8 μm). DNA analysis revealed that *C. colorata* shared less than 87.80% similarity in *tef1* sequence with *C. mundula* and 86.10% similarity with *C. popinalis*, supporting their separation. Moreover, five ITS sequences (FJ770397, KR673647, KU561066, MK217434 and MK573922) labelled "*C. popinalis*" from India, Norway, South Korea, UK and USA are probably conspecific to the new species *C. colorata* as they clustered together with *C. colorata* in ITS tree (Fig. 2) and have more than 98.4% similarity in ITS region. However, these "*C. popinalis*" collections still need more other DNA regions and detailed morphology to support this view. One collection of "*C. mundula*," namely, AFTOLID 521 from Norway, should be re-identified *C. colorata* as it clustered together with *C. colorata* in the combined nrLSU-*rpb2-tef1-atp6* tree (Fig. 1) and have more than 98.1% similarity in *tef1* region. These showed that the new species *C. colorata* maybe have a wide geographical distribution. Although *C. orientalis* is sister to *C. colorata* with strong support, these two species have obvious differences in morphology. The pileus and stipe of *C. orientalis* are usually viscid when wet and have gelatinized pileipellis and stipitipellis. *Clitocella colorata* has non-gelatinized pileipellis and stipitipellis, and its pileus is more colorful and darker (Jian et al. 2020). DNA analysis revealed that *C. colorata* shared less than 95.80% similarity in *tef1* sequence with *C. orientalis* and 90.20% similarity in ITS sequence. Moreover, *C. colorata* has a wider distribution range than *C. orientalis*, which is only distributed in China.

Discussion

Three species of *Clitocella* are confirmed from Shanxi Province, north China in this study. Of them, *C. colorata* is the most commonly encountered species, which distributes across the provincial area and grows in almost all kinds of forest. *Clitocella orientalis* and *Clitocella borealichinensis* are probably limited in southern Shanxi province, and they usually occur in the *Quercus* spp. forests.

ITS gene is rarely used in the species classification of *Clitocella* in previous studies because it contains many ambiguous sites. In the contrast, the partial sequences of three protein-coding genes (the *atp6*, *rpb2* and *tef1*) are usually used to infer the phylogeny of *Clitocella* (Kluting et al. 2014; Baroni et al. 2020; Jian et al. 2020). However, we found that ITS, *rpb2*, and *tef1* gene tree are similar to the combined (nrLSU-*rpb2*-*tef1*-*atp6*) gene regions tree when we performed phylogenetic tree construction respectively using the ITS, nrLSU, *rpb2*, *tef1* and *atp6* gene of *Clitocella* (Fig. 2, Suppl. material 1–4: Figs S1–S4). DNA analysis also showed that the intraspecific similarity of the ITS region is ≥ 98.4% and of *tef1* gene is ≥ 98.1%, the interspecific similarity of ITS region is ≤ 96.1% and of *tef1* is ≤ 95.9% (Table 2, Table 3). But for the *rpb2* gene, the intraspecific variation of *C. mundula* is more than the interspecific variation of *C. colorata* and *C. orientalis* (Table 4). Therefore, we consider that both the ITS and *tef1* may be more effective for the classification of *Clitocella* species.

Our molecular phylogenetic analysis (Fig. 1) revealed that one Norway collection O-F19454, which is labelled as *Clitocella mundula*, formed an independent clade, and it shared less than 93.40% similarity in *tef1* sequence with other *Clitocella* species. These show that it probably represents a new species of *Clitocella*. The sequences of *Clitocella fallax* formed two or three (in *rpb2* phylogeny) independent branches in our phylogenetic analyses (Fig. 2, Suppl. material 1–4: Figs S1–S4), and the similarity between the branches is less than 90.2% in *tef1* sequence and 94.9% in *rpb2* sequence. These indicate that these specimens of *C. fallax* probably represented two or three species. The specimens of *C. fallax* should be therefore re-examined to resolve this taxonomic issue. *Clitocella termitophila* is not clustered in the genus *Clitocella* (Fig. 1). Moreover, in the *rpb2* gene

Table 2. Interspecific variation and intraspecific variation of ITS in *Clitocella* species.

Species	Number (n)	Intraspecific variation (%)	Interspecific variation (%)
Clitocella colorata	9	< 1.6%	> 3.9%
C. fallax	3	< 0.3%	> 11.8%
C. mundula	1	–	> 6.0%
C. borealichinensis	2	–	> 9.6%
C. obscura	1	–	> 6.6%
C. orientalis	3	< 0.9%	> 3.9%

Table 3. Interspecific variation and intraspecific variation of *tef1* in *Clitocella* species.

Species	Number (n)	Intraspecific variation (%)	Interspecific variation (%)
Clitocella colorata	4	< 1.9%	> 4.1%
C. fallax[a]	1	–	> 9.8%
C. fallax[b]	2	< 0.1%	> 9.8%
C. mundula	6	< 0.3%	> 7.5%
'*C. mundula*'[c]	1	–	> 4.7%
C. borealichinensis	1	–	> 8.4%
C. orientalis	3	< 0.1%	> 4.1%
C. popinalis	7	–	> 4.7%

[a] represents voucher 25668OKM; [b] represents voucher O-F88953, K(M): 116541; [c] represents voucher O-F19454

Table 4. Interspecific variation and intraspecific variation of *rpb2* in *Clitocella* species.

Species	Number (n)	Intraspecific variation (%)	Interspecific variation (%)
Clitocella colorata	4	< 0.7%	> 1.7%
C. fallax[a]	1	–	> 4.0%
C. fallax[b]	4	< 0.1%	> 5.1%
C. fallax[c]	1	–	> 4.0%
C. mundula	6	< 2.1%	> 4.9%
'*C. mundula*'[d]	1	–	> 2.2%
C. borealichinensis	2	–	> 5.5%
C. orientalis	6	< 0.5%	> 1.7%
C. popinalis	9	< 0.4%	> 2.2%
C. termitophila	1	–	> 16.9%

[a] represents voucher 25668OKM; [b] represents voucher O-F88953, K(M): 116541, CBS 129.63, ME Noordeloos 1997173; [c] represents voucher ME Noordeloos 200367; [d] represents voucher O-F19454.

tree *C. termitophila* did not gather with *Clitocella*, *Clitopilopsis* or *Clitopilus* but formed a single branch (Suppl. material 2: Fig. S2). These indicate that *Clitocella termitophila* probably represents a potential taxonomic position rather than the species of *Clitocella*.

Key to the species of *Clitocella*

1 Basidiomata clitocyboid **2**
– Basidiomata pleurotoid ..... ***C. termitophila**** **(Baroni et al. 2020)**
2 Pileus surface gray, dark gray, pale yellow to yellowish brown, pigments present in pileipelli **3**
– Pileus surface almost white to pastel gray, pigments absent in pileipellis **8**
3 Basidiospores globose to subglobose **4**
– Basidiospores ellipsoid **7**
4 Pileus surface of dried samples with a positive KOH reaction **5**
– Pileus surface of dried samples with a negative KOH reaction **6**
5 Occurring in grassland systems ..... ***C. popinalis**** **(Baroni 1981; Kluting et al. 2014; Jian et al. 2020)**
– Occurring in forested systems ..... ***C. mundula**** **(Baroni 1981; Kluting et al. 2014; Jian et al. 2020)**
6 Pileus color with pink tinges ..... ***C. colorata****
– Pileus color without pink tinges ..... ***C. borealichinensis****
7 Pileus color with yellow tinges, basidiospores small, 5–8 × 3.5–5.5 µm ..... ***C. himantiigena*** **(Silva-Filho et al. 2018)**
– Pileus color without yellow tinges, basidiospores large, 7–9 × 5–6 µm ..... ***C. ammophila*** **(Contu 1999)**
8 Basidiospores globose to subglobose or ovatae **9**
– Basidiospores amygdaliform to ellipsoid **11**

* Indicates the presence of molecular data.

9	Basidia long, length > 40 μm ..... ***C. nigrescens*** **(Maire 1945)**
–	Basidia short, length < 28 μm **10**
10	Pileus infundibuliform to plano-convex, basidiospores 4–5 × 3–4.5 μm .... ***C. pallescens*** **(Silva-Filho et al. 2018; Jian et al. 2020)**
–	Pileus convex to plane, basidiospores (4–)4.5–6 × 4–5 μm..... ..... ***C. orientalis**** **(Jian et al. 2020)**
11	Basidiospores small, 5–6.2 × 2.5–3.6 μm..... ***C. blancii*** **(Contu 2009)**
–	Basidiospores large, 6.5–8 × 4–5 μm..... ***C. fallax**** **(Jian et al. 2020)**

Acknowledgements

We extend our appreciation to Dr. J.Z. Cao for collecting specimens and providing valuable suggestions. The study was supported by the National Natural Science Foundation of China (No. 31750001) and the Beijing Natural Science Foundation (No. 5172003).

References

Alfaro ME, Zoller S, Lutzoni F (2003) Bayes or bootstrap? A simulation study comparing the performance of Bayesian Markov chain Monte Carlo sampling and bootstrapping in assessing phylogenetic confidence. Molecular Biology and Evolution 20(2): 255–266. https://doi.org/10.1093/molbev/msg028

Baroni TJ (1981) A revision of the genus *Rhodocybe* Maire (Agaricales). Beih Nova Hedwigia 67: 1–194.

Baroni TJ, Angelini C, Bergemann SE, Lodge DJ, Lacey L, Curtis TA, Cantrell SA (2020) *Rhodocybe-Clitopilus* clade (Entolomataceae, Basidiomycota) in the Dominican Republic: New taxa and first reports of *Clitocella*, *Clitopilus*, and *Rhodocybe* for Hispaniola. Mycological Progress 19(10): 1083–1099. https://doi.org/10.1007/s11557-020-01619-y

Binder M, Hibbett DS (2003) Oligonucleotides. http://www.clarku.edu/faculty/dhibbett/Protocols_Folder/Primers/Primers.htm [accessed 18 Mar 2012]

Castresana J (2000) Selection of conserved blocks from multiple alignments for their use in phylogenetic analysis. Molecular Biology and Evolution 17(4): 540–552. https://doi.org/10.1093/oxfordjournals.molbev.a026334

Contu M (1999) Ecologia e tassonomia del genere Rhodocybe (Basidiomycetes, Entolomataceae) in Sardegna. Revista Catalana de Micologia 22: 5–14.

Contu M (2009) Studi sul genere *Clitopilus* (incl. Rhodocybe) 1. Prima segnalazione in Italia di Clitopilus blancii comb. nov., nuove raccolte di *Clitopilus giovanellae*, iconografia di Clitopilus carneolus comb. nov. e ulteriori nuove combinazioni. Bollettino AMER 77–78, 15–31.

Dring DM (1971) Techniques for microscopic preparation. In: Booth C (Ed.) Methods in microbiology, vol 4. Academic, New York, 98 pp. https://doi.org/10.1016/S0580-9517(09)70008-X

Gardes M, Bruns TD (1993) ITS primers with enhanced specificity for basidiomycetes – application to the identification of mycorrhizae and rusts. Molecular Ecology 2(2): 113–118. https://doi.org/10.1111/j.1365-294X.1993.tb00005.x

Hall TA (1999) BioEdit: a user-friendly biological sequence alignment editor and analysis program for Windows 95/98/NT. Nucleic Acids Symposium Series 41: 95–98.

Hillis DM, Bull JJ (1993) An empirical test of bootstrapping as a method for assessing confidence in phylogenetic analysis. Systematic Biology 42(2): 182–192. https://doi.org/10.1093/sysbio/42.2.182

Jian SP, Tolgor B, Zhu XT, Deng WQ, Yang ZL, Zhao ZW (2020) *Clitopilus*, *Clitocella*, and *Clitopilopsis* in China. Mycologia 112(2): 371–399. https://doi.org/10.1080/00275514.2019.1703089

Katoh K, Standley DM (2013) MAFFT multiple sequence alignment software version 7: Improvements in performance and usability. Molecular Biology and Evolution 30(4): 772–780. https://doi.org/10.1093/molbev/mst010

Kluting KL, Baroni TJ, Bergemann SE (2014) Toward a stable classification of genera within the Entolomataceae: A phylogenetic re-evaluation of the *Rhodocybe–Clitopilus* clade. Mycologia 106(6): 1127–1142. https://doi.org/10.3852/13-270

Kretzer AM, Bruns TD (1999) Use of atp6 in fungal phylogenetics: An example from the Boletales. Molecular Phylogenetics and Evolution 13(3): 483–492. https://doi.org/10.1006/mpev.1999.0680

Liu YJ, Whelen S, Hall BD (1999) Phylogenetic relationships among Ascomycetes: Evidence from an RNA polymerase II subunit. Molecular Biology and Evolution 16(12): 1799–1808. https://doi.org/10.1093/oxfordjournals.molbev.a026092

Maire R (1945) Études mycologiques. Fascicule 5. Bulletin de la Société d'Histoire Naturelle de l'Afrique du Nord 36: 24–42.

Matheny PB (2005) Improving phylogenetic inference of mushrooms with RPB1 and RPB2 nucleotide sequences (*Inocybe*; Agaricales). Molecular Phylogenetics and Evolution 35: 1–20. https://doi.org/10.1016/j.ympev.2004.11.014

Matheny PB, Wang Z, Binder M, Curtis JM, Lim YW, Nilsson RH, Hughes KW, Hofstetter V, Ammirati JF, Schoch CL, Langer E, Langer G, McLaughlin DJ, Wilson AW, Frøslev T, Ge ZW, Kerrigan RW, Slot JC, Yang ZL, Baroni TJ, Fischer M, Hosaka K, Matsuura K, Seidl MT, Vauras J, Hibbett DS (2007) Contributions of rpb2 and tef1 to the phylogeny of mushrooms and allies (Basidiomycota, Fungi). Molecular Phylogenetics and Evolution 43(2): 430–451. https://doi.org/10.1016/j.ympev.2006.08.024

Nylander J (2004) MrModeltest 2.2. Computer software distributed by the Evolutionary Biology Centre, University of Uppsala, Uppsala.

Page RD (2001) TreeView. Glasgow University, Glasgow.

Rehner S (2001) Primers for elongation factor 1-α (tef1). [cited 2021 Nov 1] http://www.aftol.org/pdfs/EF1primer.pdf

Ronquist F, Huelsenbeck JP (2003) MrBayes 3: Bayesian phylogenetic inference under mixed models. Bioinformatics (Oxford, England) 19(12): 1572–1574. https://doi.org/10.1093/bioinformatics/btg180

Silva-Filho AGS, Teixeira-Silva M, Cortez VG (2018) New species, new combination, and notes on *Clitocella* and *Rhodocybe* (Entolomataceae) from Paraná State, Brazil. Darwiniana 6: 58–67. https://doi.org/10.14522/darwiniana.2018.61.775

Stamatakis A (2006) RAxML-vI-HPC: Maximum-likelihood-based phylogenetic analyses with thousands of taxa and mixed models. Bioinformatics (Oxford, England) 22(21): 2688–2690. https://doi.org/10.1093/bioinformatics/btl446

Stamatakis A (2014) RAxML version 8: A tool for phylogenetic analysis and post-analysis of large phylogenies. Bioinformatics (Oxford, England) 30(9): 1312–1313. https://doi.org/10.1093/bioinformatics/btu033

Stamatakis A, Ludwig T, Meier H (2005) RAxML-III: A fast program for maximum likelihood-based inference of large phylogenetic trees. Bioinformatics (Oxford, England) 21(4): 456–463. https://doi.org/10.1093/bioinformatics/bti191

Vilgalys R, Hester M (1990) Rapid genetic identification and mapping of enzymatically amplified ribosomal DNA from several *Cryptococcus* species. Journal of Bacteriology 172(8): 4239–4246. https://doi.org/10.1128/jb.172.8.4238-4246.1990

Vizzini A, Baroni TJ, Sesli E, Antonín V, Saar I (2016) *Rhodocybe tugrulii* (Agaricales, Entolomataceae), a new species from Turkey and Estonia based on morphological and molecular data, and a new combination in *Clitocella* (Entolomataceae). Phytotaxa 267(1): 001–015. http://doi.org/10.11646/phytotaxa.267.1.1

White TJ, Bruns T, Lee S, Taylor J (1990) Amplification and direct sequencing of fungal ribosomal RNA genes for phylogenetics. In: Innis MA, Gelfand DH, Sninsky JJ, White TJ (Eds) PCR protocols: a guide to methods and applications. Academic Press, New York, 315–322. https://doi.org/10.1016/B978-0-12-372180-8.50042-1

Supplementary material 1

Figure S1

Authors: Ning Mao, Jing-Chong Lv, Yu-Yan Xu, Tao-Yu Zhao, Li Fan

Data type: JPG file

Explanation note: Phylogeny derived from Maximum Likelihood analysis of the *nrLSU* dataset of *Clitocella* and related genera in the family Entolomataceae. The bootstrap frequencies (> 70%) is shown on the supported branches. New species are highlighted in red.

Link: https://doi.org/10.3897/mycokeys.88.80068.suppl1

Supplementary material 2

Figure S2

Authors: Ning Mao, Jing-Chong Lv, Yu-Yan Xu, Tao-Yu Zhao, Li Fan

Data type: JPG file

Explanation note: Phylogeny derived from Maximum Likelihood analysis of the *rpb2* dataset of *Clitocella* and related genera in the family Entolomataceae. The bootstrap frequencies (> 70%) is shown on the supported branches. New species are highlighted in red.

Link: https://doi.org/10.3897/mycokeys.88.80068.suppl2

Supplementary material 3

Figure S3

Authors: Ning Mao, Jing-Chong Lv, Yu-Yan Xu, Tao-Yu Zhao, Li Fan

Data type: JPG file

Explanation note: Phylogeny derived from Maximum Likelihood analysis of the *tef1* dataset of *Clitocella* and related genera in the family Entolomataceae. The bootstrap frequencies (> 70%) is shown on the supported branches. New species are highlighted in red.

Link: https://doi.org/10.3897/mycokeys.88.80068.suppl3

Supplementary material 4

Figure S4

Authors: Ning Mao, Jing-Chong Lv, Yu-Yan Xu, Tao-Yu Zhao, Li Fan

Data type: JPG file

Explanation note: Phylogeny derived from Maximum Likelihood analysis of the *atp6* dataset of *Clitocella* and related genera in the family Entolomataceae. The bootstrap frequencies (> 70%) is shown on the supported branches. New species are highlighted in red.

Link: https://doi.org/10.3897/mycokeys.88.80068.suppl4

Supplementary material 5

ITS alignment

Authors: Ning Mao, Jing-Chong Lv, Yu-Yan Xu, Tao-Yu Zhao, Li Fan

Data type: PHY file

Explanation note: The ITS dataset comprised 27 samples of 11 taxa and 662 characters.

Link: https://doi.org/10.3897/mycokeys.88.80068.suppl5

MycoKeys 88: 171–192 (2022)
doi: 10.3897/mycokeys.88.82229
https://mycokeys.pensoft.net

RESEARCH ARTICLE

A peer-reviewed open-access journal
MycoKeys
Launched to accelerate biodiversity research

Morphological and phylogenetic analyses reveal two new species of Sporocadaceae from Hainan, China

Zhaoxue Zhang[1], Rongyu Liu[1], Shubin Liu[1], Taichang Mu[1], Xiuguo Zhang[1], Jiwen Xia[1]

1 *Shandong Provincial Key Laboratory for Biology of Vegetable Diseases and Insect Pests, College of Plant Protection, Shandong Agricultural University, Taian, 271018, China*

Corresponding author: Jiwen Xia (xiajiwen1@126.com)

Academic editor: Nalin Wijayawardene | Received 17 February 2022 | Accepted 29 March 2022 | Published 14 April 2022

Citation: Zhang Z, Liu R, Liu S, Mu T, Zhang X, Xia J (2022) Morphological and phylogenetic analyses reveal two new species of Sporocadaceae from Hainan, China. MycoKeys 88: 171–192. https://doi.org/10.3897/mycokeys.88.82229

Abstract

Species of Sporocadaceae have often been reported as plant pathogens, endophytes or saprophytes and are commonly isolated from a wide range of plant hosts. The isolated fungi were studied through a complete examination, based on multilocus phylogenies from combined datasets of ITS/*tub2*/*tef1*, in conjunction with morphological characteristics. Nine strains were isolated from *Ficus microcarpa*, *Ilex chinensis* and *Schima superba* in China which represented four species, *viz.*, *Monochaetia schimae* **sp. nov.**, *Neopestalotiopsis haikouensis* **sp. nov.**, *Neopestalotiopsis piceana* and *Pestalotiopsis licualicola*. *Neopestalotiopsis piceana* was a new country record for China and first host record from *Ficus macrocarpa. Pestalotiopsis licualicola* was first report from *Ilex chinensis* in China.

Keywords

Monochaetia, multigene phylogeny, *Neopestalotiopsis*, *Pestalotiopsis*

Introduction

The family Sporocadaceae was established by Corda in 1842 (type genus: *Sporocadus*). Species of Sporocadaceae are endophytic, plant pathogenic or saprobic, and associated with a wide range of host plants (Maharachch. et al. 2013; Jayawardena et al. 2015; Liu et al. 2019). Currently, the family comprises 35 genera including *Monochaetia* (Sacc.) Allesch., *Neopestalotiopsis* Maharachch. et al., *Pestalotiopsis* Steyaert, *Pseudopestalotiopsis* Maharachch.et al., and etc. Most genera have multi-septate and more or less fusiform

conidia with appendages at one or both ends, frequently with some melanised cells. Also known as pestalotioid fungi, resembling those taxa having affinities with *Pestalotia* (Liu et al. 2019).

Steyaert (1949) segregated two novel genera from *Pestalotia*, namely *Pestalotiopsis* (with 5-celled conidia) and *Truncatella* (with 4-celled conidia) based on the conidial forms. This resulted in apparent controversy from Guba (1956, 1961). He emphasised that there was no point in assembling species with similar numbers of conidial septa into distinct genera. Subsequently, Steyaert (1953, 1961, 1963) provided further evidence in support of splitting *Pestalotia*. Sutton (1980) accepted most of the genera discussed here (*Pestalotia*, *Pestalotiopsis*, *Truncatella*) which fitted into fairly well-defined groups and cited the electron microscope investigation of Griffiths and Swart (1974), which examined the conidial wall of *Pestalotia pezizoides* and two species of *Pestalotiopsis* (*P. funerea* and *P. triseta*) to support Steyaert's division of *Pestalotiopsis*. Maharachch. et al. (2014) segregated two novel genera from *Pestalotiopsis*, namely *Neopestalotiopsis* and *Pseudopestalotiopsis*, based on conidia pigment colour, conidiophores and molecular phylogeny. *Neopestalotiopsis* can be easily distinguished from *Pseudopestalotiopsis* and *Pestalotiopsis* by its versicolourous median cells (Maharachch. et al. 2014). Saccardo (1884) introduced *Monochaetia* as a subgenus of *Pestalotia* (as *Pestolozzia*). The genus *Monochaetia* was introduced by Allescher (1902), which included 23 species. Allescher (1902) designated the type *Monochaetia monochaeta* which has a single apical appendage (Guba 1961; Maharachch. et al. 2014; Senanayake et al. 2015). Steyaert (1949) transferred numerous *Monochaetia* species to *Pestalotiopsis* or *Truncatella*. More than 40 species of *Monochaetia* were recognised by the monograph of Guba (1961). There are 127 *Monochaetia* epithets in the Index Fungorum (accession date: 31 March 2022) and most have been transferred to other genera such as *Sarcostroma*, *Seimatosporium* and *Seiridium* (Nag Raj 1993; Maharachch. et al. 2011, 2014, 2016). *Seridium* and *Monochaetia* have obvious morphological differences and show separate clades (de Silva et al. 2017).

To date, most phylogenetic studies addressing genera of Sporocadaceae have been based solely on ITS and LSU sequences (Barber et al. 2011; Tanaka et al. 2011; Jaklitsch et al. 2016), or on concatenated datasets of more genes but with incomplete datasets (Senanayake et al. 2015; Wijayawardene et al. 2016). In this study, we made a collection of the established genera *Monochaetia*, *Neopestalotiopsis* and *Pestalotiopsis* species from leaves of *Ficus microcarpa*, *Ilex chinensis* and *Schima superba* in Hainan Province, China. The inventories allowed establishing two new species that are described here.

Materials and methods

Isolation and morphological studies

The samples were collected from Hainan Province, China. The strains were isolated from diseased leaves of *Ficus microcarpa*, *Ilex chinensis* and *Schima superba* using surface disinfected tissue fragments (0.5 × 0.5 cm) taken from the margin of leaf lesions

(Gao et al. 2014; Jiang et al. 2021a). Surface disinfection consisted of steps including immersion in 75% ethanol for 30 s, 5% sodium hypochlorite (Aladdin, Shanghai, China) for 1 min, and sterile distilled water for 30 s. The pieces were dried with sterilized paper towels and placed on potato dextrose agar (PDA). All plates were incubated at 25 °C for 3–4 days. Then, hyphae were picked out of the periphery of the colonies and inoculated onto new PDA plates. Photographs of the colonies were taken at 7 and 15 days using a Powershot G7X mark II digital camera. Micromorphological characters were observed using an Olympus SZX10 stereomicroscope and Olympus BX53 microscope, all fitted with Olympus DP80 high definition colour digital cameras to photodocument fungal structures. The size of conidia was measured by software Digimizer (https://www.digimizer.com/), and thirty individual measurements were obtained for each character. All fungal strains were stored in 10% sterilised glycerin at 4 °C for further studies. The holotype specimens were deposited in the Herbarium of Plant Pathology, Shandong Agricultural University (HSAUP). Ex-type cultures were deposited in the Shandong Agricultural University Culture Collection (SAUCC). Taxonomic information on the new taxa was submitted to MycoBank (http://www.mycobank.org).

DNA extraction and amplification

Genomic DNA was extracted from fungal mycelium grown on PDA using cetyltrimethylammonium bromide (CTAB) protocol as described in Guo et al. (2000). The internal transcribed spacer regions with intervening 5.8S nrRNA gene (ITS) and partial beta-tubulin (*tub2*) and translation elongation factor 1-alpha (*tef1*) genes were amplified and sequenced by using primers pairs ITS5/ITS4 (White et al. 1990), T1/Bt2b (Glass and Donaldson 1995; O'Donnell and Cigelnik 1997), and EF1-728F/EF-2 (O'Donnell et al. 1998; Carbone and Kohn 1999).

PCR was performed using an Eppendorf Master Thermocycler (Hamburg, Germany). Amplification reactions were performed in a 50 μL reaction volume, which contained 25 μL Green Taq Mix (Vazyme, Nanjing, China), 2 μL of each forward and reverse primer (10 μM) (Tsingke, Beijing, China), and 2 μL template genomic DNA, to which distilled deionized water was added. PCR parameters were as follows: 94 °C for 5 min, followed by 35 cycles of denaturation at 94 °C for 30 s, annealing at a suitable temperature for 30 s, extension at 72 °C for 1 min and a final elongation step at 72 °C for 7 min. Annealing temperature was 55 °C for ITS, 54 °C for *tub2*, 52 °C for *tef1*. The PCR products were visualised on 1% agarose electrophoresis gel. Sequencing was done bi-directionally, conducted by the Tsingke Biotechnology Company Limited (Qingdao, China). Consensus sequences were obtained using MEGA 7.0 or MEGA-X (Kumar et al. 2016). All sequences generated in this study were deposited in GenBank (Table 1).

Phylogeny

Newly generated sequences in this study were aligned with additional related sequences downloaded from GenBank (Table 1) using MAFFT 7 online service with

the Auto strategy (Katoh et al. 2019, http://mafft.cbrc.jp/alignment/server/). To establish the identity of the isolates at the species level, phylogenetic analyses were conducted first individually for each locus and then as combined analyses of three loci (ITS, *tub2* and *tef1*). Phylogenetic analyses were based on maximum likelihood (ML) and Bayesian inference (BI) for the multi-locus analyses. For BI, the best evolutionary model for each partition was determined using MrModeltest v. 2.3 (Nylander 2004) and incorporated into the analyses. ML and BI were run on the CIPRES Science Gateway portal (https://www.phylo.org/) (Miller et al. 2012) using RaxML-HPC2 on XSEDE v. 8.2.12 (Stamatakis 2014) and MrBayes on XSEDE v. 3.2.7a (Huelsenbeck and Ronquist 2001; Ronquist and Huelsenbeck 2003; Ronquist et al. 2012), respectively. Four Markov chains were run for two runs from random starting trees for 10,000,000 generations (ITS + *tub2* + *tef1*) until the split deviation frequency value < 0.01, and trees were sampled every 1000 generation. The first quarter generations were discarded as burn-in. A majority rule consensus tree of all remaining trees was calculated. The resulting trees were plotted using FigTree v. 1.4.4 (http://tree.bio.ed.ac.uk/software/figtree) and edited with Adobe Illustrator CC 2019. New sequences generated in this study were deposited at GenBank (https://www.ncbi.nlm.nih.gov; Table 1). The final concatenated sequence alignments were deposited in TreeBase (http://purl.org/phylo/treebase/phylows/study/TB2:S29480).

Table 1. Species and GenBank accession numbers of DNA sequences used in this study. New sequences are in bold.

Species	Strain	Host/substrate	Country	GenBank accession number			Reference
				ITS	*tef1*	*tub2*	
Bartalinia robillardoides	CBS 122705 T	*Leptoglossus occidentalis*	Italy	LT853104	LT853202	LT853252	Bonthond et al. 2018
Ciliochorella phanericola	MFLUCC 14-0984 T	*Phanera purpurea*	Thailand	KX789680	–	KX789682	Jiang et al. 2021b
	MFLUCC 12-0310	*Phanera purpurea*	Thailand	KF827444	KF827477	KF827478	Jiang et al. 2021b
Monochaetia castaneae	CFCC 54354 = SM9-1 T	*Castanea mollissima*	China	MW166222	MW199741	MW218515	Jiang et al. 2021b
	SM9-2	*Castanea mollissima*	China	MW166223	MW199742	MW218516	Jiang et al. 2021b
M. dimorphospora	NBRC 9980	*Castanea pubinervis*	Japan	LC146750	–	–	Liu et al. 2019
M. ilicis	KUMCC 15-0520 T	*Ilex* sp.	China	KX984153	–	–	de Silva et al. 2017
	CBS 101009	Air	Japan	MH553953	MH554371	MH554612	Liu et al. 2019
M. junipericola	CBS 143391 T	*Juniperus communis*	Germany	MH107900	MH108021	MH108045	Crous et al. 2018
M. kansensis	PSHI2004Endo1030	*Cyclobalaopsis myrsinaefolia*	China	DQ534044	–	DQ534047	Liu et al. 2006
	PSHI2004Endo1031	*Cyclobalaopsis myrsinaefolia*	China	DQ534045	–	DQ534048	Liu et al. 2006
M. monochaeta	CBS 546.80	Culture contaminant	Netherlands	MH554056	MH554491	MH554732	Liu et al. 2019
	CBS 199.82 T	*Quercus pubescens*	Italy	MH554018	–	MH554694	Liu et al. 2019
	CBS 115004	*Quercus robur*	Netherlands	AY853243	MH554398	MH554639	Liu et al. 2019
M. quercus	CBS 144034 T	*Quercus eduardi*	Mexico	MH554171	MH554606	MH554844	Liu et al. 2019
M. schimae	**SAUCC212201 T**	***Schima superba***	**China**	**MZ577565**	**OK104874**	**OK104867**	**This study**
	SAUCC212202	***Schima superba***	**China**	**MZ577566**	**OK104875**	**OK104868**	**This study**
	SAUCC212203	***Schima superba***	**China**	**MZ577567**	**OK104876**	**OK104869**	**This study**
M. sinensis	HKAS 10065 T	*Quercus* sp.	China	MH115995	–	MH115999	de Silva et al. 2018

Species	Strain	Host/substrate	Country	GenBank accession number			Reference
				ITS	*tef1*	*tub2*	
Neopestalotiopsis acrostichi	MFLUCC 17-1754 T	*Acrostichum aureum*	Thailand	MK764272	MK764316	MK764338	Norphanphoun et al. 2019
N. alpapicalis	MFLUCC 17-2544 T	*Rhizophora mucronata*	Thailand	MK357772	MK463547	MK463545	Kumar et al. 2019
N. aotearoa	CBS 367.54 T	Canvas	New Zealand	KM199369	KM199526	KM199454	Maharachch. et al. 2014
N. asiatica	MFLUCC 12-0286 T	Unidentified tree	China	JX398983	JX399049	JX399018	Maharachch. et al. 2012
	CFCC 54339 = SM32	*Castanea mollissima*	China	MW166224	MW199743	MW218517	Jiang et al. 2021b
N. brachiata	MFLUCC 17-1555 T	*Rhizophora apiculata*	Thailand	MK764274	MK764318	MK764340	Norphanphoun et al. 2019
N. brasiliensis	COAD 2166 T	*Psidium guajava*	Brazil	MG686469	MG692402	MG692400	Bezerra et al. 2018
	CFCC 54341 = ZY4	*Castanea mollissima*	China	MW166229	MW199748	MW218522	Jiang et al. 2021b
	ZY4-2D	*Castanea mollissima*	China	MW166230	MW199749	MW218523	Jiang et al. 2021b
N. chiangmaiensis	MFLUCC 18-0113 T	Dead leaves	Thailand	–	MH388404	MH412725	Tibpromma et al. 2018
N. chrysea	MFLUCC 12-0261 T	*Pandanus* sp.	China	JX398985	JX399051	JX399020	Maharachch. et al. 2012
N. clavispora	MFLUCC 12-0281 T	*Magnolia* sp.	China	JX398979	JX399045	JX399014	Maharachch. et al. 2012
N. cocoes	MFLUCC 15-0152 T	*Cocos nucifera*	Thailand	KX789687	KX789689	–	Norphanphour et al. 2019
N. coffea-arabica	HGUP 4019 T	*Coffea arabica*	China	KF412649	KF412646	KF412643	Song et al. 2013
N. cubana	CBS 600.96 T	Leaf litter	Cuba	KM199347	KM199521	KM199438	Maharachch. et al. 2014
N. dendrobii	MFLUCC 14-0106 T	*Dendrobium cariniferum*	Chiang Rai, Thailand	MK993571	MK975829	MK975835	Ma et al. 2019
N. egyptiaca	CBS 140162 T	*Mangifera indica*	Egypt	KP943747	KP943748	KP943746	Crous et al. 2015
N. ellipsospora	MFLUCC 12-0283 T	Dead plant materials	China	JX398980	JX399047	JX399016	Maharachch. et al. 2012
N. eucalypticola	CBS 264.37 T	*Eucalyptus globulus*	–	KM199376	KM199551	KM199431	Maharachch. et al. 2014
N. foedans	CGMCC 3.9123 T	Mangrove plant	China	JX398987	JX399053	JX399022	Maharachch. et al. 2012
N. formicidarum	CBS 362.72 T	Dead ant	Ghana	KM199358	KM199517	KM199455	Maharachch. et al. 2014
	CBS 115.83	Plant debris	Cuba	KM199344	KM199519	KM199444	Maharachch. et al. 2014
N. hadrolaeliae	COAD 2637 T	*Hadrolaelia jongheana*	Minas Gerais, Brazil	MK454709	MK465122	MK465120	Freitas et al. 2019
N. baikouensis	**SAUCC212271 T**	***Ilex chinensis***	**China**	**OK087294**	**OK104877**	**OK104870**	**This study**
	SAUCC212272	***Ilex chinensis***	**China**	**OK087295**	**OK104878**	**OK104871**	**This study**
N. honoluluana	CBS 114495 T	*Telopea* sp.	USA	KM199364	KM199548	KM199457	Maharachch. et al. 2014
N. iraniensis	CBS 137768 T	*Fragaria ananassa*	Iran	KM074048	KM074051	KM074057	Ayoubi et al. 2016
N. javaensis	CBS 257.31 T	*Cocos nucifera*	Indonesia	KM199357	KM199543	KM199437	Maharachch. et al. 2014
N. macadamiae	BRIP 63737c T	*Macadamia integrifolia*	Australia	KX186604	KX186627	KX186654	Akinsanmi et al. 2017
N. magna	MFLUCC 12-0652 T	*Pteridium* sp.	France	KF582795	KF582791	KF582793	Maharachch. et al. 2012
N. mesopotamica	CBS 336.86 T	*Pinus brutia*	Iraq	KM199362	KM199555	KM199441	Maharachch. et al. 2014
N. musae	MFLUCC 15-0776 T	*Musa* sp.	Thailand	KX789683	KX789685	KX789686	Norphanphour et al. 2019
N. natalensis	CBS 138.41 T	*Acacia mollissima*	South Africa	KM199377	KM199552	KM199466	Maharachch. et al. 2014
N. pandanicola	KUMCC 17-0175 T	Pandanaceae	China	–	MH388389	MH412720	Tibpromma et al. 2018
N. pernambucana	URM 7148-01 T	*Vismia guianensis*	Brazil	KJ792466	KU306739	–	Silvério et al. 2016
N. petila	MFLUCC 17-1738 T	*Rhizophora mucronata*	Thailand	MK764276	MK764320	MK764342	Norphanphoun et al. 2019
N. phangngaensis	MFLUCC 18-0119 T	Pandanaceae	Thailand	MH388354	MH388390	MH412721	Tibpromma et al. 2018
N. piceana	CBS 394.48 T	*Picea* sp.	UK	KM199368	KM199527	KM199453	Maharachch. et al. 2014
	CBS 254.32	*Cocos nucifera*	Indonesia	KM199372	KM199529	KM199452	Maharachch. et al. 2014
	SAUCC210112	***Ficus microcarpa***	**China**	**OK149224**	**OK206436**	**OK206434**	**This study**
	SAUCC210113	***Ficus microcarpa***	**China**	**OK149225**	**OK206437**	**OK206435**	**This study**
N. protearum	CBS 114178 T	*Leucospermum cuneiforme* cv. "Sunbird"	Zimbabwe	JN712498	KM199542	KM199463	Maharachch. et al. 2014

Species	Strain	Host/substrate	Country	GenBank accession number			Reference
				ITS	*tef1*	*tub2*	
N. rhizophorae	MFLUCC 17-1550 T	*Rhizophora mucronata*	Thailand	MK764278	MK764322	MK764344	Norphanphoun et al. 2019
N. rosae	CBS 124745	*Paeonia suffruticosa*	USA	KM199360	KM199524	KM199430	Maharachch. et al. 2014
	CBS 101057 T	*Rosa* sp.	New Zealand	KM199359	KM199523	KM199429	Maharachch. et al. 2014
N. rosicola	CFCC 51992 T	*Rosa chinensis*	China	KY885239	KY885243	KY885245	Norphanphour et al. 2019
	CFCC 51993	*Rosa chinensis*	China	KY885240	KY885244	KY885246	Norphanphour et al. 2019
N. samarangensis	MFLUCC 12-0233 T	*Syzygium samarangense*	Thailand	JQ968609	JQ968611	JQ968610	Maharachch. et al. 2012
N. saprophytica	MFLUCC 12-0282 T	*Magnolia* sp.	China	KM199345	KM199538	KM199433	Maharachch. et al. 2014
N. sichuanensis	CFCC 54338 = SM15-1 T	*Castanea mollissima*	China	MW166231	MW199750	MW218524	Jiang et al. 2021b
N. sonneratae	MFLUCC 17-1745 T	*Sonneronata alba*	Thailand	MK764280	MK764324	MK764346	Norphanphoun et al. 2019
N. steyaertii	IMI 192475 T	*Eucalytpus viminalis*	Australia	KF582796	KF582792	KF582794	Maharachch. et al. 2012
N. surinamensis	CBS 450.74 T	soil under *Elaeis guineensis*	Suriname	KM199351	KM199518	KM199465	Maharachch. et al. 2014
N. thailandica	MFLUCC 17-1730 T	*Rhizophora mucronata*	Thailand	MK764281	MK764325	MK764347	Norphanphoun et al. 2019
N. umbrinospora	MFLUCC 12-0285 T	unidentified plant	China	JX398984	JX399050	JX399019	Maharachch. et al. 2012
N. vitis	MFLUCC 15-1265 T	*Vitis vinifera* cv. "Summer black"	China	KU140694	KU140676	KU140685	Jayawardena et al. 2016
N. zimbabwana	CBS 111495 T	*Leucospermum cunciforme* cv. "Sunbird"	Zimbabwe	JX556231	KM199545	KM199456	Maharachch. et al. 2014
Nonappendiculata quercina	CBS 116061 T	*Quercus suber*	Italy	MH553982	MH554400	MH554641	Liu et al. 2019
	CBS 270.82	*Quercus pubescens*	Italy	MH554025	MH554459	MH554701	Liu et al. 2019
Pestalotiopsis australasiae	CBS 114126 T	*Knightia* sp.	New Zealand	KM199297	KM199499	KM199409	Maharachch. et al. 2014
P. australis	CBS 114193 T	*Grevillea* sp.	Australia	KM199332	KM199475	KM199383	Maharachch. et al. 2014
P. grevilleae	CBS 114127 T	*Grevillea* sp.	Australia	KM199300	KM199504	KM199407	Maharachch. et al. 2014
P. hollandica	CBS 265.33 T	*Sciadopitys verticillata*	The Netherlands	KM199328	KM199481	KM199388	Maharachch. et al. 2014
P. kenyana	CBS 442.67 T	*Coffea* sp.	Kenya	KM199302	KM199502	KM199395	Maharachch. et al. 2014
P. knightiae	CBS 114138 T	*Knightia* sp.	New Zealand	KM199310	KM199497	KM199408	Maharachch. et al. 2014
P. licualicola	HGUP4057 T	*Licuala grandis*	China	KC492509	KC481684	KC481683	Geng et al. 2013
	SAUCC210087	***Ilex chinensis***	**China**	**OK087323**	**OK104879**	**OK104872**	**This study**
	SAUCC210088	***Ilex chinensis***	**China**	**OK087324**	**OK104880**	**OK104873**	**This study**
P. oryzae	CBS 353.69 T	*Oryza sativa*	Denmark	KM199299	KM199496	KM199398	Maharachch. et al. 2014
P. parva	CBS 278.35	*Leucothoe fontanesiana*	–	KM199313	KM199509	KM199405	Maharachch. et al. 2014
P. portugalica	CBS 393.48 T	–	Portugal	KM199335	KM199510	KM199422	Maharachch. et al. 2014
P. spathuliappendiculata	CBS 144035 T	*Phoenix canariensis*	Australia	MH554172	MH554607	MH554845	Liu et al. 2019
Pseudopestalotiopsis cocos	CBS 272.29 T	*Cocos nucifera*	Indonesia	KM199378	KM199553	KM199467	Maharachch. et al. 2014
Pse. elaeidis	CBS 413.62 T	*Elaeis guineensis*	Nigeria	MH554044	MH554479	MH554720	Liu et al. 2019
Pse. indica	CBS 459.78 T	*Rosa sinensis*	India	KM199381	KM199560	KM199470	Maharachch. et al. 2014
Seiridium papillatum	CBS 340.97 T	*Eucalyptus delegatensis*	Australia	LT853102	MH554468	LT853250	Bonthond et al. 2018
Seir. phylicae	CBS 133587 T	*Phylica arborea*	Tristan da Cunha	LT853091	LT853188	LT853238	Bonthond et al. 2018

Isolates marked with "T" are ex-type or ex-epitype strains.

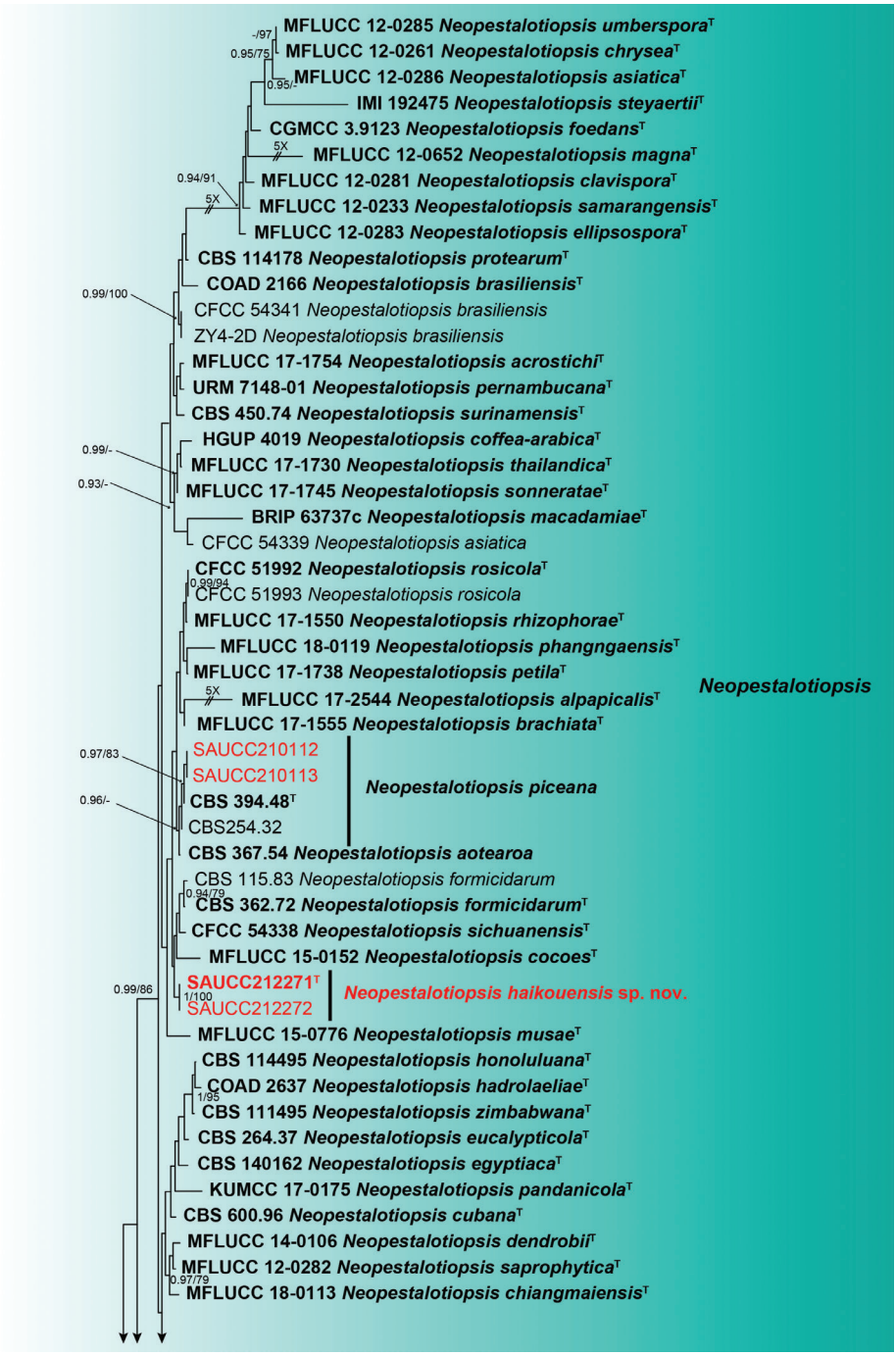

Figure 1. Phylogram of Sporocadaceae based on combined ITS, *tub2* and *tef1* sequences. The BI and ML bootstrap support values above 0.90 and 70% are shown at the first and second position, respectively. The tree is rooted to *Bartalinia robillardoides* (CBS 122705), ex-type or ex-epitype cultures are indicated in bold face. Strains from the current study are in red. Some branches were shortened according to the indicated muliplers.

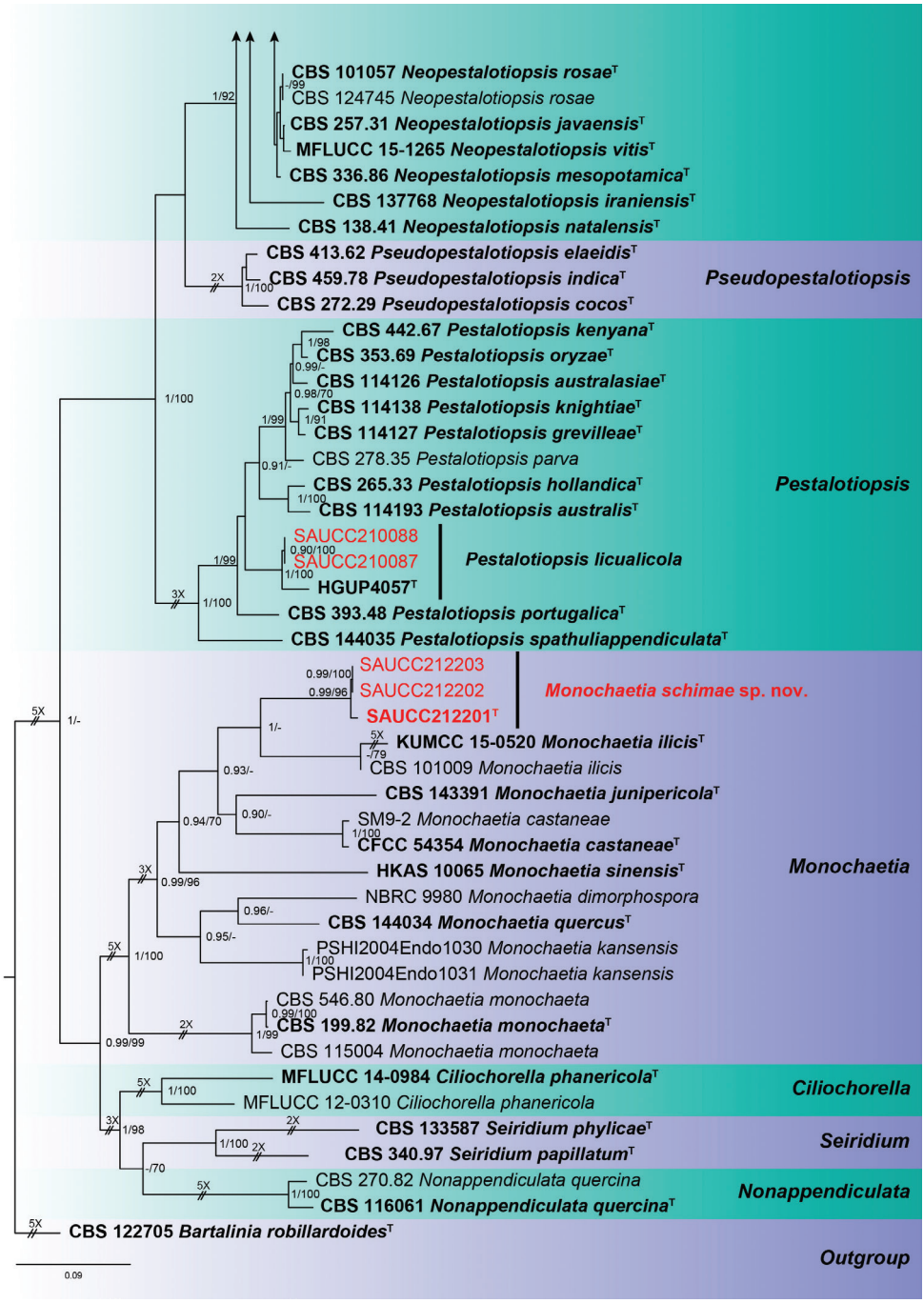

Figure 1. Continued.

Result

Phylogenetic analyses

Nine strains of Sporocadaceae isolated from plant hosts from Hainan, China, were grown in culture and used for analyses of molecular sequence data. The combined dataset of ITS-*tub2*-*tef1* has an aligned length of 2285 total characters (ITS: 1–638, *tub2*: 639–1558, *tef1*: 1559–2285) including gaps, of which 869 characters are constant, 292 variable and parsimony-uninformative, and 1124 parsimony-informative. For the BI and ML analyses, the substitution model GTR+G for ITS, HKY+I+G for *tub2* and GTR+I+G for *tef1* were selected and incorporated into the analyses. The MCMC analysis of the three concatenated genes run for 7,795,000 generations, resulting in 7796 trees. The ML tree topology confirmed the tree topologies obtained from the BI analyses, and therefore, only the ML tree is presented (Fig. 1).

Bayesian posterior probability (≥ 0.90) and ML bootstrap support values (≥ 70%) are shown as first and second position above nodes. The 96 strains were assigned to 75 species clades based on the three gene loci phylogeny (Fig. 1). Based on the multilocus phylogeny and morphology, nine isolates were assigned to four species, including *Monochaetia schimae* sp. nov., *Neopestalotiopsis haikouensis* sp. nov., *Neopestalotiopsis piceana* and *Pestalotiopsis licualicola*.

Taxonomy

***Monochaetia schimae* Z. X. Zhang, J. W. Xia & X. G. Zhang, sp. nov.**
MycoBank No: 841381
Fig. 2

Type. China, Hainan Province: East Harbour National Nature Reserve, on diseased leaves of *Schima superba*, 23 May 2021, Z.X. Zhang (holotype HSAUP212201; ex-type living culture SAUCC212201).

Etymology. Name refers to the genus of the host plant *Schima superba*.

Description. Leaf spots irregular, pale brown in centre, brown to tan at margin. Sexual morph not observed. Asexual morph on PDA: Conidiomata solitary, scattered, black, raising above surface of culture medium, subglobose, exuding black conidial droplets from central ostioles after 10 days in light at 25 °C. Conidiophores cylindrical, hyaline, smooth-walled. Conidiogenous cells 9.0–16.5 × 1.2–2.2 μm, phialidic, ampulliform, discrete, hyaline, smooth, thin-walled. Conidia 18–24 × 4.5–6.0 μm, mean ± SD = 20.5 ± 1.1 × 5.5 ± 0.4 μm, fusiform, tapering at both ends, 4-septate; apical cell 2.0–4.0 μm long, conical, hyaline and smooth-walled; three median cells doliiform, 12.5–15.5 μm long, mean ± SD = 14.2 ± 0.7 μm, olivaceous, rough-walled, upper second cell 3.8–5.3 μm long, upper third cell 3.4–5.0 μm

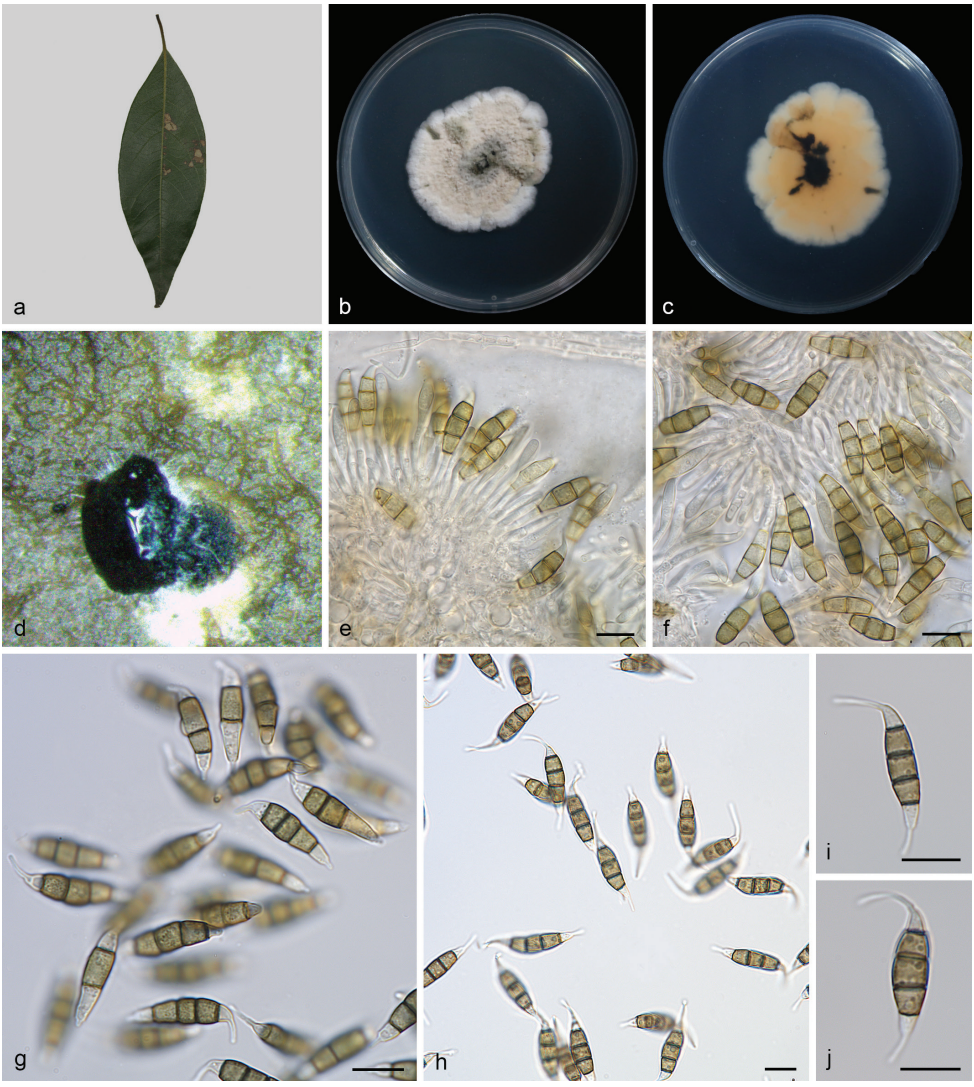

Figure 2. *Monochaetia schimae* (SAUCC212201, ex-type) **a** diseased leaf of *Schima superba* **b** surface of colony after 15 days on PDA **c** reverse of colony after 15 days on PDA **d** conidiomata **e, f** conidiogenous cells with conidia **g–j** conidia. Scale bars: 10 μm (**e–j**).

long, upper fourth cell 4.4–5.4 μm long; basal cell 2.2–4.5 μm long, conical, hyaline and smooth-walled; apical appendage 7.0–12.5 μm long (mean = 9.2 μm), single, unbranched, central, tubular, filiform; basal appendage 2.5–5.0 μm long, single, unbranched tubular, filiform.

Culture characteristics. Colonies on PDA 39.0–45.0 mm in diameter after 15 days at 25 °C in darkness, growth rate 2.5–3.0 mm/day, irregularly circular, raised, dense surface with lobate edge, zonate in different sectors, light brown at the margin, brown at the centre; reverse brown at the margin, dark brown at the centre.

Additional specimen examined. China, Hainan Province: East Harbour National Nature Reserve, 23 May 2021, Z.X. Zhang. On diseased leaves of *Schima superba*, paratype HSAUP212202, living culture SAUCC212202; on diseased leaves of *Schima superba*, paratype HSAUP212203, living culture SAUCC212203.

Notes. *Monochaetia schimae* is introduced based on the multi-locus phylogenetic analysis, with three isolates clustering separately in a well-supported clade (BI/ML = 0.99/96). *Monochaetia schimae* is phylogenetically close to *M. castaneae* from leaves of *Castanea mollissima*, *M. ilicis* from leaves of *Ilex* sp., and *M. junipericola* from twigs of *Juniperus communis*. However, *Monochaetia schimae* differs from *M. castaneae* by 148 nucleotides (11/463 in ITS, 89/743 in *tub2* and 48/403 in *tef1*), from *M. ilicis* by 94 nucleotides (18/526 in ITS, 32/698 in *tub2* and 44/456 in *tef1*), and from *M. junipericola* by 91 nucleotides (10/524 in ITS, 40/411 in *tub2* and 41/304 in *tef1*). Furthermore, they are distinguished by hosts and conidial sizes (18.0–24.0 × 4.5–6.0 µm in *M. schimae* vs. 18.8–27.3 × 4.7–6.6 µm in *M. castaneae* vs. 20.0–27.0 × 5.0–8.0 µm in *M. ilicis* vs. 22.0–28.0 × 5.0–7.0 µm in *M. junipericola*). In morphology, *Monochaetia castaneae* differs from *M. schimae* by the colour of colonies (cinnamon vs. brown), *Monochaetia ilicis* differs from *M. schimae* by the colour of median cells (brown vs. olivaceous), and *M. junipericola* differs from *M. schimae* by longer conidiogenous cells (10.0–30.0 µm vs. 9.0–16.5 µm) (de Silva et al. 2017; Crous et al. 2018; Jiang et al. 2021b).

***Neopestalotiopsis haikouensis* Z. X. Zhang, J. W. Xia & X. G. Zhang, sp. nov.**
MycoBank No: 841382
Fig. 3

Type. China, Hainan Province, Haikou City: East Harbour National Nature Reserve, on diseased leaves of *Ilex chinensis*. 23 May 2021, Z.X. Zhang (holotype HSAUP212271; ex-type living culture SAUCC212271).

Etymology. Named after the host location, Haikou City.

Description. Leaf spots irregular, grey white in centre, brown to tan at margin. Sexual morph not observed. Asexual morph on PDA: Conidiomata globose to clavate, solitary or confluent, embedded or semi-immersed to erumpent, dark brown, exuding globose, dark brown to black conidial masses. Conidiophores indistinct, often reduced to conidiogenous cells. Conidiogenous cells discrete, subcylindrical to ampulliform, hyaline, 5.0–10.0 × 2.0–6.0 µm, apex 1.0–2.0 µm diam. Conidia fusoid, ellipsoid, straight to slightly curved, 4-septate, 16.0–22.0 × 4.5–7.0 µm, mean ± SD = 20.0 ± 1.8 × 5.5 ± 0.4 µm; basal cell conical with a truncate base, hyaline, rugose and thin-walled, 3.0–4.5 µm long; three median cells doliiform, 11.5–15.0 µm long, mean ± SD = 13.2 ± 1.0 µm, wall rugose, septa darker than the rest of the cell, second cell from the base pale brown, 3.5–5.5 µm long; third cell honey-brown, 4.0–6.0 µm long; fourth cell brown, 3.8–5.7 µm long; apical cell 2.5–5.5 µm long, hyaline, cylindrical to subcylindrical, thin- and smooth-walled; with 2–3 tubular apical appendages (mostly 3), arising from the apical crest, unbranched, filiform, 13.5–24.0 µm long, mean ± SD = 19.1 ± 3.5 µm; basal appendage 2.0–7.0 µm long, single, tubular, unbranched, centric.

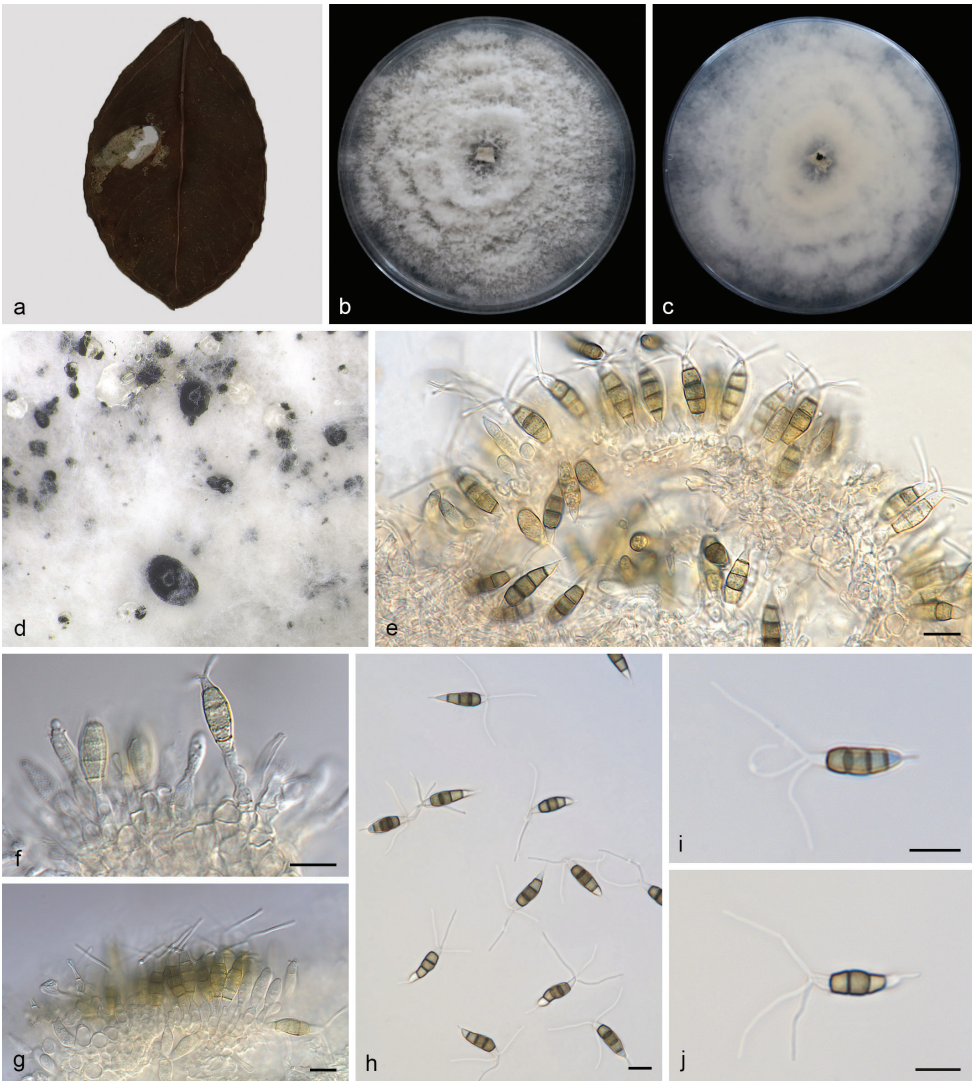

Figure 3. *Neopestalotiopsis haikouensis* (SAUCC212271, ex-type) **a** diseased leaf of *Ilex chinensis* **b** surface of colony after 7 days on PDA **c** reverse of colony after 7 days on PDA **d** conidiomata **e–g** conidiogenous cells with conidia **h–j** conidia. Scale bars: 10 μm (**e–j**).

Culture characteristics. Colonies on PDA occupying an entire 90 mm petri dish in 7 days at 25 °C in darkness, growth rate of 7.0–14.0 mm/day, edge undulate, white to grey white, with moderate aerial mycelium on the surface, with black, gregarious conidiomata; reverse similar in colour.

Additional specimen examined. China, Hainan Province: East Harbour National Nature Reserve, 23 May 2021, Z.X. Zhang. On diseased leaves of *Ilex chinensis*, paratype HSAUP212272, living culture SAUCC212272.

Notes. Phylogenetic analysis of a combined three-gene ITS-*tub2-tef1* showed that *Neopestalotiopsis haikouensis* formed an independent clade with full-supported (BI/ML = 1/100, Fig. 1) and is phylogenetically distinct from *N. cocoes* (MFLUCC 15-0152), *N. formicidarum* (CBS 362.72) and *N. sichuanensis* (CFCC 54338). *Neopestalotiopsis haikouensis* can be distinguished from the phylogenetically most closely related species *N. cocoes* by narrower conidia (4.5–7.0 vs. 7.5–9.5 μm), *N. formicidarum* by smaller conidia (16.0–22.0 × 4.5–7.0 vs. 20.0–29.0 × 7.5–9.5 μm), and *N. sichuanensis* by shorter conidia (16.0–22.0 vs. 23.2–32.8 μm). Furthermore, some species were reported from the same host genus *Ilex*, including *Pestalotia neglecta*, *Pestalotiopsis annulata*, *P. humicola* and *P. ilicis*. After comparison, *P. humicola* was closest to *N. haikouensis* in morphology, but with 78/588 differences in the ITS region (Maharachch. et al. 2014; Liu et al. 2019; Jiang et al. 2021b).

***Neopestalotiopsis piceana* S.S.N. Maharachch., K.D. Hyde & P.W. Crous, Studies in Mycology 79:146. (2014)**
Fig. 4

Description. Leaf spots irregular, pale brown in centre, brown to tan at margin. Asexual morph on PDA: Conidiomata solitary, globose to clavate, semi-immersed, brown to black; exuding globose, dark brown to black conidial masses. Conidiophores reduced to conidiogenous cells. Conidiogenous cells discrete, ampulliform to lageniform, hyaline, smooth and thin walled, simple, 4.0–12.0 × 2.0–10.0 μm, apex 2.0–5.0 μm diam. Conidia ellipsoid to clavate, straight to slightly curved, 4-septate, 19.5–26.5 × 5.5–7.0 μm, mean ± SD = 22.7 ± 0.8 × 6.1 ± 0.4 μm; somewhat constricted at septa; basal cell obconic with truncate base, rugose and thin-walled, 2.7–5.0 μm long; three median cells 12.0–16.0 μm long, mean ± SD = 14.7 ± 0.9 μm, doliiform, verruculose, versicoloured, septa darker than the rest of the cell, second cell from base pale brown, 4.0–5.7 μm long; third cell dark brown, 3.5–5.2 μm long; fourth cell brown, 3.8–5.8 μm long; apical cell obconic, hyaline, thin and smooth-walled, 2.5–5.2 μm long; with 1–3 tubular apical appendages, arising from the apical crest, flexuous, unbranched, 21.0–32.0 μm long, mean ± SD = 24.8 ± 3.5 μm; basal appendage single, tubular, unbranched, centric, 2.7–6.5 μm long.

Culture characteristics. Colonies on PDA incubated at 25 °C in the dark with an average radial growth rate of 9.0–14.0 mm/day and occupying an entire 90 mm petri dish in 7 d, with edge undulate, whitish, aerial mycelium on surface, fruiting bodies black, concentric; reverse of culture yellow to pale brown.

Specimen examined. China, Hainan Province: Five Fingers Group Scenic Area, 20 May 2021, Z.X. Zhang. On diseased leaves of *Ficus microcarpa*, HSAUP210112, living culture SAUCC210112; on diseased leaves of *Ficus microcarpa*, HSAUP210113, living culture SAUCC210113.

Notes. In the present study, two strains (SAUCC210112 and SAUCC210113) from symptomatic leaves of *Ficus microcarpa* were clustered with *Neopestalotiopsis piceana*

clade (Maharachch. et al. 2014) based on phylogeny (Fig. 1). Morphologically, our strains were the same as *N. piceana*, which was originally described with an asexual morph on wood of *Picea* sp., *Cocos nucifera* and fruit of *Mangifera indica*. The sexual morph of *N. piceana* was undetermined yet. *Neopestalotiopsis piceana* was a new record for China and first reported from *Ficus macrocarpa* (Moraceae).

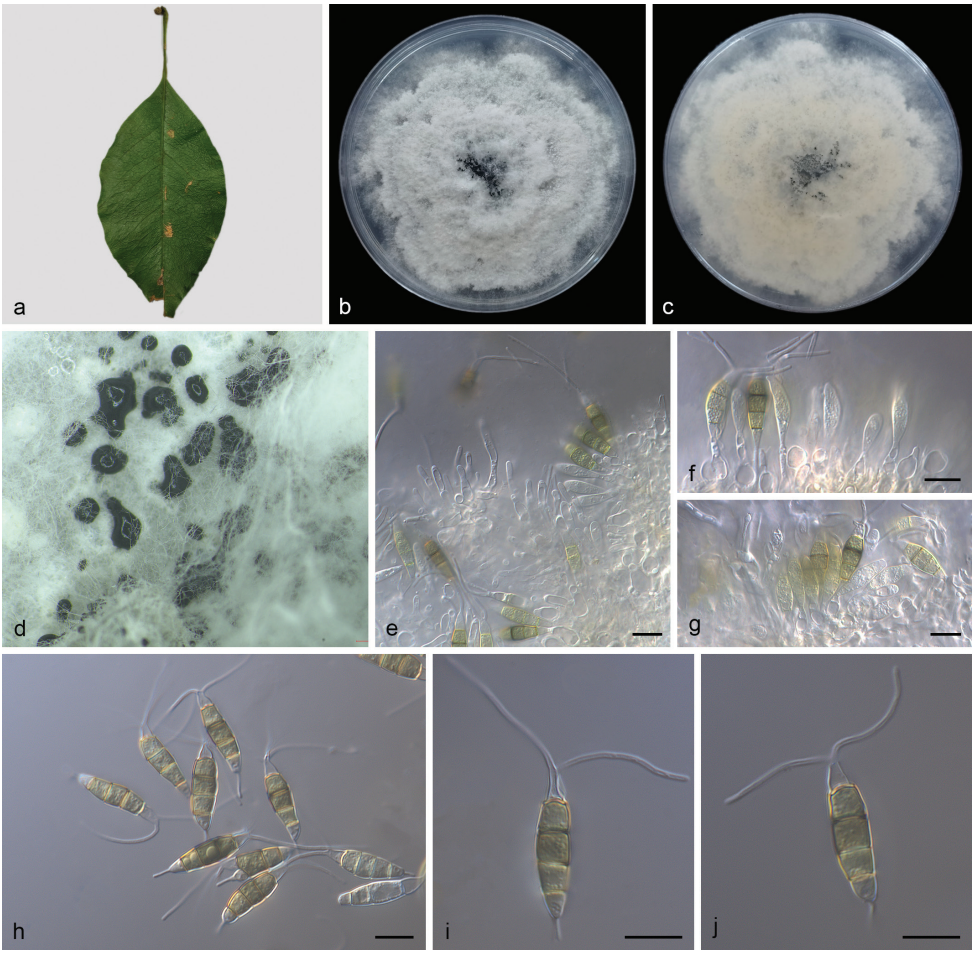

Figure 4. *Neopestalotiopsis piceana* (SAUCC210112) **a** diseased leaf of *Ficus microcarpa* **b** surface of colony after 7 days on PDA **c** reverse of colony after 7 days on PDA **d** conidiomata **e–g** conidiogenous cells with conidia **h–j** conidia. Scale bars: 10 μm (**e–j**).

Pestalotiopsis licualicola **K. Geng, Y. Song, K.D. Hyde & Yong Wang bis, Phytotaxa 88 (3):51. (2013)**
Fig. 5

Description. Leaf spots irregular, pale brown in centre, brown to tan at margin. Asexual morph on PDA: Conidiomata solitary, scattered, black, raising above surface of culture

medium, subglobose. Conidiophores cylindrical, hyaline, smooth-walled. Conidiophores often indistinct. Conidiogenous cells discrete, hyaline, simple, filiform, 5.5–10.0 µm long. Conidia 18.0–24.5 × 4.0–5.5 µm, mean ± SD = 20.5 ± 1.9 × 5.3 ± 0.3 µm, fusiform, straight to slightly curved, 4-septate, smooth, greyish brown; basal cell conical, hyaline, thin-walled, 2.8–6.0 µm long; with three median cells, dark brown, concolorous, septa and periclinal walls darker than the rest of the cell, together 11.5–16.0 µm long, mean ± SD = 13.2 ± 1.2 µm; second cell from base 3.4–5.5 µm; third cell 3.3–4.7 µm; fourth cell 3.5–5.1 µm; apical cell hyaline, conic to subcylindrical, 3.1–5.3 µm; with 1–3

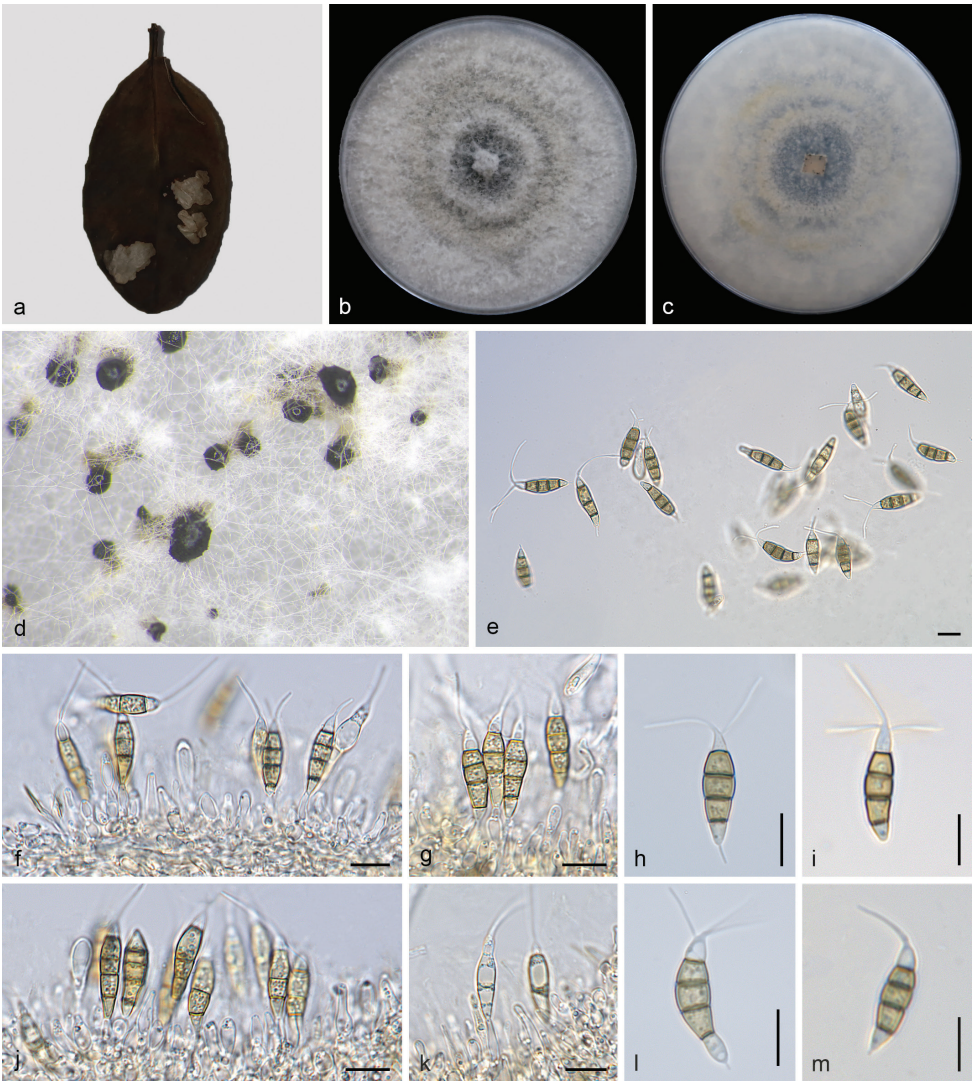

Figure 5. *Pestalotiopsis licualicola* (SAUCC210087) **a** diseased leaf of *Ilex chinensis* **b** surface of colony after 7 days on PDA **c** reverse of colony after 7 days on PDA **d** conidiomata **f, g, j, k** conidiogenous cells with conidia **e, h, i, l, m** conidia. Scale bars: 10 µm (**e–m**).

tubular apical appendages (mostly 1) without knobs, arising from the apex of the apical cell, 10.0–20.5 μm long, mean ± SD = 16.0 ± 4.0 μm; basal appendage filiform, short.

Culture characteristics. Colonies on PDA reaching 70.0–80.0 mm diam after 7 d at 25 °C, growth rate 9.0–12.0 mm/day, edge entire, whitish to pale honey coloured, with sparse aerial mycelium on the surface, with black, gregarious conidiomata; reverse similar in colour.

Specimen examined. China, Hainan Province: East Harbour National Nature Reserve, 23 May 2021, Z.X. Zhang. On diseased leaves of *Ilex chinensis*, HSAUP210087, living culture SAUCC210087; on diseased leaves of *Ilex chinensis*, HSAUP210088, living culture SAUCC210088.

Notes. In the present study, two strains (SAUCC210087 and SAUCC210088) from symptomatic leaves of *Ilex chinensis* were clustered to *Pestalotiopsis licualicola* clade (Geng et al. 2013) based on phylogeny (Fig. 1). Morphologically, our strains were the same as *P. licualicola*, which was originally described with an asexual morph on leaves of *Licuala grandis* in China. The sexual morph of *P. licualicola* was undetermined yet. This is the first time this species has been reported in *Ilex chinensis* (Aquifoliaceae) in China.

Discussion

Based on phylogeny and morphology, nine strains from three host species (*Ficus microcarpa*, *Ilex chinensis* and *Schima superba*) were described as well as two new species (*Monochaetia schimae* sp. nov. and *Neopestalotiopsis haikouensis* sp. nov.) and two known species (*Neopestalotiopsis piceana* and *Pestalotiopsis licualicola*). In the genus *Monochaetia*, most species were found on Fagaceae hosts, including *Castanea pubinervis* (*Monochaetia dimorphospora*), *Castanea mollissima* (*Monochaetia castaneae*), *Quercus pubescens* (*Monochaetia monochaeta*) and etc. In our study, the species of *Monochaetia* (*M. schimae*) was first reported from *Schima superba* (Theaceae). *Ilex* was widely grown as an evergreen tree all over the world and isolated many pathogens, endophytes or saprophytes (Alfieri et al. 1984; Maharachch. et al. 2014; de Silva et al. 2017; Solarte et al. 2018). More than 100 strains (Xylariales) have been isolated from the genus *Ilex*. Among these, there was 13 pestalotia-like fungi, and we compare morphology with my new collection. In morphology, the conidia size of *Pestalotiopsis humicola* is similar to *Neopestalotiopsis haikouensis*. Phylogenetic analyses of Maharachch. et al. (2014) and the current study show *Neopestalotiopsis* and *Pestalotiopsis* are different genus. The known species *Neopestalotiopsis piceana* was described from *Picea* sp. (Pinaceae) in United Kingdom (Maharachch. et al. 2014) and *Pestalotiopsis licualicola* was described from *Licuala grandis* (Palmaceae) in China (Geng et al. 2013). In this study, *Neopestalotiopsis piceana* was a new record for China and first reported from *Ficus macrocarpa* (Moraceae), *Pestalotiopsis licualicola* was first reported from *Ilex chinensis* (Aquifoliaceae) in China, so we described and illustrated *N. piceana* and *P. licualicola* again. Species in genera have multi-septate and more or less fusiform conidia with a single apical and basal appendage (*Monochaetia*, *Seiridium*); other genera do not form appendages (*Nonappendiculata*) or have 2–4 appendages (*Pestalotiopsis*, *Ciliochorella*,

Neopestalotiopsis, *Pseudopestalotiopsis*) (Maharachch. et al. 2014; Bonthond et al. 2018; Liu et al. 2019). Our study supported this phenomenon.

As many pestalotioid species have overlapping morphological traits, sequence data is essential to resolve these three genera and introduce new species (Jeewon et al. 2002; de Silva et al. 2017; Norphanphoun et al. 2019). Combined gene sequences of ITS, *tub2* and *tef1* can provide a better resolution for *Monochaetia*. However, more genes are needed to provide better resolution and support in *Neopestalotiopsis*. In the previous studies, members of Sporocadaceae are of particular interest with regard to the production of secondary metabolites, e.g. *Bartalinia*, *Morinia* and *Pestalotiopsis* (Collado et al. 2006; Gangadevi and Muthumary 2008; Liu et al. 2009). *Pestalotiopsis fici* was shown to possess a very high number of gene clusters involved in bioactive compound synthesis (Wang et al. 2016). Owing to *Pestalotiopsis* and other genus in this family sharing the same evolutionary history, it is important to report novel species and screen for novel metabolites in future studies.

Acknowledgements

This work was jointly supported by the National Natural Science Foundation of China (nos. 31900014, U2002203, 31750001) and National Science and Technology Fundamental Resources Investigation Program of China (2019FY100704).

References

Akinsanmi OA, Nisa S, Jeff-Ego OS, Shivas RG, Drenth A (2017) Dry Flower Disease of *Macadamia* in Australia Caused by *Neopestalotiopsis macadamiae* sp. nov. and *Pestalotiopsis macadamiae* sp. nov. Plant Disease 101(1): 45–53. https://doi.org/10.1094/PDIS-05-16-0630-RE

Alfieri Jr SA, Langdon KR, Wehlburg C, Kimbrough JW (1984) Index of Plant Diseases in Florida (Revised). Florida Dept. Agric. And Consumer Serv., Div. Plant Ind. Bull. 11: 1–389.

Allescher A (1902) Fungi Imperfecti: Gefärbt-sporige Sphaerioideen. Rabenhorst's Kryptogamen-Flora von Deutschland. Österreich und der Schweiz. 2nd edn. Kummer, Leipzig, 65–128.

Ayoubi N, Soleimani MJ (2016) Strawberry Fruit Rot Caused by *Neopestalotiopsis iranensis* sp. nov., and *N. mesopotamica.* Current Microbiology 2016(72): 329–336. https://doi.org/10.1007/s00284-015-0955-y

Barber PA, Crous PW, Groenewald JZ, Pascoe IG, Keane P (2011) Reassessing *Vermisporium* (Amphisphaeriaceae), a genus of foliar pathogens of eucalypts. Persoonia 27(1): 90–118. https://doi.org/10.3767/003158511X617381

Bezerra JDP, Machado AR, Firmino AL, Rosado AWC, Souza CAF, Souza-Motta CM, Freire KTLS, Paiva LM, Magalhaes OMC, Pereira OL, Crous PW, Oliveira TGL, Abreu VP, Fan XL (2018) Mycological Diversity Description I. Acta Botanica Brasílica 32(4): 656–666. https://doi.org/10.1590/0102-33062018abb0154

Bonthond G, Sandoval-Denis M, Groenewald JZ, Crous PW (2018) *Seiridium* (Sporocadaceae): An important genus of plant pathogenic fungi. Persoonia 40(1): 96–118. https://doi.org/10.3767/persoonia.2018.40.04

Carbone I, Kohn LM (1999) A method for designing primer sets for speciation studies in filamentous Ascomycetes. Mycologia 91(3): 553–556. https://doi.org/10.2307/3761358

Collado J, Platas G, Bills GF, Basilio Á, Vicente F, Rubén Tormo J, Hernández P, Teresa Díez M, Peláez F (2006) Studies on *Morinia*: Recognition of *Morinia longiappendiculata* sp. nov. as a new endophytic fungus, and a new circumscription of *Morinia pestalozzioides.* Mycologia 98(4): 616–627. https://doi.org/10.1080/15572536.2006.11832665

Crous PW, Wingfield MJ, Le RJJ, Richardson DM, Strasberg D, Shivas RG, Alvarado P, Edwards J, Moreno G, Sharma R, Sonawane MS, Tan YP, Altés A, Barasubiye T, Barnes CW, Blanchette RA, Boertmann D, Bogo A, Carlavilla JR, Cheewangkoon R, Daniel R, de Beer ZW, Yáñez-Morales M de Jesús, Duong TA, Fernández-Vicente J, Geering ADW, Guest DI, Held BW, Heykoop M, Hubka V, Ismail AM, Kajale SC, Khemmuk W, Kolařík M, Kurli R, Lebeuf R, Lévesque CA, Lombard L, Magista D, Manjón JL, Marincowitz S, Mohedano JM, Nováková A, Oberlies NH, Otto EC, Paguigan ND, Pascoe IG, Pérez-Butrón JL, Perrone G, Rahi P, Raja HA, Rintoul T, Sanhueza RMV, Scarlett K, Shouche YS, Shuttleworth LA, Taylor PWJ, Thorn RG, Vawdrey LL, Solano-Vidal R, Voitk A, Wong PTW, Wood AR, Zamora JC, Groenewald JZ (2015) Fungal planet description sheets: 371–399. Persoonia 35(1): 264–327. https://doi.org/10.3767/003158515X690269

Crous PW, Schumacher RK, Wingfield MJ, Akulov A, Denman S, Roux J, Braun U, Burgess T, Carnegie AJ, Vaczy KZ, Guatimosim E, Schwartsburd PB, Barreto RW, Hernandez-Restrepo M, Lombard L, Groenewald JZ (2018) New and Interesting Fungi. 1. Fungal Systematics and Evolution 1(1): 169–215. https://doi.org/10.3114/fuse.2018.01.08

de Silva N, Phookamsak R, Maharachchikumbura SSN, Thambugala KM, Jayarama Bhat D, Al-Sadi AM, Lumyong S, Hyde KD (2017) *Monochaetia ilexae* sp. nov. (Pestalotiopsidaceae) from Yunnan Province in China. Phytotaxa 291(2): 123–132. https://doi.org/10.11646/phytotaxa.291.2.3

de Silva N, Maharachchikumbura SSN, Thambugala KM, Jayarama Bhat D, Phookamsak R, Al-Sadi AM, Lumyong S, Hyde KD (2018) *Monochaetia sinensis* sp. nov. from Yunnan Province in China. Phytotaxa 375(1): 59–69. https://doi.org/10.11646/phytotaxa.375.1.2

Freitas EFS, de Silva N, Barros MVP, Kasuya MCM (2019) *Neopestalotiopsis hadrolaeliae* sp. nov., a new endophytic species from the roots of the endangered orchid *Hadrolaelia jongheana* in Brazil. Phytotaxa 416(3): 211–220. https://doi.org/10.11646/phytotaxa.416.3.2

Gangadevi V, Muthumary J (2008) Taxol, an anticancer drug produced by an endophytic fungus *Bartalinia robillardoides* Tassi, isolated from a medicinal plant, *Aegle marmelos* Correa ex Roxb. World Journal of Microbiology & Biotechnology 24(5): 717–724. https://doi.org/10.1007/s11274-007-9530-4

Gao YH, Sun W, Su YY, Cai L (2014) Three new species of *Phomopsis* in Gutianshan Nature Reserve in China. Mycological Progress 13(1): 111–121. https://doi.org/10.1007/s11557-013-0898-2

Geng K, Zhang B, Song Y, Hyde KD, Kang JC, Wang Y (2013) A new species of *Pestalotiopsis* from leaf spots of *Licuala grandis* from Hainan, China. Phytotaxa 88(3): 49–54. https://doi.org/10.11646/phytotaxa.88.3.2

Glass NL, Donaldson GC (1995) Development of primer sets designed for use with the PCR to amplify conserved genes from filamentous ascomycetes. Applied and Environmental Microbiology 61(4): 1323–1330. https://doi.org/10.1128/aem.61.4.1323-1330.1995

Griffiths DA, Swart HJ (1974) Conidial structure in two species of *Pestalotiopsis.* Transactions of the British Mycological Society 62(2): 295–304. https://doi.org/10.1016/S0007-1536(74)80038-0

Guba EF (1956) *Monochaetia* and *Pestalotia* vs. *Truncatella*, *Pestalotiopsis* and *Pestalotia.* Annals of Microbiology 7: 74–76.

Guba EF (1961) Monograph of *Pestalotia* and *Monochaetia*. Harvard University Press, Cambridge.

Guo LD, Hyde KD, Liew ECY (2000) Identification of endophytic fungi from *Livistona chinensis* based on morphology and rDNA sequences. The New Phytologist 147(3): 617–630. https://doi.org/10.1046/j.1469-8137.2000.00716.x

Huelsenbeck JP, Ronquist F (2001) MRBAYES: Bayesian inference of phylogeny. Bioinformatics (Oxford, England) 17(17): 754–755. https://doi.org/10.1093/bioinformatics/17.8.754

Jaklitsch WM, Gardiennet A, Voglmayr H (2016) Resolution of morphology-based taxonomic delusions: *Acrocordiella*, *Basiseptospora*, *Blogiascospora*, *Clypeosphaeria*, *Hymenopleella*, *Lepteutypa*, *Pseudapiospora*, *Requienella*, *Seiridium* and *Strickeria.* Persoonia 37(1): 82–105. https://doi.org/10.3767/003158516X690475

Jayawardena RS, Zhang W, Liu M, Maharachchikumbura SSN, Zhou Y, Huang JB, Nilthong S, Wang ZY, Li XH, Yan JY, Hyde KD (2015) Identification and characterization of *Pestalotiopsis*-like fungi related to grapevine diseases in China. Fungal Biology 119(5): 348–361. https://doi.org/10.1016/j.funbio.2014.11.001

Jayawardena RS, Liu M, Maharachchikumbura SSN, Zhang W, Xing QK, Hyde KD, Nilthong S, Li XH, Yan JY (2016) *Neopestalotiopsis vitis* sp. nov. causing grapevine leaf spot in China. Phytotaxa 258(1): 63–74. https://doi.org/10.11646/phytotaxa.258.1.4

Jeewon R, Liew ECY, Hyde KD (2002) Phylogenetic relationships of *Pestalotiopsis* and allied genera inferred from ribosomal DNA sequences and morphological characters. Molecular Phylogenetics and Evolution 25(3): 378–392. https://doi.org/10.1016/S1055-7903(02)00422-0

Jiang N, Voglmayr H, Bian DR, Piao CG, Wang SK, Li Y (2021a) Morphology and Phylogeny of *Gnomoniopsis* (Gnomoniaceae, Diaporthales) from Fagaceae Leaves in China. Journal of Fungi (Basel, Switzerland) 7(10): e792. https://doi.org/10.3390/jof7100792

Jiang N, Fan XL, Tian CM (2021b) Identification and Characterization of Leaf-Inhabiting Fungi from *Castanea* Plantations in China. Journal of Fungi (Basel, Switzerland) 7(1): e64. https://doi.org/10.3390/jof7010064

Katoh K, Rozewicki J, Yamada KD (2019) MAFFT online service: Multiple sequence alignment, interactive sequence choice and visualization. Briefings in Bioinformatics 20(4): 1160–1166. https://doi.org/10.1093/bib/bbx108

Kumar S, Stecher G, Tamura K (2016) MEGA7: Molecular Evolutionary Genetics Analysis Version 7.0 for Bigger Datasets. Molecular Biology and Evolution 33(7): 1870–1874. https://doi.org/10.1093/molbev/msw054

Kumar V, Cheewangkoon R, Gentekaki E, Maharachchikumbura SSN, Brahmanage RS, Hyde KD (2019) *Neopestalotiopsis alpapicalis* sp. nov. a new endophyte from tropical mangrove trees in Krabi Province (Thailand). Phytotaxa 393(3): 251–262. https://doi.org/10.11646/phytotaxa.393.3.2

Liu L, Li Y, Liu SC, Zheng ZH, Chen XL, Zhang H, Guo LD, Che YS (2009) Chloropestolide A, an antitumor metabolite with an unprecedented spiroketal skeleton from *Pestalotiopsis fici.* Organic Letters 11(13): 2836–2839. https://doi.org/10.1021/ol901039m

Liu F, Bonthond G, Groenewald JZ, Cai L, Crous PW (2019) Sporocadaceae, a family of coelomycetous fungi with appendage-bearing conidia. Studies in Mycology 92(1): 287–415. https://doi.org/10.1016/j.simyco.2018.11.001

Ma XY, Maharachchikumbura SSN, Chen BW, Hyde KD, Mckenzie EHC, Chomnunti P, Kang JC (2019) Endophytic pestalotiod taxa in *Dendrobium* orchids. Phytotaxa 419(3): 268–286. https://doi.org/10.11646/phytotaxa.419.3.2

Maharachchikumbura SSN, Guo LD, Chukeatirote E, Bahkali AH, Hyde KD (2011) *Pestalotiopsis* – morphology, phylogeny, biochemistry and diversity. Fungal Diversity 50(1): 167–187. https://doi.org/10.1007/s13225-011-0125-x

Maharachchikumbura SSN, Guo LD, Cai L, Chukeatirote E, Wu WP, Sun X, Crous PW, Jayarama Bhat D, McKenzie EHC, Bahkali AH, Hyde KD (2012) A multi-locus backbone tree for *Pestalotiopsis*, with a polyphasic characterization of 14 new species. Fungal Diversity 2012(56): 95–129. https://doi.org/10.1007/s13225-012-0198-1

Maharachchikumbura SSN, Guo LD, Chukeatirote E, McKenzie EHC, Hyde KD (2013) A destructive new disease of *Syzygium samarangense* in Thailand caused by the new species *Pestalotiopsis samarangensis.* Tropical Plant Pathology 38(3): 227–235. https://doi.org/10.1590/S1982-56762013005000002

Maharachchikumbura SSN, Hyde KD, Groenewald JZ, Xu J, Crous PW (2014) *Pestalotiopsis* revisited. Studies in Mycology 79(1): 121–186. https://doi.org/10.1016/j.simyco.2014.09.005

Maharachchikumbura SSN, Hyde KD, Jones EBG, McKenzie EHC, Jayarama Bhat D, Dayarathne MC, Huang SK, Norphanphoun C, Senanayake IC, Perera RH, Shang QJ, Xiao Y, D'souza MJ, Hongsanan S, Jayawardena RS, Daranagama DA, Konta S, Goonasekara ID, Zhuang WY, Jeewon R, Phillips AJL, Wahab MAA, Sadi AMA, Bahkali AH, Boonmee S, Boonyuen N, Cheewangkoon R, Dissanayake AJ, Kang J, Li QR, Liu JK, Liu XZ, Liu ZY, Luangsa-ard JJ, Pang KL, Phookamsak R, Promputtha I, Suetrong S, Stadler M, Wen TC, Wijayawardene NN (2016) Families of Sordariomycetes. Fungal Diversity 79(1): 1–317. https://doi.org/10.1007/s13225-016-0369-6

Miller MA, Pfeiffer W, Schwartz T (2012) The CIPRES science gateway: enabling high-impact science for phylogenetics researchers with limited resources. Proceedings of the 1st Conference of the Extreme Science and Engineering Discovery Environment. Bridging from the extreme to the campus and beyond. Association for Computing Machinery, USA, 1–8. https://doi.org/10.1145/2335755.2335836

Nag Raj TR (1993) Coelomycetous Anamorphs with Appendage-Bearing Conidia. Mycologue Publications, Waterloo, Ontario.

Norphanphoun C, Jayawardena RS, Chen Y, Wen TC, Meepol W, Hyde KD (2019) Morphological and phylogenetic characterization of novel pestalotioid species associated with mangroves in Thailand. Mycosphere: Journal of Fungal Biology 10(1): 531–578. https://doi.org/10.5943/mycosphere/10/1/9

Nylander JAA (2004) MrModelTest v. 2. Program distributed by the author. Evolutionary Biology Centre, Uppsala University.

O'Donnell K, Cigelnik E (1997) Two divergent intragenomic rDNA ITS2 types within a monophyletic lineage of the fungus *Fusarium* are nonorthologous. Molecular Phylogenetics and Evolution 7(1): 103–116. https://doi.org/10.1006/mpev.1996.0376

O'Donnell K, Kistler HC, Cigelnik E, Ploetz RC (1998) Multiple evolutionary origins of the fungus causing panama disease of banana: concordant evidence from nuclear and mitochondrial gene genealogies. Proceedings of the National Academy of Sciences of the United States of America 95(5): 2044–2049. https://doi.org/10.1073/pnas.95.5.2044

Ronquist F, Huelsenbeck JP (2003) MrBayes 3: Bayesian phylogenetic inference under mixed models. Bioinformatics (Oxford, England) 19(12): 1572–1574. https://doi.org/10.1093/bioinformatics/btg180

Ronquist F, Teslenko M, van der Mark P, Ayres DL, Darling A, Höhna S, Larget B, Liu L, Suchard MA, Huelsenbeck JP (2012) MrBayes 3.2: Efficient Bayesian phylogenetic inference and model choice across a large model space. Systematic Biology 61(3): 539–542. https://doi.org/10.1093/sysbio/sys029

Saccardo PA (1884) Sylloge fungorum omnium hucusque cognitorum 3: 797.

Senanayake IC, Maharachchikumbura SSN, Hyde KD, Jayarama Bhat D, Gareth Jones EB, McKenzie EHC, Dai DQ, Daranagama DA, Dayarathne MC, Goonasekara ID, Konta S, Li WJ, Shang QJ, Stadler M, Wijayawardene NN, Xiao YP, Norphanphoun C, Li Q, Liu XZ, Bahkali AH, Kang JC, Wang Y, Wen TC, Wendt L, Xu JC, Camporesi E (2015) Towards unraveling relationships in Xylariomycetidae (Sordariomycetes). Fungal Diversity 73(1): 73–144. https://doi.org/10.1007/s13225-015-0340-y

Silvério ML, de Cavalcanti MA (2016) A new epifoliar species of *Neopestalotiopsis* from Brazil. Agrotópica 28(2): 151–158. https://doi.org/10.21757/0103-3816.2016v28n2p151-158

Solarte F, Munoz CG, Maharachchikumbura SSN, Alvarez E (2018) Diversity of *Neopestalotiopsis* and *Pestalotiopsis* spp., causal agents of guava scab in Colombia. Plant Disease 102(1): 49–59. https://doi.org/10.1094/PDIS-01-17-0068-RE

Song Y, Geng K, Zhang B, Hyde KD, Zhao WS, Wei JG, Kang JC, Wang Y (2013) Two new species of *Pestalotiopsis* from Southern China. Phytotaxa 126(1): 22–30. https://doi.org/10.11646/phytotaxa.126.1.2

Stamatakis A (2014) RAxML Version 8: A tool for phylogenetic analysis and post-analysis of large phylogenies. Bioinformatics (Oxford, England) 30(9): 1312–1313. https://doi.org/10.1093/bioinformatics/btu033

Steyaert RL (1949) Contribution a l'etude monographique de *Pestalotia* de Not. et *Monochaetia* Sacc. (*Truncatella* gen. nov. et *Pestalotiopsis* gen. nov.). Bulletin Jardin Botanique Etat Bruxelles 19(3): 285–354. https://doi.org/10.2307/3666710

Steyaert RL (1953) New and old species of *Pestalotiopsis*. Transactions of the British Mycological Society 36(2): 81–89. https://doi.org/10.1016/S0007-1536(53)80052-5

Steyaert RL (1961) Type specimens of Spegazzini's collections in the *Pestalotiopsis* and related genera (Fungi Imperfecti: Melanconiales). Darwinia (Buenos Aires) 12: 157–190.

Steyaert RL (1963) Complementary informations concerning *Pestalotiopsis guepini* (Desmazieres) Steyaert and designation of its lectotype. Bulletin Jardin Botanique l'Etat Bruxelles 33(3): 369–373. https://doi.org/10.2307/3667200

Sutton BC (1980) The Coelomycetes. Fungi imperfecti with pycnidia, acervuli and stromata. Commonwealth Mycological Institute, Kew, Surrey.

Tanaka K, Endo M, Hirayama K, Okane I, Hosoya T, Sato T (2011) Phylogeny of *Discosia* and *Seimatosporium*, and introduction of *Adisciso* and *Immersidiscosia* genera nova. Persoonia 26(1): 85–98. https://doi.org/10.3767/003158511X576666

Tibpromma S, Hyde KD, Mckenzie E, Bhat DJ, Phillips AJL, Wanasinghe DN, Samarakoon MC, Jayawardena RS, Dissanayake AJ, Tennakoon DS, Doilom M, Phookamsak R, Tang AMC, Xu J, Mortimer PE, Promputtha I, Maharachchikumbura SSN, Khan S, Karunarathna SC (2018) Fungal diversity notes 840–928: Micro-fungi associated with Pandanaceae. Fungal Diversity 93(1): 1–160. https://doi.org/10.1007/s13225-018-0408-6

Wang B, Zhang ZW, Guo LD, Liu L (2016) New cytotoxic meroterpenoids from the plant endophytic fungus *Pestalotiopsis fici.* Helvetica Chimica Acta 99(2): 151–156. https://doi.org/10.1002/hlca.201500197

White TJ, Bruns T, Lee S (1990) Amplification and direct sequencing of fungal ribosomal RNA genes for phylogenetics. In: Innis MA, Gelfand DH, Sninsky JJ (Eds) PCR protocols: a guide to methods and applications. Academic Press Inc, New York, 315–322. https://doi.org/10.1016/B978-0-12-372180-8.50042-1

Wijayawardene NN, Hyde KD, Wanasinghe DN, Papizadeh M, Goonasekara ID, Camporesi E, Jayarama Bhat D, McKenzie EHC, Phillips AJL, Diederich P, Tanaka K, Li WJ, Tangthirasunun N, Phookamsak R, Dai DQ, Dissanayake AJ, Weerakoon G, Maharachchikumbura SSN, Hashimoto A, Matsumura M, Bahkali AH, Wang Y (2016) Taxonomy and phylogeny of dematiaceous coelomycetes. Fungal Diversity 77(1): 1–316. https://doi.org/10.1007/s13225-016-0360-2

Supplementary material 1

The combined ITS, *tub2* and *tef1* sequences

Authors: Zhaoxue Zhang, Rongyu Liu, Shubin Liu, Taichang Mu, Xiuguo Zhang, Jiwen Xia

Data type: phylogenetic

Explanation note: The combined ITS, *tub2* and *tef1* sequences.

Link: https://doi.org/10.3897/mycokeys.88.82229.suppl1